Author/s:
Ganadhiepan, Ganesharajah

Title:
Mechanobiological investigation of bone fracture healing under Ilizarov circular fixators

Date:
2020

Mechanobiological investigation of bone fracture healing under Ilizarov circular fixators

Ganesharajah Ganadhiepan

ORCID ID: 0000-0002-3401-4211

Submitted in total fulfilment of the requirements of the degree of

Doctor of Philosophy

March 2020

Department of Infrastructure Engineering

The University of Melbourne

Parkville, Victoria 3010

Australia

Abstract

Ilizarov circular fixator (ICF) is an external bone fixation device used by orthopaedic surgeons in treating variety of bone defects. Despite the fact that ICFs are being used for over seven decades, the interplay between ICF mechanics and biology of fracture healing remains poorly understood. The roles of ICF configurations on processes within the fracture site during fracture healing such as cell differentiations, solute (e.g. cell, growth factors etc.) transport and angiogenesis have not been explained well yet. Furthermore, how the interplay between ICF and other mechanical factors such as fracture geometry and loading affect these processes remains unclear. This knowledge gap in the mechanobiology of fracture healing under ICF is a barrier to address clinical problems associated with ICFs. Consequently, treatment failures and complications are significant with ICF treatments (around 10 – 30 %). This thesis intends to address this knowledge gap by conducting systematic mechanobiological investigations of fracture healing under ICFs.

In this research, various computational models to simulate various aspects of fracture healing under ICFs were developed. In developing the models, various novel methodologies and modelling techniques were adopted. Firstly, unlike in most previous studies, a fully coupled fracture healing prediction model of fractured bone stabilized with ICFs, including soft tissues and mechano-regulation was developed to simulate early stage mesenchymal stem cell (MSC) differentiations. Secondly, a model combining both mechano-regulation and bio-regulation was implemented to simulate healing of fractures stabilized with ICF under dynamic loading. Thirdly, a new regulatory model considering level of vascularity and local tissue strain was proposed and implemented to simulate angiogenesis and fracture healing under ICF. Finally, a methodology using computational modelling in conjunction with engineering reliability analysis was implemented to investigate the role of uncertainties in mechanical parameters on fracture healing under ICFs. All computational models were developed based on the theory of porous media and continuum mechanics. The models were first validated using experimental data and subsequently used for fracture healing predictions. Mechanical experiments involving measurement of bone interfragmentary movements (IFM) using an advanced 3D optical

measuring system (ARAMIS) were conducted in this research for model validation purposes. Wherever possible, the predictions of the models were corroborated by experimental and clinical data.

Through systematic analyses, this thesis contributes to the existing body of knowledge by providing new insights into the mechanobiology of fracture healing under ICFs. This thesis elucidates the following mechanobiological aspects of fracture healing under ICF that have not been systematically studied so far:

1. The effects of ICF configuration, loading and fracture geometry on the early stage mesenchymal stem cell (MSC) differentiations during fracture healing;
2. The roles of physiologically relevant dynamic loading on cell differentiations and cell / growth factors transport within the early stage fracture site;
3. The effects of subject specific factors (i.e. body weight, fracture geometry and ICF configuration) on angiogenesis and optimal time dependent weight bearing levels for bone fractures treated with ICFs; and
4. The effects of uncertainties in mechanical factors (i.e. fracture geometry, weight bearing and ICF configuration) on fracture healing under ICF.

In addition, the models presented in this thesis could potentially be used for further systematic investigations and in clinical settings for designing and comparing ICF treatment strategies.

List of Publications

The following publications were made based on the work of this thesis:

1. **G. Ganadhiepan**, S. Miramini, M. Patel, P. Mendis, and L. Zhang, "Bone fracture healing under Ilizarov fixator: Influence of fixator configuration, fracture geometry, and loading," International Journal for Numerical Methods in Biomedical Engineering, vol. 35, no. 6, p. e3199, 2019.

2. **G. Ganadhiepan** et al., "The Effects of Dynamic Loading on Bone Fracture Healing Under Ilizarov Circular Fixators," Journal of Biomechanical Engineering, vol. 141, no. 5, pp. 051005-051005-12, 2019.

3. **G. Ganadhiepan**, S. Miramini, P. Mendis, and L. Zhang, "The effects of direct and indirect loading on bone fracture healing under Ilizarov circular fixator," in 6th International Conference on Computational and Mathematical Biomedical Engineering, Japan, 2019, vol. 2, pp. 855-858.

4. **G. Ganadhiepan**, S. Miramini, P. Mendis, and L. Zhang, "The role of physiological loading on bone fracture healing under Ilizarov circular fixator : the effects of load duration and loading frequency " in Computer Methods, Imaging and Visualization in Biomechanics and Biomedical Engineering, vol. 36, G. A. Ateshian, K. M. Myers, and J. M. R. S. Tavares, Eds. Lecture Notes in Computational Vision and Biomechanics: Springer, 2020, pp. 218-236.

Declaration

This is to certify that:

1. this thesis comprises only my original work towards the PhD except where indicated in the preface;

2. due acknowledgement has been made in the text to all other material used; and

3. this thesis is fewer than 100,000 words in length, exclusive of tables, maps, bibliographies and appendices as approved by the Research Higher Degrees Committee.

Ganesharajah Ganadhiepan

Preface

This thesis includes contents from published materials and manuscripts in press or under review for publication, which are direct outcomes of this research work. I (Ganesharajah Ganadhiepan) was the first and the primary author and my supervisors A/Prof. Lihai Zhang, Prof. Priyan Mendis and Dr. Saeed Miramini were co-authors of all these works. In addition, some of these works include our collaborators who gave their inputs as co-authors. As the first and primary author of these works, I was responsible for conceptualizing, planning, execution of the works, writing the first draft of the manuscripts and revising the manuscripts based on the comments from both internal and publishers' review processes. In each work my contribution was at least 55 %.

My supervisors A/Prof. Lihai Zhang, Prof. Priyan Mendis and Dr. Saeed Miramini regularly discussed with me, monitored my progress and provided their inputs and feedback throughout each of these works. The contributions of collaborators and where these works appear in this thesis are briefly described below.

The contents of chapters 3 and 4 are primarily from the journal article **Bone fracture healing under Ilizarov fixator: Influence of fixator configuration, fracture geometry, and loading** published by the **International journal for numerical methods in biomedical engineering** (published on 14/03/2019). Prof. Minoo Patel of Epworth Richmond was a co-author of this article.

Chapter 5 is based on the journal article **The Effects of Dynamic Loading on Bone Fracture Healing Under Ilizarov Circular Fixators** published by the **Journal of Biomechanical Engineering** (published on 25/03/2019). Prof. Minoo Patel of Epworth Richmond, Prof. Peter Ebeling of Monash University and Prof. Yulong Wang of Shenzhen University were co-authors of this article.

In the aforementioned works, Prof. Minoo Patel of Epworth Richmond, Prof. Peter Ebeling of Monash University and Prof. Yulong Wang of Shenzhen University provided clinical perspectives to the problems investigated and helped me design the studies.

Furthermore, **The role of physiological loading on bone fracture healing under Ilizarov circular fixator : the effects of load duration and loading frequency** which was published as a book chapter in **Lecture Notes in Computational Vision and Biomechanics** book series (published on 01/04/2020) and **The effects of direct and indirect loading on bone fracture healing under Ilizarov circular fixator** published in the **proceedings of the 6th International Conference on Computational and Mathematical Biomedical Engineering** (published on 10/06/2019) are included in the appendix as additional outcomes of this research project.

Acknowledgements

Firstly, I thank my supervisors A/Prof. Lihai Zhang, Prof. Priyan Mendis and Dr. Saeed Miramini for their guidance, motivation, mentorship and support. My principal supervisor A/Prof. Lihai Zhang's encouragement and the freedom he gave me were the primary reasons that I managed to make a few publications during my PhD. He was always ready to give time for his students, even during busy times and weekends. In addition, he was so generous to ask me to drop by his office whenever I needed to discuss about anything so that I could solve my issues quickly and move forward. Without his support throughout, I would not have completed my project on time.

I would like to express my sincere gratitude to Prof. Priyan Mendis for introducing me to A/Prof. Lihai Zhang in 2016 and making my PhD dream come true. In addition, I thank him for providing me the opportunity to teach his subject which helped me discover my teaching potentials. My sincere thanks are due to Dr. Saeed Miramini for helping me getting started with computational modelling and continuously providing support in all aspects of my research work. I specially thank him for his help in planning and conducting mechanical experiments and generously training me to use ARAMIS 3D optical measuring system. I would also like to thank my chair Dr. Felix Hui for his helpful advice and support in progress reviews.

I gratefully acknowledge the University of Melbourne for funding my studentship via Melbourne Research Scholarship. In addition, I would also like to thank Melbourne School of Engineering Conference Travel Scholarship and the Department of Infrastructure Engineering's conference support grant for providing me funding to support my conference travels.

Moreover, I take this opportunity to thank our department administrators Ms. Pauline Woolcock and Ms. Eileen Doufas Shea and collaborators Prof. Minoo Patel of Epworth Richmond, Prof. Peter Ebeling of Monash University and Prof. Yulong Wang of Shenzhen University for all their supports throughout. My special thanks are due to Mr. Steve Adams, senior technical officer (Wet Labs) and master's students Sifan Liu and

Lijia Guo for their help in conducting the mechanical experiments. I would also like to thank my colleagues Ms. Smriti Ghimire, Mr. Babar Nasim Khan Raja and Mr. Jin Liao for helping me during the experiments and for the useful discussions we had about many aspects of research. Especially, I benefitted a lot from the discussions we had on computational modelling and believe they would have benefitted a lot too. I thank them and all my other fellow mates for making the past 3.5 years so memorable and enjoyable.

Last but not least, I would like to express my sincerest gratitude to my parents Mr. Kumarasamy Ganesharajah and Mrs. Sivasakthy Ganesharajah for their selfless love and the guidance, encouragement and support they gave me in every step I took in my life. I am equally grateful to my sister Mrs. Mayoorini Majuran and brother-in-law Mr. Arudsothy Majuran, for never making me feel that I am thousands of miles away from my parents. Words can never express how grateful I am to my parents, sister and brother-in-law. Thank you so much for everything you have done.

Table of Contents

List of Tables

List of Figures

List of Third-Party Copyright Materials

Citation Information for Third party copyright material	Location of item in thesis	Permission granted Y/N
Figure 6-1 in V. Scanlon and T. Sanders, Essentials of Anatomy and Physiology. Philadelphia, UNITED STATES: F. A. Davis Company, 2014.	p.10	Y
Figure 3 on Page 625 (Chapter 43) in A. L. Firth, W. Yao, and J. X.-J. Yuan, "Identification of Adult Stem and Progenitor Cells in the Pulmonary Vasculature," in *Textbook of Pulmonary Vascular Disease*: Springer, 2011, pp. 621-636.	p.12	Y
Figure 1 in P. Andrzejowski and P. V. Giannoudis, "The 'diamond concept'for long bone non-union management," *Journal of Orthopaedics and Traumatology*, vol. 20, no. 1, p. 21, 2019. This file is licenced under Creative Commons CC BY licence.	p.27	Y
Figure 3 in V. Coppa, M. Marinelli, and N. Specchia, "Unilateral uniplanar modular external fixator for percutaneous proximal femoral osteotomy in children: surgical technique," *European Journal of Orthopaedic Surgery & Traumatology*, vol. 29, no. 1, pp. 205-211, 2019.	p.35	Y
Figure 1 in M. S. Alqahtani, A. Al-Tamimi, H. Almeida, G. Cooper, and P. Bartolo, "A review on the use of additive manufacturing to produce lower limb orthoses," *Progress in Additive Manufacturing*, pp. 1-10, 2019. This file is licenced under Creative Commons CC BY licence.	p.35 and p.37	Y
Figure 3 and Table 1 in A. Vetter *et al.*, "Temporal tissue patterns in bone healing of sheep," *Journal of Orthopaedic Research*, vol. 28, no. 11, pp. 1440-1447, 2010.	p.150 and p.151	Y

1 Introduction

1.1 Background

Musculoskeletal injuries make up a significant proportion of the total world health expenses [1]. In particular, long bone fracture which occurs due to various reasons such as osteoporosis and trauma is one of the frequent non-fatal injuries reported worldwide [1, 2]. In Australia, it is reported that a bone breaks every 3.4 minutes and results in over 150,000 hospitalisations and almost one million bed-days each year [3]. This makes bone fractures the most common form of hospitalised trauma in Australia [3]. The nationwide costs of poor bone health in Australia exceeded 2 billion dollars in 2016 alone and the total cost since 2012 is predicted to exceed a staggering 33 billion dollars by 2022 [4]. From these numbers of Australia, one could imagine how big the total global economic burden of skeletal problems would be. These are just the direct costs and not inclusive of the indirect costs due to reasons such as loss of productivity. The indirect costs associated with bone fractures could be much higher than the direct costs and account for around 65 – 95 % of the total cost of fractures [5]. These facts clearly suggest that bone fracture is a serious health problem that needs to be addressed as it is becoming increasingly burdensome.

In working age adults, long bone fracture is the most common type of fracture [3]. Out of all bone fractures, thigh bone (femur), upper arm bone (humerus) and shinbone (tibia) fractures alone account for 3 %, 14 % and 24 %, respectively [3]. Long bone fractures mainly result from high energy trauma such as falls or transport accidents and often these fractures are complex to manage due to high risk of treatment failures [3, 5, 6]. A recent Australian study considering 3886 patients with humeral, femoral and tibial fractures reported healing complication rates as high as 8.1 % with non-union being the most common complication [3]. Therefore, is essential to treat long bone fractures effectively so that the time and cost associated with treatment could be minimized. Minimizing treatment time can also minimize the risk of complications and the indirect costs due to loss of productivity [7].

The need for effective treatment has been driving the advancements in the field of orthopaedics for several decades. While bone has natural capacity to heal by itself after

fracture, the intrinsic healing capacity of bones may not always be enough [7]. Therefore, some external intervention may be required depending on the nature of fracture and other subject specific factors that affect healing. Both biology and mechanics are equally important for the success of healing [8]. The principle behind treating fractures is to provide the best possible mechanical environment within the fracture site so that the intrinsic biological healing capacity of bone is best utilized [7, 9]. Traditionally, most fractures are treated with plaster casts by stabilizing fractures and minimizing disturbance to the fracture site [10]. However, plaster casts may not always be suitable.

Number of different bone fixation devices have come into existence in the past several decades [11]. The use of such devices requires some level of surgical procedure. Fixation devices are mainly categorized into either internal fixations or external fixations. Internal fixation devices are mounted into patients' bodies and thus require complex surgical procedures. In addition, modifications to internal fixations are impossible without additional surgical procedures. Moreover, internal fixation devices need to be left within the patient's body permanently in most cases.

External bone fixations devices on the other hand are mounted outside of patients' bodies and possess numerous advantages over internal fixations. The main advantages of external fixation devices include (i) being minimally invasive, (ii) being tailorable to patient specific needs, (iii) being adjustable depending on the progress of healing and (iv) being removable upon satisfactory healing [9, 12]. These advantages led to the development of number of external bone fixation devices in the past.

Ilizarov circular fixator (ICF) is one such external device that has been used by orthopaedic surgeons in treating variety of bone defects such as fractures, length discrepancies, deformities and osteomyelitis [13]. It is a modular fixator consisting of rings, wires, half pins, struts and rods which can be assembled in endless possible ways to cater patient specific needs [14]. The ICF components such as rings and wires come in variety of sizes and specifications. This gives surgeons the freedom to choose the most suitable components to get the best configuration on a case-by-case basis. Furthermore, ICFs allow early weight bearing which helps patients to get mobile relatively early during healing. It is also suggested that early weight bearing is beneficial for fracture healing

[12]. Clinical observations indicate that ICFs have enormous potential in treating bone defects effectively.

1.2 Problem statement

The first use of ICFs dates to the 1950s [14, 15]. Even though ICFs have been in existence for nearly seven decades now, it still remains a secondary treatment option [12]. One of the important reasons for this situation is lack of understanding of the mechano-biology of healing under ICFs. Most of the existing clinical and experimental studies are limited in fully elucidating how ICF interacts with the fracture environment and affects healing. Therefore, many aspects of fracture healing under ICFs such as how ICF configuration affects cell differentiations or angiogenesis within the fracture site remains poorly understood. This is one of the reasons why clinical decisions about ICF treatments are often made on a trial and error basis [15]. Therefore, there is a need for systematic investigation on how ICF interacts with fracture environment and understand the mechano-biology of healing under ICFs to utilize the full potential of the device.

It is known that patient specific factors such as fracture geometry, body weight, age, sex and comorbidities (e.g. osteoporosis) can influence the fracture healing process. Therefore, it is essential that these factors are considered when making patient specific treatment plans. Since ICF could be assembled in endless possible configurations, it is necessary to consider the ICF configuration parameters when planning treatments. This is because, they influence the stability of fracture site and thus affect the healing process. Owing to the number of factors involved and their complex interrelationships, patient specific treatment planning is often challenging in treatments involving ICFs.

1.3 Research objective

The objective of this research is to conduct systematic investigations into the mechano-biology of fracture healing under ICF. This research mainly focuses on how ICF interacts with the fracture environment and other patient specific factors during healing in order to determine ways to promote healing under ICFs. The effects of ICF configurations, patient specific factors and their interplays on fracture healing are investigated in this research. The results of this research would enable surgeons to make decisions based on facts rather than trial and error. Initially this research focuses on the early stages of bone fracture

healing as it is known that early stage fracture environment is very sensitive and capable of affecting the whole healing process [16, 17]. Subsequently the research focus moves into the next stages of fracture healing.

The specific objectives of this research are as follows:

- Developing a reliable method to study different aspects of fracture healing under ICFs
- Investigating the effects of ICF configuration, loading and fracture geometry on the early stages of fracture healing
- Investigating the effects of physiologically relevant dynamic loading on early stage bone fracture healing under ICFs
- Determining optimal time dependent levels of weight bearing for bone fractures treated with ICFs.
- Investigating how uncertainties in mechanical factors (i.e. fracture geometry, weight bearing and ICF configuration) affect fracture healing under ICF.

1.4 Methodology and scope of this research

As the research problem is inherently complex owing to the large number of factors involved, experimental or clinical approaches could be either too expensive, time consuming or impractical with currently available techniques [18]. On the other hand, validated computational models provide an excellent solution to this problem. Using computational models, it is possible to handle multiple inputs and provide reasonably accurate solutions relatively quickly. With computational power growing exponentially, simulation of very complex processes is increasingly becoming time and cost effective. Moreover, computational models offer perfect repeatability and eliminate inter-subject differences which are generally inevitable in experimental and clinical approaches.

Therefore, in this research, computational models of bone fractures treated with ICF were developed to address the research objectives. The models were validated using experimental data and subsequently used to simulate fracture healing under various conditions to address the research objectives. Wherever possible, model predictions were compared with experimental and clinical results.

This research focuses specifically on fractures of long bones in weight bearing limbs (e.g. tibia). Human bones were considered wherever possible. However, due to lack of experimental data under controlled environments for human models, animal models with similarities to humans had to be considered in some investigations. Due to the availability of experimental data [19, 20], sheep models were used in some investigations of this research. It should also be noted that assumptions and simplifications had to be made wherever necessary without affecting the fundamental behaviours when developing the computational models. These are explained in detail in relevant sections of this thesis.

1.5 Thesis structure

The structure of the thesis is as follows:

Chapter 1: Introduction

This refers to the current chapter.

Chapter 2: Literature Review

This chapter gives a comprehensive literature review on the current state of knowledge in this research area to provide background to this thesis. Initially, bone composition, their functions, material properties, bone fractures and fracture healing are reviewed. Next, studies on fracture healing are reviewed with special focus on computational models. Subsequently, bone fracture treatment methods are reviewed, and the use of external fixation devices are discussed. Finally, the applications, advantages and limitations of ICFs are described and the research gaps are identified.

Chapter 3: Mechanical Experiment on Tibial Fractures Stabilized with Ilizarov Circular Fixator

This chapter describes the mechanical experiment carried out on tibial fractures stabilized with ICFs. Transverse tibial fractures stabilized with different configurations of ICF were subjected to axial loading and the interfragmentary movements were measured using a 3D optical measurement system ARAMIS (GOM, Braunschweig, Germany). The mechanical behaviour of bone-ICF assembly was observed in the study and the experimental data was later used for validation purposes. Detailed description of the experimental methodology and discussion of the mechanical test results are given in this

chapter. Thus, this chapter has an experimental focus into the mechanical behaviour of bone-ICF assembly and provides useful new biomechanical data to complement existing understanding. The subsequent chapters are dedicated primarily to computational simulations of the mechanobiology of fracture healing under ICFs. Most of the contents of this chapter were published in an article in the *International Journal for Numerical Methods in Biomedical Engineering* [21].

Chapter 4: Bone fracture healing under Ilizarov circular fixator: influence of fixator configuration, fracture geometry and loading

Development of a fully coupled computational model of tibial fractures stabilized with ICF is described in this chapter. First the chapter explains how the fracture healing model was developed and validated against the experimental data presented in Chapter 3. Then the roles of ICF configuration, fracture geometry and loading on early stage cell differentiations were investigated using the validated model. In contrast to Chapter 3 which focuses into the mechanical behaviour of bone-ICF assembly, this chapter focuses into the mechanobiology of fracture healing via computational modelling. The outcomes of this study were published in an article in the *International Journal for Numerical Methods in Biomedical Engineering* [21].

Chapter 5: The Effects of Dynamic Loading on Bone Fracture Healing Under Ilizarov Circular Fixators

The role of dynamic loading (resulting from weight bearing activities) on early stage healing under ICF is investigated in this chapter. Starting from the work described in Chapter 4, the early stage fracture healing model was further extended to include various cells, growth factors and their transport and interactions within the fracture site. Then the model was used to study the spatial and temporal changes in the cell and growth factor concentrations during the early stage healing under various patient specific factors. This chapter presents the details of model development followed by results, discussion and conclusions. An article was published based on this work in the *Journal of Biomechanical Engineering* [22].

Chapter 6: Optimal time-dependent levels of weight-bearing for bone fracture healing under Ilizarov circular fixators

Broadening the investigation from early stage to full course of healing, this chapter deals with determining time dependent and subject specific optimal weight bearing range for bone fractures treated with ICF. Based on the works in Chapters 4 and 5, a model was developed to simulate the time dependent healing of bone fractures incorporating angiogenesis. Taking sheep model as an example, this chapter describes how optimal weight bearing could be established for a given set of conditions and subject specific parameters. A manuscript written based on this work is currently under review by a journal.

Chapter 7: A probabilistic approach to address uncertainties in Ilizarov circular fixator-based fracture treatments

This chapter builds on top of Chapter 6 to incorporate uncertainties in subject specific parameters and investigates their effects on the probability of successful healing. A probabilistic approach using computational modelling in conjunction with engineering reliability analysis techniques is presented in this chapter. This chapter provides key insights about the sensitivity of fracture site to different mechanical variables. Furthermore, the method presented in this chapter could be used to investigate reliability of different ICF treatment strategies.

Chapter 8: Conclusions and Recommendations

This chapter summarizes the findings of this research and makes recommendations for future work.

References

The list of references is provided at the end of chapter 8.

Appendix: Additional outcomes of this research

Additional outcomes of this research project that are not included in the chapters are included in the appendix.

2 Literature Review

2.1 Introduction to Bone

Bones provide structural framework which defines the overall body shape and ensures safer transmission of mechanical loads acting on it. Bones are also responsible for protecting vital organs made of soft tissues (e.g. brain, liver etc.) within a body. The role of bones in a body could be compared to that of structural members of a building such as beams and columns. These structural elements bear their own self weight, carry the weight of the non-structural elements and take the external loads such as wind and transmit them safely to the ground to protect the building and its occupants.

However, bones in living bodies involve themselves in more complex activities than those of structural members of a building. In living bodies, bones could be attached to muscles, joints, tendons, ligaments, cartilage and connective tissues and collectively form the musculoskeletal system which is responsible for precise body motion [23, 24]. Bones continuously undergo a process known as 'remodeling' by which it restructures and reshapes itself in response to its biological and mechanical environments [25, 26]. This self-adaptive nature of bone is vital for proper functioning of the musculoskeletal system. It is also one of the reasons for the interspecific and intraspecific differences in the bone material properties, despite the same mineralogical composition. Noticeable differences in bone material properties, even within the same organism at different skeletal locations is possible [27]. In addition, factors such as age, sex and comorbidities can also affect the material properties of bone [26]. Likewise, geometric features of bones (i.e. size, shape, thickness etc.) are also subjected to interspecific and intraspecific differences due to the influence of these factors [28]. Therefore, it is hard to define universal geometries or material properties for bone.

In addition to structural and locomotive purposes, bone serves number of important biological purposes in living bodies. This includes, acting as a mineral reservoir (especially for calcium); providing the environment for marrow which is responsible for new blood cell formation and capable of storing fat; acting as a reservoir for growth factors (GFs) and cytokines and taking part in maintaining the acid-base balance in the

body [29]. Thus, bone plays a key role in the overall functioning of living organisms with skeletal system.

2.1.1 Bone morphology

In humans, there are four different categories of bone based on their shape, namely, (i) long bones such as tibiae, femurs, humeri, ulnae etc.; (ii) short bones such as carpal bone, tarsal bone etc.; (iii) flat bones such as skull, mandible, ribs etc.; and (iv) irregular bones such as vertebrae, sacrum, coccyx etc. [30]. Since this research project focuses on long bone fractures, this chapter will focus mainly on long bones.

Long bones have long hollow shafts known as diaphyses and rounded ends known as epiphyses. Diaphysis is composed of dense and compact bone known as cortical bone on the outer which surrounds an inner hollow known as the medullary cavity. This cavity, which is also known as medullary/marrow canal, is occupied by yellow bone marrow which is rich in adipose tissue. Epiphysis on the other hand is composed primarily of highly porous trabecular bone surrounded by a thin cortical bone shell. Trabecular bone has a honeycomb-like structure which is responsible for its high porosity and referred to as spongy or cancellous bone [30, 31]. Figure 2.1 illustrates the two different types of bones in a typical long bone (i.e. femur).

Cortical bone is made of structured ‘osteons’ or ‘Haversian system’ which consists of microscopic cylinders made up of concentric rings of osteocytes (i.e. bone forming cells) with a central canal known as ‘Harversian canal’. Blood vessels invade bones via these canals to supply oxygen and nutrients to bone (Figure 2.1). In trabecular bones, the interconnected pores contain red bone marrow, which is responsible for red blood cell, platelet and white blood cell productions [26, 30, 31]. Cortical bones are covered by an outer layer of fibrous connective tissue known as periosteum which consists of blood vessels and bone forming osteoblasts which could assist bone tissue repair. The collagen fibres of periosteum merge with those of the tendons and ligaments attached to the bones. A similar, but thinner layer of connective tissue is also found on the inner side of cortical bone, which lines the medullary cavity. This is referred to as ‘endosteum’. Both periosteum and endosteum play an important role in the remodelling process of bones [26, 30, 31].

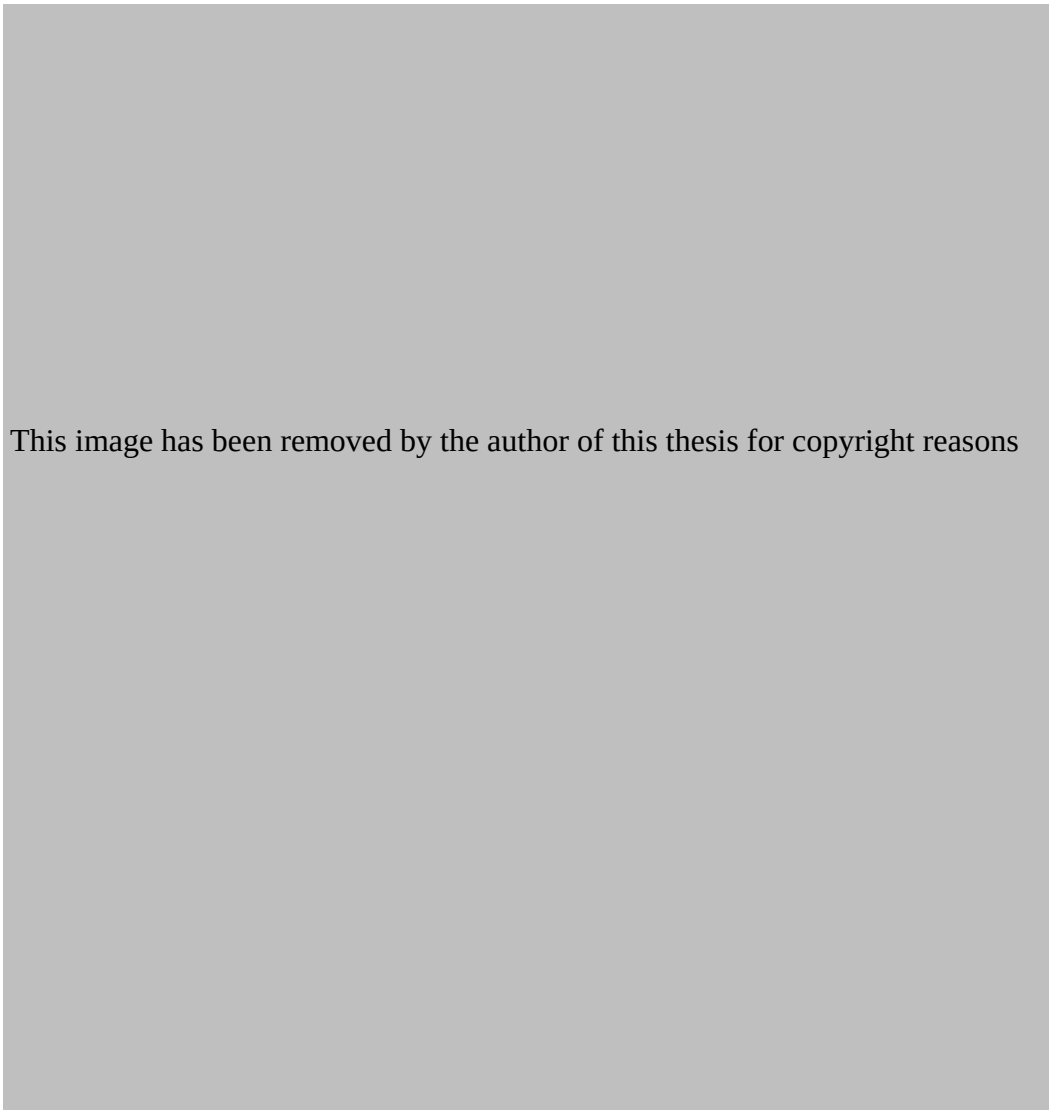

Figure 2.1 Typical human femoral bone and the Harversian system
Adopted from Scanlon and Sanders [31] with permission

2.1.2 Bone development and the underlying cellular processes

The development of bones can take place in two fundamentally different ways. One is by direct apposition (i.e. de novo) and the other is by replacing existing tissues [32, 33]. During embryonic growth, bones are first made of cartilage and fibrous connective tissues which gets replaced gradually by bone tissue. Interestingly, the underlying cellular and molecular events in embryonic skeletal development, bone remodelling and fracture healing are virtually identical [34]. Detailed studies on these three different processes

have shown striking similarities amongst them in terms of histology, physiology and functionality. This phenomenon is attributed to the fact that, these three distinctly different processes (in terms of space and time) originate from the common progenitor cells known as mesenchymal stem cells (MSC). These cells (MSCs) are multipotent and have the ability to continuously replicate themselves and differentiate along multiple cell lineages. MSCs respond to biochemical and mechanical environmental cues and thus, commitment of MSCs to cell lineages could be influenced by the local biochemical and mechanical microenvironments [34].

For example, during fracture repair, MSCs could take either (i) the osteogenic pathway and differentiate into osteoblasts to synthesise bone tissue or (ii) chondrogenic pathway and differentiate into chondrocytes to synthesise cartilage tissue or (iii) fibrogenic pathway and differentiate into fibroblasts to synthesise fibrous connective tissue. Commitment to a specific pathway depends on the microenvironmental factors and once committed, the cells would start to synthesise the extracellular matrix specific to the committed pathway [34]. It is known that the level of blood supply, presence of growth factors (GF) and mechanical stability can influence the cell fate (i.e. commitment of MSCs to a specific pathway).

In addition, MSCs can differentiate into various other types of mesenchymal tissues including tendon, muscle, marrow, fat and dermis. Figure 2.2 illustrates the mesengenic process, indicating differentiation pathways of MSC and their stages, from proliferation of MSCs to synthesis of tissues.

During embryonic development of long bones, the original cartilage tissue starts to ossify around three months of gestation and osteoblasts gradually synthesis bone matrix to replace cartilage. The ossification process occurs at the centre of the diaphysis and continue even after birth throughout childhood. Epiphyseal discs at the junction of the diaphysis and epiphysis, remains cartilaginous to enable growth of long bones and eventually gets replaced by bone matrix between 16 – 25 years after which bone growth ceases [31].

Osteoclast is another type of cell present in bones which is responsible for the resorption and remodelling processes. Resorption is the process by which mineralized bone is degraded. This process is essential for skeletal growth, maintaining bone integrity,

maintaining calcium balance in blood and bone repair [35]. Remodelling of bones refer to the process by which mature bone tissue is resorbed and replaced with new bone tissue. This process is responsible for changes in bone architecture and material properties to meet the changing mechanical needs [36]. Remodelling is a process that continues throughout life. Thus, microstructural architecture and material properties of bones are always dynamic and depend on the biochemical and mechanical environments.

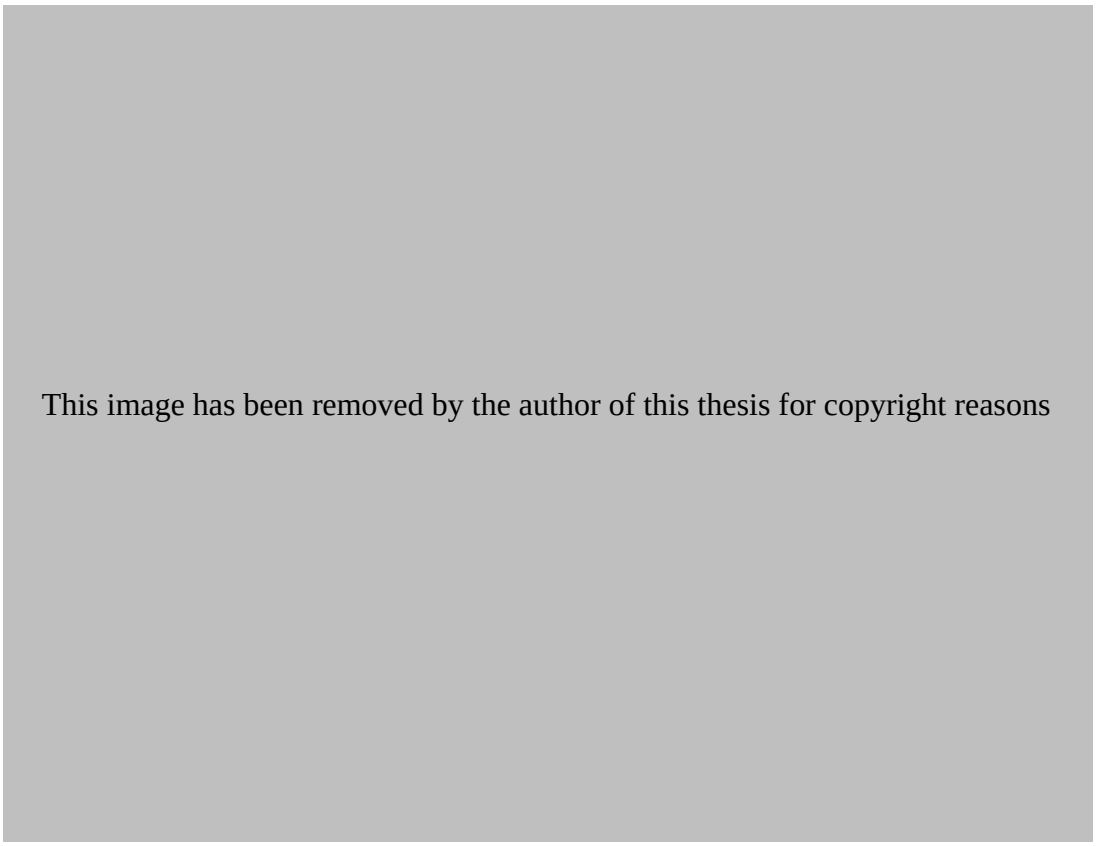

Figure 2.2 The mesengenic process
Adopted from Firth et al. [37] with permission

2.2 Composition and material properties of bone

As a material, bone can be viewed at different scales. At macroscopic scale, bone is either compact (low porosity) or spongy (high porosity); at microstructural scale, it is either lamellar (well organised) or woven (randomly organised); and at nanoscale, bone is a composite material composed of collagens, minerals (mainly hydroxyapatite), water and

non-collagenous proteins [32]. The material properties of bone are often related to its macroscopic composition [26, 38].

Both compact (cortical) and spongy (trabecular or cancellous) bones are porous, non-homogenous and anisotropic materials. At macroscopic level, these two types are mainly characterised by their porosity and apparent density. Porosity of compact bone is generally very low and ranges between 0.05 – 0.10; whereas, the same of spongy bone is generally very high and ranges between 0.50 – 0.95 [26]. Apparent density is defined as mass divided by the total volume including the pores, and thus, varies with porosity [27]. Many studies have related mechanical properties of bone to its apparent density. For example, Carter and Hayes [39] and Lotz, et al. [40] related the elastic modulus and compressive strength of cortical and trabecular bones to their apparent densities. Some other studies [41-43] have shown that the mechanical properties of bone depends also on mineral content in addition to the apparent density.

Overall, adult human skeleton is composed of approximately 80 % cortical bone and 20 % trabecular bone. However, this ratio is not the same throughout the skeleton. For example, the ratio of cortical to trabecular bone is about 25:75 in vertebra, 50:50 in femoral head and 95:5 in radial diaphysis [30]. Therefore, the mechanical properties of the bone could very well vary from one to another or even within different regions of the same bone. In bones, the combination of both cortical and trabecular bone forms a sandwich-like structural arrangement which is attributed to its optimal engineering properties [26].

Structural and hence mechanical heterogeneity of bone arises from its material composition, pores and interfaces (e.g. solid-solid, solid-fluid etc.). Living bones are multiphasic and composed mixture of soft and hard tissues, fluid and solutes. The inorganic constituents of bone are responsible for its strength and stiffness in compression while the organic constituents are responsible for the same in tension [26]. The anisotropy of bone, which arises from its microstructural arrangement, is responsible for its direction dependent mechanical properties. In cortical bones, lamellar and osteonal directions govern its anisotropy; whereas, it is governed by trabecular orientation in trabecular bones [26].

In engineering perspective, living bone is one of most complex materials as its composition and material properties are highly variable. It is a hierarchically arranged, porous, multiphasic, dynamic, heterogeneous and anisotropic material, the composition and properties of which are subjected to interspecific, intraspecific, temporal and spatial variations. However, bone is highly desirable as a material because it is extremely tough, lightweight, adaptive, multifunctional and possesses the capacity to resist fracture in a variety of different loading conditions [44]. Yet, musculoskeletal injuries are very common and responsible for significant global health burden. In particular, long bone fractures is one of the frequent non-fatal injuries reported worldwide [1].

2.3 Bone fractures

In simple, bone fractures occur when the stresses in bone exceed its strength. There are two ways by which this could happen: (i) stress exceeding its strength under extreme loading levels or (ii) strength falling below the stress under normal physiological loading levels. The former is generally spontaneous and traumatic (as in the case of fall) or non-traumatic (as in the case of sudden internal muscle contractions), which could result in bone stresses exceeding its strength [26]. The latter is generally chronic and results from creep or fatigue. When bones are subjected to prolonged and repetitive loading conditions, micro-damages can occur. Generally, bones can repair the micro-damages by remodelling; however, there is a limit to this potential. If the rate of microdamage exceeds the rate of repair, bone would start to lose its stiffness and strength until it fractures [26]. Therefore, the second case can result in bone fractures occurring even at normal or subnormal levels of loading. Athletes, soldiers and dancers who undergo high levels of repetitive physical activities are prone to this type of fracture. In addition, weakening of bone due to biological conditions such as osteoporosis or bone tumours could also lead to fractures at lower activity levels.

The type and nature of bone fracture could differ from one to another. Therefore, number of different bone fracture classification systems have been put forward for naming and describing the fractures, grouping and ordering them, predicting the outcomes and guiding actions [45]. These systems can be mainly categorised into: (i) fracture specific systems; (ii) patient specific systems; (iii) generic / universal systems; and (iv) soft tissue injury related systems. Fracture specific classifications describe fractures of specific

skeletal locations; whereas, patient specific classifications are for specific type of patients such as children. Generic or universal classifications describe fractures of any kind anywhere in the skeleton. Unlike these three types, soft tissue injury related classifications do not deal with the fracture, but the level of soft tissue injury associated with it [45].

Classifying fractures enables the use of same language amongst surgeons and to make comparison of subjects easier. Moreover, description of the morphological features associated with fractures could help deciding the course of treatment and predict the outcome [46]. In the realm of long bones, 'Arbeitsgemeinschaft für Osteosynthesefragen (AO)' system is one such fracture classification systems, which was developed with the objective of assisting surgeons in treatment planning. This is in fact the only generic type classification system in use today [45].

AO classification uses a descriptive five-digit alphanumeric coding system, which is based on the bone and the specific segment under consideration, fracture type, its group and subgroup. There are 27 possible classifications at the sub group level for any bone segment, which leads to very accurate classification and hence, better understanding of the morphology of fracture [45]. Such an understanding is essential for predicting healing outcome and planning treatments; because, morphological features play a very dominant role in fracture healing [8]. Unfortunately, none of the classification system, including the AO system can reliably predict the outcome of the most common types of fractures [45]. This owes to the fact that fracture healing is a highly complex process, which is under the influence of multitude of biochemical and mechanical factors [8]. Therefore, accurate classification of fractures could only supplement deep understanding of the fracture healing process in predicting the outcomes and planning treatments.

2.4 Bone fracture healing

Bone fracture healing is a very complex biological process which involves many cellular, molecular and tissue level events in an orchestrated manner [47, 48]. Although fracture healing has been studied for decades, there is still plenty to be learned to fully comprehend this process [49]. Nevertheless, the current state of knowledge provides thorough overall understanding and deep insights into many aspects of fracture healing.

Bone fractures heal either by primary or secondary healing pathways. The former which is also called direct healing, involves direct attempt of cortex to re-establish anatomical lamellar bone and Harversian system [49, 50]. Secondary healing is also known as indirect healing and involves formation of fracture callus which serves as a temporary scaffold during the initial phases of healing and later transforms into bone as healing progresses [50]. The two healing pathways differ from each other based on the histological events that take place during the healing process [50]. To understand these different pathways of healing better, it is essential to understand the histological events that take place in each of these healing pathways.

2.4.1 Primary or direct healing

Primary or direct healing takes place when there is correct anatomic reduction of the fracture fragments and stable fixations. Often these conditions are achieved by open reductions and rigid internal fixations. In this healing pathway, cortical bone tends to re-establish lamellar bone structure by direct remodelling without any intermediate stages such as periosteal response or callus formation. Harversian canals and blood vessels are directly established in primary healing [49, 50]. There are two different types of primary healing as described below.

2.4.2 Contact healing

This type of primary healing occurs when the fracture gap is very small (< 0.01 mm) and the fracture site is stable [49]. Generally, stability of fracture site is given either by 'Interfragmentary movement (IFM)' of 'Interfragmentary strain (IFS)'. The former refers to the relative movement between the fracture fragments and the latter refers to the ratio between IFM and initial fracture gap [19]. For contact healing to occur, it is suggested that IFS should be less than 2 % [49]. When the fracture environment is favourable for contact healing, cutting cones are formed at the osteons closest to the fracture site. The tips of the cone which consists of osteoclasts crosses the fracture line and creates longitudinal cavities which is soon filled by newly forming bone by osteoblasts residing at the rear of the cutting cone [49]. In this way mechanical continuity is re-established in contact healing by simultaneous bony bridging and haversian system formation in the axial direction. The newly formed osteons are later remodelled into lamellar bone.

2.4.3 Gap healing

Gap healing occurs under stable microenvironments when the fracture gap is less than 1 mm [49]. In this type of primary healing, bone formation first occurs perpendicular to the longitudinal direction to minimize the gap. Once the gap size reduces sufficiently, bone bridging occurs similar to that in contact healing [47, 49]. Therefore, Harversian remodelling does not occur simultaneously with bone bridging in gap healing which is the main difference between the two types of primary healing [49].

Although, achieving primary healing is the objective of most open reductions and internal fixation surgeries, it is not the common type of fracture healing [49]. This is mainly because perfect anatomical reduction and absolute stability does not naturally occur in most fractures. Even carefully reduced fractures stabilized with rigid internal fixations could experience micromotions depending on the nature of fracture, level of weight bearing and rigidity of fixation. Therefore, most fractures tend to heal by secondary healing.

2.4.4 Secondary or indirect healing

Secondary or indirect fracture healing recapitulates many aspects of embryonic skeletal development [51, 52]. In this fracture healing pathway, bridging of bone fragments occur via formation of fracture callus, which acts as a biological splint. Contrary to primary healing, secondary healing does not require anatomic reduction or rigid fixations. As fracture callus is a result of IFM [53], rigid fixations that restrict IFMs tend to inhibit the formation of callus and compromise healing. Relatively flexible fixations causing moderate IFMs tend to promote formation of callus; however, too much IFM can result in delayed union or non-unions. Secondary healing involves the following three distinct but partially overlapping phases: inflammation, repair and remodelling.

Inflammatory phase

Soon after bone fracture, bleeding due to rupture of blood vessels within bone and surrounding soft tissues leads to formation of haematoma within the fracture site. This initiates the inflammatory response. Blood clotting prevents further bleeding and blood-derived inflammatory cells and pro-inflammatory cells present in haematoma initiates inflammation. The inflammatory response peaks 24 h post injury and gets completed by

the first week. Additional inflammatory cells actively invade haematoma during this phase and the inflammatory signals give rise to macrophages [54]. Macrophages in turn release signalling molecules that are essential for the healing cascade such as cytokines and growth factors within haematoma [54]. Disruption of blood supply leads to bone necrosis to variable distances from the broken bone ends depending on the nature of fracture. Furthermore, hypoxic conditions due to interrupted blood supply induce release of angiogenic factors. As a result, endothelial cells invade into haematoma from pre-existing vessels to form new blood vessels [47]. Blood vessels, along with blood, supply osteoprogenitor cells to the fracture site. Subsequently, fibroblasts appear within the fracture site to replace haematoma with granulation tissue which forms the early callus [47]. Early callus filled with fibrous granulation tissue provides a suitable environment for cell migration, proliferation, differentiation and tissue synthesis to facilitate the fracture repair process.

Reparative phase

Reparative process begins with the formation of callus while the inflammatory response is still on [47]. Periosteal response plays a vital role in the reparative phase and stripping of periosteum has been reported to inhibit callus formation [47]. Undifferentiated MSCs present in the periosteum migrates into the callus, proliferate and differentiate into different tissue forming cells depending on the local microenvironment [55]. Adjacent to periosteum far from the fracture gap where the blood vessels are undisturbed and the tissue strains are low, MSCs differentiate directly into osteoblasts to synthesis woven bone tissue, which is known as ‘intramembranous ossification’ [47]. With bone forming along periosteum, the regions swells and forms the initial hard callus [56]. The bone forming front gradually moves from periosteum towards the fracture gap as healing progresses [57]. Periosteal callus which is also referred to as ‘external’ or ‘peripheral’ callus is an indicator of progression of healing. Since bone marrow is also a source of both MSCs and blood supply, bone formation occurs within the endosteal callus (medullar region) as well parallel to periosteal bone formation. Thus, fracture repair occurs partially by intramembranous ossification within these regions of the callus.

However, the key to successful fracture repair in secondary healing is via formation of soft cartilaginous callus, which hardens later and subsequently undergoes mineralization

and resorption to eventually get replaced by woven bone [49]. This process is known as 'endochondral ossification' which recapitulates some aspects of embryonic skeletal development [49]. In the early stages of healing, the callus regions away from undisturbed periosteum that are closer to the fracture line gets deprived of blood supply [47]. Avascular conditions impair differentiation MSCs into osteoblasts; but, give rise to MSC differentiation into chondrocytes as they are well suited for avascular and hypoxic conditions [47]. On the other hand, fracture gap and adjacent callus regions would predominantly consist of fibrous connective tissue due relatively high tissue strains [47]. Under relatively high strains MSCs tend to differentiate into fibroblasts and form fibrous connective tissue [47, 58]. However, the newly formed chondrocytes proliferate and synthesize cartilage tissue to form soft callus. Soft callus provides stability to the fracture site and minimizes strains within the fracture gap under loading [59].

With time chondrocytes undergo hypertrophy, release calcium and die off (i.e. apoptosis). Hypertrophic chondrocytes secrete growth factors that attract osteoclasts which degrades calcified cartilage [59]. As the cartilaginous callus regions bridge, IFMs and tissue strains within the fracture gap reduces significantly and allows blood vessels to invade the degrading calcified callus. Blood vessels bring in monocytes and MSCs that differentiate into osteoclast-like cells and osteoblasts, respectively. The former actively involves in resorption of calcified callus while the latter synthesises new bone to fill in the resorbed regions [47]. After bony bridging, IFMs and tissue strains within the fracture gap reduces further to allow intramembranous ossification to occur. Subsequently, fibrous connective tissue is replaced fully with woven bone tissue.

Remodelling phase

Although formation of woven bone during the reparative phase stabilizes the fracture site and allows load bearing, it does not restore the pre-fracture morphology or properties of bone [49]. Therefore, secondary healing involves a remodelling phase in which hard callus made of woven bone is gradually replaced with lamellar bone. Osteoclastic resorption occurs in the periosteal callus once the fracture gap is filled with woven bone. Within the cortical zone, woven bone is remodelled by osteon formation similar to primary healing. During this phase medullary cavity is re-established by resorption of

endosteal callus [47]. Thus, the fractured bone restores its morphology and properties during this phase which can last for prolonged periods. In general, it is approximated that the inflammatory, reparative and remodelling phases can take around 10 %, 40 % and 70 % of the total healing times respectively with overlaps as shown in Figure 2.3.

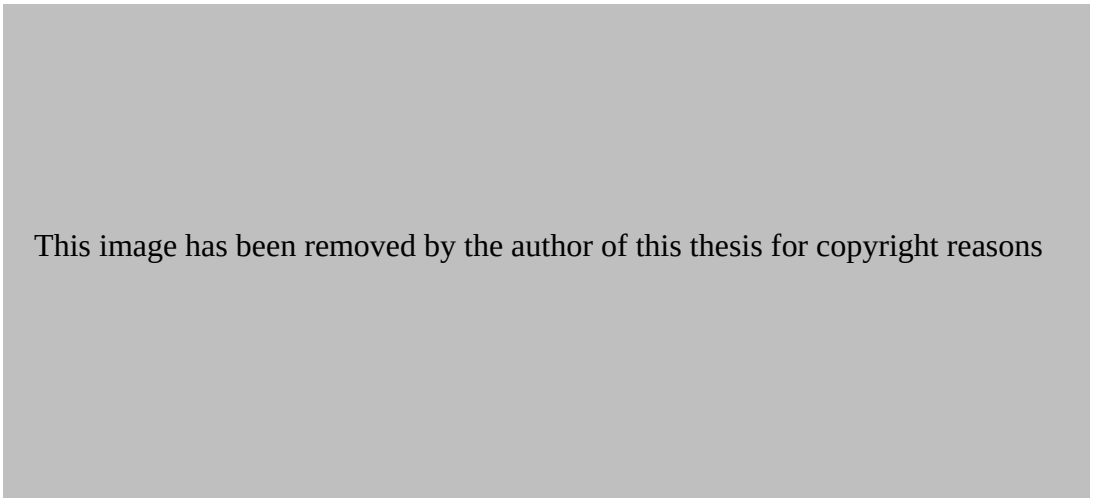

Figure 2.3 Approximate relative times for different phases of secondary healing expressed as percent of total healing time and the time dependent intensities of response
Based on Richard et al. [60]

2.4.5 Fracture union, delayed union and non-union

Different bones take different times to heal following fracture. Moreover, any two fractures on the same type of bone could take different healing times depending on other factors that influence healing. Therefore, universal definition of healing time is impossible. In clinical point of view, a fracture is deemed to have healed if clinical union of bone fragments is detected [5]. Clinical union refers to the point when bone reaches sufficient strength beyond which no further treatment is generally necessary. For fractures treated with external bone fixation devices, clinical union marks the time for removal of fixators [61]. It should be kept in mind that clinical union does not refer to an end point of healing but some point during the reparative phase when bone reaches sufficient strength to take physiological loads [60]. Generally, whether a fracture has achieved clinical union or not is judged both by clinical and radiographic assessments [62]. Clinical criteria used to define clinical union includes : no pain / tenderness when bearing weight,

ability to bear weight, no motion at fracture site on examination etc. [63] On the other hand, radiographic criteria for defining clinical union includes : bridging of fracture, obliteration of fracture line, absence of hardware loosening etc. [63] Out of these different criteria, no pain when weight bearing and bridging of fracture are the most commonly used clinical and radiographic criterions, respectively, for defining clinical union [63]. Judging clinical union purely based on clinical criteria is rare and surgeons most frequently use radiographic methods in the recent times [63].

Bony bridging of peripheral callus, which is an indicator of successful healing occurs in humans typically between 8 – 16 weeks post fracture [47]. However, this depends on numerous subject specific factors that influence fracture healing [47]. However, in certain cases healing takes longer than usual which could be indicative of impaired healing. Unlike in other tissues, most bone fractures can heal without scars and restore most or all its pre-fracture properties. Once fully healed, newly formed bone becomes indistinguishable from the old bone [56]. However their intrinsic healing capacity may not always be enough, and some external intervention may be required in some cases [7]. Generally, 90-95 % of the fractures heal without problems [64]. But there is a small proportion of fractures in which the bone repair process is impaired. This leads to undesirable conditions such as delayed union or non-union.

When healing takes longer than acceptable time frames it is referred to as delayed healing. Acceptable time frame is subjective and depends on many patient specific factors [65]. In delayed healing, it is expected that fracture should eventually heal without additional interventions. Non-union on the other hand is a condition where there is no possibility of healing without further intervention. However, judgement of the possibility of healing without further intervention is up to the physician treating the fracture. It is suggested that a fracture that is at least 9 months old could be a non-union if either many different therapeutic measures have been tried already [66] or no signs of healing is seen for 3 consecutive months [64]. When a fracture results in non-union or delayed union, patients may experience prolonged functional disability and pain. Furthermore, these conditions can financially affect patients due to their inability to return to work for longer periods and additional treatment costs. Therefore, it essential that undesirable healing conditions such as delayed union or non-union are eliminated.

Delayed unions and non-unions result from poor healing conditions arising from one or more of the factors that influence fracture healing being unfavourable. Lack of blood supply or mechanical stability are some of the main reasons that cause unfavourable healing environments [49]. However, there are number of other factors that can affect the healing environment unfavourably and result in delayed union or non-union. Therefore, it is crucial to understand these factors to ensure satisfactory healing outcomes.

2.4.6 Factors controlling fracture healing

In the cascade of fracture healing, both biological and mechanical factors play influential roles in controlling the progression of healing. They interact with each other and result in complex fracture healing pathways [53]. A diamond concept for fracture healing was proposed to describe the complex interaction of the following four key factors that affect fracture healing : Osteogenic cells, osteoinductive mediators, osteoconductive matrix and mechanical environment [53, 67].

Osteogenic cells

Availability of a vibrant cell population is a fundamental requirement for unimpaired fracture healing. Early granulation tissue, cartilaginous tissue and bone tissue are formed as a result of cellular activities. MSCs migrating into the fracture site differentiate into tissue forming cells such as fibroblasts, chondrocytes and osteoblasts to synthesise tissues. Evidence suggests that periosteum is the greatest source of MSCs during fracture healing [55]. In addition, MSCs migrate into the fracture callus from bone marrow and surrounding soft tissues as well [68]. Osteoblasts and committed pre-osteoblasts residing in cortical bone migrate into fracture callus and contribute to intramembranous ossification [59, 68, 69]. Fibroblasts present in bone marrow [70] and surrounding soft tissues [71] could also migrate into fracture callus and take part in connective tissue formation [59]. Chondrocytes on the other hand are believed to form within callus via cell differentiation processes [55, 59].

In addition to the tissue forming cells, osteoclasts and endothelial cells are also activated during fracture healing to play their respective roles. Osteoclasts are derived from hematopoietic macrophage or monocyte lineage precursors [72]. Bone marrow is one of the origins of hematopoietic precursors [73]. Osteoclasts along with fibroblasts initiates

the conversion of haematoma into granulation tissue in the very early stages of healing. Later, osteoclasts take part in degradation of calcified cartilage and resorption of woven bone in the reparative and remodelling phases, respectively [59, 72]. Endothelial cells that are responsible for angiogenesis originate mainly from cortical bone and bone marrow from very early stages of healing to drive intramembranous and endochondral ossifications [74].

Osteoinductive mediators

The differentiation of MSCs and subsequent synthesis of tissues is governed by several osteoinductive mediators (i.e. growth factors) present within the fracture site. It is known that signalling molecules such as interleukins (IL), tumour necrosis factor – α (TNF- α), fibroblast growth factor (FGF), insulin-like growth factor (IGF), platelet-derived growth factor (PDGF), vascular endothelial growth factor (VEGF) and transforming growth factor β (TGF- β) are expressed at different timepoints within the fracture site to regulate different activities of the healing cascade [53]. These factors are secreted by MSCs, osteoblasts, chondrocytes, osteoclasts, monocytes, macrophages, endothelial cells and platelets. The sources and functions of some of the important growth factors are briefly summarized below:

- Interleukin – 1 (IL-1) : IL-1 is produced by macrophages mainly during the inflammatory and remodelling phases. The functions of IL-1 include increasing fibroblastic collagens, collagen cross-linking, stimulating angiogenesis and selectively degrading callus tissue [48, 75].
- Interleukin – 6 (IL-6) : IL-6 is produced by osteoblasts mainly during the inflammatory and remodelling phases. The main function of IL-6 is stimulating bone resorption [48, 75].
- Tumour necrosis factor – α (TNF- α) : TNF- α is produced by macrophages, lymphocytes and monocytes mainly during the inflammatory phase and by the end of endochondral ossification. The main functions of TNF- α include stimulating osteoclast function, recruiting MSCs and inducing apoptosis of hypertrophic chondrocytes [48].
- Fibroblast growth factor -I (FGF-I) : FGF-I is produced by macrophages, osteoblasts and immature chondrocytes at different time points of healing. The

main functions of FGF-1 include promoting blood vessel formation and stimulating collagenase [75].

- Fibroblast growth factor - II (FGF-II) : FGF-II is produced by macrophages, osteoblasts, chondrocytes and hypertrophic chondrocytes at different time points of healing. The main functions of FGF-II include promoting blood vessel formation, stimulating collagenase and acting as chemoattractant and mitogen for chondrocytes [75].
- Insulin-like growth factor – I (IGF-I) : IGF-I is produced by osteoblasts during intramembranous ossification and pre-hypertrophic chondrocytes. The main functions of IGF-I include increasing collagen synthesis, stimulating pre-osteoblastic cells and increasing osteoclast precursors [75].
- Insulin-like growth factor – II (IGF-II) : IGF-II is produced by proliferating chondrocytes and osteoclasts mainly during bone resorption . The main functions of IGF-II include increasing collagen synthesis, increasing osteoblast precursor cell proliferation during resorption, promoting cartilage synthesis and modulating osteoclast function [75].
- Platelet-derived growth factor (PDGF) : PDGF is produced by platelets, monocytes, activated tissue macrophages and endothelial cells constantly post-inflammation. The main functions of PDGF include stimulating MSC proliferation, helping cartilage and bone formation, acting as mitogen for connective tissue cells and promoting resorption [75].
- Vascular endothelial growth factor (VEGF) : VEGF is produced by endothelial cells, macrophages, fibroblasts, smooth muscle cells, osteoblasts and hypertrophic chondrocytes at different time points of healing. The main functions of VEGF include controlling angiogenesis, inducing proliferation and differentiation of osteoblast precursor cells and promoting MSC chemotaxis [76].
- Transforming growth factor β (TGF- β) : TGF- β is produced by platelets, monocytes, macrophages, osteoblasts, osteoclasts, MSCs, endothelial cells and chondrocytes mainly during intramembranous ossification, chondrogenesis and endochondral ossification. The main functions of TGF- β include acting as chemoattractant for macrophages, promoting angiogenesis, inducing MSC

differentiation into chondrocytes and osteoblasts, and promoting cartilage calcification [75].

Thus, the interplay between different cells and growth factors is a key aspect of fracture healing. So far, various cell and growth factor therapies have been developed to biologically enhance fracture healing potential. For example, genetically engineered MSCs, differentiated osteoblasts and TGF-β superfamily members such as bone morphogenetic proteins (BMP) are being used clinically to treat delayed unions and non-unions [53].

Osteoconductive matrix

The next important factor controlling fracture healing is osteoconductive matrix, which refers to the extracellular matrix (ECM) that provides the environment for the cellular processes and their interactions with other factors to take place. ECM is a dynamic meshwork of self-assembled macromolecules composed of collagens, proteoglycans / glycosaminoglycans, elastin, fibronectin, laminins and several other glycoproteins [77, 78]. When natural scaffold provided by ECM is inadequate, external intervention is necessary [67]. Current clinical strategies include the use of natural and engineered grafts as filler materials to provide scaffold to the fracture site. Sometimes such materials are enriched with osteogenic or osteoconductive factors to maximize the healing potential [53].

Mechanical Environment

Another important factor that controls fracture healing is mechanical environment [53]. Mechanical stability controls the mechanical environment of the fracture site which has a direct influence on cellular activities. Cells are sensitive to biophysical stimuli; therefore, mechanical environment could be used to stimulate cells in specific pathways [58]. Fracture sites require mechanical environment to be favourable throughout the course of healing starting from early callus formation to remodelling. The objectives of most fracture treatments whether it is a simple application of plaster cast or open surgical reduction with internal fixations is to ensure that the fracture site is adequately stable and thereby enhance healing [53].

Mechanical environment at the fracture site depends on number of factors such as fracture geometry, fixation rigidity and mechanical forces [19, 79, 80]. Experimental evidence shows that unfavourable mechanical environments arising from large gap sizes, loose fixations and excessive IFSs (due to physiological loading) increase the risks of delayed unions and non-unions [8, 19]. Conversely, small gap sizes and moderate fixation stiffness and loading were shown to be beneficial for healing as these conditions can promote osteogenic and chondrogenic pathways [8]. However too rigid fixations or too little IFS (due to little or no loading) could also affect callus formation and bone quality [8, 81, 82]. Therefore, care and caution are essential during reduction of fractures, application of fixation and design of post-operative physiological exercises for successful fracture treatment.

Vascularity

The original diamond concept was later extended to incorporate vascularity and the host factors [67, 83] due to their importance. Vascularity is one of the most influential factors that affect healing. It has been shown that adequate blood supply is a prerequisite for osteogenesis; whereas, avascular environments are conductive to chondrogenesis. VEGF plays an important role in regulating angiogenesis (i.e. formation of new blood vessels) and production of VEGF is suggested to be the main coupling mechanism between angiogenesis and osteogenesis [84]. During endochondral ossification, angiogenesis plays an important role in transforming cartilaginous tissue into woven bone. VEGF is produced by both osteoblasts and hypertrophic chondrocytes and known to attract endothelial cells which are responsible for vasculature development [59]. Mechanical stability is an essential requirement for vasculature development because high tissue strains at the fracture site can rupture blood vessels and inhibit angiogenesis.

Host factors

In addition to the aforementioned factors, fracture healing can be influenced by pre-existing co-morbidities such as diabetes or osteoporosis. These subject specific biologic conditions are referred to as host factors and need to be taken care of when treating fractures [67]. Healing under such biological conditions would be different from normal fracture healing. For example, it has been reported that osteoblasts from osteoporosis patients did not exhibit same level of proliferation or TGF-β release as observed in healthy

donors [8]. Studies have also reported that genetic variations can positively or negatively impact healing [83]. Fracture healing time and rate of strength / stiffness gain could be influenced by subject specific genetic conditions. Therefore, all these factors have their roles in influencing fracture healing. Thus, fundamental understanding of their interplay is essential for successful treatment. Figure 2.4 depicts the diamond model of bone fracture healing interaction. This has gained wide acceptance as a conceptual model for identifying what is essential for successful healing and to manage unfavourable conditions such as delayed union and non-unions [67].

It is essential that any enhancement done based on the diamond concept be contained locally within the target site for the maximum effect. The need for containment has led to the incorporation of the concept of 'biological chamber' in the diamond concept. The concept suggests that a bio-reactor would be developed locally to confine the treatment to a non-union site via modifications to soft tissue or biological membranes [67].

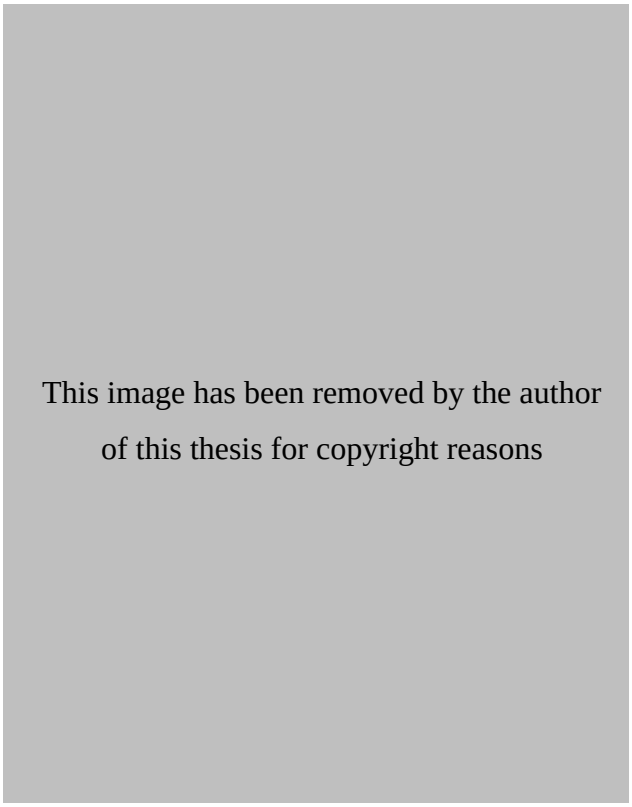

Figure 2.4 The diamond model of bone fracture healing interactions
Adopted from Andrzejowsk and Giannoudis with permission [67]

Timing

Successful treatment of fractures not only requires manipulation of any one or more of the aforementioned factors favourably but also the right time to do it. Many studies on different treatment strategies have demonstrated the criticality of timing in fracture treatments. Animal experiments and clinical studies on fractures/osteotomies treated with external bone fixators have demonstrated the beneficial and adverse effects of early and late weight bearing, respectively on fracture healing [85, 86]. Studies investigating the effects of different cell or osteoinductive mediator administrations on animal fracture healing have shown that timing of delivery is a pivotal factor in deciding the outcome of administration [87, 88]. Similarly, timing is crucial for the placement of bone grafts and 'dynamization' of bone fixation devices [89-91]. Therefore, for a treatment to be effective, it is important to determine the most suitable timings for the chosen treatment strategy.

Notably, the early stage of fracture healing is of prime importance as it is very sensitive to external factors and decisive of the differentiation pathways of MSCs (i.e., chondrogenic, osteogenic, etc.). Therefore, actions taken during the early stages are crucial as they could influence the whole healing process [16, 17]. Healing time and bone quality could be significantly changed as a result of initial conditions [19].

In the myriad of factors that affect fracture healing and their complex interplays, obtaining a comprehensive understanding of the roles of individual factors on healing process is very challenging. Nevertheless, the advancements in the fields of biomedicine, tissue engineering and computational biology in the past few decades have unravelled many unknowns of fracture healing biology and continue to provide new insights.

2.5 Types of studies on bone fracture healing

In studies on fracture healing, data can be obtained from different observational levels. Generally, there are three main observational levels : cellular level, tissue level and clinical level [81]. Data obtained at each level is essential for comprehensive understanding of the process and subsequent clinical applications. Studies on fracture healing could generally take either clinical or experimental or computational approach. Each of these approaches have its own advantages and limitations.

2.5.1 Clinical studies

Clinical studies report findings obtained under realistic conditions and therefore have direct clinical relevance. However, standardization of clinical data across multiple studies or sometimes even within the same study could be difficult due to the high levels of inter subject variabilities present in clinical trials [92]. Therefore, it is not always possible to draw clear conclusions from clinical studies. Nevertheless, they are indispensable in field of biomedicine to assess clinical significance of any new treatment strategy.

2.5.2 Experimental studies

Experimental studies on fracture healing could be of different types such as *in-vivo*, *ex-vivo* or *in-vitro* and are usually designed to mimic realistic conditions under controlled environments to obtain useful data for comparative analysis. In most experimental studies, animal models are used as alternatives to human models due to ethical issues associated with using human models in research. Although the use of animal models poses limitations in directly translating findings to clinical applications, animal experiment is still one of the best options available to gain fundamental understanding of any biological process. Generally, animal models are used in research studies based on the "August Krogh Principle" which states that "*for a large number of problems there will be some animal of choice, or a few such animals, on which it can be most conveniently studied* " [93]. Therefore, researchers are left with the decision of choosing the right animal model that best fits the purpose of study [93].

Experiments may require state of the art equipment, well controlled environments and careful planning [94]. Sometimes, due to the inherent complexity of fracture healing process, experimentation could be either too expensive, time consuming or impractical [18]. Furthermore, inter-subject variabilities arising from host factors such as comorbidities or other factors cannot be fully eliminated in experiments [94].

2.5.3 Computational studies

Computational models in fracture healing studies have been used to overcome the limitations associated with experimental and clinical approaches [94]. Owing to the ability of computers in handling multiple inputs and processes, computer models provide an excellent framework to study the complex fracture healing process systematically and

effectively. With computational power growing exponentially, simulation of very complex processes is becoming increasingly affordable in terms of time and money [95]. Moreover, computational models offer perfect repeatability and eliminate the issues due to inter-subject differences which are generally inevitable in experimental and clinical approaches.

Nevertheless, experimental and clinical evidence are essential elements of any biomedical research. Therefore, the purpose of computer models in fracture healing studies is to be used as reliable tools in simulating healing process under specific conditions [96]. The main advantage of such models is that they could be used to test new hypotheses prior to experiments which can help in deciding whether an experimental study is worth the time and resources in the first place [96]. It also helps to identify any unforeseen aspects of experiments beforehand and make changes accordingly. This enables experiments to be conducted efficiently. Computational models could even prompt development of new hypotheses. Thus, computational models augment clinical and experimental studies to elucidate our understanding on the complex fracture healing process [97]. However careful consideration of the modelling assumptions and/or simplifications and their effects on model predictions is crucial with computational studies. In addition, validity of the model should be ensured by comparing model predictions with clinical and experimental data.

2.6 Computer methods in bone fracture healing

It is known that fracture healing is controlled by a variety of biological and mechanical factors. However, most fracture healing models in literature describe healing process using specific biological or mechanical variables. Based on the nature of these variables, computational models of bone fracture healing can be classified into either mechano-regulatory models or bio-regulatory models or mechano-bio-regulatory models [98].

2.6.1 Mechano-regulatory Models

Mechano-regulatory models assume that fracture healing is regulated by mechanical factors and do not directly consider the effects of bio-chemical factors such as growth factors. Many mechano-regulatory models have been proposed so far [57, 99, 100]. Perren [10], described tissue differentiation in fracture healing using the level of tissue

elongation within the callus. Elongations below 2 % were suggested to result in bone formation and those between 2 – 10 %, 10 -15 % and 15-100 % were suggested to form cartilage, fibrous and granulation tissues, respectively.

Claes and Heigele [57] used principal strain and hydrostatic pressure within the callus to describe tissue differentiation. Based on animal experiments, they defined threshold values for different types of tissue differentiation. It was suggested that local strains less than 5 % and hydrostatic pressure between -0.15 - 0.15 MPa were conductive to bone formation; principal strains less than 15 % and compressive hydrostatic pressures less than -0.15 MPa were conductive to cartilage formation and all other combinations of the two variables would result in connective and fibrocartilaginous tissues [57].

Prendergast et al. [58, 100] described fracture healing based on stimulation index "S" defined as $S = \gamma / a + v / b$, where, γ is the octahedral shear strain of solid phase, v is the interstitial fluid flow, a = 0.0375, and b = 3 $\mu m\ s^{-1}$. As per this model, S values less than 1 would lead to bone formation; S values between 1 and 3 would lead to cartilage formation; and S values above 3 would lead to fibrous tissue formation.

Pauwels [101] and Carter et al. [102] proposed similar mechano-regulation models to describe fracture healing using two mechanical variables. The model of Pauwels [101] was based on volumetric and deviatoric deformations; whereas, principal tensile strain and hydrostatic pressure were used in the model of Carter et al. [102]. However, these models did not specify quantitative threshold values for tissue differentiation.

Isaksson et al. [103] tested the possibility of describing fracture healing using either (i) deviatoric strain or (ii) fluid pressure or (iii) fluid velocity and concluded that deviatoric strain alone could be used to describe fracture healing satisfactorily. In a different study, Isaksson et al. [99] simulated a well-controlled sheep tibial fracture healing experiment using different mechano-regulatory models. The study compared the predicted tissue differentiation patterns with those observed histologically at different time points. The results showed that the model proposed by Prendergast et al. [58, 100] is more accurate and versatile than the alternatives.

The original model of Prendergast et al. [58, 100] was extended by Lacroix et al. [104] to incorporate distribution of MSCs within the callus. Later, the model was further extended

by Lacroix and Prendergast [105] to incorporate bone resorption process and used to investigate the effects of loading and gap size on fracture healing. The model [105] was able to predict formation and removal of different tissues within the callus and reduction of interfragmentary strains (IFS) with time, very similar to those observed in sheep experiments. In another study, Steiner et al. [106] showed that the model of Claes and Heigele [57] is also versatile and capable of simulating fracture healing process accurately, after sufficient calibration of the uncertain input parameters in the model. They showed this by comparing the calibrated model results with multiple in-vivo sheep experiment results. Similarly, numerous improvements have been made to many of the original models in the past such as incorporating angiogenesis, oxygen supply etc. [106-109]. These studies demonstrate that mechano-regulatory models can successfully simulate many of the key aspects of fracture healing such as spatial tissue distribution patterns, stiffening of callus with time and the effects of fracture geometry and loading on fracture healing.

2.6.2 Bio-regulatory Models

Bio-regulatory models on the other hand, describes fracture healing in terms of bio-chemical factors such as growth factors. Bailon-Plaza and Van Der Meulen [110] first proposed a bone fracture healing model taking into account the roles of Osteogeneic Growth Factor (OGF) and Chondrogenic Growth Factor (CGF) on tissue differentiation during fracture healing. In their study, the following seven variables were used to describe fracture healing: MSC, osteoblasts, chondrocytes, bone tissue, connective/cartilage tissue, OGF and CGF.

Based on their study [110], Geris et al. [59] developed a bioregulatory model to investigate the roles of VEGF and angiogenesis on fracture healing. Geris et al.[59] added separate variables for fibroblasts, endothelial cells, fibrous tissue, vasculature and VEGF. Thus, fracture healing process was described using twelve interdependent variables. Using their model, Geris et al. [59] predicted the tissue patterns within the endosteal, cortical and periosteal regions of the callus after 1,3 and 5 weeks post-fracture and compared the same with those observed in a rat experiment. The results indicated that the model successfully predicted many key aspects of fracture healing such as intramembranous ossification, endochondral ossification, cell migration, angiogenesis

and the effects of impaired angiogenesis on healing. Since then, the model was improved by Geris et al. number of times [74, 111] and some of the recent improvements include the incorporation oxygen as a critical determinant of fracture healing [112].

Bio-regulatory models provide key insights into the fundamental bio-chemical processes involved in fracture healing. However, they totally neglect the role of mechanical factors on fracture healing. Therefore, these models are suitable to study the cause-effect relationships of biochemical variables during fracture healing.

2.6.3 Mechano-bio-regulatory Models

There are bone healing models that incorporate both mechano-regulation and bioregulation, hence, called mechano-bio-regulatory models. Bailon-Plaza and Van Der Meulen [113] improved their original model [110] to include the effects of mechanical forces on bone healing. Their model assumed deviatoric strain to stimulate bone formation and dilatational strains to inhibit it. The model [113] predicted positive effects due to moderate loading and negative effects due to excessive loading on fracture healing. The study also demonstrated the negative effects of delaying mechanical stimulation in rigidly fixed fractures.

Later, Geris et al. [114], based on the work of Bailon-Plaza and Van Der Meulen [113], incorporated mechano-regulation into their original bio-regulatory model [59]. Their model [114] considered the effects of mechanical factors on both angiogenesis and osteogenesis and demonstrated its capability to simulate fracture healing similar to those observed in many experimental studies. The model [114] provided an excellent framework to study the interrelationships between mechanics, angiogenesis and osteogenesis in fracture healing.

Thus, number of studies in literature so far have already demonstrated the potential of computer models in simulating fracture healing reliably. This prompted many researchers to use computational models to test different treatment methods, which is discussed briefly under section 2.9. Before moving to there, this thesis discusses about different treatment strategies available for bone fractures.

2.7 Treatment of bone fractures

Biology and mechanics are the two cornerstones of fracture healing [8]. As bones have intrinsic capacity to heal by itself, fracture treatments usually focus on providing suitable mechanical environment at the fracture site to best utilize the biological healing capacity of bones [7, 9]. In general fracture treatments involve reduction and stabilization of the fracture site followed by rehabilitation [9].

Depending on the nature of fracture and other factors, treatments follow either non-operative or operative procedures [9]. In general, most stable fractures could be treated with simple non operative procedures as they maintain position. But for unstable fractures, often surgical interventions are required. The primary aim of both operative and non-operative procedures is to restore functionality [115]. Some of the common treatment procedures to manage fractures include the followings [9]:

- Plaster casts : Under functional loading, plaster casts provide controlled motion which permits callus development and leads to secondary healing.
- Traction : Traction is an old-fashioned method which involves application of forces to maintain reduction. As micro-motion is permitted within the fracture site, secondary healing takes place via callus formation.
- Internal fixations : Internal fixations require surgical procedure and are often used to treat unstable fracture. Examples of internal fixations include bone plates and intramedullary nails. Depending on the level of stability internal fixations may lead to either primary or secondary healing.
- External fixations : External fixations also require surgical procedure but are minimally invasive in nature. These are particularly useful when fractures involve extensive soft tissue damage. External fixations generally permit micromotions and allow secondary healing to take place.

Majority of the fractures are treated successfully without complications [8]. In the rest, causes of treatment failure need to be systematically investigated to take remedial actions to enhance healing. The diamond concept (Figure 2.4) provides a conceptual framework to plan and manage unfavourable healing outcomes [67]. Possible methods for fracture healing enhancement include : cell therapy, stimulation by growth factors, bone grafting, mechanical intervention, ultrasound or electromagnetic stimulation and gene therapy

[116]. These methods could also be used to minimize healing time or enhance bone quality in normally healing fractures.

When stabilizing fractures, the choice of fixation is mainly governed by the nature of the fracture and patient specific conditions. Stable fractures could be easily managed without surgical procedures [9]. However, when a fracture is unstable, surgical techniques could become necessary. In such cases minimal invasive techniques are preferable as they minimize additional damage to the fracture site [115]. External bone fixations are advantageous in this regard [12].

External fixation devices

Unlike in the past where use of external bone fixation devices was often a last resort, the use of external bone fixation devices has gained popularity in the recent decades and are gradually becoming one of the mainstream techniques to treat various bone defects [12]. In external bone fixation devices, bone fragments are held in position by pins, nails or wires which are attached to an external scaffolding [12, 117].

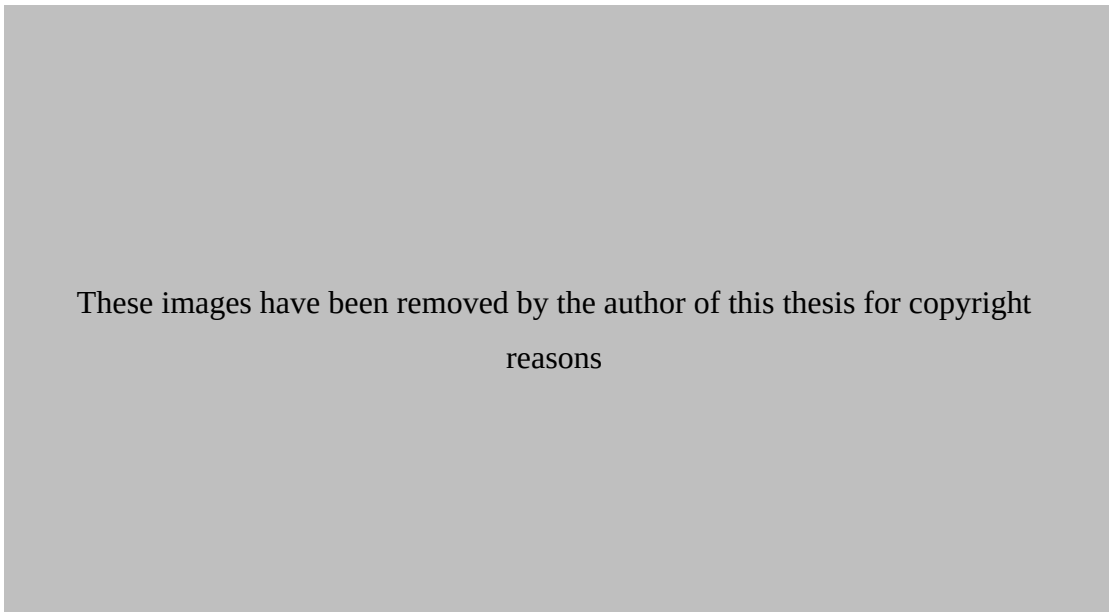

Figure 2.5 Typical (a) unilateral fixator and (b) ring fixator
Adopted from Valentino et al. [118] and Alqahtani et al. [119] with permission

In addition to being minimally invasive, external bone fixations provide numerous advantages such as tailorability to patient specific conditions, post-operative adjustability throughout the course of healing and removability upon satisfactory healing [12]. External bone fixations are very beneficial in cases where fracture include soft tissue damage as open fractures which could preclude internal fixations [9]. Furthermore, external fixations are relatively flexible which is beneficial for callus development in the early stage of healing [9]. There two basic types of external fixators [12]:

- Unilateral fixators : These fixators (Figure 2.5 a) consist of percutaneously placed pins or screws connected using an external rod. Rods or screws need to penetrate near cortex, medullary canal and far cortex and should be terminated without penetrating further into the soft tissue on the far cortex side [120].
- Ring fixators : These fixators (Figure 2.5 b) consist of very fine wires and attached to circular or semi-circular rings. In ring fixators, fine wires pass through the limb and attached to the rings on either side of the limb. Ring fixators are more commonly referred to as Ilizarov circular fixators (ICFs) or simply Ilizarov fixators, named after the surgeon who introduced it.

While both unilateral fixators and ICFs can provide excellent fracture site stability and lead to successful union, ICFs possess some unique features that are highly desirable for treating number of different bone defects [12]. A good understanding about ICF and how it differs from unilateral fixators is necessary to appreciate the full potential of ICF in treatments.

2.8 Ilizarov circular fixators (ICFs)

ICF was introduced by Prof. Gavriil Abramovich Ilizarov from Kurgan, Russia in the early 1950s [14, 15]. As shown in Figure 2.6, ICF is a modular fixator which could consist of rings, rods, wires, pins and nuts and be assembled in countless possible configurations depending on patient specific requirements [14]. Choosing appropriate ICF configuration depends on several factors such as location and geometry of the bone defect, level of soft tissue damage and functional requirements. In contrast to unilateral fixators which use pins of diameters in the range of 4 – 6 mm, ICFs use only 1.5 or 1.8 mm diameter smooth or beaded Kirschner wires to affix bone fragments to the fixator

[14, 121]. Thus, ICFs minimize damage to the fracture site further by minimizing invasion.

ICF rings are available in different diameters ranging from 80 – 300 mm. In general the smallest diameter ring that will fit the limb with at least 2 cm clearance from the skin is used for maximal stability and minimal skin damage [12]. To ensure that the fixation is stable enough, fine wires are generally pretensioned between 491 – 1275 N (i.e. 50 – 130 kg) and secured to the rings using slotted bolts and nuts [122]. However, some or all wires in ICFs could be substituted with half pins if required. In such cases the fixation is referred to as hybrid fixation [14].

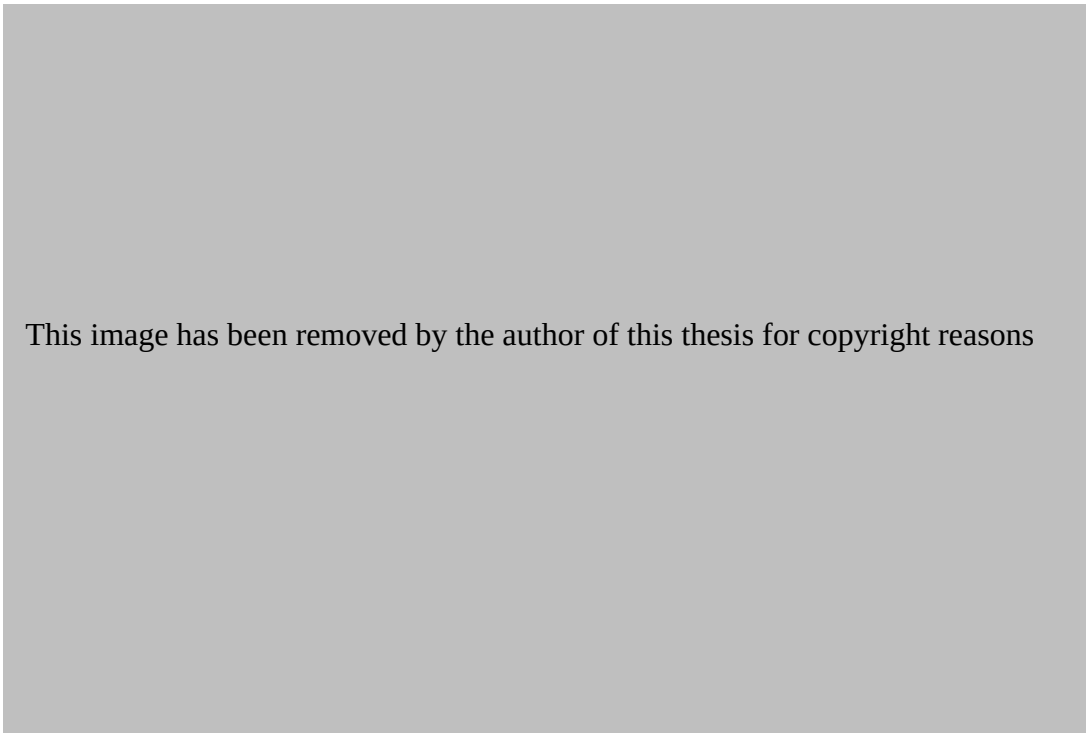

Figure 2.6 Components of a typical Ilizarov circular fixator (ICF)
Adopted from Alqahtani, et al. [119] with permission

Although the exact definition of optimal mechanical environment for fracture healing is not defined, it is known the low levels of axial strains have positive effects whereas high axial strains and shear strains have inhibitory effects on fracture healing [123]. Therefore, an ideal fracture fixation should have nonlinear axial stiffness and high shear stiffness. In other words, the fixation should allow low axial motion but prevent high axial or shear

motions within the fracture site [123]. It has been shown that ICFs fulfil these criteria as crossed pretensioned wires provide high shear stiffness and non-linear axial stiffness [123]. Nonlinear axial stiffness of ICF is attributed to pretension wire behaviour under loading. When bone fragments are subjected to axial loading, pretensioned wires undergo transverse movement and develop additional wire tensions beyond the initial wire pretension levels. With the increase of wire tension, ICF will develop more resistance to axial movement as the axial stiffness of ICF depends on wire tension. This will lead to ICF becoming increasingly stiffer with axial load, exhibiting a non-linear behaviour [124]. Nonlinear axial stiffness of the fixator permits relatively more motion under low loads which presumably stimulates callus formation; but, prevents damage from excessive movements under high loads [12].

2.8.1 Comparison of ICF with unilateral fixator

Unilateral fixators were shown to be relatively more rigid which prevents axial movements [125]. This could possibly explain why ICFs were successful in promoting osteogenesis where unilateral fixators failed [12]. In addition, unilateral fixators undergo cantilever bending when subjected to axial loading and demonstrate non inform loading at the fracture site [12]. This can cause significantly different sizes of peripheral callus on the near and far cortex sides [126]. However, when ICFs are subjected to axial loading, even loading is produced at the fracture site [12]. This could prevent malunion and enhance healing.

Furthermore, when multiplanar fixations are necessary, ICFs could be beneficial over unilateral fixators. With unilateral fixators, additional frames may be required in different planes for this purpose. However, owing to its circular nature, ICF provides circumferential access to limbs making multiplanar fixations relatively simple [12]. Moreover, with the advent of Taylor spatial frame (TSF), which is an advanced variant of ICF, almost any multiplanar correction could be done with precision and ease [127, 128]. Figure 2.7 shows a typical TSF with six adjustable length struts (i.e. hexapod) which permits easy manipulation of the fracture site.

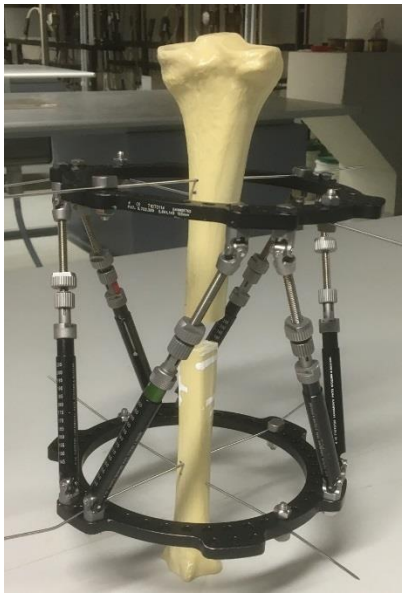

Figure 2.7 Taylor spatial frame (TSF) mounted on a surrogate human tibia (shinbone)

It is important to note that unilateral fixators are advantageous over ICFs to treat defects in humerus (upper arm bone) and femur (thigh bone) which have bulky surrounding soft tissues [12]. Having full rings around upper arms or thighs could cause discomfort to patients. In most cases use full ICF rings at these locations could be impractical. Furthermore, drilling wires through muscle compartments at these locations could be unsafe [12]. Therefore, unilateral fixators are more suited in such cases.

Nevertheless, humeral or femoral defects do not preclude the use of ICFs. It possible to use ICFs in hybrid form with arches, open rings and half pins at these locations. However, the fixator behaviour of hybrid ICFs would be different to those of traditional ICFs. Some studies have shown that both hybrid and traditional ICFs are comparable in terms of stiffness [121, 129] while some others have shown that hybrid ICFs have superior bending and torsional stiffness [130]. However, stiffness of ICF is configuration specific, therefore it is necessary to ensure that the configuration chosen is of adequate stiffness. As ICFs are modular and versatile, surgeons usually have plenty of different options to choose from.

2.8.2 Limitations of ICF

Despite being advantageous in many aspects, ICFs do have a few limitations. Clinical studies have reported that ICFs are inherently flexible and result in large IFMs under

weight-bearing in the early stages of healing [131, 132]. Since fracture site environment in the early stage could have lasting effects, larger IFMs resulting from ICFs could be detrimental to healing. However, traditionally early weight bearing is suggested to have beneficial effects on fracture healing under ICFs [12]. These contradicting clinical observations could be due to inter subject differences in factors such as fracture geometry, body weight and ICF configuration which can significantly influence IFMs within the fracture site. Therefore, it is essential that surgical fixation of ICF is carried out based on sound biomechanical principles taking subject specific parameters into consideration. However, predicting biomechanical behaviour of ICF under clinical settings to choose the best configuration on a case-by-case basis is not easy.

Patient intolerance is one of the major problems associated with treatments using ICFs [133]. Since ICFs are bulky external fixators, they can cause discomfort to patients during daily activities. In addition, wrongly placed wires through muscles could cause functional limitations [13]. Furthermore, wires and pins may loosen and cause pain to patients [13].

Another important drawback of ICFs is the risk of pin tract infections [133]. Colonized bacteria present in pins and wires that are inserted into bone and soft tissues could cause infections and require special care [134]. Although pin tract infections have been reported not to affect the outcome, this continues to be a matter of argument as infected wire or pin tracts could become loose and affect the overall stability of the fixation [135]. It is believed that longer treatment durations (> 3 months) increase the risk of pin tract infections [134].

Therefore, minimization of treatment time with ICFs is of utmost importance as longer treatment times would increase the duration of physical discomfort, financial burden, risk of complications such as infections and risk of additional surgical procedures [7]. However delayed healing is a common problem associated with external fixations and the mechanical conditions imposed by the fixator at the fracture site in an important cause for this [86]. It is beneficial to optimize fixation configuration to produce the best mechanical environment within the fracture site throughout healing as this can speed up healing. Nonetheless, determining optimal mechanical environment within the fracture site has been one of the biggest challenges in treating bone fractures [81].

2.8.3 The knowledge gap: Mechanobiology of fracture healing under ICF

To achieve optimal mechanical environments within the fracture site, sound understanding of the biomechanics of ICF and its effects on fracture healing is essential. This requires systematic investigations on ICF to be carried out. Although the mechanical behaviour of ICFs has been studied extensively, systematic investigations on the effects of ICF on fracture healing is still lacking [15, 136, 137]. As ICFs could be assembled in endless possible configurations, the complex interplay between ICF configuration and fracture site environment needs special attention.

ICF configuration is governed by several factors such as ring diameter, configuration of ring blocks, pretension wire diameter, number of pretension wires, pretension levels, use of wires/half pins etc [138]. In the past, several experimental studies have been dedicated to understanding the biomechanics of ICF.

Bronson et al. [139], studied the effect of ring diameter on the biomechanical properties of ICF using single-ring configurations and reported reduction in axial, bending and torsional stiffness in response to increase in ring diameter. Increasing the ring diameter from 120 mm to 160 mm resulted in 30 % axial stiffness reduction while only 10 % bending and torsional stiffness reductions in ICFs. Similarly, the experimental study on four-ring ICF constructs by Cross et al. [140] reported average axial stiffness reductions around 75 % when increasing the ring diameter from 50 mm to 118 mm.

The investigations of Podolsky and Chao [141] using 4-ring ICF constructs reported 10 – 20 % stiffness increase due to increasing the wire diameter from 1.5 mm to 1.8 mm. Similarly, axial and torsional stiffness increase around 10 % has been reported by Bronson et al. [139] due to the increase of wire diameter from 1.5 mm to 1.8 mm in a single ring block of ICF. On the other hand, it has also been reported that under equal wire tensions, a single 1.8 mm diameter wire could be 50 % stiffer than a 1.5 mm diameter wire [142].

Orbay et al. [143] reported that axial and torsional rigidities of single-ring blocks is directly proportional to the number of wires. Watson et al. [144] conducted mechanical tests on four-ring ICF constructs with two mutually perpendicular pretension wires (with a pretension of1275 N) per ring and reported nearly 25 % reduction in axial stiffness of

ICF due to removal of one wire each from proximal and distal ring blocks. The study of Bronson et al. [139] reported increase in axial and torsional stiffness of double ring ICF up to 30 % in four wire configurations compared to those with just three wires.

Studies on wire pretension levels have revealed inconsistencies in the effect of wire pretensions on the biomechanics of ICF. The investigations on single ring block ICFs by Bronson et al. [139] did not show any noticeable effects due to the increase of wire pretension from 90 kg (883 N) to 130 kg (1275 N). On the other hand, Kummer et al. [124], based on a single wire study reported 33 % stiffness increase in response to wire pretension increase from 60 kg (589 N) to 120 kg (1178 N). A different study using rigid ICF frames demonstrated much larger stiffness increases up to 53 % for the same wire tension increase (i.e. from 60 to 120 kg) [145].

The effect of use of half pins in place of or in combination with pretensioned wires has also been investigated in previous studies. Khurana et al. [136] conducted a series of mechanical tests to study the effect of replacing two 1.8 mm diameter wires pretensioned to 110 kg (1079 N) with two 6.5 mm diameter half pins on the stiffness of a single-ring ICF construct. The results revealed that the constructs with half pins had 20 – 50 % more axial stiffness than those with pretension wires. This suggested that inclusion of half pins at appropriate locations could enhance fixator stiffness. This idea was further strengthened by a different study on single ring constructs which exhibited significantly greater stability for an ICF construct with two 5 mm diameter half pins and a single 1.8 mm diameter pretension wire compared to that of a construct with four 1.8 mm diameter wires[138]. Conversely, the experimental investigation of Yilmaz et al. [146]on different configurations of standard (wire only) an hybrid (wires and half pins) ICF configurations reported that all hybrid configurations considered in the study had lower axial and bending stiffness compared to those of the standard ICF configuration.

It is evident from the existing studies that ICF configuration has a major role to play in the stability of fracture site. However, the main limitation of these studies is that they only focus on the mechanical aspects of ICF such as its stiffness and fail to elucidate how the changes in mechanical properties of ICF influence the biology of healing. Studies investigating the mechanobiology of fracture healing are very limited if not totally unavailable. Furthermore, it is hard to draw meaningful conclusions regarding the

mechanical performance of ICF from the existing studies as different studies use different set of configuration parameters (e.g. ring diameter, configuration of ring blocks, pretension wire diameter, number of pretension wires, pretension levels, use of wires/half pins etc.).

For example, in the study of Khurana et al. [136], no statistically significant difference ($p > 0.05$) in axial stiffness between ICF configurations with transverse wires and those with half pins were reported when 180 mm diameter rings were used. However, for 155 mm rings, the configuration with half pins demonstrated higher axial stiffness which was statistically significant ($p = 0.036$). In another study, Kummer [124] reported that the effect of wire tension on fixation stiffness plateaued once the wire tension reached 90 kg (883 N) for 1.5 mm diameter wires while that for 1.8 mm diameter wires was 130 kg (1275 N). Moreover, Cross et al. [140], based on their experimental study on the roles of ring diameter and wire pretension on the mechanical performance of four-ring ICF constructs, indicated that while both ring diameter and wire pretension each significantly ($p < 0.001$) affected construct stiffness, their interaction was also significant ($p < 0.001$) for construct stiffness. Therefore, the interpretation of biomechanical results are specific to the ICF configuration under consideration. For example, how much stiffness change can be achieved by changing the pretension wire diameter from 1.5 mm to 1.8 mm depends on the ring diameter, number of rings used and other configuration parameters. This makes it difficult to compare outcomes across different studies as different configurations may be adopted in different studies.

Therefore, there is still lack of deeper understanding about the interrelationships between different configuration parameters of ICF which makes it hard to predict the mechanical behaviour of a given ICF configuration. This combined with lack of understanding of the mechanobiology of fracture healing under ICF poses a significant challenge in treating fractures using ICFs.

In addition to the fixator parameters, there are several other mechanical factors that affect ICF performance and fracture healing such as magnitude of external loading (e.g. weight bearing), type of loading, fracture geometry etc. Podolsky et al. [141] conducted a series of mechanical tests on four-ring ICF constructs. The ICFs consisted of two 150 mm diameter rings for each fragment; two 1.5 mm diameter pretension wires per ring with

each wire pretensioned to 110 kg (1079 N). Under axial loading between 0 – 100 kg (0 – 981 N), the axial stiffness of the ICF construct was calculated from the slope of load - displacement curve. On average, the ICF construct was 2.7 stiffer (axial) for the load range of 668 – 891 N than for the load range of 0 – 222 N. This demonstrates the nonlinear mechanical behaviour of ICF. Similarly, Kummer [124] pointed out that the effect of wire tension on the overall rigidity of ICF is most noticeable under low axial loads which is due to the non-linear behaviour of pretension wires [138]. Thus, the mechanical behaviour of ICF would be specific to the load range considered.

In addition, many experimental studies have shown that the type of loading (e.g. dynamic or static, direct or indirect etc.), load duration, loading frequency can all have significant influence on the mechanical behaviour of ICFs [147-151].Therefore, when comparing results across different biomechanical studies it is also essential to compare the loading under which the testing was conducted. This again poses a significant challenge in comparing results across different experimental studies as different studies adopt different types and ranges of loading.

A common shortcoming in most studies involving mechanical tests is that the load transfer via the soft bone tissues within the fracture site is often neglected in mechanical tests. Almost all mechanical tests represent fracture as a gap and soft tissues within the fracture gap are not incorporated. Therefore, a complete understanding on how an ICF construct affects the mechanical environment of the fracture site cannot be obtained with mechanical tests alone. It is well known that fracture gap size is an important mechanical factor that influences the mechanical environment of fracture healing [19, 20]. However, when the fracture is represented as a gap, it is practically impossible to study the effect of fracture gap size on the mechanical environment of fractures. For example, in a mechanical test where the fracture is represented as a gap, when all other conditions remain the same, a 2 mm and 20 mm gap would demonstrate the same mechanical behaviour under axial loading before the fragments come into contact. However, 2 mm and 20 mm fracture gaps would result in two totally different mechanical environments within the fracture site during healing.

Furthermore, mechanical experiments representing fractures as mere gaps are mostly representative of the behaviour of ICFs in the very early stages of fracture healing when

the tissues within the fracture site are too soft to take any load. With time, as the fracture heals, the bone starts to take more load and the load share between bone and ICF modifies. Under such conditions, the mechanical behaviour of the fracture site would be very different to those investigated in mechanical experiments. Therefore, mechanical experiments have limited capabilities in studying fracture healing under ICFs.

Animal experiments provide a solution to this problem as they allow the time dependent effects of individual parameters on fracture healing to be studied in a controlled manner. However, animal experiments focusing on the mechanobiology of fracture healing under ICF are very limited. Claes et al. [19] conducted a series experiments on sheep to investigate the influence of fracture gap size, interfragmentary movement and interfragmentary strains on the quality of healing under a circular external fixator. Transverse osteotomies of different gap sizes (i.e. 1 mm, 2 mm and 6 mm) were created in the right metatarsus in 42 sheep and subjected to either small or large initial interfragmentary strain (7 % or 31 %). Weekly interfragmentary movements were monitored and after 9 weeks the animals were sacrificed. Later, their metatarsus were explanted and subjected to mechanical and radiographic tests. The study revealed that the healing process was inferior for 6 mm fracture gap. In addition, the study showed that increase in fracture gap size results in reduction in bending stiffness. Furthermore, larger interfragmentary movements (31 %) stimulated larger callus formation for small gaps (1-2 mm), but not for larger gap sizes (6 mm).

In a different study, Claes et al. [20] investigated the role of fracture gap size on vascularization and tissue differentiation within the fracture site stabilized with a circular external fixator using sheep model. The study revealed that medium gap sizes (i.e. 2.1 mm) result in significantly more revascularization (91 %) and bone formation (168 %), but less fibrocartilage tissue formation (54 %) than large gap sizes (i.e. 5.7 mm) when subjected to physiologically relevant loading (30 – 32 % interfragmentary strain).

In another sheep experimental study, Claes et al. [152] investigated the role of interfragmentary strain on vascularization and tissue differentiation within the fracture site stabilized with a circular external fixator. In this study 2 mm osteotomy was created in all sheep and subjected to either small (i.e. 0.2 mm) or large (i.e. 1 mm) axial interfragmentary movements. The study revealed that larger interfragmentary movements

led to significantly more fibrocartilage (248 %) and less bone formation (45 %) than in smaller interfragmentary movements. On average, the periosteal vascularization was significantly more in the group with smaller interfragmentary movements than that with larger interfragmentary movements. These results explain the role of external loading on the process of healing. Furthermore, these sheep experimental studies [19, 20, 152] indicate that there has to be a range of optimal combination of a given set of mechanical parameters for fracture healing. Since the mechanical properties of the fracture site change with time, the optimal combinations of parameters must also change with time as healing progresses. However, studies focused on this aspect of fracture healing under ICF are very limited.

Although the animal experiments of Claes et al. [19, 20, 152] provide useful insights into the mechanobiology of fracture healing under circular external fixations, the primary focus of these studies was to investigate the effects of fracture geometry and stability on fracture healing. Those studies do not investigate the role of the fixator configurations on fracture healing. Furthermore, these animal studies used custom made circular fixators that are extremely rigid in bending and torsion. Therefore, the fixator behaviour in these studies is not directly comparable with the performance of standard ICFs. Other existing experimental studies on ICFs focus mostly on the mechanical behaviour of the fixator under different configurations and loading conditions [137]. Therefore, they do little to explain the effects of mechanical factors on the biology of healing.

On the other hand, many aspects of ICF have been studied clinically [153-156]. However, clinical results are limited in explaining the effects of ICF on the biology of fracture healing as they lack cell and tissue level observations. Furthermore, high levels of variabilities in subject specific factors makes clinical results less standardisable. In certain cases, contradicting observations are also reported in clinical studies [132, 157]. Therefore, it is not always easy to make clear conclusions from clinical observations across different studies or sometimes even within the same study.

Consequently, the mechanobiology of fracture healing under ICF remains poorly understood. As a result, the roles of external mechanical factors on cell and tissue level biological events within the fracture site stabilized with ICFs during healing remains unclear. Therefore, fundamental questions such as the followings remain unanswered:

(i) What are the effects of ICF configuration, loading and fracture geometry on the early stage mesenchymal stem cell (MSC) differentiations during fracture healing ?

(ii) What are the roles of physiologically relevant dynamic loading on cell differentiations and cell / growth factors transport within the early stage fracture site ?

(iii) What are the effects of subject specific factors (i.e. body weight, fracture geometry and ICF configuration) on angiogenesis and optimal time dependent weight bearing levels for bone fractures treated with ICFs ?

(iv) What are the effects of uncertainties in mechanical factors (i.e. fracture geometry, weight bearing and ICF configuration) on fracture healing under ICF ?

This fundamental knowledge gap is a barrier to achieve optimal mechanical environments within the fracture site for timely healing with adequate bone quality. Therefore, achieving timely healing with ICFs remains a clinical challenge. Another important clinical challenge associated with ICFs is deciding the time of removal of the fixator. Premature removal of fixator could result in refracture or malunions; whereas, late removals can prolong the treatment time. This decision requires determination of time dependent load bearing capacity of fracture site to judge when it can tolerate full weight bearing [12].

However, clinical decisions about ICF treatments are often made on trial and error basis without systematic investigations [15]. As a result, rates of unfavourable conditions such as non-unions and complications remain significant (around 10 – 30 %) with ICF treatments [137]. In addition, there is also tendency in surgeons to use more familiar unilateral fixators than ICFs despite the advantages ICF [12].

The knowledge gap in linking ICF mechanics with biology of fracture healing prompts for further fundamental research in this area. Proper understanding of the mechanobiology of fracture healing under ICF is the key to utilize the full potential of ICFs and minimize healing time and complications. The complex nature of this problem demands systematic investigation into the effects of multiple factors and their interplays on fracture healing in a controlled manner. Computational models provide an excellent

solution for this purpose. Many previous studies have demonstrated the potential of computational models in systematically studying various treatment strategies.

2.9 Computational models to study fracture treatment strategies

Computational models have been used in full spectrum of orthopaedic devices for over four decades [158]. In long bone fracture fixation devices, models reported in literature include those of unilateral frames, compression plates, intramedullary nails and Ilizarov fixators. The primary reasons for the use of computational models of fixation devices are (i) gaining fundamental understanding of the bone – device interaction and (ii) designing and pre-clinical testing of new devices and comparing them with existing ones [158].

Some models [159, 160] focus only on the mechanical behaviour of the bone – device interaction. Such models provide important information about the mechanical aspects relevant to fracture treatment such as the relationship between fixator stiffness and interfragmentary movement (IFM) or stress distribution across the fixation sites under loading. However, they are limited in interpreting the effects of mechanical factors on the biology of healing. Overcoming this issue, some models [161, 162] have attempted to include fixations as mathematical abstractions such as springs. This helped gaining fundamental understanding of the effects of fixator stiffness on fracture healing. However, such models have limitations in clinical applications as they do not simulate the actual fixation behaviour. With the improvements in computational power and developments of sophisticated software, fully coupled models simulating fracture healing under fixation devices [126, 163-165] have started to emerge in the recent years.

Another important application of computer models in fracture treatment studies is investigating the effects of different growth factor and cell therapies. Using bio-regulatory models, which incorporate separate variables for cells and GFs, it is possible to test if the injection of cells or GFs or both at different time points can enhance healing; and if so, decide optimal dosage levels, administration times, injection locations etc. [59]. This is particularly useful for delayed healing or non-union cases. For example, Geris et al. [166] simulated postoperative administration of MSCs to promote healing in atrophic non-unions and investigated the effects of injection locations on the healing patterns. Furthermore, computational models could be used to conveniently study the effects of

periosteal stripping or reaming of marrow canals which could result directly due to fracture or following surgical procedures [167].

It is evident that computational models could be extremely helpful in systematically investigating the effects of different treatment strategies on fracture healing. When comparatively studying the effects of different configurations of ICF on fracture healing, computer models could be very convenient. Because, making changes to fixator configurations or other subject specific parameters is very easy in computational models. Number of studies have presented computational models of ICFs in the past to investigate different problems related to ICF. The following subsection briefly discusses about some of them.

Computational models of ICF

Prat et al. [168], developed one of the earliest computational models of ICF and investigated load sharing between callus and fixation under rigid and dynamic cases. Load transmission via callus at different stage of healing were investigated by exponentially increasing callus elastic modulus in 5 stages. The model predicted nearly 85.5 % of load transmission via callus when the callus elastic modulus was just 1 % of that of intact bone. In the same study, experiments on rabbit tibial fractures were conducted to corroborate their findings. The study indicated that rigid configurations are preferable than flexible configurations in the early stages to minimize damage to callus.

An important feature of ICF is the non-linear behaviour of pre-tension wires under loading which influences both fixator stiffness and allowable level of weight-bearing. Due to the importance of pretension wires in ICFs, number of studies in the past [169, 170] have specifically focused on the analytical investigation of pre-tensioned wires using computational modelling.

Zhang [171], pointed out the need of the entire load deflection curve of the ICF in describing the mechanical behaviour of wires. His study demonstrated that computational modelling is a valid and cost-effective way to obtain a whole spectrum of information about pretensioned wire behaviour. In a different computational study, Zhang [172], developed a diagram to estimate the number of wires required for a chosen wire

pretension and estimate the stiffness of ICF. Such simple diagrams can be very helpful in assisting clinical decision making.

Since ICFs are modular and could be assembled in endless possible configurations, they pose a significant challenge in determining how a given configuration would perform under a given loading scenario. This led some researchers to develop computational methods to quickly and accurately determine the performance of fixator by taking fixation configuration as model input. Nielsen et al. [173], developed an interactive computational model, which would take bone position, ring diameter, wire pretension, load, half pin clamp height, number of pins/wires and pin/wire mounting positions as inputs from users to construct the computational model of ICF and to determine the bone displacements with reasonable accuracy in less than 30 s. A similar approach was taken in the model of Watson et al. [144], which used a master input file to specify the instructions to model different configurations of ICF. Both these studies [144, 173], corroborated their models using mechanical tests.

Despite these advancements in computational modelling of ICFs, no models coupling mechanics with biology of fracture healing has been developed so far. Thus, the existing computational models can be used primarily to study the mechanical behaviour of ICFs. Therefore, there is a need for developing advanced computational models to investigate mechanobiology of fracture healing under ICFs.

2.10 The need for further research

Computational models of ICF so far have shown potential in investigating clinically relevant problems and treatment planning. However, due of lack of coupling between mechanics and biology, the existing models are still a step away in elucidating the complex mechanobiology of fracture healing under ICF. Therefore, how ICF configurations influence processes within the fracture site such as cell differentiations, solute (e.g. cell, growth factors etc.) transport and angiogenesis during fracture healing has not been explained well. Furthermore, how the interplay between ICF and other mechanical factors such as fracture geometry or loading affect these processes remains unclear. This knowledge gap in the mechanobiology of fracture healing under ICF is a barrier to address clinical problems associated with ICFs as described under section 2.8.3.

This thesis intents to the address this knowledge gap via the followings:

- Developing reliable computational models to study different aspects of fracture healing under ICFs
- Investigating the effects of ICF configuration, loading and fracture geometry on the early stages MSC differentiation during fracture healing
- Investigating the effects of physiologically relevant dynamic loading on cell differentiations and cell / growth factors transport during early stage bone fracture healing under ICFs
- Determining the effects of subject specific factors (i.e. body weight, fracture geometry and ICF configuration) on angiogenesis and optimal time dependent weight bearing levels for bone fractures treated with ICFs.
- Investigating how uncertainties in mechanical factors (i.e. fracture geometry, weight bearing and ICF configuration) affect fracture healing under ICF.

This thesis presents computational models that couple both mechanics and biology to simulate fracture healing under ICF. Different models were developed to investigate different aspects of fracture healing under ICF. The development of the models, validation of them using experimental data and subsequent investigations into different aspects of healing using the validated models are presented in detail in the following chapters of this thesis.

3 Mechanical Experiment on Tibial Fractures Stabilized with Ilizarov Circular Fixator

Chapter summary

In order to develop reliable computational models, it is essential to test their validity by comparing model predictions with data obtained under controlled environments. As this research intends to study fracture healing under ICFs using computational models, mechanical experiments on bone fractures stabilized with ICFs were conducted to obtain data for validation purposes. This chapter presents the details of the mechanical experiment conducted.

Most of the contents of this chapter were adapted from the article titled "**Bone fracture healing under Ilizarov fixator: Influence of fixator configuration, fracture geometry, and loading**" published in the **International Journal for Numerical Methods in Biomedical Engineering** [21] where I was the first and the primary author of the article. In this work, as the main researcher, I proposed the research idea, designed the mechanical experiment and discussed the results. My supervisors A/Prof. Lihai Zhang, Dr. Saeed Miramini and Prof. Priyan Mendis regularly discussed with me, monitored my progress and provided their inputs and feedback throughout this work. Prof. Minoo Patel of Epworth Richmond provided his help in designing the experiment.

3.1 Introduction

One of the key objectives of this thesis is to systematically investigate how ICF configuration influences the mechanobiology of fracture healing. To achieve this, it was proposed to develop computational models which can take user inputs to define the ICF configuration and simulate fracture healing under the specified configuration. By taking this approach, the role of each ICF configuration specific factor on biological processes during fracture healing can be studied in a controlled manner while isolating the influence of other factors. For example, if the role of ICF ring diameter on cell differentiation within the fracture site is to be studied, the user could run simulations under different ring

diameters while keeping all other factors the same for all simulation cases. Then cell concentrations under each simulation case could be quantified from the model and comparatively studied to predict how ring diameter influences cell differentiations.

However, to test the validity of the model predictions, it is essential to compare model predictions with experimental data obtained under controlled environments. Therefore, it was decided to first conduct a mechanical experiment to obtain data for validation purposes. As ICFs are modular fixators, there are plenty of options for the configuration of choice. In the experiment, the choice of ICF configuration was made based on two criteria. First, to keep the configuration simple to minimize complexity. Second, to test a clinically relevant configuration that has not been adequately investigated in existing literature. This criterion was set so that useful data can be obtained to complement the existing understanding about the biomechanical behaviour of the chosen configuration.

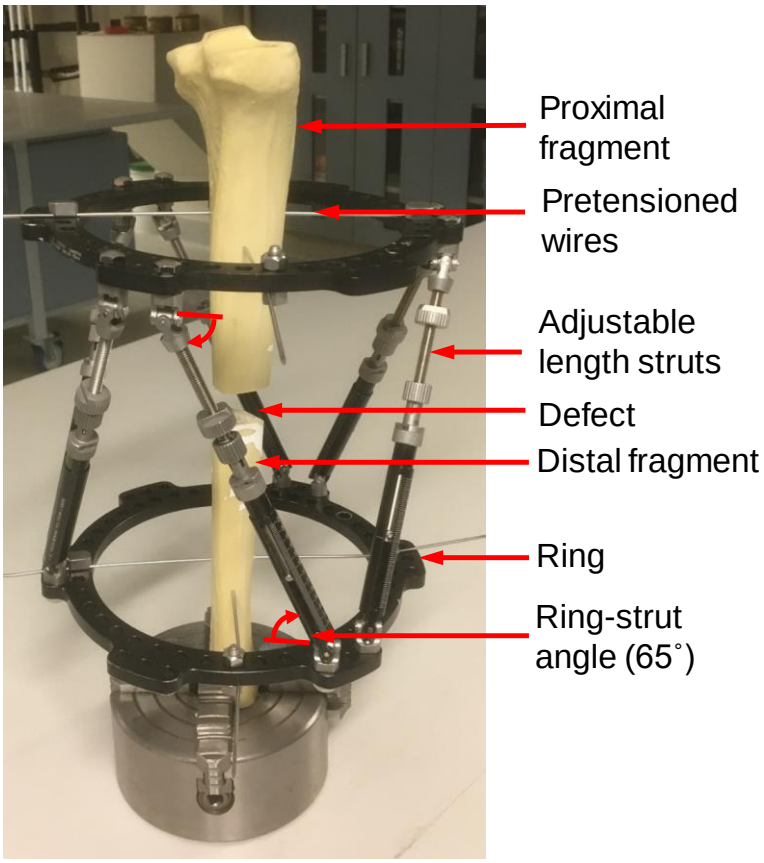

Figure 3.1 ICF configuration with hexapod system (i.e. TSF) used in the mechanical experiment

It is known that Taylor spatial frame (TSF) is an advanced variant of ICF, which uses a hexapod system with six adjustable length telescopic struts at the fracture site (Figure 3.1). The hexapod system is advantageous over the conventional 'ring and threaded rod' ICF system as it allows the fracture site to be manipulated three dimensionally with six degrees of freedom. This enables TSF to correct almost any multiplanar deformity easily and accurately [127, 128]. Thus, it makes TSF one of the most versatile external bone fixator devices. Most importantly, due to its feature of computer aided fixator adjustment, TSF is regarded as more reliable than the conventional ICF [174].

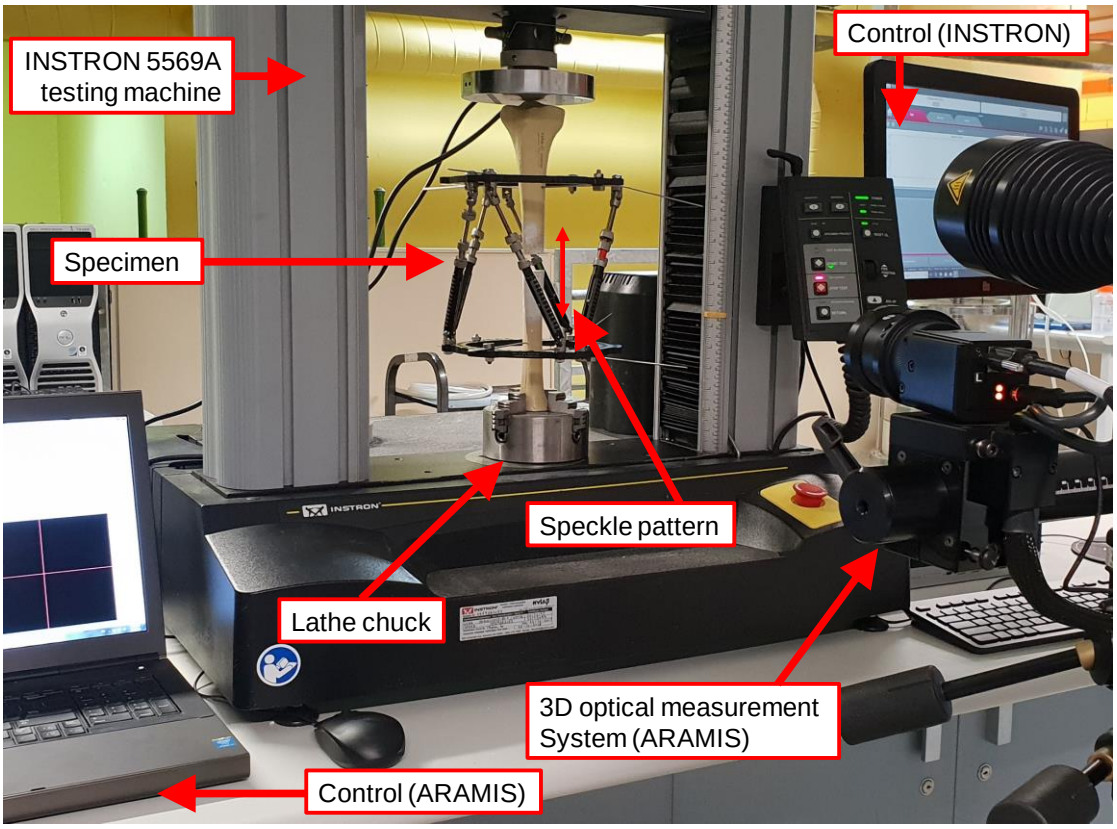

Figure 3.2 Details of experimental setup using INSTRON 5569A testing machine and 3D optical measurement system (ARAMIS)

Numerous experimental studies have investigated the influence of ICF frame elements and configurations on the biomechanical properties of the conventional ICF [121, 144, 146, 175]. However, there is only limited amount of data available on the biomechanical properties of TSF under different configurations [127]. Henderson et al.[128] investigated

the influence of ring-strut angle on the fixator stability using an isolated TSF hexapod. Khurana et al.[136] compared the effect of wires and half pins using a single ring experimental setup. However, these studies mainly focused on isolated behaviour of different parts of TSF. A few other studies investigated the mechanical behaviour of different TSF constructs by using tubes to represent bones [127, 176]. However, the influence of the stiffness characteristics of the frame constructs (TSF) on the fracture site movements (i.e. IFM) has not been fully investigated yet. This is one of the current areas of interest in orthopaedic research [127, 177].

Therefore, ICF configuration with hexapod system (i.e. TSF) was chosen for this experiment. Mechanical tests were carried out on surrogate human tibial bone specimens with transverse fractures stabilized by a two ring TSF (Figure 3.1). The details of the experimental setup are shown in Figure 3.2. The specimens were axially loaded using INSTRON universal testing machine and the interfragmentary movements (IFM) were measured using a 3D optical measurement system (ARAMIS).

3.2 Materials and Methods

Surrogate adult human tibiae manufactured by SYNBONE AG (Malans, Switzerland) was used in the mechanical testing. The bone was made of specially formulated polyurethane foam that has the mechanical properties similar to those of adult human tibiae [178, 179]. It comprises of outer cortical bone and inner cancellous bone and imitates the anatomical structure of a real bone very closely. The average compressive Young's modulus (E) and Poisson's ratio (υ) of the surrogate bones used are 1500 MPa and 0.25 respectively [178]. The surrogate bone fractures were stabilized using TSFs manufactured by Smith & Nephew PLC (Memphis, Tennessee, USA).

The TSF constructs used in the mechanical test (Figure 3.1) consisted of (i) two identical aluminium (E = 69 GPa and υ = 0.33) rings (one for the proximal fragment and another for the distal fragment); (ii) four 1.8 mm diameter stainless steel (E = 197 GPa and υ = 0.29) pretension wires (two mutually perpendicular wires per ring), and (iii) six stainless steel FAST FX struts (Smith & Nephew) per assembly. The rings and FAST FX struts were assembled to have a ring-strut angle of 65˚ (as shown in Figure 3.1) and the bone specimens were centred to the rings.

Figure 3.3 Wires affixed to drill driver (Milwaukee, Wisconsin, USA).

It should be noted that ring-strut angle plays an important role in the stability of TSF. An experimental study [128] showed that TSFs would reach instability as the ring-strut angle reduces and recommended to avoid ring-strut angles less than 30°. The study [128] also showed that TSFs are generally stable under compression for ring-strut angles in the range of 30-70°. Within this range, larger angles lead to lower stresses in the struts which could be explained using simple truss mechanics. Therefore, a ring-strut angle of 65° was used in this experiment (Figure 3.1).

The wires were affixed to a drill driver (Milwaukee, Wisconsin, USA) and their bayonet ends were used to directly drill through the bones and secured in position at both ends of the rings with slotted wire fixation bolts (Figure 3.3 and Figure 3.4). Once the TSF was affixed to the bones, a 20 mm fracture gap was created at mid height of the tibia. The reason for choosing a relatively larger gap size was to prevent bone fragment apposition during loading.

In the next step, the wires were pretensioned by keeping one end of the wire tightly fixed to the ring (using slotted wire fixation bolt and nut) and stretching the other end using a dynamometric wire tensioner (Smith & Nephew). This device provides graduations of the standard range of clinical wire pretension levels in kilograms (i.e. 50 – 130 kg) which

was used to measure the pretension level in the wires as they were stretched. Once the desired pretension was achieved, the wire tensioner was locked in position and the wire was secured to the ring tightly at the stretching end using slotted wire fixation bolt and nut (Figure 3.5).

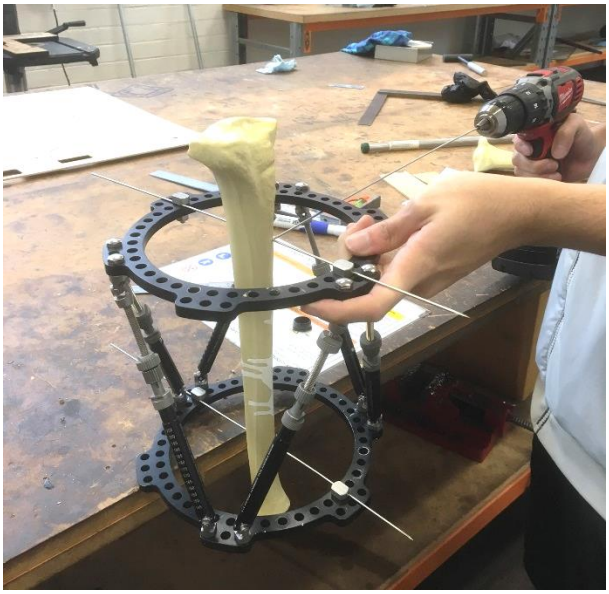

Figure 3.4 Drilling of surrogate bone specimens using wires and securing of wires using slotted wire fixtion bolts

To test the validity of the model under different configurations, it was decided to conduct the experiment under two different TSF configurations. As it is known that ring diameter is one of the most influential configuration parameters that affect the biomechanical behaviour of TSF [124, 180], it was decided to conduct the experiment under different ring diameters. Two different TSF constructs, one with 130 mm ring diameter and another with 155 mm ring diameter were used in the mechanical testing. It should be noted that these diameters refer to the internal diameter of the rings. In both cases, wire pretension of 883 N (90 kg) was applied to all wires. The distal bone ends of the assembled TSF constructs were fixed to a lathe chuck and the assembly was loaded at the intercondylar eminence of the tibia in the axial direction using the universal testing machine (INSTRON 5569A, Massachusetts, USA). This test setup attempts to mimic the physiological load application (e.g. standing) on tibia from knee and ankle joints [178, 181].

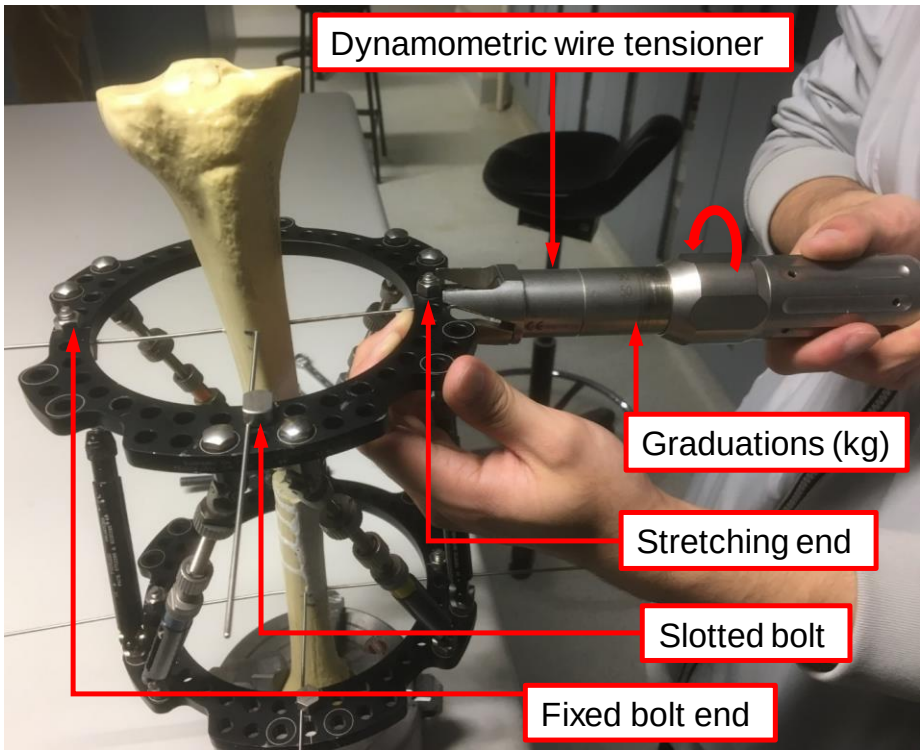

Figure 3.5 Pretensioning of wires using dynamometric wire tensioner

With the help of the cross hairs of ARAMIS, the specimens were placed in the INSTRON machine each time carefully so that the fragments are vertical and properly aligned. This was done to ensure that the compressive load is applied axially and to minimize the lateral movements of the fragments during axial loading. To simulate a partial weight bearing condition after surgery, an axial compressive load of 150 N (i.e. around 20 % of the body weight) was ramped over 0.5 s [179] using the INSTRON machine. Each test was repeated five times and the IFMs were recorded using ARAMIS 3D optical measuring system at 25 N intervals.

IFM measurement using ARAMIS 3D optical measuring system

In this mechanical test, it was intended to measure the fracture site movements at number of points along the fracture ends rather than at just one point (e.g. mid-point). This was achieved using the ARAMIS 3D optical measuring system (GOM, Braunschweig, Germany) which allows full field measurements at multiple points to be taken

simultaneously. ARAMIS provides very accurate non-contact measurements, eliminating the sources of measurement errors that are present in contact measurements. It can measure deformations as small as 0.0002 mm with a strain accuracy of 0.01 %. Thus, ARAMIS makes the effect of measurement errors insignificant for the range of displacements measured in this experiment.

To capture the displacements using ARAMIS, a stochastic speckle pattern consisting of black dots on white background was created using spray paints around the fracture gap of the tibia (Figure 3.2) as per the specifications of the GOM [182]. ARAMIS creates facets (small rectangular areas) from this speckle pattern and uses them to determine the displacements based on the relative movements of the facets between subsequent images captured.

In this study, two cameras (50 mm focal length lenses) of the ARAMIS system, set up according to the specifications of GOM [182] were used to capture the images. The facets were of 19 x 19 pixel (15 x 15 pixels with 2 pixel overlapping) which is the recommended facet size of ARAMIS for normal deformation measurements [182]. Before each test, to ensure that the speckle pattern is adequate, an image covering the fracture gap and the surrounding areas with speckle pattern was captured and processed using the ARAMIS control machine (Figure 3.2). This was done to check if ARAMIS could detect the fragment ends and the surrounding areas which are the areas of interest. Mechanical test and displacement measurements were carried out only after ensuring this.

Full field displacements of multiple points along the proximal end of the fracture gap and the corresponding points (lying vertically below) in the distal end of the fracture gap were measured and the relative movements between the proximal points and the corresponding distal points were calculated as IFM in each direction. In each test, the first image was captured when the axial load was zero and then images were captured at every 25 N intervals up to 150 N.

3.3 Results and Discussions

The mechanical test results showed that the IFMs were predominantly vertical and both vertical and lateral components of IFMs increased with axial load. However, the largest lateral IFMs were observed to be 0.077 mm and 0.101 mm for TSF with 130 mm and 155

mm diameter rings, respectively at 150 N axial load. Since the lateral components of the IFMs were negligible compared to the vertical components (less than 2.5 % of the vertical components for both rings), the lateral and rotational components were ignored from further analysis. Therefore, IFM would refer to the axial IFM (vertical direction) hereinafter.

To obtain more representative values of IFM, the mean values of IFMs were calculated from three points along the proximal end and the corresponding points in the distal ends. Figure 3.6 presents the mean axial IFM components calculated from the mechanical test. The axial stiffness of TSF with 130 mm diameter rings was significantly higher than that of TSF with 155 mm rings. On average TSF with 155 mm diameter rings was around 31 % less stiff that with 130 mm rings. As demonstrated by previous experimental and computational studies, this behaviour is due to the differences in clear wire lengths supporting the axial loading [124, 169, 170]. While all other factors remain the same, increasing the wire span reduces the lateral stiffness of the wires and increase lateral deflection. It has been shown analytically that the lateral deflection of pretensioned wires is sensitive to the clear span of the wires between supports [169, 170]. As the ring diameter changes, so does the clear span of the wires and the axial stiffness of the fixator. Experimental studies elsewhere have reported axial stiffness reductions around 30 % as a result of changing the ring diameter from 120 mm to 160 mm [138] which is comparable with the 31 % reduction recorded in this experiment.

The non-linear relationship between axial load and IFM can also be seen in Figure 3.6 which is due to stress stiffening effect of the pretensioned wires [171]. This nonlinearity is geometric as reported in many studies [169-171] and depends on the level of transverse movements of the wires. This explains the difference in the levels of nonlinearities under different ring sizes.

Furthermore, the experimental results suggest that the effect of ring diameter is more evident at lower axial loads. The increase in axial IFM due to the increase of ring diameter from 130 mm to 155 mm was 43 % for 25 N axial loading while it reduced to 19 % for 150 N axial loading. This again is attributed to the non-linear behaviour of wires as reported in studies elsewhere [138, 180]. Clearly the axial stiffness of the fixator is dependent on axial loading and ring diameter.

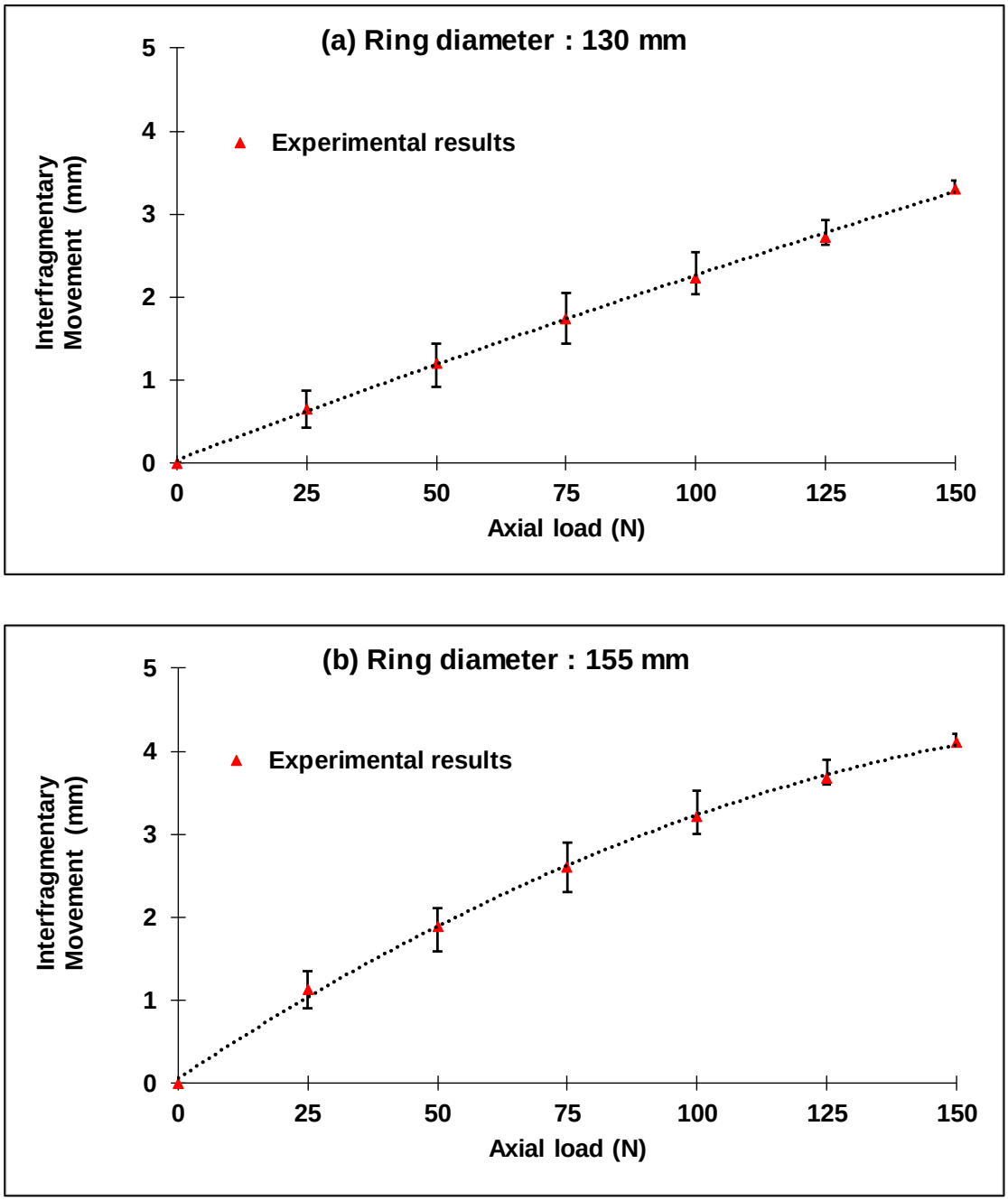

Figure 3.6 Axial interfragmentary movements (IFMs) obtained from the mechanical experiment for TSF (gap size = 20 mm, wire pre-tension = 883 N [90 kg]) with (a) 130-mm diameter rings and (b) 155-mm diameter rings

To further investigate the effects of these factors, a simple two-way ANOVA test on the mechanical results was carried out. The test revealed that both axial load and ring diameter have strong effects on the axial stiffness of the fixator ($p < 0.05$) with ring

diameter having the strongest effect. However, their interaction did not appear to affect the axial stiffness significantly (p = 0.06).

Axial stiffness measured from the mechanical experiment for TSFs with 130 mm and 155 mm diameter rings varied from 36 – 46 N/mm and 22 – 37 N/mm, respectively within the load range considered. Experimental tests on two-ring conventional ICF configuration with two mutually perpendicular wires per ring reported average axial stiffness values around 30 N /mm [144]. However, the ring diameter (i.e. 180 mm), wire pretension (i.e. 1275 N), spacing between the rings and location of the defect between the rings were different in that study [144] compared to those used in this experiment. In a different mechanical study, four-ring conventional ICF configuration with 150 mm diameter rings measured axial stiffness around 50 N/mm [121]. Although the results obtained from the present mechanical experiment are comparable to those obtained elsewhere, direct comparison of the results is not possible. This is due to the differences in load ranges and configuration parameters (e.g. ring diameter, wire pretension, number of rings, and distance between rings etc.) used in the present experiment and experiments elsewhere. However, the results suggest that axial stiffness comparable to those of conventional ICFs could be achieved with TSF constructs as well.

It should be noted that this mechanical experiment has some limitations. Firstly, only axial loading condition was tested in this experiment as it is the predominant loading condition that occurs in lower extremities such as tibia [180]. Secondly the tests were not conducted on cadaveric bones but on surrogate bones. While the use of surrogate bones minimizes the uncertainties in geometric and material properties associated with cadaveric bones, surrogate bone behaviour could be different to that of cadaveric bones. In addition, the behaviour of bones with comorbidities such as osteoporosis would be much different to those demonstrated in this experiment. Therefore, the biomechanical behaviour of defects stabilized using TSF observed in this experiment is mostly representative of bone defects under healthy conditions. Furthermore, axial loading only up to 150 N was considered in this experiment. As axial stiffness of TSF is dependent on axial loading due to non-linear behaviour of pretension wires, it is very well possible for the fixator to behave differently under higher loading ranges (i.e. above 150 N). It is expected that the configurations tested in this experiment will exhibit more rigid

behaviour under higher axial loading. Thus, the behaviour demonstrated by the tibial defects stabilized by TSF in this experiment is mostly representative of the early stages of healing post-surgery where weight bearing is limited (around 20 % of body weight).

Nevertheless, the experiment provides some useful biomechanical data relevant to a clinically relevant ICF configuration that has not been tested adequately before (i.e. TSF). The results obtained in this experiment may have clinical relevance as it reports fracture site movements (i.e. IFMs) of bones with anatomic geometries as opposed to displacements measured at the top of circular pipes which are used to mimic bones as in previous experimental studies on TSFs [127, 176]. It should be noted that the main objective of this mechanical experiment is to obtain data to validate computational models that are to be developed later. For this purpose, the experiment served satisfactorily as biomechanical data under controlled environments for two different fixator configurations has been obtained from this experiment. The next chapter discusses the development and validation of the computational model in detail.

4 Bone fracture healing under Ilizarov circular fixator: influence of fixator configuration, fracture geometry and loading

Chapter summary

This chapter aims to enhance the understanding of the relationship between ICF configuration and its effects on bone fracture healing. Taking Taylor spatial frame (TSF) as an example, the roles of critical parameters (i.e. TSF ring diameter, wire pretension, fracture gap size and axial load) that govern fracture healing during the early stages were investigated by using computational modelling. A single fully coupled 3D computational model of a fractured tibia stabilized with ICF (i.e. TSF) was developed with the help of CT scan image reconstruction. The bone tissues and fracture callus were modelled as poroelastic materials and the mechanical behaviour of the tissues were modelled using porous media theory. To simulate the response of mesenchymal stem cells (MSCs) to the early mechanical environment of the callus, a previously developed mechano-regulatory theory based on deviatoric strain and fluid velocity was adopted. The computational model was first validated using the results obtained from mechanical experiments (Chapter 3). Then, the model was used to simulate mesenchymal stem cell (MSC) differentiations within different regions of the fracture site under various combinations of TSF ring diameter, wire pretension, fracture gap size and axial load values. Predicted spatially dependent MSC differentiation patterns and the influence of each parameter on differentiations were compared with *in vivo* results. This chapter provides key insights into the mechanobiology of fracture healing under ICF. In addition, this chapter exhibits the potential of computational models in assessing the performance of ICFs as well as assisting surgeons in patient specific clinical treatment planning.

This chapter is based on the article titled **"Bone fracture healing under Ilizarov fixator: influence of fixator configuration, fracture geometry and loading"** published in **International Journal for Numerical Methods in Biomedical Engineering** [21]. As the first and primary author of the article, I was responsible for the proposal of the research idea, development and validation of the computational model, analysis of results,

discussions, drawing conclusions and writing the article. My supervisors A/Prof. Lihai Zhang, Dr. Saeed Miramini and Prof. Priyan Mendis regularly discussed with me, monitored my progress and provided their inputs and feedback throughout this work. Prof. Minoo Patel of Epworth Richmond provided clinical perspectives to the problem and helped me design this study.

4.1 Introduction

Computational methods are becoming increasingly popular in orthopaedic research [99, 105, 164, 165, 178]. As described in detail in Chapter 2, several mechano-regulatory algorithms for predicting mechanobiological processes of fracture healing have been proposed so far [58, 99]. Based on such algorithms, numerous computational models have been developed to study the influence of different fixator devices on fracture healing [164, 165, 183]. However, computational studies on ICF or its influence on fracture healing are very limited and it is still not clear how ICF configuration alters the fracture environment and affect the healing process.

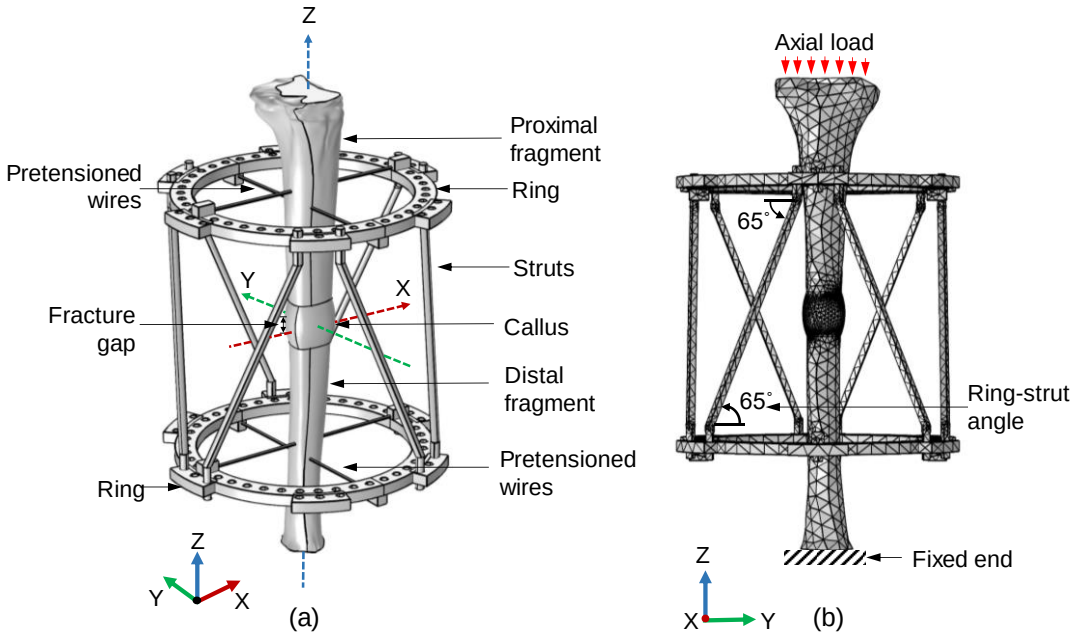

Figure 4.1 (a) Schematic diagram showing the configuration of the Taylor spatial frame (TSF) used in this study; (b) finite element model of the fractured tibia stabilised using TSF

In this chapter, Taylor spatial frame (TSF) was used as an example to study this problem (Figure 4.1). By developing computational models validated using mechanical experimental data (Chapter 3), this study aims to investigate the influence of TSF configuration (i.e. ring diameter and wire pretension) on the mechanical environment of the fracture site. It was specifically focused on the influence of TSF configurations on MSC differentiation during the early stages of healing as this is one of the most important biological processes responsible for tissue synthesis during fracture repair. In addition, the effects of axial loading and fracture gap size on fracture environment are also investigated. This chapter mainly focuses on the early stage of fracture callus (i.e. post inflammatory phase callus consisting of granulation tissue) as it has been shown that the early stage fracture site is very critical and decisive of the cell fate which could affect the entire healing process [16, 184].

4.2 Materials and Methods

The methodology adopted in this study is depicted in Figure 4.2. As described in detail in Chapter 3, mechanical tests were carried out on surrogate bone specimens with transverse fractures stabilized by a two ring TSF. The IFM measurements obtained in the experiment were used to validate the numerical predictions made using a computational model (Figure 4.1) developed in this study. After model validation, the computational model was used to predict MSC differentiations within the early callus under different combinations of gap size, axial load, ring diameter and wire pretension.

4.2.1 Computational modelling

The 3D geometry of the tibia was reconstructed from CT scan images of the surrogate tibia, which enabled the tibial geometry to be reconstructed with its inner open volumes. The geometry was then imported to the commercial CAD software SOLIDWORKS (Dassault Systèmes, Massachusetts, USA) where the geometric operations were carried out. The finalised geometry of the fractured tibia was then imported to the commercial finite element software package COMSOL Multiphysics (COMSOL AB, Stockholm, Sweden) where the geometry of the TSF was developed around the tibia. Subsequently meshing and numerical analysis were conducted using COMSOL Multiphysics.

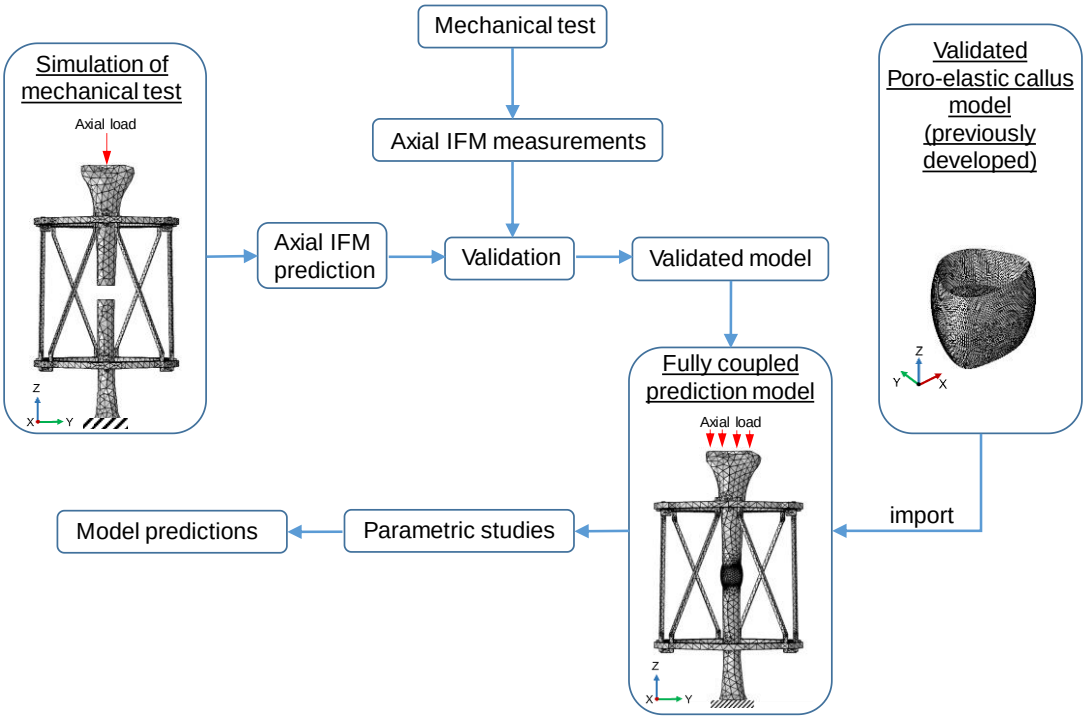

Figure 4.2 Methodology adopted in this study

Table 4.1 Properties of materials used in this study

Material	E (MPa)	υ	Φ	k ($m^4 N^{-1} s^{-1}$)	K_s (MPa)	K_f (MPa)
Cortical bone	20000 [105]	0.3 [105]	0.04 [105]	10^{-17} [105]	13920 [105]	2300 [105]
Bone Marrow	2 [105]	0.167 [105]	0.8 [105]	10^{-14} [105]	2300 [105]	2300 [105]
Granulation Tissue	0.05 [185]	0.167 [105]	0.8 [105]	10^{-14} [105]	2300 [105]	2300 [105]
Stainless Steel [a]	197000 [144]	0.29 [144]	--------	--------	--------	--------
Aluminium [b]	69000 [186]	0.33 [186]	--------	--------	--------	--------

E – Young's modulus **υ** - Poisson's Ratio **Φ** – Porosity **k** –Permeability

K_s – Solid compression modulus **K_f** – Fluid compression modulus

[a] FAST FX struts and stainless-steel pretension wires
[b] TSF rings

First, the computational model was validated using the axial IFMs measured in the mechanical test. The purpose of this validation process is to ensure that the computational

model could be implemented to simulate IFMs (which is the mechanical stimulus for cell differentiation within the callus) under different combinations of the parameters studied (e.g. wire pretension, axial load etc.). As shown in Figure 4.2, to simulate the mechanical test, the model was created with a gap at mid height of the tibia and the material properties of SYNBONE surrogate tibia were assigned to the bone fragments. The TSF components (i.e. aluminium rings, stainless steel FAST FX struts and stainless-steel pretension wires) were modelled as linear elastic materials and axial loading was applied as a point load to represent the narrow loading region in the mechanical test (Figure 3.2 and Figure 4.2). The IFM predictions were then compared with the mechanical test results. After validation, a previously developed poroelastic callus model [165, 178, 179] was imported into the model and added around the fracture gap as shown in Figure 4.2 where the bone-callus interface was connected using continuous solid to solid connections. The properties of the materials used in this study are given in Table 4.1.

4.2.2 Governing equations

Based on the theory of porous media, the mechanical behaviour of the early stage fracture callus could be explained as given below [165, 187]. The stress tensor $\boldsymbol{\sigma}$ of the callus could be expressed as

$$\boldsymbol{\sigma} = -p\mathbf{I} + \boldsymbol{\sigma}^{\mathbf{e}} \tag{4.1}$$

where, p is the incremental interstitial fluid pressure, $\mathbf{I}$ an identity matrix and $\boldsymbol{\sigma}^{\mathbf{e}}$ the elastic stress of solid matrix [165]. Neglecting the body forces and assuming that the tissue is under quasi static condition, the momentum equation could be expressed as [165]

$$\nabla.\boldsymbol{\sigma} = -\nabla p + \nabla.\boldsymbol{\sigma}^{\mathbf{e}} = \mathbf{0} \tag{4.2}$$

where, ∇p is the gradient of p, $\nabla.\boldsymbol{\sigma}$ and $\nabla.\boldsymbol{\sigma}^{\mathbf{e}}$ are the divergences of $\boldsymbol{\sigma}$ and $\boldsymbol{\sigma}^{\mathbf{e}}$, respectively.

The continuity of solid and fluid phases could be expressed by the following divergence equation:

$$\nabla.(\mathbf{v}^{\mathbf{s}} - \mathbf{k}\nabla p) = \mathbf{0} \tag{4.3}$$

where, $\mathbf{v}^{\mathbf{s}}$ is the velocity of the solid phase and $\mathbf{k}$ is the tissue permeability tensor.

4.2.3 Mechano-regulation

As discussed in Chapter 2, several mechano-regulatory theories for fracture healing have been proposed so far [10, 57, 58, 102, 103]. These theories either use a combination of mechanical parameters such as principal strain and hydrostatic stress [102], strain and hydrostatic pressure [57], deviatoric strain and fluid velocity [58, 105] or single mechanical parameter such as interfragmentary strain [10] or deviatoric strain [103] to simulate mechano-regulation at fracture site. Isaksson et al. [99] compared several of these mechano-regulatory theories with *in vivo* sheep experimental data and concluded that the algorithm for poroelastic formulations based on deviatoric strain and fluid velocity by Prendergast et al. [58, 100, 105] was reasonably accurate, more versatile and shows better agreement with the experimental observations than the alternatives. Therefore, the theory of Prendergast et al. [58, 100, 105] was incorporated in the present study along with the material properties (Table 4.1) used in their models.

The mechano-regulatory theory of Prendergast et al. [58, 100] suggests that the differentiation of MSCs into osteoblast, chondrocytes or fibroblasts depends on the stimulation index *'S'* ($S = \gamma/a + v/b$; where, γ is the octahedral shear strain of solid phase, v is the interstitial fluid flow, a = 0.0375 and b = 3 μm s^{-1}) [100, 105]. During the early stage fracture healing, small magnitudes of S (< 1) would lead to osteoblast differentiation, S in the range of $1 < S < 3$ would lead to chondrocyte differentiation, while large magnitudes of S (> 3) would lead to fibroblast differentiation [100].

4.2.4 Boundary conditions and loading protocol

In this study, the early callus was assumed to be filled with MSC, and its external boundaries were assumed to be impermeable to fluid flow [99]. As shown in Figure 4.1a, right-handed Cartesian coordinate system was used in the model with positive X pointing the anterior direction; positive Y pointing the medial direction; and positive Z pointing proximal direction. Wire pretensions were applied as initial stress (initial condition at t = 0) to the wire elements along their axial direction (i.e. either X or Y direction depending on the orientation of the wires). The bottom end of the distal fragment was fixed. The axial compression was then applied over a period of 0.5 seconds at the top of the proximal end (in the -Z direction) as depicted in Figure 4.1b.

In real circumstances, around 60 % of the knee load is taken by the medial condyle and 40 % is taken by the lateral condyle [188]. Therefore, the distribution of load on the tibial plateau is generally nonuniform across the surface [188]. For simplification, the axial load was assumed as uniformly distributed and applied on the tibial plateau [163]. This simplification would only have little effect on the mechanical microenvironment of the bone cells. During the mechanical test, the pretension wires drilled through the bones had a very firm grip on the bones. Therefore, the wire-bone interface was modelled using rigid connections as in the study of Nielsen et al. [173] and the simulation results fitted the experimental data reasonably well (Figure 4.3).

4.2.5 Geometric non-linearity of pretension wires

The relationship between the transverse load and the corresponding deflection of the pretension wires is generally non-linear [171] due to the stress stiffening effect of the wires. This tends to increase the resistance to deflection as the transverse load increases [139]. Therefore, the geometric non-linearity of the wires was considered in the analysis.

4.2.6 Numerical solutions

As shown in Figure 4.1b, the entire geometry (including pretension wires) was meshed using second order solid tetrahedral elements. A mesh convergence analysis was conducted to determine the optimum mesh size for the model and the numerical model was solved using the time dependent solver with absolute tolerances of 10^{-1} Pa and 10^{-4} m for pore pressure and displacement, respectively. These tolerance values were chosen based on the degree of accuracy required for the solution and computational efficiency. Based on previous studies [165, 179], the dependent variables, i.e. displacement and pore pressure were calculated to 10^{-4} m (or 0.1 mm) and 10^{-1} Pa (or 0.1 Pa) accuracies. The mesh sizes were chosen such that the differences between subsequent solutions in the convergence analysis were less than 2 %. As pore pressure and fluid velocity are rapidly changing variables within the callus, the convergence analysis resulted in finer mesh for the callus than the other elements in the model. The entire geometry was meshed with 216496 and 207595 tetrahedral elements for 155 mm and 130 mm ring TSFs respectively.

4.2.7 Parametric studies

Using the developed computational model, a series of parametric studies were conducted to investigate the influence of different TSF configurations, fracture gap sizes and loading conditions on cell differentiations within the callus during the early stage of healing.

Table 4.2 Simulation cases used in this study

Case	Control Case	Gap size (mm)	Ring diameter (mm)	Wire pre-tension (N)	Axial load (N)
1) Effect of gap size					
G1	G3	1	155	883 (90 kg)	150
G3	-	3	155	883 (90 kg)	150
G5	G3	5	155	883 (90 kg)	150
2) Effect of axial load					
F1a	G1	1	155	883 (90 kg)	100
F1b	G1	1	155	883 (90 kg)	200
F3a	G3	3	155	883 (90 kg)	100
F3b	G3	3	155	883 (90 kg)	200
F5a	G5	5	155	883 (90 kg)	100
F5b	G5	5	155	883 (90 kg)	200
3) Effect of ring diameter					
R1	G1	1	130	883 (90 kg)	150
R3	G3	3	130	883 (90 kg)	150
R5	G5	5	130	883 (90 kg)	150
4) Effect of wire pre-tension					
P1a	G1	1	155	491 (50 kg)	150
P1b	G1	1	155	1275 (130 kg)	150
P3a	G3	3	155	491 (50 kg)	150
P3b	G3	3	155	1275 (130 kg)	150
P5a	G5	5	155	491 (50 kg)	150
P5b	G5	5	155	1275 (130 kg)	150

Two different ring diameters (i.e. 130 mm and 155 mm) and three different wire pretensions (i.e. 491 N (50 kg), 883 N (90 kg) and 1275 N (130 kg)), gap sizes (i.e. 1 mm, 3 mm and 5 mm) and axial loads (i.e. 100 N, 150 N and 200 N) were considered in this study as shown in Table 4.2. The cell differentiations within different regions of the fracture callus, namely, periosteal callus, intercortical callus and endosteal callus (Figure 4.4b) were numerically predicted under each of the cases (Table 4.2).

4.3 Results

4.3.1 Model validation

Figure 4.3 compares the mean axial IFM components calculated from the mechanical test with those predicted numerically. It was observed that the numerical predictions were either within the experimental error range or very close to the mean IFM values (maximum of 7 % deviation) for the entire range of loading considered. Therefore, the developed computational model could reproduce the mechanical experiment reasonably well.

4.3.2 Parametric studies

Spatially dependent MSC differentiation pattern

After validation, the model was used to investigate the effects of fracture gap size, axial load, TSF ring diameter and wire pre-tension on MSC differentiations during the early stage healing. Figure 4.4 shows cell differentiations within the fracture callus, stabilized with TSF (ring diameter = 155 mm, wire pre-tension = 883 N (90 kg) and axial load = 150 N) under different gap sizes (i.e. 1 mm, 3 mm and 5 mm).

The 3D contour results in Figure 4.4c show the MSC differentiation patterns within the callus. In addition, the longitudinal sections have been given to illustrate the results better by showing the typical MSC differentiation patterns within periosteal, intercortical and endosteal regions of the callus. Thus, the longitudinal section results supplement the 3D contour results of the model. As seen from the 3D contour results, by far, the MSC differentiation patterns in each region throughout the callus are similar to those illustrated in the corresponding longitudinal sections. Thus, the longitudinal section results in

conjunction with the 3D contour results give a better understanding of the MSC differentiation patterns within the callus.

It can be seen that, MSC differentiation in the fracture callus is spatially dependent with osteoblast differentiation occurring in both proximal and distal ends of the external callus (i.e. periosteal callus) far from the fracture gap, chondrocyte differentiation occurring in the external callus and fibroblast differentiation occurring within the internal callus (i.e. intercortical and endosteal callus).

Histological observations of early stage bone fracture healing [47, 189, 190] have shown that (i) bone forming from intramembranous ossification (i.e. directly from osteoblasts) takes place farther away from the fracture site in the external callus adjacent to periosteum where the IFMs cause very little strain; (ii) formation of cartilaginous tissue from chondrocyte differentiation takes place in the external callus adjacent to the fracture line; and, (iii) fibrous connective tissue forms within the fracture gap and between the cartilaginous zones where the tissue strains are high. It can be seen that, the predicted differentiation patterns in Figure 4.4 agree reasonably well with patterns observed histologically [47, 189, 190]. Furthermore, as shown in Figure 4.4, the model predicts that the internal and external callus regions are in different mechanical environments. The internal callus is affected more than the external callus as a result of IFM which concurs with other studies in the literature [19, 105]. Figure 4.5 – Figure 4.8 presents the influence of each parameter (i.e. gap size, axial load, wire pretension and ring diameter) on the cell contents within different regions of the callus (i.e. periosteal, intercortical and endosteal). But, the results of callus regions where there were no significant changes (all changes < 5%) are not presented in those figures.

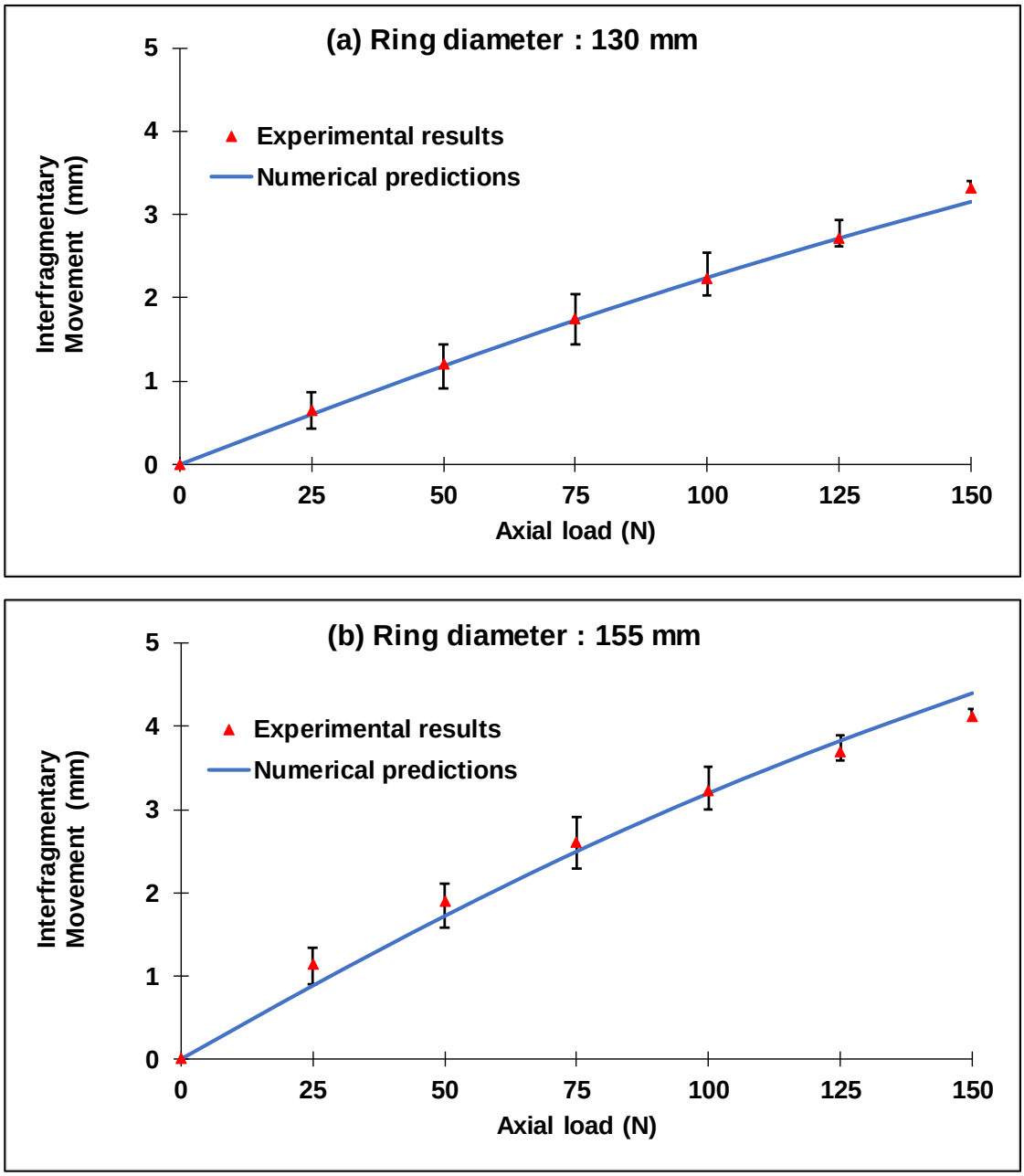

Figure 4.3 Comparison of axial interfragmentary movements (IFMs) obtained from the experiment and numerical simulation of the experiment (gap size = 20 mm, wire pre-tension = 883 N [90 kg]): (a) 130-mm diameter ring and (b) 155-mm diameter ring

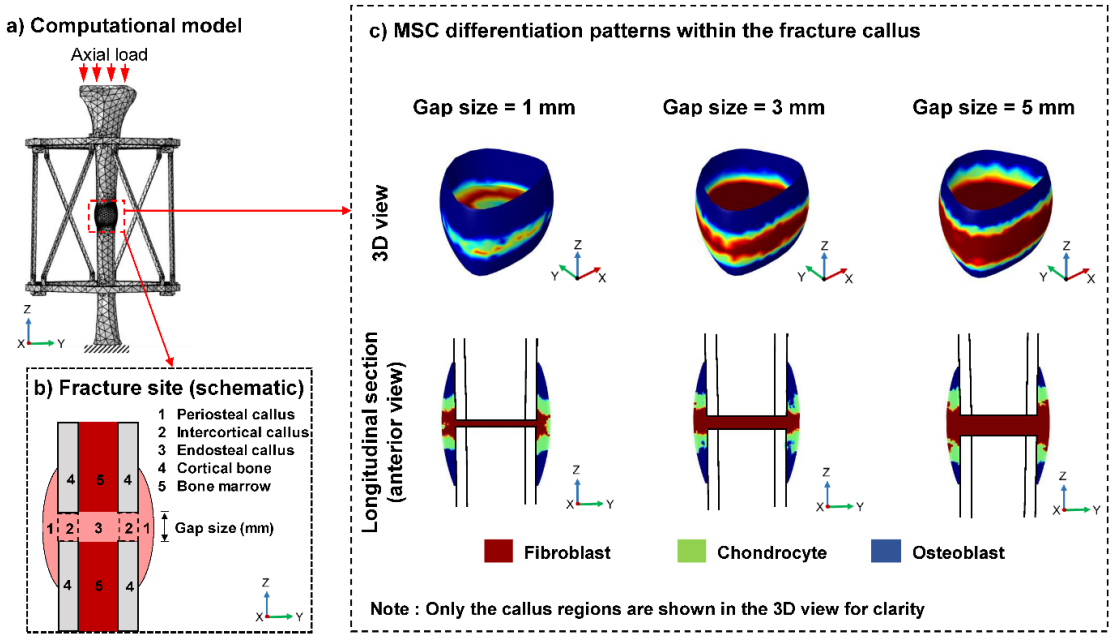

Figure 4.4 (a) Computational model of the fractured tibia; (b) schematic diagram of the longitudinal section of the fracture site showing different regions of the fracture site; and (c) spatially dependent cell differentiations within the fracture callus stabilised with Taylor spatial frame (ring diameter = 155 mm, wire pre-tension = 883 N [90 kg], and axial load = 150 N) under different gap sizes (i.e. 1, 3, and 5 mm)

Gap size

Figure 4.5 shows the change of fibroblast, chondrocyte and osteoblast contents relative to the control case G3 (i.e. gap size = 3mm (Table 4.2)) under different gap sizes (i.e. 1 mm and 5 mm). The results show that cell differentiation is very sensitive to gap size. Decreasing the gap size from 3 mm to 1 mm increased the osteoblast content by around 120 % but decreased the chondrocyte and fibroblast contents by around 70 % and 90 %, respectively in the periosteal callus. On the other hand, increasing the gap size from 3 mm to 5 mm, increased the fibroblast content in the periosteal callus by around 80 % but decreased the osteoblast content by around 55 %. In the intercortical callus, the changes were relatively small (< 4 %) and the cells were mostly fibroblasts. However, in the endosteal callus, chondrocyte content increased (by 35 %) and the fibroblast content decreased (by 35 %) as the gap size decreased from 3 mm to 1 mm. However, no noticeable changes were seen when the gap size increased.

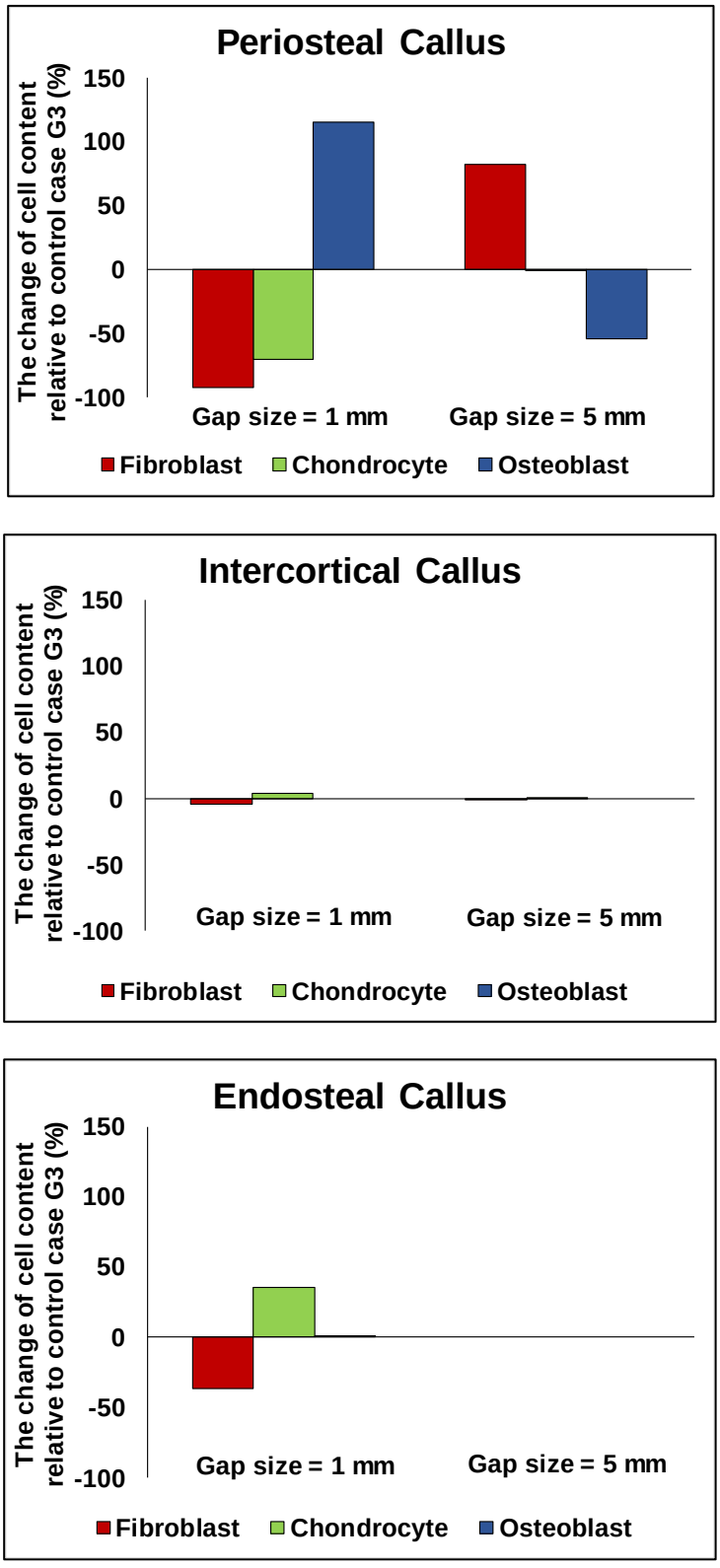

Figure 4.5 The change of cell contents within different regions of the callus relative to control case G3 (ring diameter = 155 mm, gap size = 3 mm, wire pre-tension = 883 N [90 kg], and axial load = 150 N) under different gap sizes (i.e. 1 and 5 mm)

Axial load

(a) Gap size = 1 mm

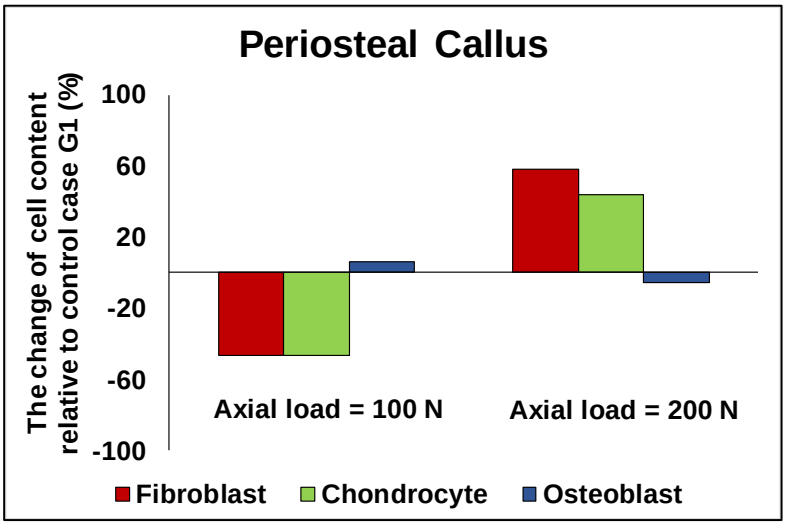

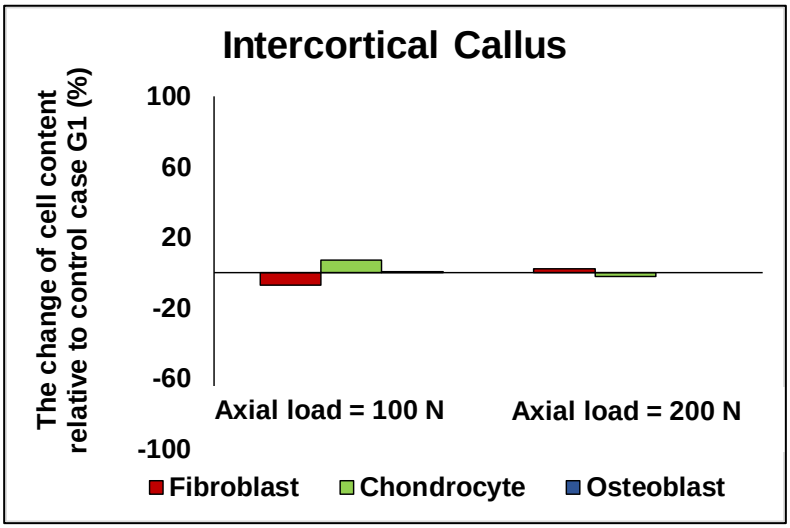

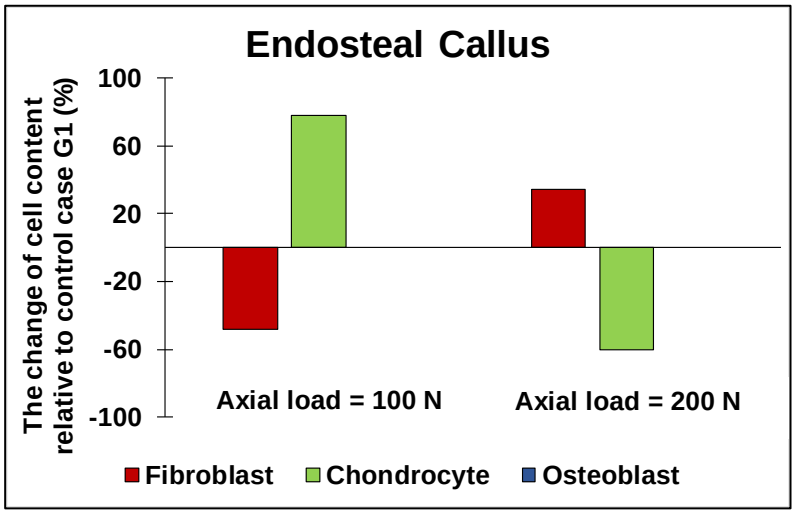

(b) Gap size = 3 mm

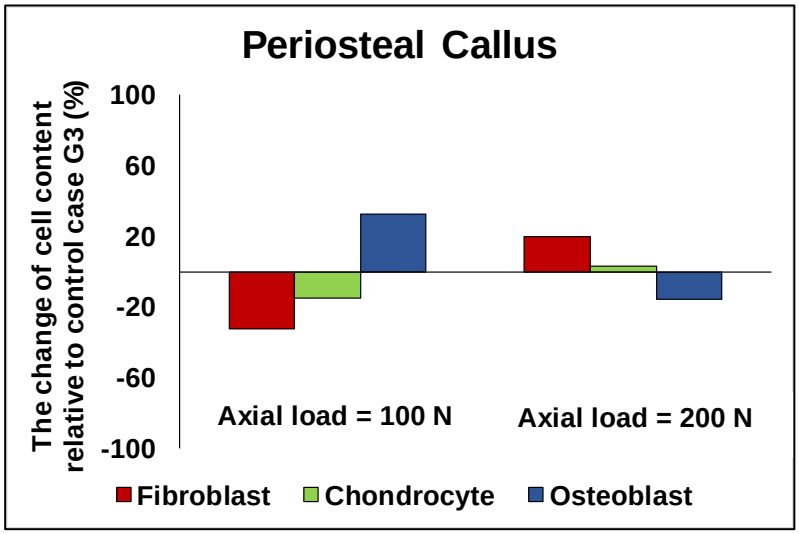

(c) Gap size = 5 mm

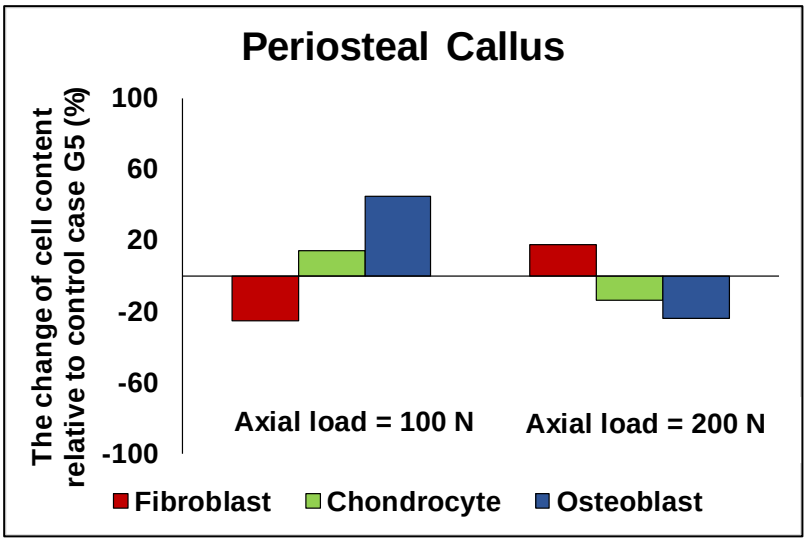

Figure 4.6 The change of cell contents within different regions of the callus under different axial loads (i.e. 100 and 200 N) relative to control case G1 for (a) 1 mm, relative to control case G3 for (b) 3 mm, and relative to control case G5 for (c) 5-mm gap sizes
(note : callus regions with negligible cell content changes are not shown)

Figure 4.6 shows the changes in cell contents within different zones of the callus under different axial loads (i.e. 100 N and 200 N) relative to control case (i.e. axial load = 150 N (Table 4.2)). It indicates that the influence of axial load on cell differentiation is location and gap size dependent. For example, under a small gap size (i.e. 1 mm), the change in the magnitude of axial load had little influence on osteoblast content; however,

under mid and large gap sizes (i.e. 3 mm and 5 mm), obvious increase (i.e. up to 45%) was seen in the periosteal callus when reducing axial load from 150 N to 100 N. In the endosteal and cortical callus no noticeable changes were seen in the osteoblast content.

Differentiation of chondrocytes in the periosteal zone, increased with the axial load for small and medium sized gaps (i.e. 1 mm and 3 mm); however, under a large gap size (i.e. 5 mm), increase in axial load predicted decrease in chondrocyte content. The fibroblast content in the periosteal callus generally increased with axial load and the increase was more prominent under relatively small gap sizes (e.g. 1 mm) as shown in Figure 4.6. No noticeable changes in the chondrocyte or fibroblast contents were predicted in the intercortical or endosteal callus due to changes in axial load magnitude for mid and large gap sizes (i.e. 3 and 5 mm). However, for 1 mm gap, endosteal callus showed increase of chondrocytes (up to 80 %) and decrease of fibroblasts (50 %) as the load reduced to 100 N; but, decrease of chondrocytes (up to 60 %) and increase of fibroblasts (35 %) were noticed as the load increased to 200 N.

TSF ring diameter and wire pretension

Figure 4.7 shows the changes in cell contents within different callus regions under 130 mm diameter ring relative to control case (i.e. ring diameter = 155mm (Table 4.2)) for different gap sizes. The results show that decreasing the ring diameter from 155 mm to 130 mm affects osteoblast content significantly (around 20 % increase); but, only in the periosteal callus for large gap sizes (e.g. 5mm). The increase in TSF mechanical stiffness resulting from the reduction of the ring diameter from 155 mm to 130 mm was insufficient to affect the fibroblast or chondrocyte contents significantly except in the endosteal callus for small gap sizes (e.g. 1 mm) where chondrocytes increased and fibroblasts decreased by 20 % and 15 % respectively. Figure 4.8 shows the effects of different wire pretensions on cell contents within different regions of the callus relative to control case (i.e. 883N or 90 kg (Table 4.2)). The changes in wire pretension significantly changed the osteoblast content (around 10 %) only in the periosteal callus under a large gap size (i.e. 5 mm). The fibroblast contents did not change significantly by changing the wire pretensions and the chondrocyte content was also not predicted to change significantly, except in the endosteal callus for a small gap size (i.e. 1 mm) where 10 % increase was observed as the wire pretension increased to 1275 N.

(a) Gap size = 1 mm

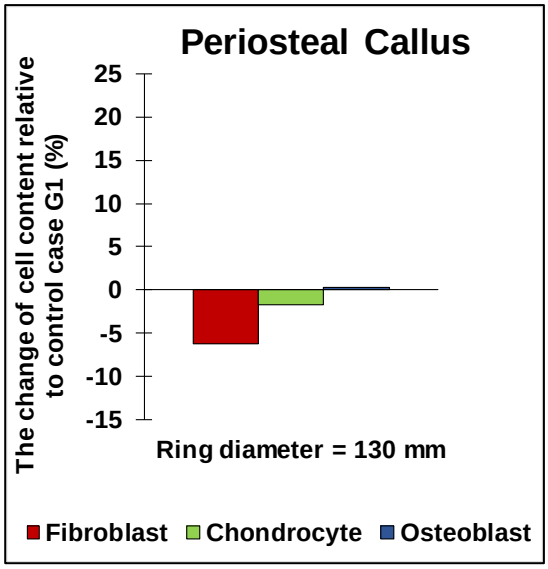

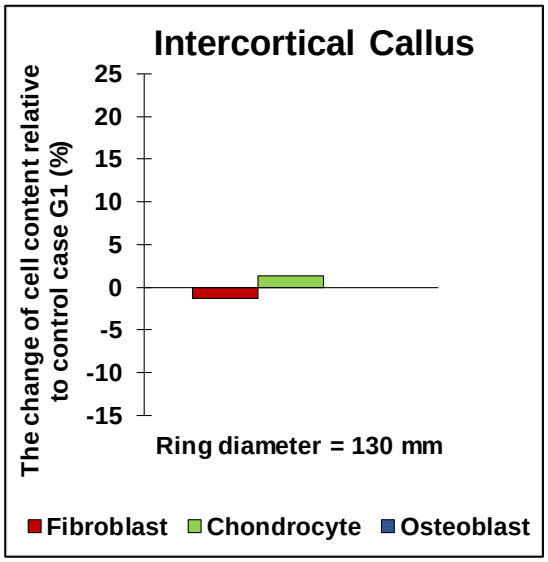

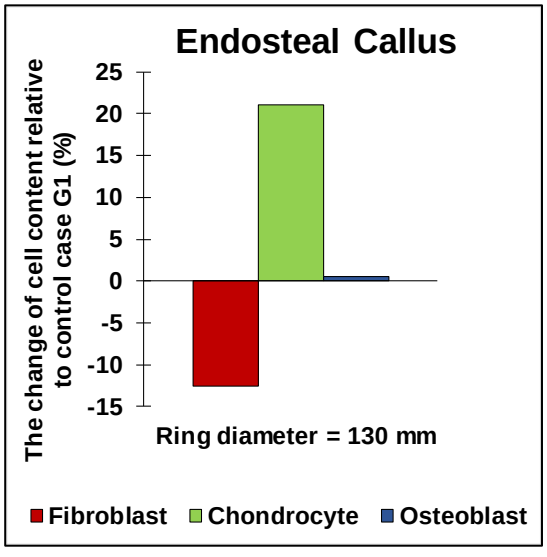

(b) Gap size = 3 mm

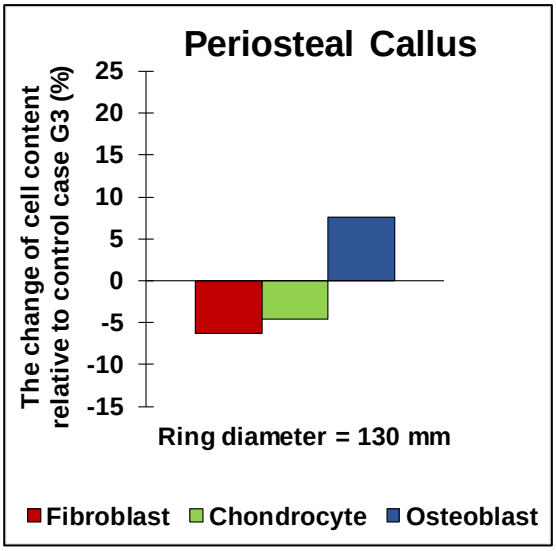

(c) Gap size = 5 mm

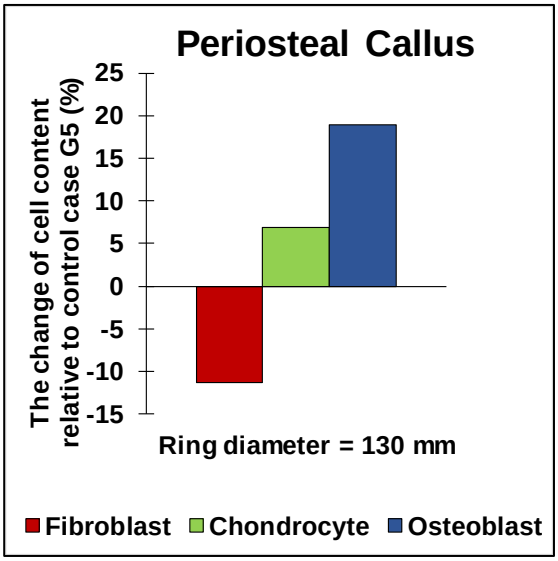

Figure 4.7 The change of cell contents within different regions of the callus under 130-mm diameter ring relative to control case G1 for (a) 1 mm, relative to control case G3 for (b) 3 mm, and relative to control case G5 for (c) 5-mm gap sizes
(note : callus regions with negligible cell content changes are not shown).

(a) Gap size = 1 mm

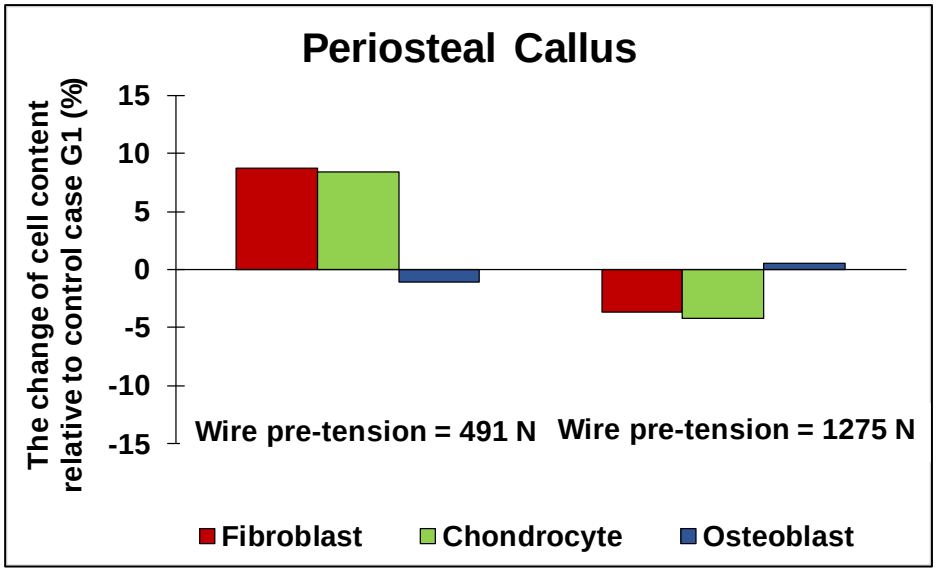

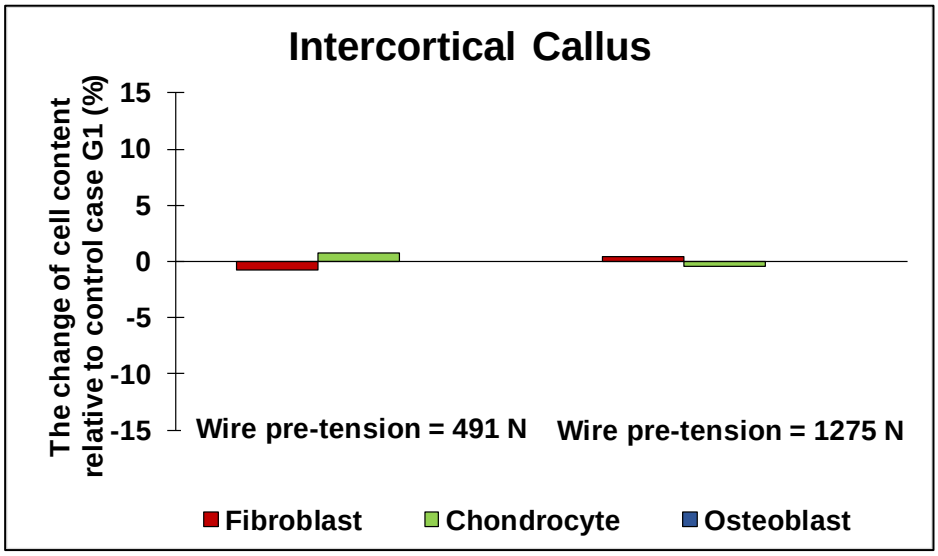

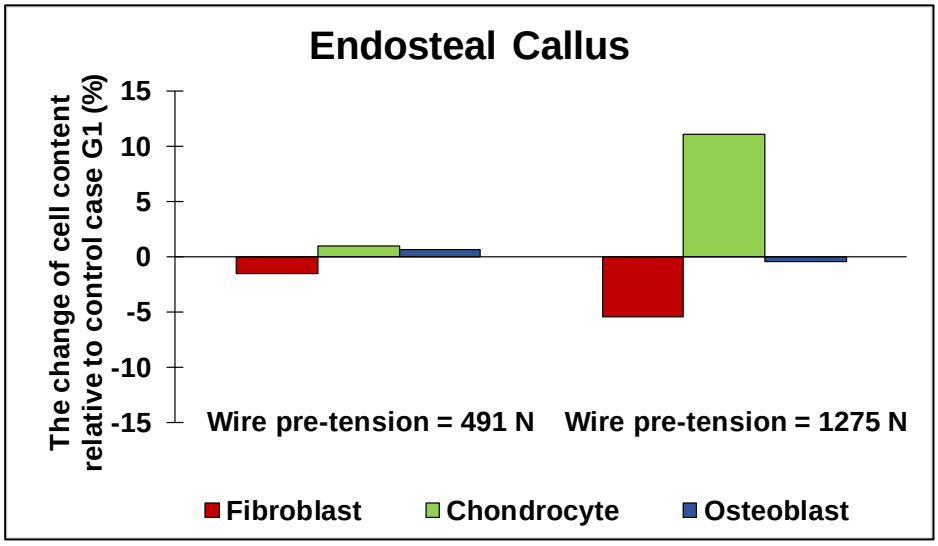

(b) Gap size = 3 mm

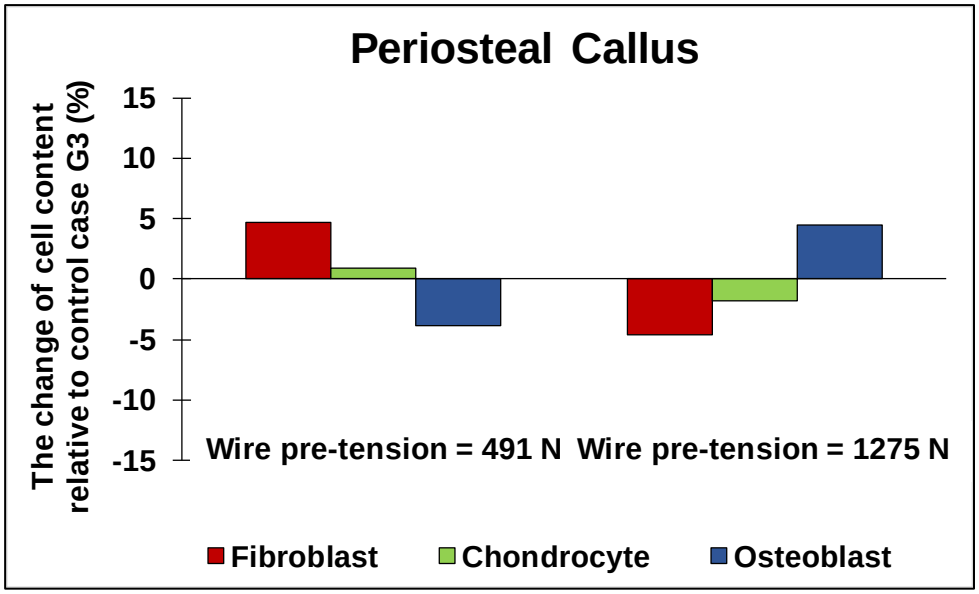

(c) Gap size = 5 mm

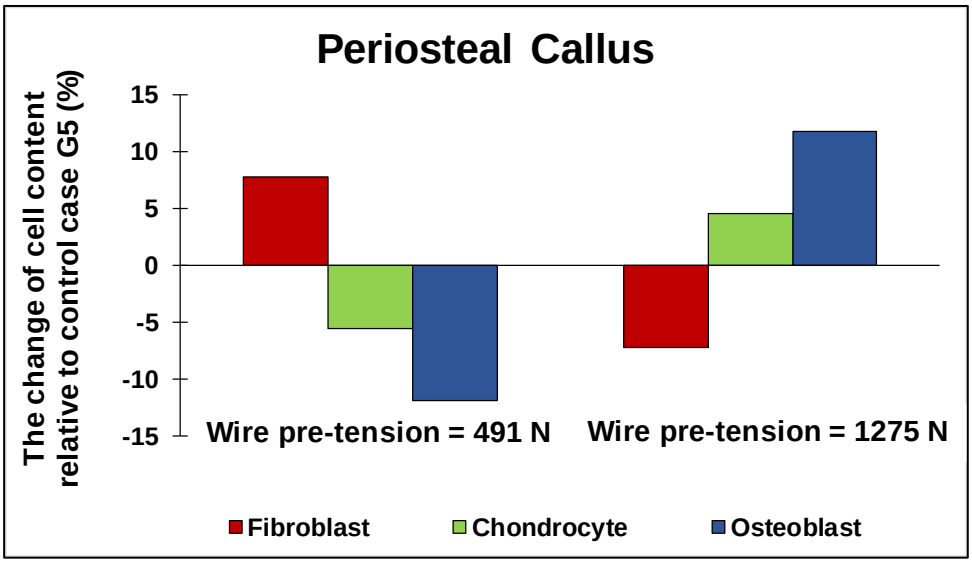

Figure 4.8 The change of cell contents within different regions of the callus under different wire pre-tensions (i.e. 491 [50 kg] and 1275 N [130 kg]) relative to control case G1 for (a) 1 mm, relative to control case G3 for (b) 3 mm, and relative to control case G5 for (c) 5 mm gap sizes
(note : callus regions with negligible cell content changes are not shown)

4.4 Discussion

Differing from previous studies in literature which mainly focus on the mechanical behaviour of Ilizarov circular fixators (in this case TSF), the current study provides a mechanobiological perspective to its performance. A single fully coupled 3D

computational model of ICF (TSF) including poroelastic soft tissues of bone is presented in this study. This enables mechanobiological assessment of the effects of fixator configuration and patient specific geometric and load conditions on the biomechanical microenvironment of the fracture site to be conducted.

Since the axial stiffness of TSF is dependent upon the IFM itself (due to stress stiffening of pretensioned wires), important parameters that affect IFM such as gap size and axial load were also considered in this study along with TSF ring diameter and wire pretension. The present study closely mimics realistic bone fracture conditions stabilized by TSF and a range of clinically relevant values were chosen for the parametric studies as follows : (i) Axial loading ranging from 100 N to 200 N, which represents the allowable weight bearing after surgery [178]; (ii) Common wire pretensions ranging from 491 N (50 kg) to 1275 N (130 kg) [121]; and (iii) TSF ring diameters of 130mm and 155mm (Smith & Nephew).

Although the computational model developed in this study mainly focuses on the early stage cell differentiations within the callus, it provides very useful data for two reasons. Firstly, the early environment is of prime importance as it is decisive of the cell fate which can affect the healing pathway of the progenitor cells and subsequently affect the entire healing process [16, 184]. Secondly, the fixator's role in the fracture stability is predominant in the early stage [79] when the fracture callus stiffness is too low with very soft tissues.

4.4.1 Predictive capacity of the model

The predictive capacity of the developed computational model was assessed by comparing the IFMs predicted by the computational model with the IFMs measured experimentally using the ARAMIS 3D optical measuring system (Figure 4.3). It was observed that the IFM predictions for 155 mm ring showed larger differences from the mechanical test compared to those of 130 mm ring. This could be possibly attributed to the relative movement of the wire in the bone-wire interface. As the wires deflect under transverse load, they tend to elongate and move relative to the bone. For 155 mm ring the effect would be more compared to that of 130 mm as the axial stiffness of 155 mm ring would be relatively low and the movements would be relatively big. Also, this effect would be more perceptible at relatively small loads, because the axial stiffness would be

low at low loads. As the load increases, the axial stiffness would increase due to stress stiffening effect and the incremental deflection of wires for a given load increment would get smaller. However, in the present model, the bone-wire interface was modelled as rigidly connected to each other. Incorporating the relative movement in the computational model would have resulted in relatively more axial movements as reported in the study of Zamani and Oyadiji [170]. Nevertheless, it could be seen that the computational model can reproduce the experimental observations reasonably well as the numerical predictions were always either within the experimental error range or very close to the mean values (maximum of 7 % deviation).

In addition, the model predicted cell differentiations were consistent with, *in vivo* observations [19, 47, 189, 190] and predictions of well-established computational models [99, 105]. For example, the cell differentiation patterns predicted in this study (Figure 4.4) concur with patterns observed in histological studies [47, 189, 190] and those predicted by the computational models of Lacroix and Prendergast [105] and Isaksson et al. [99]. In addition, the model predicted that the cell differentiations within the fracture gap is affected very much by the IFM; but, the effect of IFM gradually diminishes with the increase of distance from the fracture gap which is in line with other studies [105].

4.4.2 Parametric study and comparison with *in vivo* studies

In studying human orthopaedic conditions, rat, mouse and rabbit models are the most commonly used in laboratories [191]. However, due to the size of these animals, their applicability is limited to basic orthopaedics and acceptable only in the early stages [191]. To study more complex issues (e.g. fracture fixations) larger animals with limbs and skeletal segments of sufficient sizes such as non-human primates, sheep, goats, dogs and pigs [191] are required. Among these, sheep is found to be (i) easy to handle; (ii) more feasible in terms of economy, emotions and ethics and (iii) similar to humans in terms of body weight [191]. A lot of studies using external fixations have been carried out on sheep models in the past [19] [192-194].The present study compares the model predictions with some of the relevant sheep experiment results in the literature.

The model predicted that most of the changes resulting from parametric changes were within the periosteal region of the callus and the changes in the internal callus

(intercortical and endosteal callus) were insignificant in most cases. This is because the internal callus would be highly affected (S >> 3) by IFM in the early stages of the healing and varying the external parameters within the physiological range would not be enough to turn the mechanical microenvironment favourable (S<=3). Only reducing the fracture gap to very small sizes (e.g. 1 mm) could stabilize the environment and make it more favourable for healing as observed in sheep experiments[19, 192]. The present model was able demonstrate this as the internal callus was predicted to be favourable and responsive to other parameters only for 1 mm gap size (Figure 4.6 - Figure 4.8).

The changes in external callus (periosteal) are thought to be very crucial in the early stages as external callus plays the role of surrounding the fracture site and stabilizing it in the early stages so that the fracture site movements can be limited [47, 103, 189]. This would gradually turn the fracture site environment favourable for healing (S<=3). Therefore, this study focuses mainly on the changes within the periosteal region of the callus.

Among the four parameters explored in this study (i.e. gap size, axial load, ring diameter and wire pretension), gap size is the most critical parameter affecting the cell differentiations within the callus. As shown in Figure 4.5, relatively smaller gap sizes (e.g. 1 mm) result in larger osteoblast differentiation within the periosteal callus, which is indicative of osteogenic pathway and faster bridging of the fragments. In contrast, larger gap sizes (e.g. 5 mm) lead to the increase of fibroblast content which is indicative of delayed healing. These observations are consistent with the sheep experiment of Claes et al. [19] which investigated the roles of gap size and fracture stability on fracture healing and showed delayed healing with the increase of gap size from 1 to 6 mm. This observation could be attributed to the increase of interfragmentary strain (IFS) with gap size (when all other parameters are kept unchanged) [19, 105]. Smaller IFSs (under small gap sizes) result in more stable mechanical microenvironments (S<1) which is conductive to osteoblast differentiation, whereas relatively unstable microenvironments (S>3) resulting from larger IFS (under large gap sizes) are conductive to fibroblast differentiation.

The present study suggests that the chondrocyte content is high in the periosteal region of mid-sized (e.g. 3 mm) fractures (up to 70 % more than other gap sizes) which is indicative of greater cartilage tissue formation (Figure 4.5). This prediction is also

comparable with the results of the sheep experiment [19] which reported that a 2 mm gap size induced more cartilage formation (up to 60 %) than those of 1 mm or 6 mm gap sizes [19]. This is because mid-sized gaps (i.e. 3 mm) result in moderate IFSs which gives rise to mid-range S values (i.e. 1<S<3) within the callus which is conductive to chondrocyte differentiation and subsequently cartilage formation.

Physiologically relevant loading imposed on the fractured bone after surgery is another important factor that influences the healing outcomes. The results in Figure 4.6 show that the increase of axial load (from 150 N to 200 N) could increase the fibroblast content (up to 60 %) but decrease the osteoblast content (up to 25 %) in the periosteal callus. However, chondrocyte content could increase with the axial load only for small (i.e. 1 mm) and mid-sized (i.e. 3 mm) gaps (up to 45 % and 5 % respectively). For large gap sizes (i.e. 5 mm) chondrocyte content tends to decrease with the axial load (up to 15 %). This observation too concurs with the sheep experiment results of Claes et al.[19] where IFS increase from 7 % 31 % resulted in callus area increase of 19 % and 29 % for 1 mm and 2 mm gaps respectively; but a 37 % decrease for 6 mm gap. This is because fractures with relatively small and mid-sized gaps (i.e. 1-3 mm) are relatively stable. Therefore, moderate loading (100 – 200 N) would give rise to moderate stimulation (1<S<3), increasing the chondrocyte content. However, for relatively large gaps (i.e. 5 mm), where the fracture site is unstable, the same magnitude of load would result in larger IFS and hence higher S values (S>3), which could lead to increase in fibroblast differentiation. The implication of the model predictions is that the amount of weight bearing must be carefully chosen considering the patient specific parameters such as gap size to prevent delayed healing or non-union.

Within the range of values considered in this study, the stiffness changes due to change of TSF ring diameter or wire pretension appeared to be insufficient to make significant changes to the cell contents within the periosteal callus for small and moderate gap sizes (i.e. 1 – 3 mm). However, for a large gap size (i.e. 5 mm) significant changes were observed, especially with osteoblast content (Figure 4.7 and Figure 4.8). The results suggest that, in the early stages of healing, for small or mid-sized fractures (i.e. 1-3 mm), controlling the loading (i.e. partial weight) could be more effective than striving to modify the stiffness of TSF by changing the wire pretension or ring diameter. However, for

relatively large gap sizes (e.g. 5 mm) surgeons would also have the option of adjusting these parameters to a certain extent to control biomechanical environment of the fracture site. But the most important of all is careful reduction of the fragments; because, it would decide the gap size which is the most influential parameter of all.

In the internal callus (intercortical and endosteal), it could be seen from Figure 4.5 that reducing the gap size to 1 mm from 3 mm could result in chondrocyte increase and fibroblast decrease (around 35 % each) in the endosteal region. Furthermore, Figure 4.6-Figure 4.8 show that significant changes occur in the endosteal callus in response to other parameters only for 1 mm gap size. In general, stabilizing the fracture site increases chondrocyte content and decreases fibroblast content within the endosteal zone for small gap sizes (e.g. 1 mm). For example, decreasing the axial load (from 150 N to 100 N) or decreasing the ring diameter (from 155 mm to 130 mm) or increasing the wire pretension (from 883 N to 1275 N) could increase the chondrocyte content up to 80 %, 20 % and 10 % and decrease the fibroblast content up to 50 %, 15 % and 5 % respectively. The histological observations of sheep osteotomy sites by Claes et al.[195] showed fracture bridging to take place via both periosteal and endosteal callus for all sheep with 1 mm osteotomy which was not observed for sheep with 2 mm or 6 mm osteotomies. In addition, increasing the gap size from 1 mm to 2 mm and increase of IFS from 7 % to 31 % in the 1 mm group was observed to considerably increase the fibrous connective tissue within the fracture site. These observations are in agreement with the model predictions of this study.

A different sheep study by Yamaji et al. [192] with external ring fixators have indicated that even a larger IFS (35 %) in smaller fractures (2 mm) could result in relatively lesser connective tissues (around 50 %) within the callus than those with a smaller IFS (12 %) in larger fractures (6 mm). So, it appears that smaller fracture gap sizes could result in better mechanical environments throughout the callus.

Because of this, it is recommended that reduction of fragments need to be carried out carefully under flexible fixations such as TSF to improve fracture healing [19]. Generally, it is suggested that reductions should be made with small gap sizes as possible [19]. However, relatively large gap sizes (i.e. 5 mm or more) may sometimes become inevitable

in clinical situations. Especially, where there is significant bone loss due to high energy fractures [196] or surgical removal of bone tumours [13].

Therefore, to determine the most desirable environment within the fracture site, it is necessary to consider the patient specific parameters such as gap size and loading levels along with the fixator stiffness parameters. In this regard, models like the one presented in this study would be of assistance to surgeons in making patient specific treatment planning.

4.4.3 Limitations

It is known that tibial bone is an anisotropic material, the mechanical properties of which depend on its microstructure and mineral composition [197]. Therefore, the mechanical response of human tibia in different directions would be different [197, 198]. However, in this study, mechanical tests were carried out using surrogate tibia and the bone tissues were assumed to be isotropic to simplify the computational analysis.

It should be mentioned that, to simplify the complex loading scenarios, only axial compressive load (representing knee joint loading as uniform compression) was considered and the growth of fracture callus and change of mechanical properties were ignored in this study. In addition, bio-regulatory effects (e.g. growth factors) were not considered in this study. Moreover, as the current study was focused on the early stage, only the initial response is predicted in this study. Most importantly, further experimental and clinical evidence is required to validate the model predictions.

4.5 Conclusions

The outcomes of this study provide new insights (in a mechanobiological perspective) into the use of ICF (in this study TSF) in treating bone fractures. The computational model developed in this study enables the selection of optimal parameters (i.e. fracture gap, TSF ring diameter, wire pretension and axial loading) during the early stage fracture healing. A summary of the main findings of this study are as follows:

- The developed model was able to predict the spatially dependent MSC differentiation patterns observed in histological studies. Also, the numerical

predications from the parametric study concur well with *in vivo* observation which exhibits the potential of numerical modelling in assisting treatment planning.

- Gap size is the most important parameter that affects cell differentiations within the callus. Small gap sizes (e.g. 1 mm) could result in better healing environments throughout the callus; whereas, mid (e.g. 3 mm) and large size (e.g. 5 mm) gaps tend to rely mostly on periosteal stabilization. Therefore, careful reduction of the fracture is of paramount importance.
- The influence of axial loading on cell differentiation is gap size dependent. The changes in cell differentiation due to axial load changes are mainly noticeable in the periosteal callus; but for small gap sizes (e.g. 1 mm) changes are noticeable throughout the callus.
- The change in TSF mechanical stiffness resulting from change of ring diameter (i.e.155 mm to 130 mm) or wire pretension (491 N – 1275 N) could only change the cell contents in the periosteal callus significantly for large gap sizes (e.g. 5mm). In addition, the changes are mainly noticeable in the osteoblast content. For smaller gap sizes (e.g. 1 mm) significant changes (up to 20 %) could be achieved within the internal callus as well.
- It is preferable to achieve gap sizes as small as possible. But, when larger gap size (e.g. 3 – 5 mm) are unavoidable, controlling the axial load (i.e. partial weight bearing) would be more effective than adjusting the TSF stiffness by changing the ring diameter or wire pretension in the early stages of healing.

5 The Effects of Dynamic Loading on Bone Fracture Healing Under Ilizarov Circular Fixators

Chapter summary

This chapter is adapted from the article of the **same title** published in the **Journal of Biomechanical Engineering** [22]. As the first author of the article, the key responsibilities of proposing the research idea, developing the methodology, analysing and interpreting the results, drawing conclusions and writing the article were mine. My supervisors A/Prof. Lihai Zhang, Dr. Saeed Miramini and Prof. Priyan Mendis provided their inputs and feedback throughout and were actively involved in all phases of this work. Prof. Minoo Patel, Prof. Peter Ebeling and Prof. Yulong Wang provided clinical perspectives to the problem and helped me in designing the study.

This material has been removed by the author of this thesis for copyright reasons

This material has been removed by the author of this thesis for copyright reasons

This material has been removed by the author of this thesis for copyright reasons

This material has been removed by the author of this thesis for copyright reasons

This material has been removed by the author of this thesis for copyright reasons

This material has been removed by the author of this thesis for copyright reasons

This material has been removed by the author of this thesis for copyright reasons

This material has been removed by the author of this thesis for copyright reasons

This material has been removed by the author of this thesis for copyright reasons

This material has been removed by the author of this thesis for copyright reasons

This material has been removed by the author of this thesis for copyright reasons

This material has been removed by the author of this thesis for copyright reasons

This material has been removed by the author of this thesis for copyright reasons

This material has been removed by the author of this thesis for copyright reasons

This material has been removed by the author of this thesis for copyright reasons

This material has been removed by the author of this thesis for copyright reasons

This material has been removed by the author of this thesis for copyright reasons

This material has been removed by the author of this thesis for copyright reasons

This material has been removed by the author of this thesis for copyright reasons

This material has been removed by the author of this thesis for copyright reasons

This material has been removed by the author of this thesis for copyright reasons

This material has been removed by the author of this thesis for copyright reasons

This material has been removed by the author of this thesis for copyright reasons

This material has been removed by the author of this thesis for copyright reasons

6 Optimal time-dependent levels of weight-bearing for bone fracture healing under Ilizarov circular fixators

Chapter summary

It is known that weight-bearing exercises under Ilizarov circular fixators (ICF) could enhance bone fracture healing by mechano-regulation. However, interfragmentary movements (IFMs) at the fracture site induced by weight-bearing may inhibit angiogenesis and ultimately delay the healing process. To tackle this challenge, a computational model is presented in this chapter. The model incorporates angiogenesis and considers the spatial and temporal changes in mechanical properties of fracture callus to predict optimal levels of weight-bearing during fracture healing under ICF. The study takes sheep fracture as example and shows that the developed model has the capability of predicting patient specific, time-dependent optimal levels of weight-bearing which enhances mechano-regulation mediated healing without hindering the angiogenesis process. The findings of this study have potential applications in designing post-operative weight bearing exercises.

6.1 Introduction

It is well known that bone fracture healing is a very complex process involving many cellular, molecular and tissue level events in an orchestrated manner [48]. These events are regulated by many biological and mechanical factors and are controllable externally. The basis behind choosing a treatment strategy is to provide the most favourable environment for healing. One of the most important requirements of successful healing is re-establishment of vasculature within the fracture site [20, 152]. Therefore, it is essential that the angiogenesis process is not hindered within the fracture site during healing. The other prerequisite for the fracture healing is mechanical stability [152]. It is known that unstable fractures end up in delayed unions or non-unions. One of the reasons behind this phenomenon is that unstable fracture environments can affect both angiogenesis and synthesis of bone tissue [152, 224]. As explained in Chapter 2, if fracture site is rigidly fixed, fractures tend to heal by primary healing where bone tends to re-establish itself from the existing bone fragments [19, 49, 223].

Under flexible fixations, most fractures heal by secondary fracture healing, where the healing process goes through three distinct but overlapping phases [47, 49]. The phases of secondary fracture healing are explained in detail under Chapter 2. However, they are briefly described again to provide background to the research problem addressed in this chapter.

Secondary healing begins with the ‘inflammation phase’. Soon after fracture, due to rupture of blood vessels, blood flows into the fracture site to form haematoma which is soon followed by inflammatory response [94]. Haematoma is subsequently replaced with very soft fibrous granulation tissue which forms the initial fracture callus. This acts as a temporary scaffold for the cascade of cellular activities in the subsequent phases [94].

Early callus provides an excellent environment for multipotent mesenchymal stem cells (MSCs) to migrate within the fracture site and differentiate into tissue forming cells like osteoblasts, chondrocytes and fibroblasts [48]. This differentiation process is regulated by the local mechanical and biological environments and thus spatially varying within the callus. Osteoblasts are formed to synthesise woven bone tissue via intramembranous ossification at relatively low strain environments close to the periosteum and far from the fracture gap [47]. Within the unstable fracture gap, MSCs predominantly differentiate

into fibroblasts to synthesis fibrous connective tissue. In other regions MSCs differentiate into chondrocytes to synthesis cartilage tissue [47]. Bone forming front gradually moves towards the fracture gap as healing progresses, while cartilage stabilizes the areas surrounding the fracture gap [47, 57]. Subsequently, cartilage gets transformed into woven bone tissue by endochondral ossification as the environment becomes favourable for osteogenesis. These changes lead to stiffening of external callus and minimization of interfragmentary movement (IFM) within the fracture gap. As the fracture gap becomes increasingly stable, fibrous tissue gets replaced by woven bone tissue via intramembranous ossification [47]. In summary, during this phase, fracture is repaired by transforming the initial soft granulation tissue filled callus entirely into woven bone via different pathways and hence called the reparative phase.

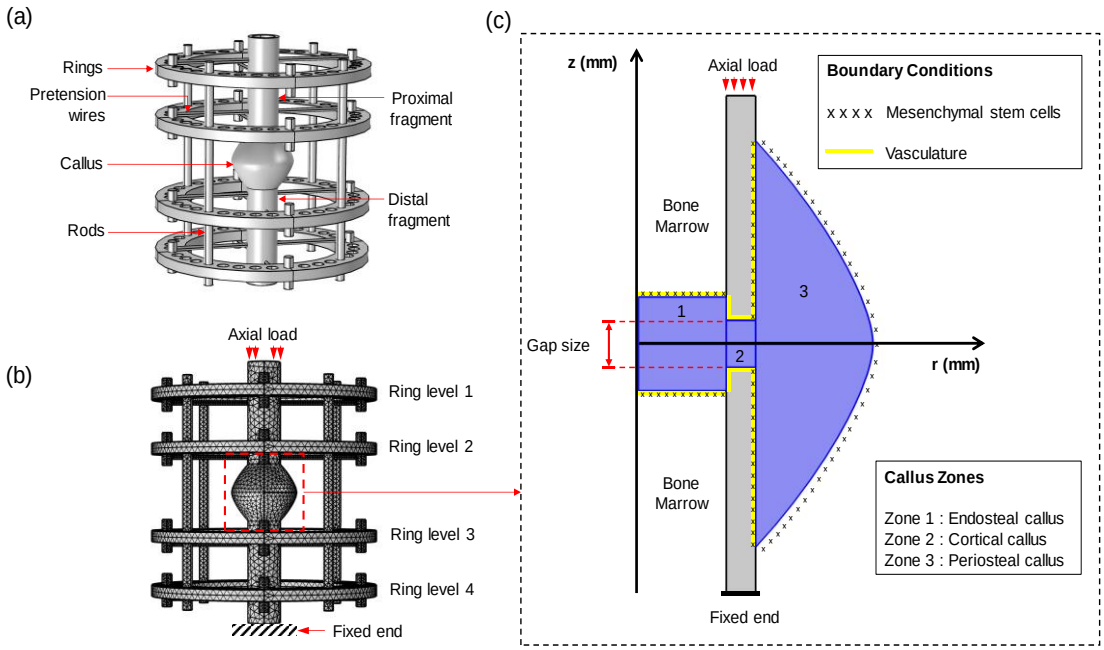

Figure 6.1 (a) Schematic diagram showing the configuration of the Ilizarov circular fixator (ICF) used in this study; (b) 3D finite element model of the ICF; and (c) boundary conditions of the 2D axisymmetric model .
The 2D model was used to simulate the spatial and temporal changes in angiogenesis, cell differentiations and material properties within the fracture site and the 3D model was used to simulate the corresponding mechanical response at the fracture site under different ICF configurations and physiological loading (weight-bearing).

In the next phase, woven bone is fully replaced by well organised lamellar bone by a process known as remodelling. This process may take several months to years after the fracture is fully bridged by woven bone. During the remodelling phase, bone regains its pre-fracture geometry and strength [26, 225]. In clinical point of view, no further

treatment is generally necessary after the end of reparative phase. The fracture is deemed to have healed if clinical union of bone fragments is detected [5]. Therefore, the objective of surgeons is to shorten the reparative phase and achieve clinical union within accepted timeframes. This requires maintenance of conductive environments within the fracture site as much as possible. Experimental evidence suggests that, level of vascularity and local mechanical stability play vital roles in regulating tissue synthesis in the reparative phase [20, 152]. Therefore, it is essential to have deeper understanding about these factors.

Fracture healing involves enhanced metabolic activities, which requires additional supply of oxygen and other essential factors such as nutrients [226]. However, due to rupture of blood vessels, enough blood supply does not prevail within the fracture site, which leads to shortage of these essential factors. Studies have revealed that angiogenesis begins from existing vasculature at a very early stage of fracture healing [47, 190]. As angiogenesis progresses, the increase of blood supply increases the supply of oxygen and other essential factors and removal of metabolic wastes. Studies have reported that angiogenesis precedes osteogenesis, which suggests that enough blood supply is a prerequisite for osteogenesis [226]. On the other hand, avascular environments with insufficient blood supply are conductive to chondrogenesis [47, 102]. Clearly, the level of blood supply is a regulator of differentiation pathway and tissue synthesis. However, the level of blood supply alone may not be enough to fully describe the differentiation process as vascularized zones of callus do not always lead to osteogenesis but also fibrogenesis [152, 227]. This indicates that there should be at least one more factor that governs the differentiation pathway.

It has been reported that bone tissues form under relatively stable environments, whereas fibrous tissue forms under relatively high strains [152]. If good blood supply condition exists, mechanical stability controls whether osteogenic or fibrogenic pathway is taken during the healing process. Histological studies have shown that, bone formation begins adjacent to periosteum, but far from the fracture gap [47, 190], where the early blood vessels are observed and the tissue strains are relatively small. The progression of ossification follows revascularization and occurs adjacent to previously formed bone tissues where the tissue strains are minimal [47, 57, 226]. On the other hand, fibrous tissue begins to form within the fracture gap, which is in proximity to vasculature under

relatively high tissue strains. Cartilage is formed in avascular and hypoxic regions where there is no formation of other two types of tissues [47, 107]. Later on, with blood vessels invading the callus, cartilage is gradually replaced by woven bone (*i.e.* endochondral ossification) [47, 190]. Therefore, fracture healing process can be described based on the local level of blood supply and tissue strain. It should also be noted that tissue strain does not only affect the differentiation pathways and tissue synthesis, but also angiogenesis. Relatively high tissue strains lead to blood vessel rupture and inhibition of angiogenesis [47]. Thus, tissue strain has a direct and indirect effect on differentiation pathways.

To enhance intramembranous or endochondral ossifications during bone repair, it is essential that angiogenesis process is not hindered. This requires relatively low mechanical strains within the fracture site. However, very low strains can lead to significant resorption which leads to loss of bone mass, stiffness and strength [81, 82, 228]. Therefore, there should be an optimal range of tissue strains that promote both angiogenesis and osteogenesis. Determining the level of weight-bearing corresponding to the optimal tissue strain range would have clinical significance as it would allow therapists to determine patient specific physiological exercises under different fixation configurations.

Many studies in the past have reported that too rigid or too flexible fixations are not very beneficial for healing and there should be an optimal range of stiffness for the ideal healing conditions [19, 165, 183, 229]. However, there is no clear consensus as to what this range is. Therefore, the selection of the most appropriate fixation type and configuration is often challenging. Since there is lack of systematic investigation into this problem, surgeons generally take a trial and error approach [179]. The problem gets more complex as stiffening of callus with time constantly modifies the load share between the fixator and callus. This makes it necessary to regulate the fixation stiffness or load to maintain the optimal level of IFM throughout the course of healing.

Ilizarov circular fixators (ICF) are very beneficial in this regard as they allow adjustment of stiffness as required. The modular nature of ICF allows it to be constructed in many possible configurations to suit patient specific needs. In addition, ICFs are minimally invasive which makes them desirable. Even though ICFs are in existence for over six decades, systematic investigations on weight-bearing for the optimal healing conditions

under ICF are still lacking. Therefore, the full potential of ICFs cannot be utilized yet. It is known that patient specific parameters such as fracture geometry and fixator configuration influence fracture healing [19, 21, 178]. Therefore, the optimal weight-bearing for fracture healing need to be determined on a case-by-case basis taking patient specific parameters into account.

However, this is very challenging owing to number of patient specific factors that need to be considered and their complex interrelationships. Computational models provide an excellent framework for this problem as it can handle multiple inputs and provide reasonably accurate solutions relatively quickly. As discussed in Chapter 2, different aspects of ICF have been studied numerically using computational models in the past [21, 22, 144, 169, 170]. However, studies on determining optimal weight-bearing for fracture healing under ICF are very limited, if not totally unavailable.

The purpose of this chapter is to develop a computational framework for determining optimal weight-bearing levels for fractures treated with ICF taking patient specific factors as inputs. In this study, different ICF configurations, fracture gap sizes (GS) and body weights (BW) were considered and how these important patient specific factors affect time dependent optimal weight bearing levels for fracture healing under ICF was investigated.

6.2 Materials and Methods

This study mainly focuses on the reparative phase (second phase) of fracture healing without considering the initial inflammatory responses and the transformation of woven bone into lamellar bone (remodelling) [55, 99, 104, 230, 231]. In addition, it is assumed that local vascularity and tissue strain are two critical determinants of fracture healing. Due to availability of experimental data for validation and comparison purposes [19, 20], sheep fractures were used as an example to study the problem.

6.2.1 Problem description

The computational framework proposed in this study consists of two models. The first model is an adaptive two-dimensional (2D) axisymmetric model (Figure 6.1) of a sheep

metatarsal fracture that simulates the spatial and temporal changes of angiogenesis and cell differentiations within the fracture site during healing. When the simulation begins, vascularization starts within the post inflammation callus from existing vasculature. In parallel, MSCs start to migrate into the callus from different boundaries and differentiate into either osteoblasts, chondrocytes or fibroblasts (which are responsible for the synthesis of bone, cartilage and fibrous tissue, respectively), depending on the local tissue strain (deviatoric strain) and level of blood supply (indicated by vessel density). The mechanical properties at each spatial point of the fracture callus are calculated using the rule of mixtures from cell densities as described elsewhere [104, 107]. The model was first validated using sheep experimental data [19, 20] and then used to predict healing under different simulation cases.

The second model is a parameterized three-dimensional (3D) model of fractured sheep metatarsal stabilized with ICF, which was developed based on Chapter 5 [22]. It was used to simulate the mechanical response at the fracture site under different ICF configurations and physiological loading. The model is reconstructed before each simulation based on the parameters specified by the users (e.g. geometric, material and configuration specific parameters). The material properties of the fracture callus in the 3D model were updated at each time point based on the simulation results of the 2D model. All components of ICF including pretension wires and half pins were assumed to be made of stainless steel. Table 6.1 summarises the mechanical properties of different materials used in the model.

In this way, the complex mechano-biological simulation was reduced to a 2D axisymmetric model while the overall fixator-fracture site interaction was studied using the 3D model. This simplification is reasonable as the bone elements were assumed to be cylindrical and only uniform axial load was considered in this study [22]. Under these conditions, a circular fixator (ICF) with the configuration depicted in Figure 6.1 would result in axisymmetric displacements in response to axial loads. Therefore, the bone fragments and fracture callus (without ICF) could be treated as a 2D axisymmetric problem. This simplification improved the computational efficiency. Using this approach, the optimal weight-bearing under different combinations of ICF configurations (Table 6.2), body weights (i.e. 50-100 kg) and transverse fracture gaps (i.e. 3 - 6 mm) were

predicted as these are three important factors that affect fracture healing and weight-bearing [12].

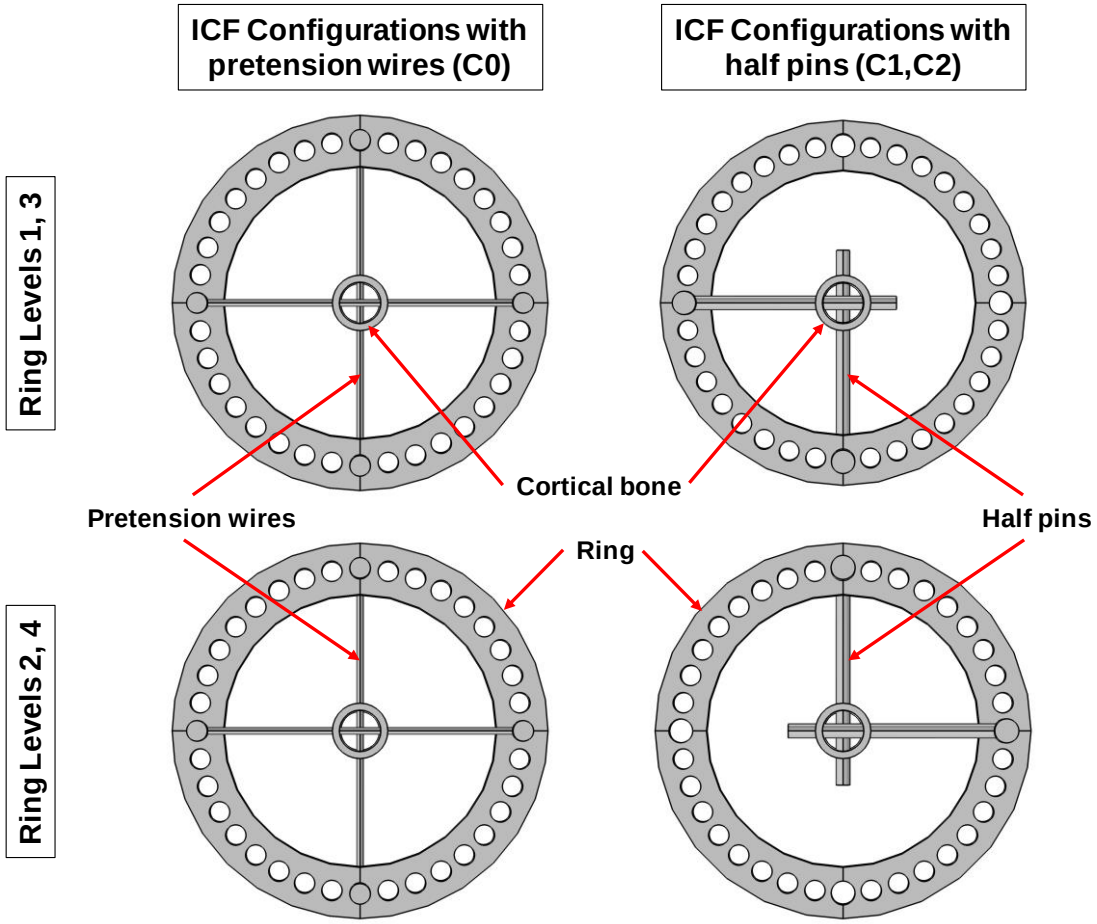

Figure 6.2 Schematic diagram showing the top view of ICF ring and pretension wire / half pin arrangement at each ring level under different ICF configurations (i.e. C0, C1, C2) considered in this study
(Note : Details of ICF configuration are summarised in Table 6.2)

6.2.2 Model Geometry

The geometry (Figure 6.1) of the fracture site was based on the geometry adopted by Claes and Heigele [57], which was established from histological observations of sheep metatarsal fractures. The cortical bone was assumed to be a hollow cylinder with an outer diameter of 16 mm and inner diameter of 12 mm, with a gap at mid height representing a transverse fracture. The fracture callus was assumed to be formed with a maximum diameter of 32 mm (Figure 6.1). Taking the approach of previous studies [55, 104, 106, 224], the same callus geometry throughout the study was assumed, neglecting callus

growth. As described in Table 6.2, the fracture site was stabilized with three different configurations of ICF: C0, C1 and C2. Each ICF configuration consists of (i) four rings in total with two rings each for proximal and distal fragments; and (ii) two wires / half pins per ring; to ensure stability [12, 232]. Figure 6.1 shows the schematic diagram of configuration C0. For configurations C1 and C2, wires were replaced with half-pins. At alternating ring levels, half pins were fixed to rings on the opposite sides to ensure uniform distribution of load (Figure 6.2).

Table 6.1 Properties of materials used in this study

Material	E (MPa)	υ	Φ	k ($m^4 N^{-1} s^{-1}$)	K_s (MPa)	K_f (MPa)
Cortical bone	20000 [a]	0.3 [a]	0.04 [a]	10^{-17} [a]	13920 [a]	2300 [a]
Mature bone	6000 [a]	0.3 [a]	0.8 [a]	3.7×10^{-13} [a]	13920 [a]	2300 [a]
Cartilage	10 [a]	0.167 [a]	0.8 [a]	5×10^{-15} [a]	3400 [a]	2300 [a]
Fibrous Tissue	2 [a]	0.167 [a]	0.8 [a]	10^{-14} [a]	2300 [a]	2300 [a]
Granulation Tissue	2 [b]	0.167 [a]	0.8 [a]	10^{-14} [a]	2300 [a]	2300 [a]
Stainless Steel [1]	197000 [c]	0.29 [c]	--------	--------	--------	--------

E – Young's modulus **υ** - Poisson's Ratio **Φ** – Porosity **k** –Permeability

K_s – Solid compression modulus **K_f** – Fluid compression modulus

[a] Lacroix and Prendergast [105] [b] Steiner et al. [106] [c] Watson et al. [144]

[1] All components of ICF including pretension wires and half pins

6.2.3 Development of the model

Fracture callus is a porous material composed of different tissues, interstitial fluid and solutes (e.g. cells). Therefore, callus was treated as a tri-phasic poroelastic material and the fracture healing model was developed using the theory of porous media. The formulation of tri-phasic callus is described in detail in Chapter 5 and previous studies [22, 233, 234]. In the poroelastic model, tissues and interstitial fluid represent the solid and fluid phases, respectively and the following four cells constituted the solute phase: MSC (c^m), osteoblasts (c^b), chondrocytes (c^c) and fibroblasts (c^{fb}).

Table 6.2 ICF Configurations considered in this study

Configuration	Description
C0	• 4-rings of 80 mm diameter (internal) • 2 x 1.8 mm diameter mutually perpendicular wires per ring • 130 kg (1275 N) wire pretension
C1	• 4-rings of 80 mm diameter (internal) • 2 x 4.0 mm diameter mutually perpendicular half pins per ring • Pins affixed on opposite sides at alternating ring levels
C2	• 4-rings of 80 mm diameter (internal) • 2 x 6.0 mm diameter mutually perpendicular half pins per ring • Pins affixed on opposite sides at alternating ring levels

Based on the model of Burke and Kelly [107], angiogenesis during fracture repair was modelled using a continuous variable, vessel density (v), to represent the level of blood supply (Figure 6.3). The values of v ranges from 0 to 1 indicating 'no blood supply' (0) and 'full blood supply' (1) conditions. New blood vessels grow from existing ones and invade callus to establish a network of blood vessels. As shown in Figure 6.3, vasculature development occurs from well vascularised zones (i.e. high values of v) towards poorly vascularized zones (i.e. low values of v) through a diffusion-like process [107, 235]. The effect of mechanical factors on revascularization was incorporated into the model by defining a tissue strain-dependent diffusion coefficient which describes the rate of angiogenesis. In other words,

$$\frac{dv}{dt} = D^v \nabla^2 v \tag{6.1}$$

where, D^v is the angiogenic diffusion coefficient defined by the following function,

$$D^v = f(\varepsilon) = \begin{cases} D^{v0}, & \varepsilon \leq \varepsilon_{ang} \\ 0, & \varepsilon > \varepsilon_{ang} \end{cases} \tag{6.2}$$

where D^{v0} is the free angiogenic diffusion coefficient, ε is the deviatoric strain and ε_{ang} is the deviatoric strain threshold for angiogenic inhibition which is in the range of 6-9 % based on previous studies [107, 108].

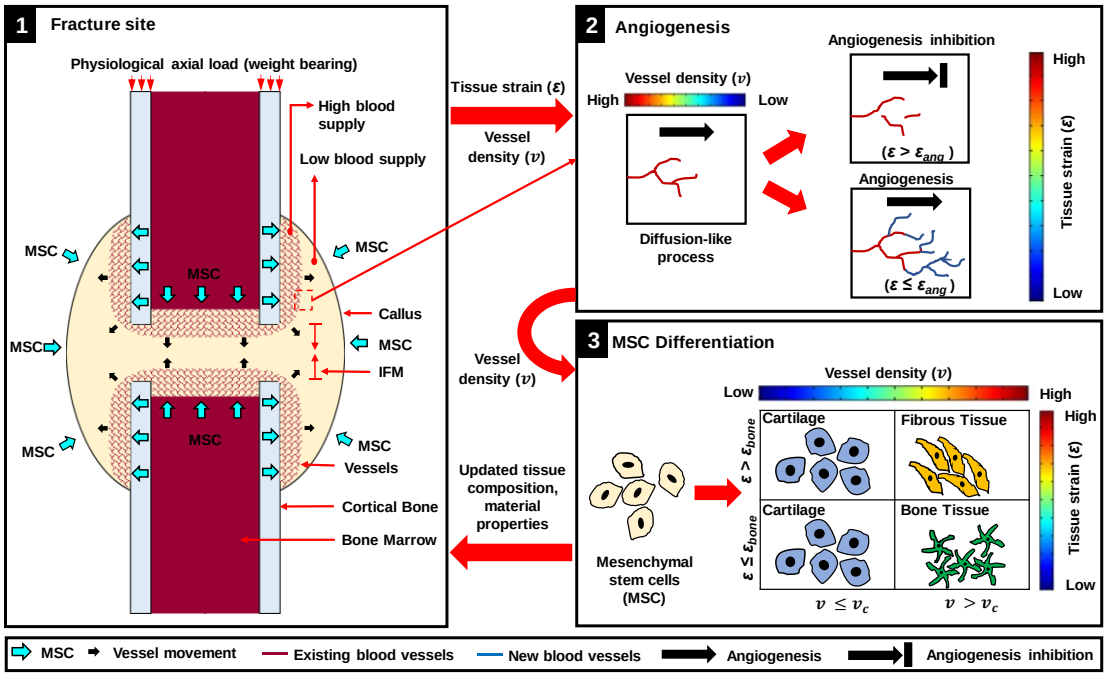

Figure 6.3 Schematic diagram showing mesenchymal stem cell (MSC) migration, differentiation and angiogenesis processes during fracture healing.

The distribution of MSCs inside the fracture callus is a complex process which involves multiple mechanisms. MSCs possess the capacity to self-renew and proliferate [236]. Inside the callus, MSCs migrate by both random and directed motions [237] involving crawling and convective transport [104]. It was assumed that proliferation and migration of MSCs can be described as the advancement of MSCs from regions of high densities to those of low densities through a diffusive process [104, 105, 107]. In addition, the distributions of osteoblasts, chondrocytes and fibroblasts within the callus were also assumed to be analogous to diffusion [55].

MSCs were assumed to take chondrogenic pathway when vessel density is below a threshold value ($v \leq v_c$) based on the study of Burke and Kelly [107]. When the vessel density is above this threshold value ($v > v_c$), MSCs take the osteogenic or fibrogenic pathways when the tissue strain is smaller than ($\varepsilon \leq \varepsilon_{bone}$) or greater than ($\varepsilon > \varepsilon_{bone}$) the allowable strain of bone tissue (ε_{bone}), respectively. Previous studies have reported

that chondrocytes can trans-differentiate directly into osteoblasts during endochondral ossification [238, 239]. There is also evidence that fibroblasts could trans-differentiate into osteoblasts [240, 241]. In this study, endochondral ossification and trans-differentiation of fibroblasts into osteoblasts were assumed to occur when the combination of v and ε are favourable for osteogenesis. The time-dependent changes of cell concentration within the callus can be described by

MSC: $$\frac{\partial \bar{c}^{\,m}}{\partial t} = -\nabla \cdot \left(-D^m \nabla \bar{c}^{\,m} + \mathbf{v^f}\, \bar{c}^{\,m}\right) - F_1 \bar{c}^{\,m} - F_2 \bar{c}^{\,m} - F_3 \bar{c}^{\,m} \qquad (6.3)$$

Fibroblast: $$\frac{\partial \bar{c}^{\,fb}}{\partial t} = -\nabla \cdot \left(-D^{fb} \nabla \bar{c}^{\,fb} + \mathbf{v^f}\, \bar{c}^{\,fb}\right) + F_1 \bar{c}^{\,m} - F_4 \bar{c}^{\,fb} \qquad (6.4)$$

Chondrocyte: $$\frac{\partial \bar{c}^{\,c}}{\partial t} = -\nabla \cdot \left(-D^c \nabla \bar{c}^{\,c} + \mathbf{v^f}\, \bar{c}^{\,c}\right) + F_2 \bar{c}^{\,m} - F_5 \bar{c}^{\,c} \qquad (6.5)$$

Osteoblast: $$\frac{\partial \bar{c}^{\,b}}{\partial t} = -\nabla \cdot \left(-D^b \nabla \bar{c}^{\,b} + \mathbf{v^f}\, \bar{c}^{\,b}\right) + F_3 \bar{c}^{\,m} + F_4 \bar{c}^{\,fb} + F_5 \bar{c}^{\,c} \qquad (6.6)$$

where, D^m, D^{fb}, D^c and D^b are the diffusion coefficients of MSC, fibroblast, chondrocyte and osteoblast, respectively; $\mathbf{v^f}$ is the true fluid velocity; F_1, F_2, F_3 are the rates of fibrogenic, chondrogenic and osteogenic differentiations of MSC, respectively; and F_4, F_5 are the rates of osteogenic differentiation of fibroblast (i.e. trans differentiation) and chondrocytes (i.e. endochondral ossification), respectively. F_1, F_2, F_3, F_4 and F_5 can be defined as

$$F_1 = p_1(\varepsilon) \times q_1(v) \qquad (6.7\text{ a})$$

$$F_2 = p_2(\varepsilon) \times q_2(v) \qquad (6.7\text{ b})$$

$$F_3 = p_3(\varepsilon) \times q_3(v) \qquad (6.7\text{ c})$$

$$F_4 = p_4(\varepsilon) \times q_4(v) \qquad (6.7\text{ d})$$

$$F_5 = p_5(\varepsilon) \times q_5(v) \qquad (6.7\text{ e})$$

where, $p_i(\varepsilon)$ is the rate of production depending on deviatoric strain and $q_i(v)$ is the production rate modifier depending on the vessel density that define cell specific production or degradation rates ($i = 1,2,3,4,5$). For simplicity, the production rates of osteoblasts by all the different processes (F_3, F_4 and F_5) were assumed to be the same (i.e. $F_3 = F_4 = F_5$) in this study. Figure 6.4 shows the $p_i(\varepsilon)$ and $q_i(v)$ functions adopted in this study.

Deviatoric strains less than 7 % [242], 3.75 % [105] and 2.5 % [103] have been reported as allowable for osteogenesis in previous studies. Perren and Cordey [243] suggested a tissue strain limit of 2 % for bone tissue synthesis based on its allowable strain limit before rupture. Another previous study [244] reported a volumetric strain threshold of 1.5 ± 0.5 % for bone formation. Likewise, blood perfusion less than 30 % has been estimated as 'low', and assumed to be conductive to chondrogenesis [230]. Another study [108], which assumed linear relationship between vessel density and oxygen tensions, estimated that oxygen tensions below a third (33 %) of the maximum oxygen tension inhibits osteogenesis and promotes chondrogenesis. This indicates that vessel densities below 33 % of the maximum vessel density is conductive to chondrogenesis. Based on these studies, ε_{bone} = 2 % and v_c = 30 % were assumed in this study.

The tissue strain-dependent production rates, $p_i(\varepsilon)$, were defined based on the study of Andreykiv et al. [210]. As shown in Figure 6.4, no fibroblast production was assumed for $\varepsilon \leq \varepsilon_{bone}$. The production rate of fibroblast was assumed to be constant (maximal) when $\varepsilon > \varepsilon_{bone}$. Osteoblast production rate was assumed to be minimal when ε is zero and increase linearly with ε until it reaches ε_{bone}, beyond which osteoblast production ceases. The production rate of chondrocytes was assumed to be constant (maximal) for all ε values as chondrogenesis is governed by the level of blood supply.

The production rates were modified using modifiers, $q_i(v)$, to account for the blood supply available locally at any given location within the callus. Since the increase in vascularization increases the supply of oxygen, nutrients and other elements necessary for metabolism [226, 245], it was assumed that vessel density dependent modifiers, $q_i(v)$, increase with vasculature density when the conditions are favourable. The production modifiers of both fibroblasts and osteoblasts were assumed to be zero for $v \leq v_c$ and reach maximum when there is enough blood supply, which was assumed to occur

for a vasculature density of 80 % (v = 0.80). In addition, it was assumed that this transition is smooth over the v interval of 0.30 to 0.80.

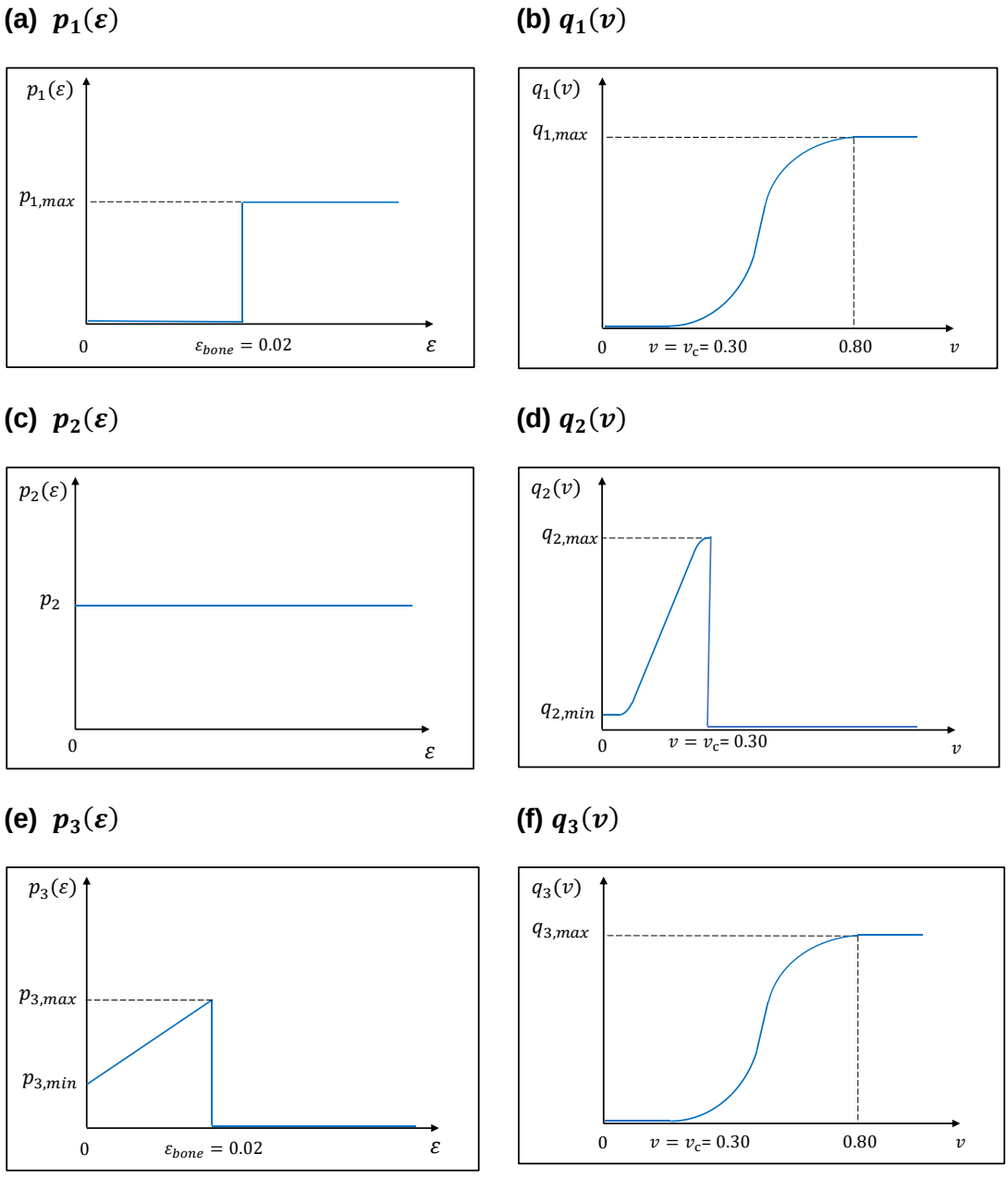

Figure 6.4 Tissue strain dependent cell production rates p_i (ε) and vessel density dependent production rate modifiers q_i (v) for fibroblasts (*i*=1); chondrocytes (*i*=2) and osteoblasts (*i*=3).

The values of the production rates adopted in this study are given in Table 6.3.

Table 6.3 Parameters related to angiogenesis and cell evolution within the callus

Parameters	Expression
Diffusion coefficient of MSC (D^m)	0.10 mm^2/day [a]
Diffusion coefficient of osteoblasts (D^b)	8.64×10^{-20} mm^2/day [b]
Diffusion coefficient of chondrocytes (D^c)	8.64×10^{-20} mm^2/day [b]
Diffusion coefficient of fibroblasts (D^{fb})	0.67 mm^2/day [c, d]
Diffusion coefficient of angiogenesis (D^v)	$f(\varepsilon)$ [e, 1]
Free diffusion coefficient of angiogenesis (D^{v0})	7.5×10^{-2} mm^2/day [f,*]
Strain threshold for angiogenesis inhibition (ε_{ang})	6 % [e]
Maximum strain limit for osteogenesis (ε_{bone})	2 % [g,h]
Maximum strain limit for bone resorption (ε_{res})	0.005 % [h]
Maximum vasculature density limit for chondrogenesis (v_c)	30 % [f,i]
Maximum tissue strain-dependent production rate of fibroblasts ($p_{1,max}$)	0.2/day [j]
Tissue strain-dependent production rate of chondrocytes (p_2)	0.2/day [j,k,*]
Minimum tissue strain-dependent production rate of osteoblasts ($p_{3,min}$)	0.004/day [k,*]
Maximum tissue strain-dependent production rate of osteoblasts ($p_{3,max}$)	0.007/day [k,*]
Maximum blood supply dependent production rate modifier for fibroblasts ($q_{1,max}$)	1 [j,*]
Minimum blood supply dependent production rate modifier for chondrocytes ($q_{2,min}$)	0.2 [*]
Maximum blood supply dependent production rate modifier for chondrocytes ($q_{2,max}$)	1 [j,k,*]
Maximum blood supply dependent production rate modifier for osteoblasts ($q_{3,max}$)	1 [k,*]

[a] Ghiasi et al. [246] [b] Zhang et al. [209] [c] Geris et al. [59] [d] Bailón-Plaza and van der Meulen [113] [e] Burke and Kelly [107] [f] Lu and Lekszycki [247] [g] Perren and Cordey [243] [h] Isaksson et al. [103] [i] Simon et al. [230] [j] Isaksson [55] [k] Andreykiv et al. [210] [*] Estimated

[1] The function $f(\varepsilon)$ is given by Eq. 6.2. The angiogenic diffusion coefficient $D^v = D^{v0}$ for $\varepsilon \leq \varepsilon_{ang}$ and drops to 0 for $\varepsilon > \varepsilon_{ang}$. The transition was smoothened over an ε interval of 6 - 10 % instead of a sudden drop at $\varepsilon = \varepsilon_{ang}$ = 6 %.

It has been reported that, even chondrogenesis, which is well adopted to avascular, hypoxic environments, need a minimal level of oxygen for basic metabolic activities [112]. Recent studies have pointed out that angiogenesis is needed for chondrogenesis (especially in the earliest phases of chondrogenesis) and inhibition of angiogenesis affects the autocrine and paracrine processes that control chondrocyte progression [248]. Therefore, we assumed the production modifiers of chondrocytes to be minimal at very low values of v and subsequently increase with v to reach the maximum when $v = v_c$, beyond which chondrocyte production ceases. Table 6.3 summarizes the parameters related to angiogenesis and cell evolution used this study.

6.2.4 Initial and boundary conditions

It was assumed that the initial callus was filled with soft granulation tissue. Therefore, the initial material properties of the callus was specified to be those of granulation tissue. The initial densities of vessels and cells within the callus were set to zero (*i.e.* at $t = 0$, and $v = 0$ and $c^m = c^b = c^c = c^{fb} = 0$). In addition, in the ICF configuration C0, the wire pretension (i.e. 1275 N), was specified as initial stress to the wires.

As shown in Figure 6.1, the axial loads were applied on the top of the proximal fragment of the cortical bone and the bottom of the distal fragment was assigned fixed boundary condition. Periosteum, bone marrow and surrounding soft tissues were assumed to be the sources of MSC [59, 105]. The boundary concentration of MSC was specified as 2×10^4 cells / ml [74]. The blood vessels were assumed to propagate from periosteum, endosteum, bone ends and medullary cavity [59, 107, 108]. At these boundaries, the vasculature density was set to be 100 % [107]. In the 2D model, axisymmetric boundary condition was specified along the z axis.

6.2.5 Numerical solutions

The model was developed using the commercial finite element software package COMSOL Multiphysics® v. 5.3a (COMSOL AB, Stockholm, Sweden). A convergence study (with an error limit of 2 %) was conducted to choose the mesh size for the models. The 3D model was meshed using solid tetrahedral elements, the 2D model was meshed using triangular elements and the models were solved using the time-dependent solver of the software. Using the models, the optimal weight-bearing levels were determined under different combinations of parameters as described in detail under section 6.2.7.

6.2.6 Model validation

The 2D axisymmetric model of fracture healing was validated using the experimental data reported by Claes et al. [19, 20]. The experimental data used in this study were of 3.1 mm transverse osteotomies on sheep metatarsals. The animals were subjected to loading for producing an initial IFM of 1 mm. The weekly IFMs were measured *in vivo* for 8 weeks post osteotomy. After the ninth week, the animals were sacrificed, and the metatarsals were explanted. These explanted metatarsals were subjected to bending tests [19] to

determine the callus stiffness, and histological observations [20] to measure vascular densities within different regions of the callus. Using the model, the axial load required to produce 1 mm initial IFM was predicted to be 150 N. Under this loading model predictions were compared with the experimental results.

6.2.7 Parametric studies

After validation, weekly optimal weight-bearing levels for fracture healing were predicted using the models. The upper limit was calculated by ensuring angiogenesis is not inhibited anywhere within the callus (i.e. $\varepsilon \leq \varepsilon_{ang}$ throughout the callus), while the lower limit was calculated by ensuring that areas conductive to resorption (i.e. $\varepsilon \leq \varepsilon_{res}$) are insignificant (< 5 %) within the callus. The optimal weight-bearing ranges for fracture healing were predicted under different combinations of gap sizes (i.e. 3 and 6 mm), ICF configurations (i.e. C0, C1 and C2) and body weights (50, 75 and 100 kg); The predicted weights were normalised to the body weight considered in each case to standardize the results.

6.3 Results and Discussion

6.3.1 Model validation

The axial IFMs predicted by the model were in good agreement with the *in vivo* IFMs reported by Claes et al. [19]. As shown in Figure 6.5a, the IFMs predicted by the model were within the experimental error ranges. The model predictions show that there is no significant change in callus stiffness in the first two weeks, which is evident from the flat profile of the IFM versus healing time curve and large IFMs around 1 mm in the first two weeks. The IFMs began to reduce from the third week and continued to drop until ninth week to reach insignificant values (< 0.01 mm). The drop between the third to fifth weeks (from 0.88 mm to 0.42 mm) was predicted to be steeper than those at other times during healing. This behaviour is also consistent with the experimental IFM vs healing time data [19].

As temporal changes in vessel density and Young's modulus within the callus were not recorded in the sheep experiments [19, 20]. Therefore, the comparisons of model predictions with experimental data for these two parameters were made only on the ninth

week post-operation. As shown in Figure 6.5b, the average vessel densities within the periosteal, endosteal and cortical zones of the callus were predicted. The vessel densities increased with time in all three zones and tended to reach steady densities. The rate of increase diminished as the density increased, which is typical for any diffusion-like process. By the end of nine weeks, cortical and endosteal zones were well vascularized with vessel densities around 90 %; whereas, the vessel density within the periosteal zone was just around 40 %. The vessel densities predicted at the end of ninth week were well within the experimental error range and thus, consistent with the experimental results [20].

a) Axial interfragmentary movements

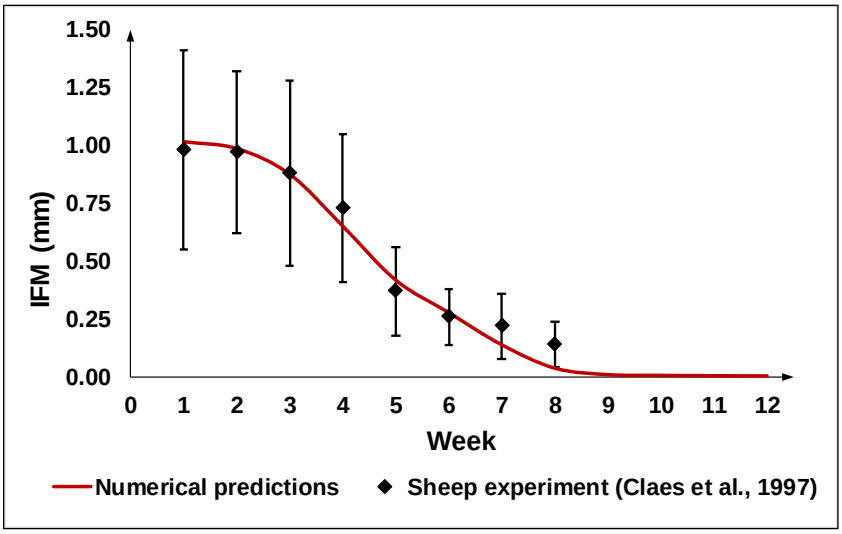

b) Normalised Young's modulus

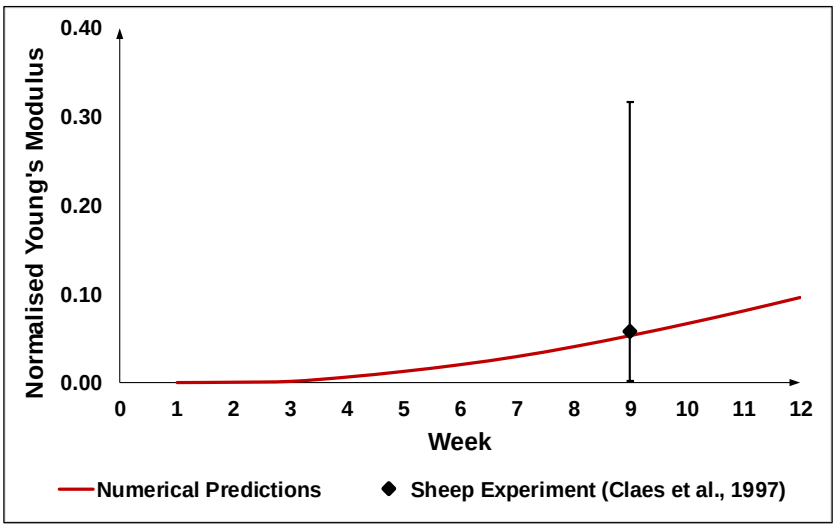

c) Normalised Vessel density

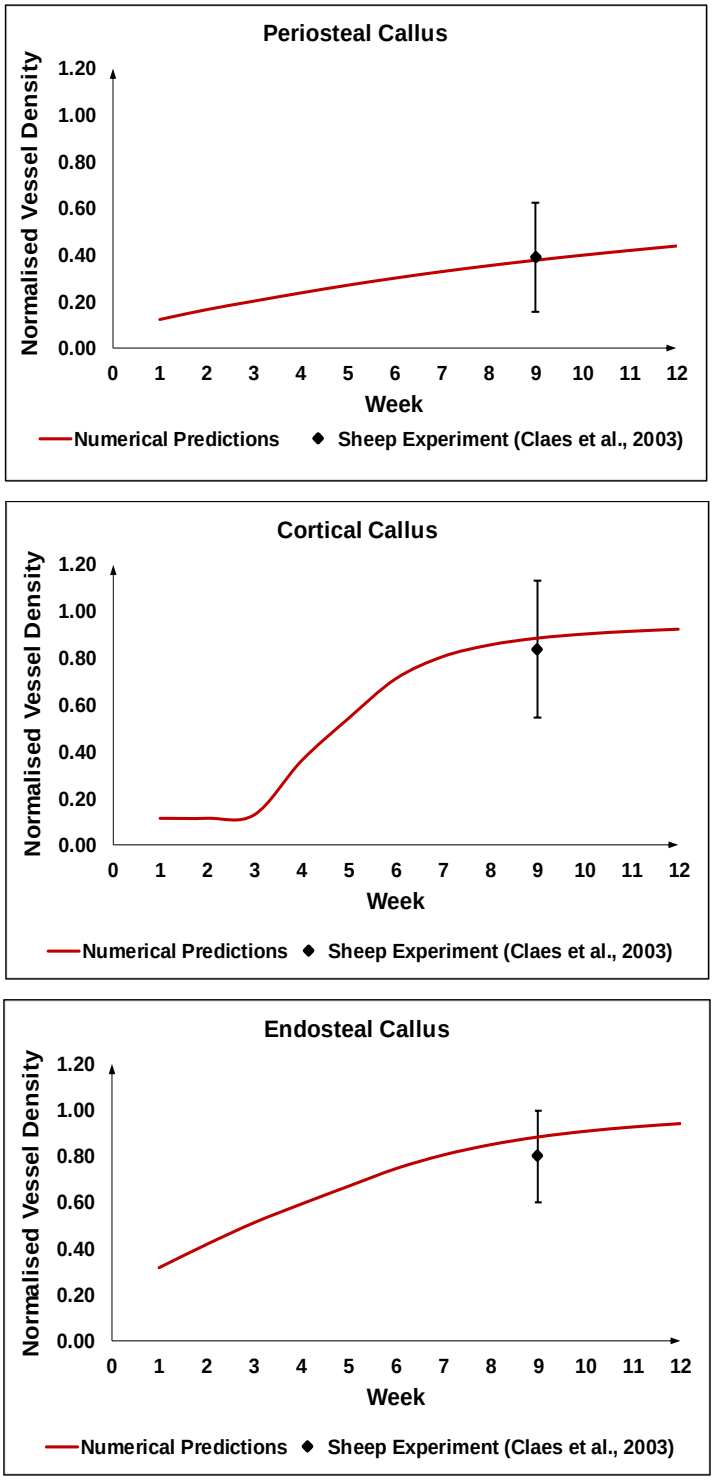

Figure 6.5 Comparison of the model predictions with sheep experiments of Claes et al. (1997,2003) : (a) axial interfragmentary movement; (b) normalised Young's modulus and (c) normalised vessel density, in the periosteal, cortical and endosteal zones of the callus

Based on the method of Wehner, et al. [249], the overall Young's modulus of the experimentally tested fracture calluses on the ninth week was estimated using the bending test data of Claes, et al. [19]. Then, the Young's modulus of the callus predicted by the model was compared with that estimated from the experimental data as shown in Figure 6.5c. It was seen that, the overall Young's modulus of the callus on the ninth week predicted by the model was very close to that estimated using the experimental data [19]. The results suggest that the model developed in this study is reasonably accurate and capable of predicting many aspects of fracture healing such as callus stiffening and angiogenesis.

6.3.2 The role of angiogenesis on callus stiffening

The numerical results show that the model was able to simulate the interrelationships between angiogenesis and callus stiffness. It can be seen from Figure 6.5 that callus stiffness is positively correlated with the level of vascularity. During the first two weeks, no significant enhancement to callus stiffness is observed, which is evident from high IFMs (Figure 6.5a) and low Young's moduli (Figure 6.5b). It can be seen from Figure 6.5c that, none of the three callus zones had enough vascularity (i.e. vessel density) during the first two weeks. However, from the third week onwards IFM decreased as Young's modulus increased, which indicates callus stiffening. By the end of fifth week, IFM reduced significantly to 0.42 mm, which corresponds to significant vessel densities of 27 %, 54 % and 67 % within periosteal, cortical and endosteal zones, respectively. In the following weeks, IFM reduced steadily as the vessel densities increased. These predictions indicate that callus stiffening during fracture healing is positively correlated to the level of vasculature and highlights the need to preserve angiogenesis for faster and stronger callus development.

Apparently, angiogenesis in the endosteal and periosteal zones are not severely affected due to external loading (i.e. weight-bearing) as in the cortical zone. Vessel densities were predicted to increase steadily within endosteal and periosteal zones (Figure 6.5c). However, within the cortical zone, weight-bearing appeared to inhibit angiogenesis during the early stages of healing (i.e. first three weeks), as indicated by the flat profile of vessel density versus healing time curve (Figure 6.5c). After the third week, when the zone became increasingly stable, angiogenesis progressed within the cortical zone, which

is indicated by rising vessel density. By the end of seventh week, cortical zone became well vascularized (i.e. v > 80 %).

6.3.3 The role of gap size

The results suggest that the allowable weight-bearing, and timing are strongly influenced by the fracture gap size (Figure 6.6). In the first four weeks post fracture, even very little weight-bearing (for BW = 75 kg) was predicted to inhibit angiogenesis within some parts of the callus for medium sized fractures (i.e. GS = 3 mm). Between fourth to eighth weeks post-operation, moderate weight-bearing (around 15 - 30 % of BW) was predicted to be optimal for medium sized fractures. During this period, weight-bearing below 16 % and above 29 % of BW were predicted to result in significant resorption, and inhibition to angiogenesis, respectively. The model predicted rapid increase in the maximum allowable weight-bearing from the eighth week onwards, while the minimum recommended weight-bearing remained around 22 % of BW. By the eleventh week, 100 % BW was permissible for medium sized fractures. On the other hand, weight-bearing had inhibitory effects on angiogenesis till the eleventh week for 6 mm fractures. On the eleventh week, the model predicted no inhibitory effects to angiogenesis for weight-bearing up to 31 % of the BW and recommended a minimum of 21 % of BW for 6 mm fractures.

Claes, et al. [20] studied revascularization and tissue formation in sheep metatarsal fractures under different gap sizes. Ten sheep were divided into two groups based on osteotomy sizes as either M / medium (i.e. 3.1 mm) or L / Large (i.e. 8.1 mm) and given the same level of axial interfragmentary strain (30-32 %) in a controlled manner using a custom-made external ring fixator. After 9 weeks post-operation, sheep were sacrificed and subjected to histological analysis, where the level of vascularization and tissue formations were measured. The results showed nearly 91 % more vessel density and 168 % more bone tissue within the callus for the ‘M’ group compared to ‘L’ group. The histological observations suggested partial bony bridging for the ‘M’ group and delayed healing for the ‘L’ group. The present model predicted allowable weight-bearing around 69 % of BW without angiogenesis inhibition for medium sized fractures (3 mm) which suggests that the fracture has partially healed and reached enough stiffness by the end of ninth week. However, the large fracture (6 mm) predicted that the callus is unable to bear weight without affecting angiogenesis after nine weeks which is suggestive of delayed

healing. Therefore, the model predictions agree reasonably with experimental observations.

Current predictions reiterate the need for careful reduction of fractures and osteotomies in surgical procedures in a different perspective by highlighting its effect on angiogenesis and weight-bearing. As reported in many previous experimental [19, 20] and computational studies [21, 105, 126], fracture gap has strong influence on fracture healing. Larger gaps can result in persistence of large IFMs for a longer time, which leads to poor vascularization and bone formation. This in turn leads to delayed healing and prolong the time post-operation for patients to get involved in physiological activities.

a)

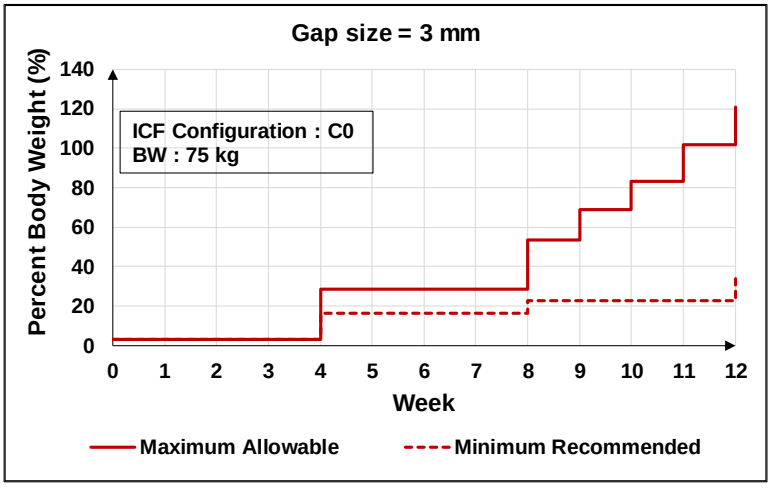

b)

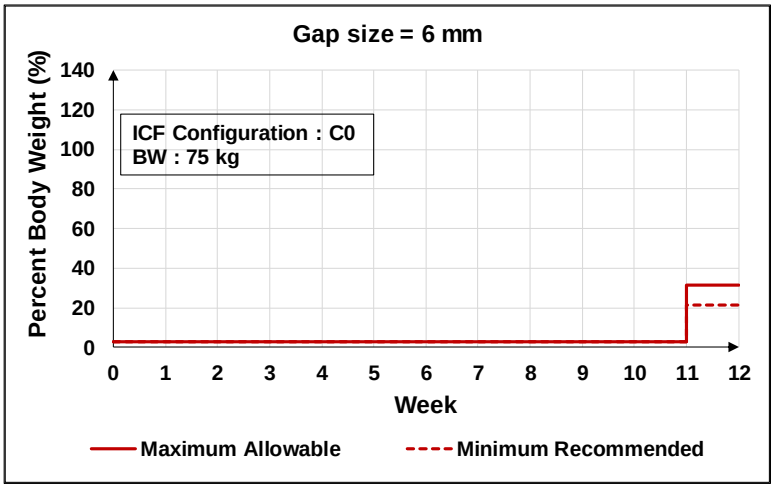

Figure 6.6 Optimal weight-bearing for fracture healing under ICF (Configuration : C0) expressed as percent body weight (BW = 75 kg) for (a) gap size = 3 mm and (b) gap size = 6 mm

6.3.4 The role of body weight

Whether a specific physiological activity is beneficial or detrimental to fracture healing is a subject specific decision, as it is driven very much by the body weight of the subject. This is evident from the predictions for allowable and recommended weight-bearings for different body weights. The model results suggest that lighter patients can get involved in a specific type of physiological activity faster than heavier patients. For example, in sheep metatarsals, maximum internal forces may reach 110 % of the body weight during normal walking [92]. As seen from Figure 6.7, sheep of 50 kg and 75 kg could walk safely post-fracture by the end of tenth and twelfth weeks respectively, whereas a 100 kg sheep would not reach this state within twelve weeks.

The clinical study of Leet, et al. [250] reported correlation between body weight and post-operative complications in femoral fractures. In their study, obese patients had an increased rate of post-operative complications compared to non-obese patients. Patil and Baseer [251] reported significant delays in healing and complications with higher body mass indices (BMI). Similarly, number of other studies have reported correlations between body weight (or BMI) and compromised healing / complications [252, 253].

a)

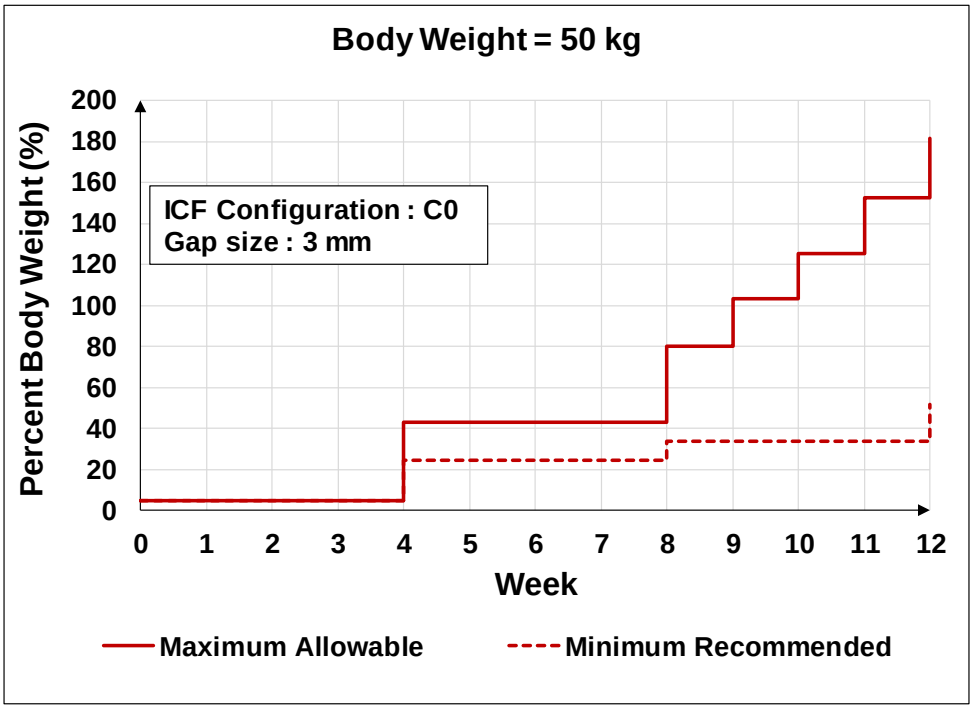

b)

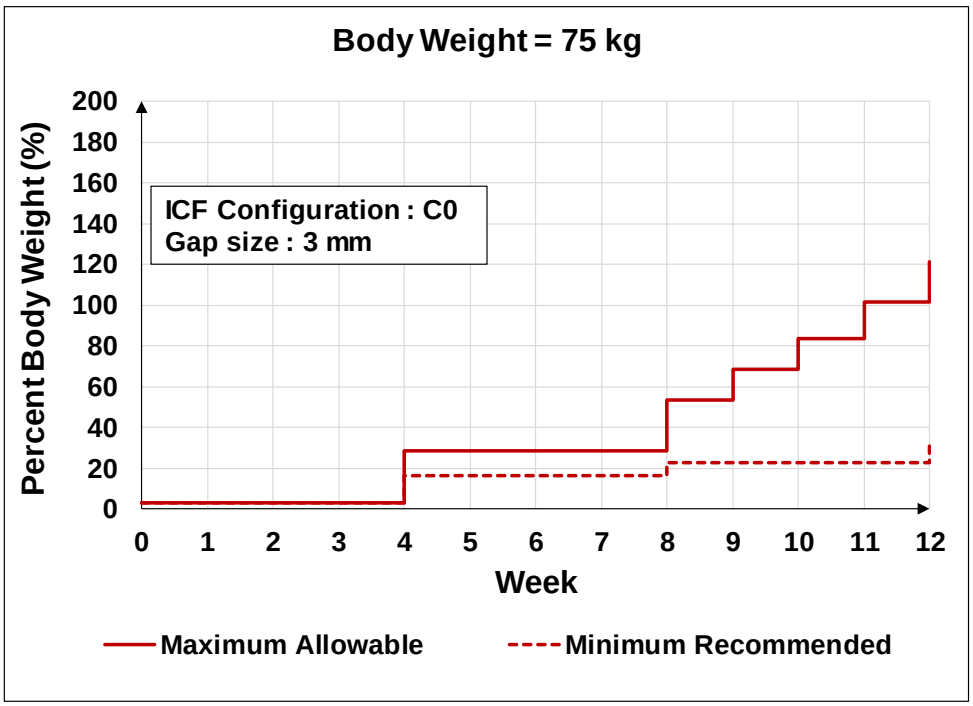

c)

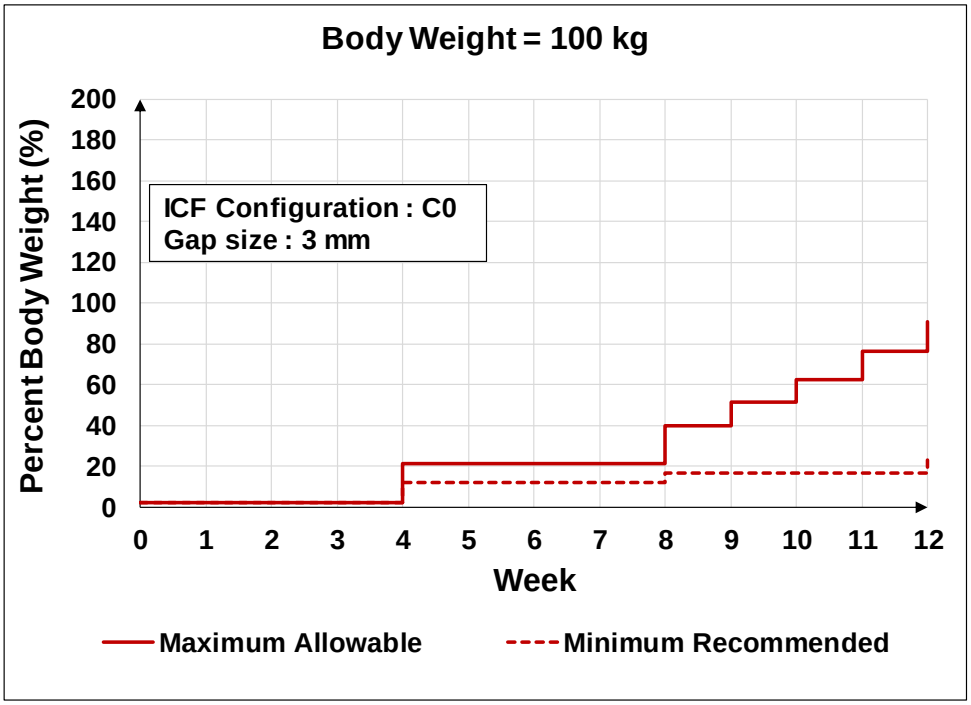

Figure 6.7 Optimal weight-bearing for fracture healing (gap size = 3 mm) under ICF (Configuration : C0) expressed as percent body weight for body weights (BW) = (a) 50 kg ; (b) 75 kg ; and (c) 100 kg.

These studies suggest that increase in body weight may affect fracture healing, safe weight-bearing capacity and delay the healing process, which agrees well with the current predictions. On the other hand, lack of weight-bearing has been reported to decrease the amount of woven bone formation during fracture healing in animals [254]. Therefore, it is essential that patients get involved in adequate levels of weight-bearing exercises. The model predictions suggest that patients with relatively low body weights need to get involved in relatively high weight-bearing exercises compared to heavier patients to enhance bone formation and stronger callus development as shown in Figure 6.7.

6.3.5 The role of ICF configuration

It is well established that fixation stiffness can alter fracture site stability and affect healing. Too rigid and too flexible fixations are both thought to be not very beneficial for healing. Therefore, it is essential that fixation configuration is carefully chosen for the patient specific case. With ICFs, bone fragments are affixed to the fixator either using fine wires or half pins or a combination of both [12]. Wires pass through the injured limb fully and affixed on opposite sides of ICF rings (Figure 6.1 and Figure 6.2). As wires are small in diameter (1.5 – 1.8 mm), it is essential to pre-tension wires adequately to ensure that the fixation is stiff enough. Clinical pretension levels range between 491 – 1275 N (50 - 130 kg). During weight-bearing, wire tension further increases above initial pre-tension levels to support weight. Thus, the axial stiffness of the fixation increases with the level of weight-bearing and exhibits a non-linear behaviour [170]. Half pins on the other hand have relatively bigger diameters (3.5 – 6 mm) and penetrate the limb only from one side (Figure 6.2). They support weight-bearing by cantilever action and thus the axial rigidity of the fixation increases with the diameter of the half pins used. Generally ICF configurations with half pins provide more rigidity to the fixation compared to those with wires [12].

In this study, two ICF configurations with half pins (i.e. C1 and C2) were considered and compared with traditional wire-only ICF configuration (C0), for medium sized fractures. ICF configuration C0, consisted of 1.8 mm diameter wires pre-tensioned to 1275 N; whereas, configurations C1 and C2 consisted of 4 mm and 6 mm diameter half pins, respectively.

a)

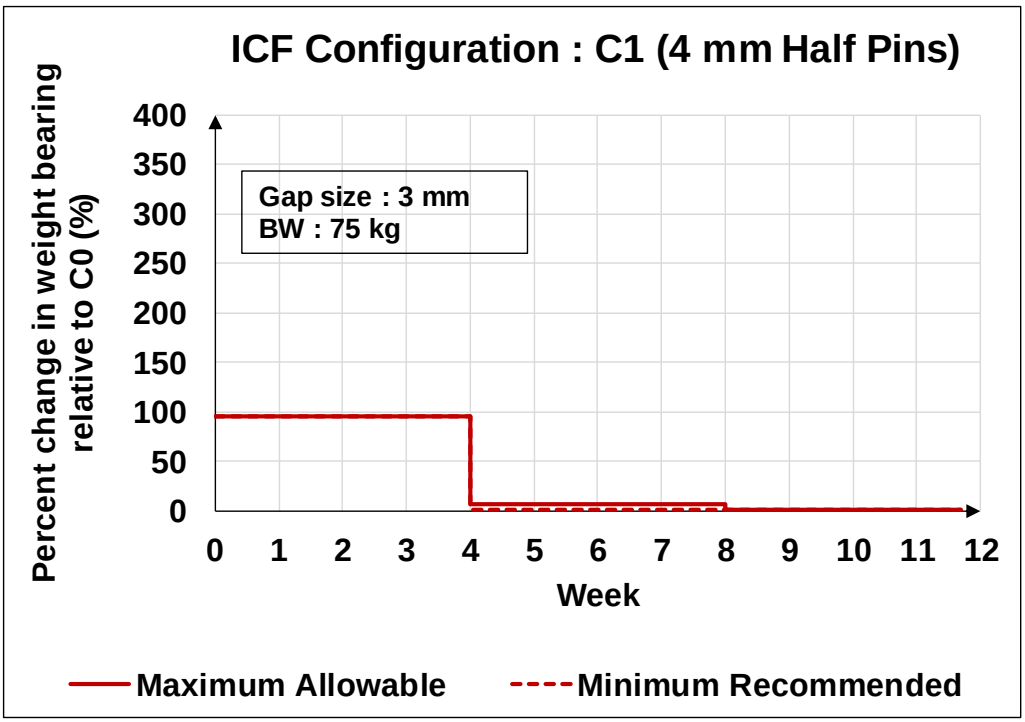

b)

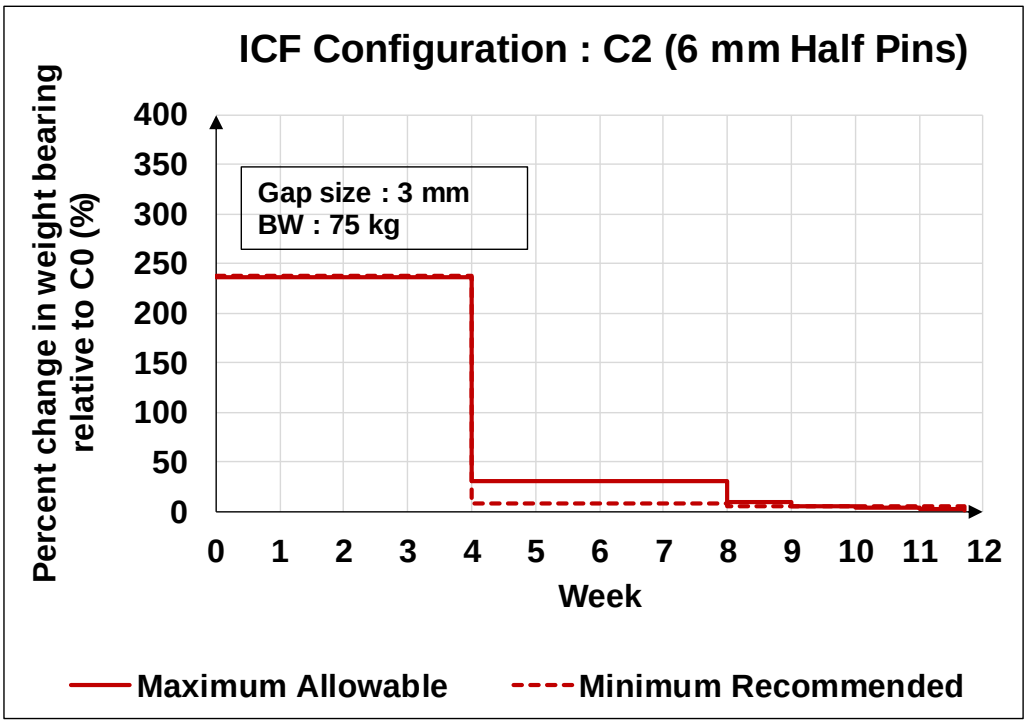

Figure 6.8 Percent change in weight-bearing (BW = 75 kg ; gap size = 3 mm) relative to ICF configuration C0 (1.8 mm pretension wires) for ICF configurations (a) C1 (4 mm half pins); and (b) C2 (6 mm half pins).

As shown in Figure 6.8, the results suggest that the allowable weight-bearing increases with ICF rigidity. In the first four weeks, the allowable maximum weight-bearing for C1 and C2 configurations increased by 96 % and 236 %, respectively, relative to the allowable weight-bearing for C0. Between the fourth and eighth weeks, the respective increases were 7 % and 30 %. This suggests that relatively stable ICF configurations permit more weight-bearing without damage to angiogenesis during healing, which can be beneficial for patients' mobility. Using half pins instead of pretension wires and using relatively larger diameter half pins instead of smaller ones could enhance the level of weight-bearing in the early stages. However, rigid configurations also require relatively higher levels of minimum weight-bearing compared to those of flexible configurations to enhance bone formations and callus stiffening. Therefore, both maximum allowable and minimum recommended loads increase with the rigidity of the fixation. After 8 weeks no noticeable differences in weight-bearing between different configurations were predicted (Figure 6.8).

It has been reported that inadequate axial load (weight bearing) under adequate blood supply or weight bearing under inadequate blood supply are both not beneficial for fracture healing [12, 255]. The former leads to bone resorption while the latter inhibits osteogenesis. Only the right combination of blood supply and weight-bearing under stable conditions promote healing [12]. In a clinical study where IFM measurements were taken on patients with tibial osteotomies treated with ICFs reported very high IFMs due to early weight bearing under ICFs [132]. The study concluded that early weight bearing under ICFs could have detrimental effects on fracture healing. A later clinical study [131] reported similar observations and supported the findings of the previous study [132].

Clinical experience suggests that stable fixation configurations make weight-bearing comfortable by controlling IFMs and recommends fixations to be very stable in the early stages of healing for weight bearing [12]. As healing progresses, bone takes greater load and the fixation becomes gradually ineffective [12]. In this study, the model predicted that medium sized fractures (e.g. 3 mm) under flexible ICF configurations (i.e. configurations with pretension wires alone) are susceptible to inhibition of angiogenesis under relatively low weight-bearing in the early weeks (e.g. 4 weeks) of healing. Relatively rigid ICF configurations (i.e. configurations with half pins) appear to minimize the inhibitory effects. However, no noticeable benefits in terms of safe weight-bearing

may be reached beyond a certain time point (e.g. 8 weeks). Therefore, the model predictions are consistent with clinical observations.

6.3.6 Limitations

The developed model was based on several assumptions and simplifications. Firstly, simplified fracture geometry and loading conditions (only axial) were used to minimize the computational time and resources needed for the analysis. In addition, the growth of fracture callus was ignored, and the analysis was carried out within a fixed domain. This approach has been adopted by many previous studies [55, 105]. Secondly, the model parameters (i.e. material properties, differentiation rates, boundary conditions etc.) obtained from literature may reflect the conditions of a small cohort of subjects. Thirdly, the focus of this study is mainly on the reparative phase; therefore, the inflammatory (first phase) or remodelling (third phase) phases of healing were not modelled. Most importantly, further experimental and clinical evidence is required to corroborate the findings of this study.

6.4 Conclusions

In the present study, a computational framework was developed to determine the optimal levels of weight-bearing based on angiogenesis and mechano-regulation mediated fracture healing process under ICF. The model takes into account the spatial and temporal changes in vascularization and callus mechanical properties. The following are the major findings of this study:

- There is time-dependent and subject (i.e. patient) specific optimal levels of weight-bearing which enhances mechano-regulation mediated healing without inhibiting angiogenesis throughout the fracture healing process.
- The allowable levels of weight-bearing under ICF and their timings are dependent on fracture geometry. For a medium fracture gap size (e.g. 3mm) in sheep, weight-bearing with 30 % BW could start in week 4 post-operation and gradually increase to 100 % BW by week 11. In contrast, for a relatively large fracture gap size (i.e. 6 mm), weight-bearing could only start in week 11 post-operation.
- Due to the relatively high flexibility of traditional ICF configurations with pretension wires (C0), partial weight-bearing is recommended for relatively

longer periods post operation (up to 9 weeks or more for sheep fractures) as full weight bearing during this period could affect angiogenesis.

- Relatively rigid ICF configurations with large diameter half pins (e.g. 6 mm), could enhance the allowable level of weight-bearing (up to 236 %) compared to those under traditional ICF configurations with pretensioned wires in the early stages of healing. However, no noticeable benefits in terms of safe weight-bearing may be reached beyond a certain time point (e.g. 8 weeks).

7 A probabilistic approach to address uncertainties in Ilizarov circular fixator-based fracture treatments

Chapter summary

Treating bone fractures involves dealing with uncertainty about the mechanical environment at the fracture site. When treating fractures using Ilizarov circular fixators (ICF), it may be necessary to deal with higher degrees of uncertainties due to the inherently complex non-linear mechanical behaviour of ICFs. However, most of the existing investigations into fracture healing under ICF take deterministic approaches ignoring the uncertainties associated with the mechanical variables. This chapter addresses this problem by taking a probabilistic approach which uses computational modelling in conjunction with engineering reliability analysis techniques. In this chapter, the effects of uncertainty in fracture gap size (GS), level of weight bearing (P), ICF wire pretension (T) and wire diameter (WD) on the probability of successful healing (PoS) at the beginning of reparative phase was predicted. The findings of this study provide key insights about the sensitivity of fracture site to different mechanical variables. Furthermore, the method presented in this study has potential applications in studying reliability of different treatment strategies using ICFs.

7.1 Introduction

Treating bone fractures involves dealing with uncertainties associated with biological and mechanical factors that affect the healing process. Such uncertainties can very well influence the progression of healing and the outcome. While it may be preferable to minimize the uncertainties associated with such factors, doing so may not always be possible. Therefore, it is essential that the uncertainties associated with the factors that affect fracture healing be considered to determine the reliability of treatment strategies. As fracture treatments usually focus on providing suitable mechanical environment at the fracture site to best utilize the intrinsic biological healing capacity of bones [7, 9], it is of prime importance to consider the uncertainties associated with mechanical factors in bone healing treatments.

It is known that most fractures heal by secondary healing which requires certain amount of interfragmentary movement (IFM) at the fracture site for callus formation. IFMs depend primarily on fracture geometry (e.g. fracture gap size) and external loading (e.g. weight bearing). Uncertainties in fracture geometry arise from imperfect reduction of bone fragments. On the other hand, uncertainties regarding loading arise from patients' noncompliance to clinical weight bearing instructions following surgery [256]. This may be partially due to patients' difficulties in controlling the loading exerted on the injured limb.

When treating fractures using Ilizarov circular fixators (ICF), it may be necessary to deal with higher degrees of uncertainties about the mechanical environment at the fracture site due to number of reasons. Firstly, ICFs are affixed to bones using fine pretensioned wires which exhibit nonlinear stiffness behaviour [257]. This leads to uncertainties in predicting fixation behaviour as the ICF stiffness depends on number of other uncertain factors such as level of weight bearing. Secondly, pretension loss and loosening of wires is a common problem associated with ICFs which leads to uncertainties in fixation rigidity [151, 257]. In addition, being a modular external fixation could potentially lead to uncertainties in fixation configuration. These uncertainties could result in deviation of IFMs at the fracture site from those expected and possibly affect the healing process. This adds an element of uncertainty in the ICF treatment outcomes.

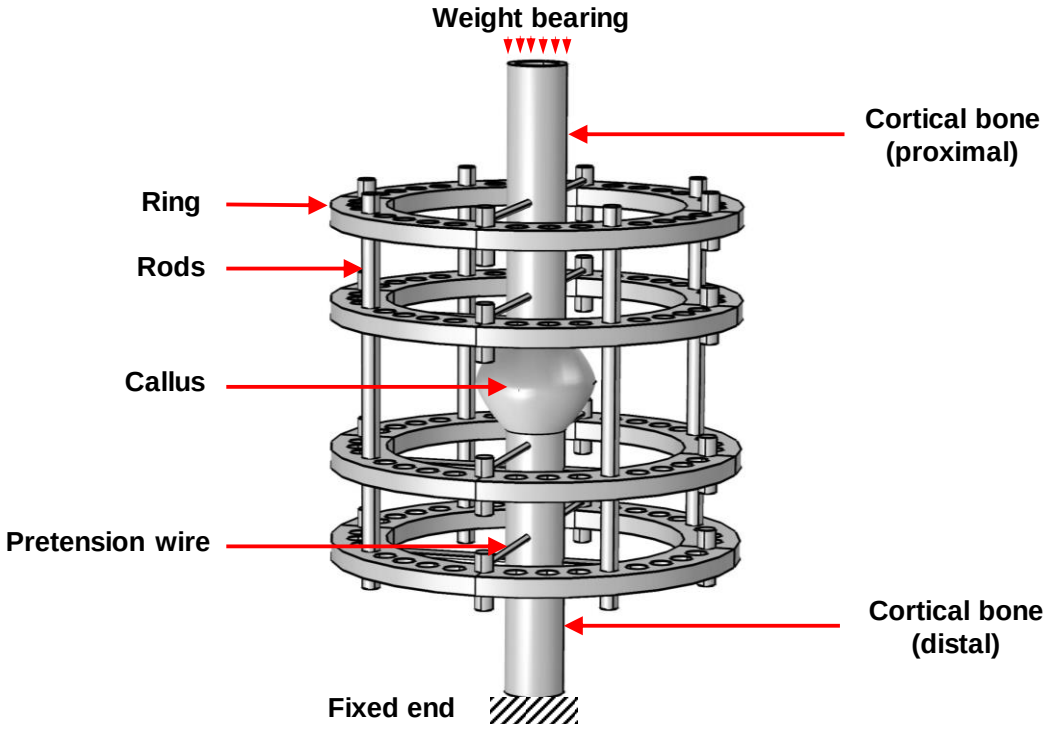

Figure 7.1 Schematic diagram of the configuration of Ilizarov circular fixator (ICF) used in this study

It is possible to estimate the level of uncertainties in treatment outcomes quantitatively. This requires systematic parametric investigations into fracture healing under controlled environments which can be achieved using validated computational models. However, most of the existing computational studies on fracture healing have neglected the uncertainties associated with the factors that affect healing and taken deterministic approaches.

In this chapter, a probabilistic approach is taken to address this challenge by considering the uncertainties in some of the important mechanical variables that affect fracture healing under ICFs. Probabilistic methods have been used in number of engineering applications (e.g. structural reliability of infrastructure facilities) in the past. In the recent times, probabilistic approaches have been used in the field of orthopaedics to design new orthopaedic components and assess structural reliability of orthopaedic constructs [258-261]. However, no studies so far have incorporated probabilistic methods to investigate the effects of uncertainties in mechanical variables on fracture healing under ICFs.

In this chapter, sheep fracture model is taken as an example and the uncertainties associated with fracture gap size (GS), axial loading resulting from weight bearing (P) and ICF configuration were considered. As pretension wires are an important source of uncertainties in ICF, the effects of wire pretension level (T) and wire diameter (WD) were specifically considered in this study. In Chapter 6, optimal ranges of weight bearing under different fracture gap sizes and ICF configurations were presented. It was predicted that the optimal level of weight bearing would be between 16-29 % of the body weight (75 kg) during the post early stages of healing (i.e. reparative phase) for a mid-sized fracture (i.e. GS = 3 mm), stabilized with a four ring ICF as shown in Figure 7.1 (T = 130 kg and WD = 1.8 mm). Starting from these optimal conditions, this chapter investigates how probability of fracture healing changes within the periosteal, cortical and endosteal zones of the callus in response to the changes in the level of uncertainty in GS, P, T and WD. Based on Chapter 6, probability of successful fracture healing (PoS) was defined as the probability of tissue strain (deviatoric) lying between strain limits for bone resorption (lower bound) and angiogenesis inhibition (upper bound) as explained in detail under section 7.2.

7.2 Materials and Methods

To investigate how the uncertainties associated with GS, P, T and WD affect the probability of successful healing (PoS) in sheep fractures, the computational model presented in Chapter 6 was used in conjunction with the principles of engineering reliability analysis as shown in Figure 7.2. In the analysis a 3 mm metatarsal fracture stabilized with a four ring ICF was considered. Based on the results of Chapter 6 it is known that weight bearing could have inhibitory effects on angiogenesis and fracture healing during the very early stages of healing. Therefore, this analysis focuses on the stages of healing where partial weight bearing is allowed (post-early stage).

However, fracture healing involves many subsequent stages following the early stage. Therefore, an important challenge here is to decide what point of the healing pathway to carry out the analysis at. This requires deeper understanding about the stages of healing within the broadly defined healing phases (i.e. inflammation, repair and remodelling). For

this purpose, this study makes use of data from the experimental study of Vetter et al. [262] on sheep fractures.

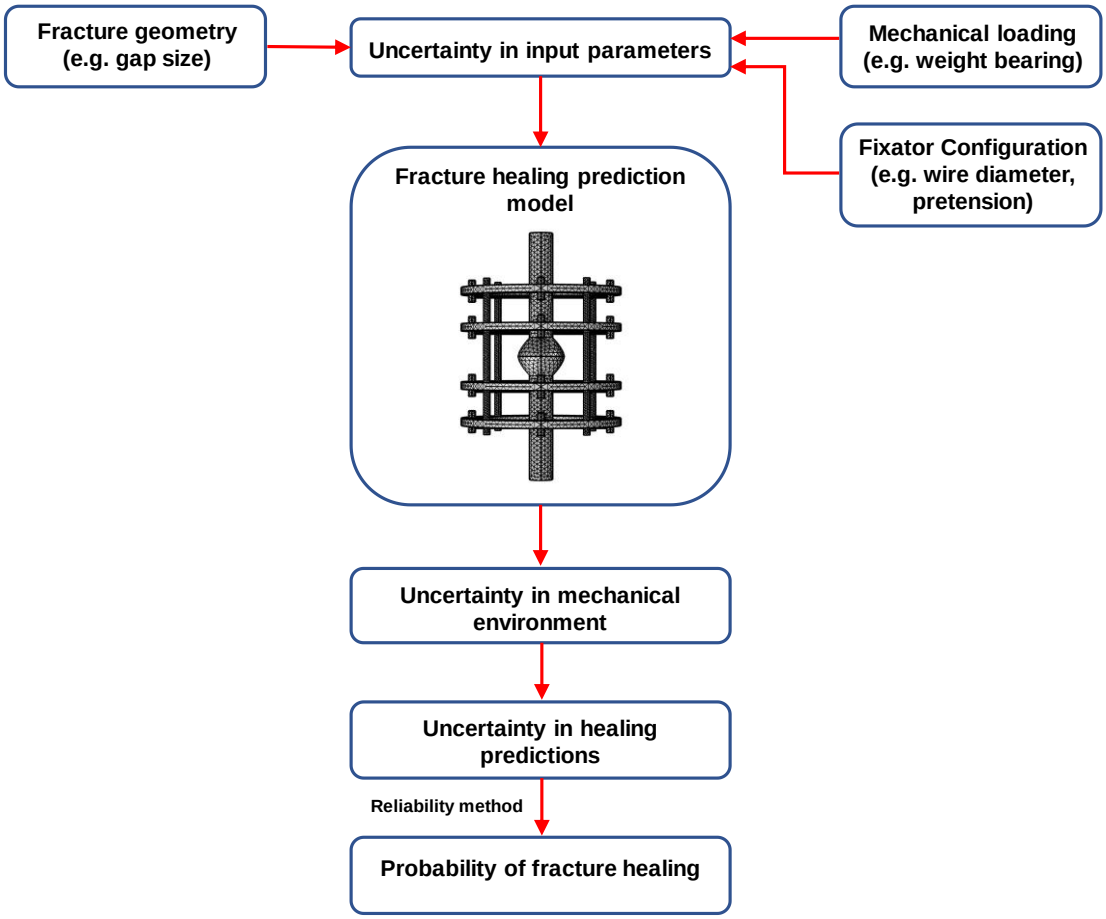

Figure 7.2 Methodology used in this study

In their experimental study on sheep long bone osteotomies stabilized with external fixations, Vetter et al. [262] demonstrated six different stages (stage I-VI) of secondary healing based on the tissue distribution patterns within the callus (Figure 7.3 and Table 7.1). The experiment involved 64 sheep of 63 (± 8) kg which were subjected to 3 mm osteotomies and subdivided equally into 'rigid' and 'semirigid' groups based on the rigidity of the external fixation. At different time points of healing, equal number of sheep were sacrificed from both groups and their calluses were subjected to histological analysis. Subsequently, image processing techniques were used to quantitatively describe the tissue patterns and produce averaged tissue distribution images at different stages of healing.

Based on the results of Vetter et al.[262], stage I of secondary healing in sheep represents the late inflammatory phase where remnants of haematoma is present in callus. Stage II corresponds to early reparative phase where neither remnants of haematoma nor cartilage tissues are observed within the callus. By the end of stage II, the internal callus (i.e. cortical and endosteal zones) and the region at the level of osteotomy gap in external callus (periosteal callus) are filled fully with remnants of haematoma indicating no repair within these regions.

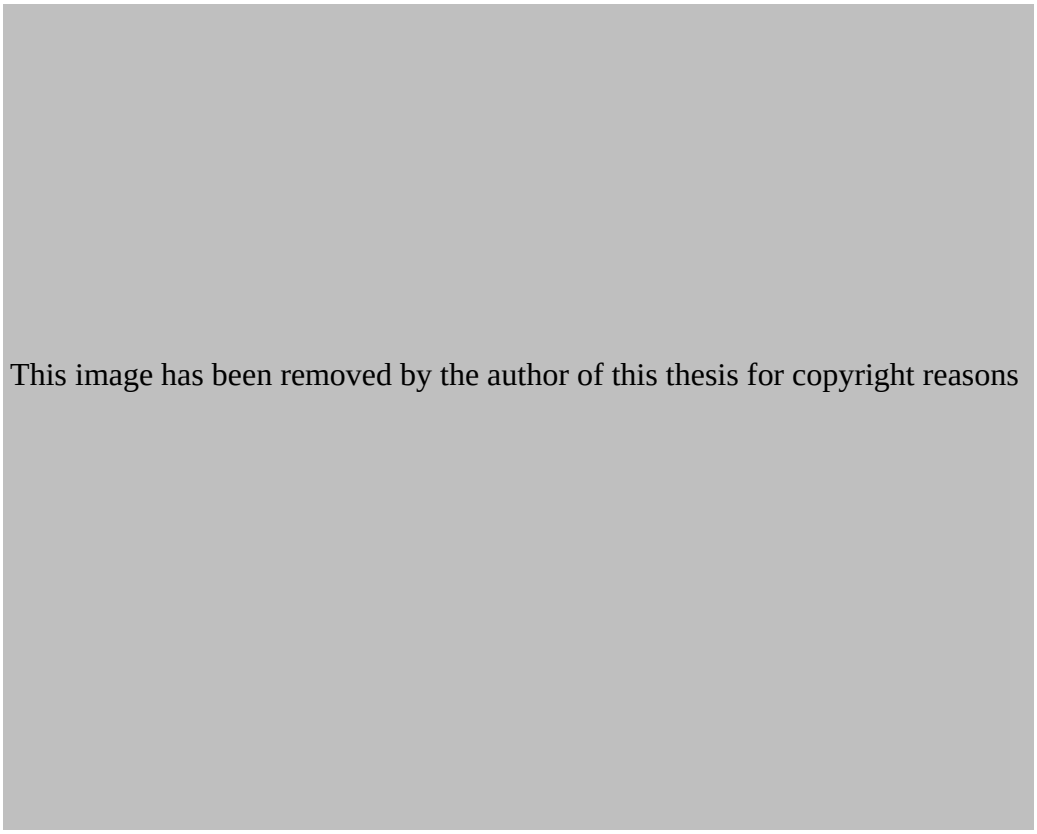

Figure 7.3 Six stages of secondary healing in sheep fractures
Adopted from Vetter et al. [262] with permission.

Stage III marked the reparative phase where bone formation within the fracture gap, cartilage formation and subsequent periosteal bridging occurs. This is also the stage when endochondral ossification begins. Therefore, this is the stage of fracture healing when angiogenesis and bone formation are critically important. It is essential to promote angiogenesis while minimizing bone resorption during stage III as it is a crucial stage of

secondary healing for successful outcomes. If the mechanical conditions are unfavourable during this stage, the repair process and the weight bearing capacity could be hindered. In addition, periosteal bony bridging of proximal and distal fragments (stage IV), endosteal bony bridging of medial and lateral sides of the callus (stage V) and subsequent remodelling of bone (stage VI) could also be delayed. Therefore, in this chapter, the probability of fracture healing as a result of uncertainties in GS, P, T and WD was investigated at the beginning of reparative phase (stage III).

Table 7.1 Stages of secondary healing and corresponding healing phases
adopted from Vetter et al. [262] with permission

It should however be noted that the timepoint at which stage III (reparative phase) of healing begins is subjective and depends on number of subject specific factors [262]. Considering the present study, GS, T and WD are variables that are fixed at the time of surgery. It is obvious that these variables could affect the rate of healing progression and the time taken to reach stage III. For example, a fracture with smaller gap size may reach stage III of healing faster than that with a larger gap size when all other variables remain unchanged. In addition, differences in healing rates could even result from differences in subject specific factors. This is evident from the differences in healing rates observed for sheep within same group in the experiment of Vetter et al. [262]. Therefore, this analysis focuses on a specific point in the healing pathway rather than a specific point in time during healing.

The inherent assumption in this analysis is that the ‘healing pathway’ as defined by the succession of healing stages remains unchanged and the differences in variables (i.e. GS, P, T and WD) only alter the speed at which the healing path is followed [262]. Vetter et

al. [262] reported that 3 mm sheep osteotomies stabilized using both rigid and semi -rigid external fixations marked the beginning of stage III on average on the fourth week post osteotomy and concluded in most cases before the end of week 6 post osteotomy. In the absence of further experimental data relevant to this study, it was assumed that stage III of healing for 3 mm sheep fractures stabilized with external fixators begin at similar time points as reported in Vetter et al. [262] and the material properties of the callus at this stage were estimated using the previously developed sheep fracture healing model (Chapter 6). All the cases considered in this analysis would achieve the estimated callus stiffness at some time point which marks the beginning of stage III of fracture healing. This chapter investigates how the uncertainties associated with GS, P, T and WD affect the probability of fracture healing once this stage is reached. It is reasonable to assume that the bone fracture treatment variables (GS, P, T and WD) are normally distributed [126]. The mean values of these variables were assumed based on Chapter 6 and a relatively wide range of uncertainty was assumed as shown in Table 7.2.

Table 7.2 Mean and coefficients of variation (COV) of mechanical variables used in this study.

Variable	Mean	Coefficient of variation (COV)
Fracture gap size (GS)	3 mm [a]	0.1 – 0.9 [b]
Weight bearing loading (P)	150 N [a]	0.1 – 0.9 [b]
Wire pretension (T)	130 kg (1275 N) [a]	0.1 – 0.9 [b]
Wire diameter (WD)	1.8 mm [a]	0.1 – 0.9 [b]

[a] The mean values of variables were obtained based on Chapter 6 for optimal fracture healing.

[b] Relatively wide range of COV were assumed for each variable to investigate the role of uncertainty of each parameter on the probability of fracture healing.

7.2.1 Computational simulations

In this study, the computational model presented in Chapter 6 was used to conduct numerical simulations. The callus properties were estimated from the model and assumed to be representative of the beginning of reparative phase (stage III) of secondary healing. First, the model was solved with all four variables set to their optimal (mean) values (i.e. GS = 3 mm; P = 150 N; T = 130 kg; WD = 1.8 mm) and the average deviatoric tissue

strain (ε) within the periosteal, endosteal and cortical regions were calculated. Subsequently, each variable was considered one by one and the model was solved for different of levels of uncertainties (i.e. COV) of the variables. In each case the average ε values within periosteal, endosteal and cortical were calculated and the plot of ε versus parametric values were generated for each variable for each callus zone. Subsequently these data were used to carry out reliability analysis as described in section 7.2.2. The properties of materials used in the model are summarised in Table 7.3 and the simulations were carried out using the finite element software package COMSOL Multiphysics v 5.3a (COMSOL AB, Stockholm, Sweden).

Table 7.3 Properties of materials used in this study

Material	E (MPa)	υ	Φ	k ($m^4 N^{-1} s^{-1}$)	K_s (MPa)	K_f (MPa)
Cortical bone	20000 [a]	0.3 [a]	0.04 [a]	10^{-17} [a]	13920 [a]	2300 [a]
Fracture callus	12 [b]	0.167 [a,b]	0.8 [a,b]	10^{-14} [a,b]	2300 [a,b]	2300 [a,b]
Stainless steel	197000 [c]	0.29 [c]	--------	--------	--------	--------

E – Young's modulus υ - Poisson's Ratio **Φ** – Porosity **k** –Permeability

K_s – Solid compression modulus K_f – Fluid compression modulus

[a] Lacroix and Prendergast [105] [b] Estimated based on the results of Chapter 6 and Vetter et al. [262]

[c] Watson et al. [144]

7.2.2 Reliability analysis

A reliability analysis was carried out to investigate how the probability of fracture healing changes within different zones of fracture callus. In structural engineering, this is a common technique used to investigate the structural reliability of infrastructure facilities. The principle behind this approach is that there are uncertainties regarding loading acting on a structure and the resistance of it. The probability of failure of a structure is defined as the probability of loading exceeding the resistance. This could be calculated by plotting the probability density functions of both loading and resistance and calculating the area of overlap.

In this study, a similar approach was taken to calculate the probability of fracture healing. When tissue strain (ε) exceeds the strain threshold for angiogenesis inhibition (ε_{ang}= 6 %), existing blood vessels are ruptured and no formation of new blood vessels take place.

This could hinder the healing process and lead to unfavourable conditions such as delayed union or non-union. On the other hand, when tissue strain (ε) is smaller than the maximum strain limit for bone resorption ($\varepsilon_{res} = 0.005\ \%$), bone is resorbed. This could compromise bone quality and result in poor healing. Therefore, the probability of failure (PoF) is defined as the sum of probabilities of having unfavourable tissue strains. In other words, PoF = P ($\varepsilon < 0.005\ \%$) + P ($\varepsilon > 6\ \%$). On the other hand, probability of successful healing (PoS) is defined as PoS = P ($0.005\ \% \leq \varepsilon \leq 6\ \%$).

In order to calculate the probability of successful healing (PoS), the probability density function (PDF) of tissue strain (ε) is required. As tissue strain (ε) depends on GS, P, T and WD, it could be described as follows :

$$\varepsilon = f(GS, P, T, WD) \tag{7.1}$$

In this function, it is reasonable to assume that GS, P, T and WD are independent variables as their values are not correlated. For example, there is no correlation between the load exerted by patient post-surgery and the gap size (GS) or fixation configuration (T,WD). Furthermore, GS, P, T and WD were assumed to be normally distributed. To approach this problem, let's consider a dependent variable X defined as follows:

$$X = g(X_1, X_2, X_3, \ldots, X_n) \tag{7.2}$$

where, $X_1, X_2, X_3, \ldots X_n$ are random variables. By Taylor series expansion, the mean and standard deviation of X (i.e. μ_X and σ_X) could be expressed as

$$\mu_X \approx g(\mu_{X1}, \mu_{X2}, \mu_{X3}, \ldots, \mu_{Xn}) \tag{7.3}$$

$$\sigma_X \approx \sqrt{\sum_{i=1}^{n}\sum_{j=1}^{n} \frac{\partial g}{\partial X_i}\frac{\partial g}{\partial X_j} Cov(X_i, X_j)} \tag{7.4}$$

where, $\mu_{X1}, \mu_{X2}, \mu_{X3}, \ldots, \mu_{Xn}$ are means of $X_1, X_2, X_3, \ldots, X_n$, respectively and $Cov(X_i, X_j)$ is the covariance of X_i and X_j. If X is linearly related to $X_1, X_2, X_3, \ldots, X_n$, this relationship could be expressed by Eq. 7.5 and μ_X could be expressed by Eq. 7.6.

$$X = a_0 + a_1X_1 + a_2X_2 + a_3X_3, \ldots . + a_nX_n \quad (7.5)$$

$$\mu_X = a_0 + a_1\mu_{X1} + a_2\mu_{X2} + a_3\mu_{X3} + \ldots . + a_n\mu_{Xn} \quad (7.6)$$

In Eq. 7.5 and 7.6, $a_0, a_1, a_2, \ldots , a_n$ are constants. If the variables $X_1, X_2, X_3, \ldots , X_n$ are independent, σ_X could be expressed as

$$\sigma_X = \sqrt{(a_1\sigma_{X1})^2 + (a_2\sigma_{X2})^2 + (a_3\sigma_{X3})^2 + \cdots + (a_n\sigma_{Xn})^2} \quad (7.7)$$

The unknown constants $a_0, a_1, a_2, \ldots , a_n$ could be determined from regression analysis. Once μ_X and σ_X are known the probability of different ranges of X could be calculated by considering the PDF of X. For a given set of values for the independent variables $X_1, X_2, X_3, \ldots . X_n$, the effect of uncertainty (variability) in any specific variable on the probability of X falling within a specific range could be studied by considering the variability of only that variable while keeping others constant at the given values. In such cases, if the variable considered is normally distributed, the distribution of X will also be normal.

7.2.3 Parametric studies

In this study, the mean values of the input variables (Table 7.2) were obtained from previous analysis (Chapter 6). It was assumed that the fragments were surgically reduced with a gap size (GS) of 3 mm. However, there is uncertainty in how perfect the reduction is. Therefore GS = $\mu_{GS} \pm \sigma_{GS}$ = 3 mm ± σ_{GS}. To investigate how probability of successful healing (PoS) varies with the level of uncertainty in GS, a wide range of standard deviation (σ_{GS} = COV × μ_{GS}) were considered. As given in Table 7.2, values of COV_{GS} were assumed between 0.1 – 0.9. Similarly, P = $\mu_P \pm \sigma_P$ = 150 N ± σ_P, T = $\mu_T \pm \sigma_T$ = 130 kg ± σ_T and WD = $\mu_{WD} \pm \sigma_{WD}$ = 1.8 mm ± σ_{WD} were assumed for P, T and WD, respectively. This set of mean values were found to result in optimal healing conditions in Chapter 6. Starting from the optimal healing settings (i.e. all variables set to mean values), each variable was considered one at a time and the model was solved under different values of COV (between 0.1 - 0.9) of the variable and average tissue strains within the periosteal, cortical and endosteal zones of the callus were recorded.

7.3 Results

7.3.1 Regression analysis

First, to establish the relationship between each independent variable and tissue strain, the average tissue strains predicted within periosteal, cortical and endosteal callus were plotted against each variable as shown in Figure 7.4. Then least square curve fitting was used to determine the relationship between average tissue strain and the independent variables within each callus zone (Table 7.4). All four variables exhibited a linear relationship with average tissue strain within all three regions. In addition, it was noted that the average tissue strain within the cortical zone was always the highest and that of the periosteal zone was always the lowest under all cases. Out of the four variables, the axial load resulting from weight bearing (P) was the most influential parameter at the beginning of stage III (reparative phase) of secondary healing. This is evident from the relatively steeper slopes of lines seen in Figure 7.4 b. Particularly, a relatively strong positive correlation between the average tissue strain and P was predicted within the cortical zone. In addition, positive correlations between P and average tissue strain were seen within the endosteal and periosteal zones as well.

The correlation between average tissue strain and GS was predicted to be negative within the cortical zone but positive in the other two regions. On the other hand, a weak negative correlation between the average tissue strain and the ICF configuration parameters (i.e. T and WD) was predicted within the cortical zone. However, no significant changes (very weak negative correlation) were predicted in average tissue strains in response to variabilities in T or WD within the periosteal or endosteal zones of the callus. As the correlations between the average tissue strain and independent variables (i.e. GS, P, T and WD) in all three regions of the callus are linear, the average tissue strain ε could be expressed as

$$\varepsilon = a_0 + a_{GS} \times GS + a_P \times P + a_T \times T + a_{WD} \times WD \qquad (7.8)$$

a)

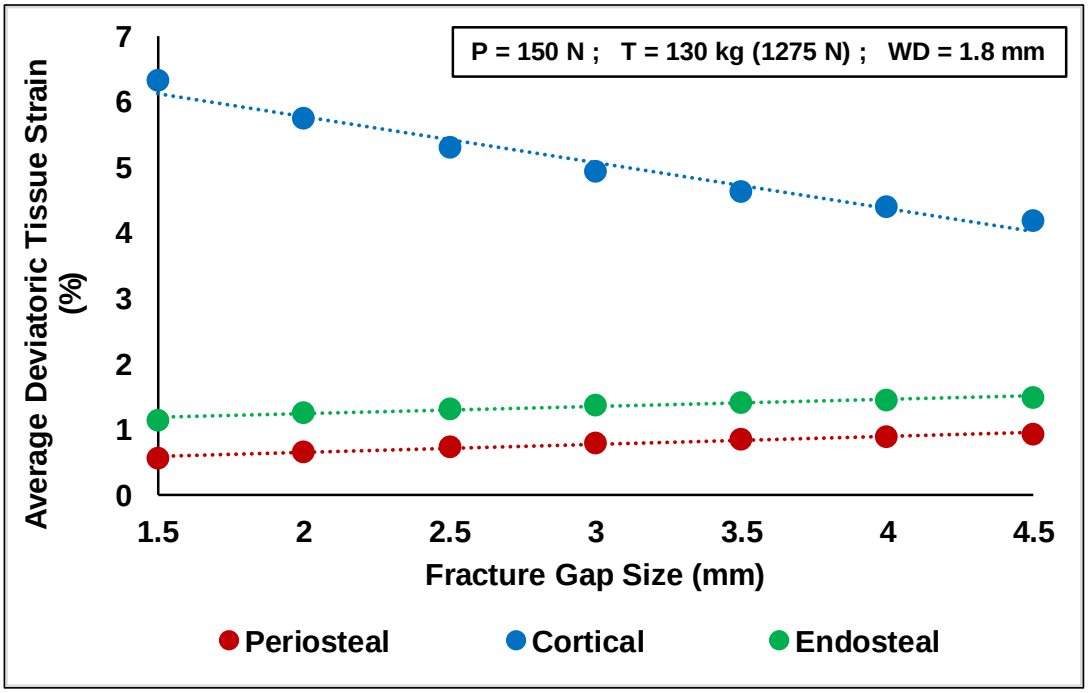
P = 150 N ; T = 130 kg (1275 N) ; WD = 1.8 mm
Average Deviatoric Tissue Strain (%)
0
1
2
3
4
5
6
7
1.5
2
2.5
3
3.5
4
4.5
Fracture Gap Size (mm)
Periosteal
Cortical
Endosteal

b)

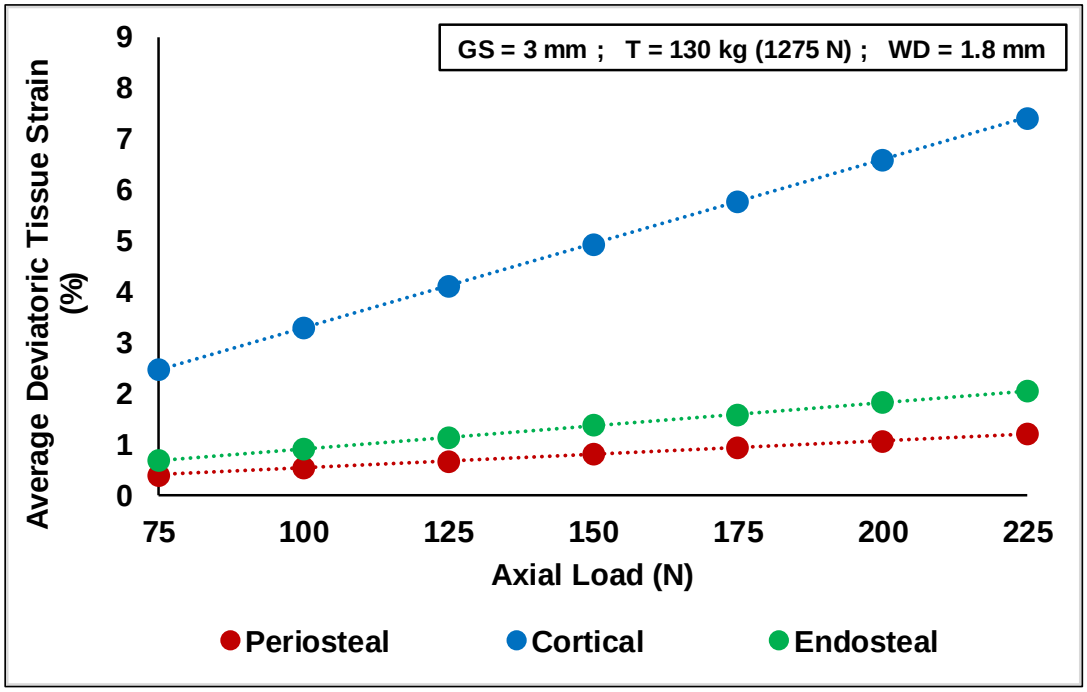
GS = 3 mm ; T = 130 kg (1275 N) ; WD = 1.8 mm
Average Deviatoric Tissue Strain (%)
0
1
2
3
4
5
6
7
8
9
75
100
125
150
175
200
225
Axial Load (N)
Periosteal
Cortical
Endosteal

c)

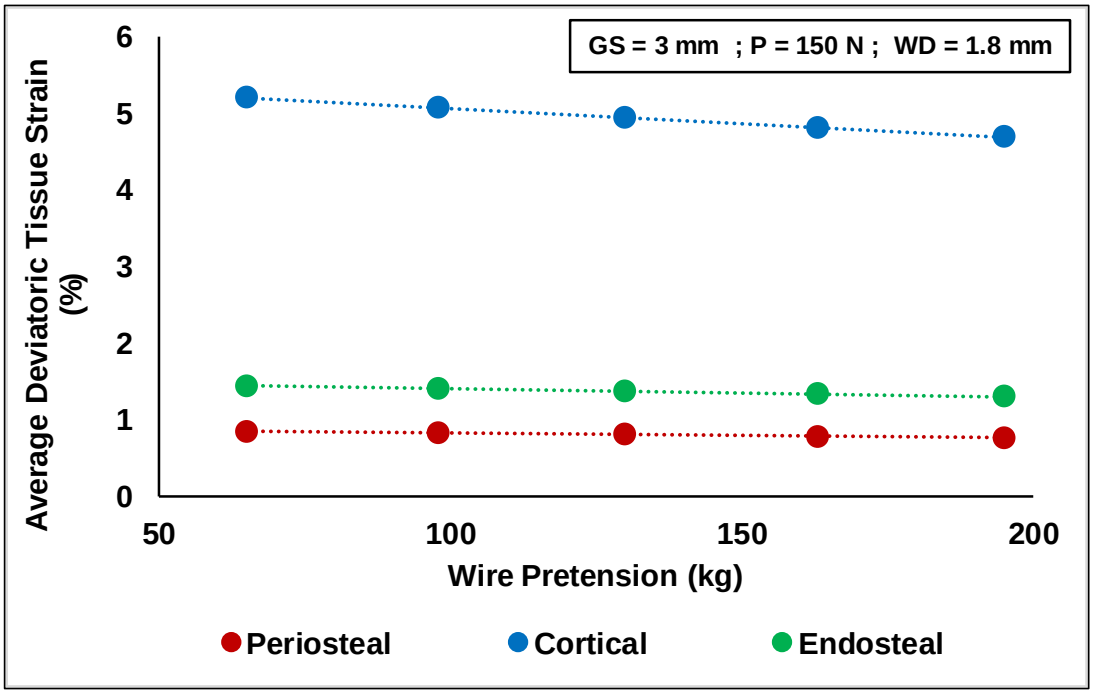

d)

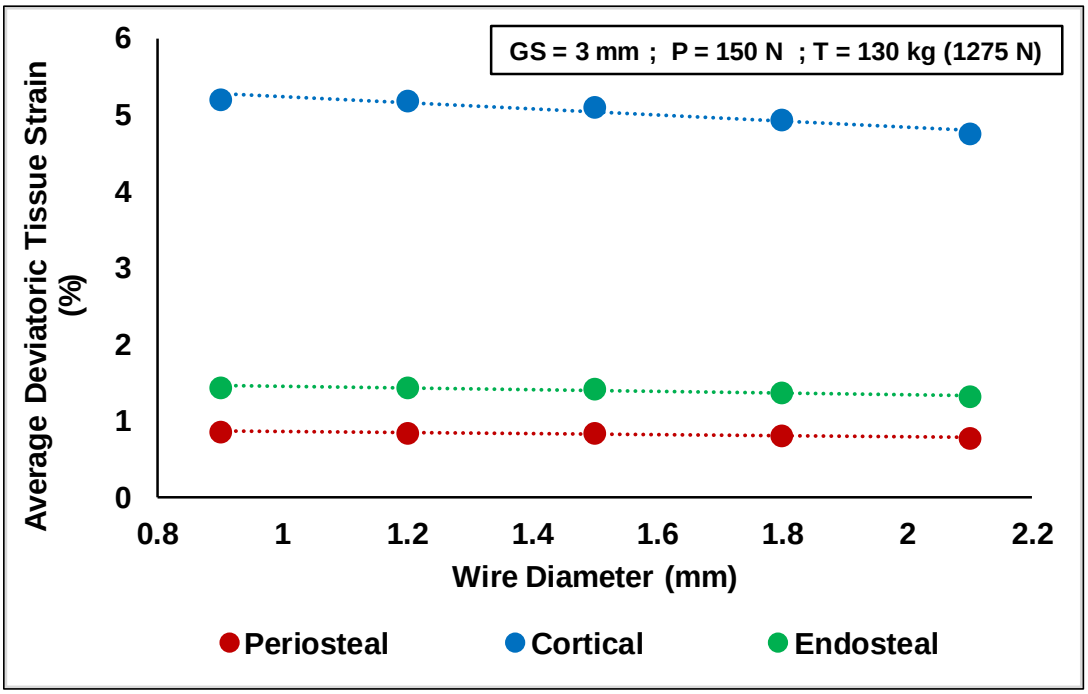

Figure 7.4 The relationship between average tissue strain and (a) gap size, (b) weight bearing, (c) wire pretension and (d) wire diameter.

Table 7.4 Relationships between independent variables and average tissue strains within periosteal, cortical and endosteal callus

X_n	Periosteal	Cortical	Endosteal
GS	ε = 0.1204 × GS + 0.4198	ε = -0.7000 × GS + 7.1800	ε = 0.1071 × GS + 1.0300
P	ε = 0.0053 × P + 0.0017	ε = 0.0329 × P - 0.0014	ε = 0.0091 × P + 0.0029
T	ε = -0.0006 × T + 0.8877	ε = -0.0039 × T + 5.4588	ε = -0.0011 × T + 1.5082
WD	ε = -0.0637 × WD + 0.9137	ε = -0.3867 × WD + 5.618	ε = -0.1067 × WD + 1.552

Notes: The units of GS, P, T and WD are mm, N, kg and mm, respectively.
The means of variables are GS = 3 mm, P = 150 N, T = 130 kg and WD = 1.8 mm
When a variable is considered, the other three variables are set to their means.

Based on the predicted data (Figure 7.4), the unknowns a_0 , a_{GS} , a_P, a_T and a_{WD} were determined by regression analysis using Microsoft Excel 365 (Microsoft Corp., Washington, USA) and the equations for ε in each callus zone were obtained as follows:

Periosteal zone:

$$\varepsilon = -0.1588 + 0.1204 \times GS + 0.0053 \times P - 0.0006 \times T - 0.0691 \times WD \quad (7.9)$$

Cortical zone:

$$\varepsilon = 3.2218 - 0.7000 \times GS + 0.0329 \times P - 0.0039 \times T - 0.3118 \times WD \quad (7.10)$$

Endosteal zone:

$$\varepsilon = 0.0069 + 0.1071 \times GS + 0.0091 \times P - 0.0011 \times T - 0.1068 \times WD \quad (7.11)$$

7.3.2 Reliability analysis

By using Eqs. 7.9-7.11, the probability of healing within each callus zone was calculated by considering the probability density function of ε. Since each variable was assumed to be normally distributed and considered one by one in the analysis, ε will also be normally distributed. Therefore, the probability of successful healing (PoS) can be calculated as

$$PoS = P(0.005\ \% \leq \varepsilon \leq 6\ \%) = \phi(6\ \%) - \phi(0.005\ \%) \quad (7.12)$$

where ϕ is the cumulative density function (CDF) of ε.

a) COV = 0.1

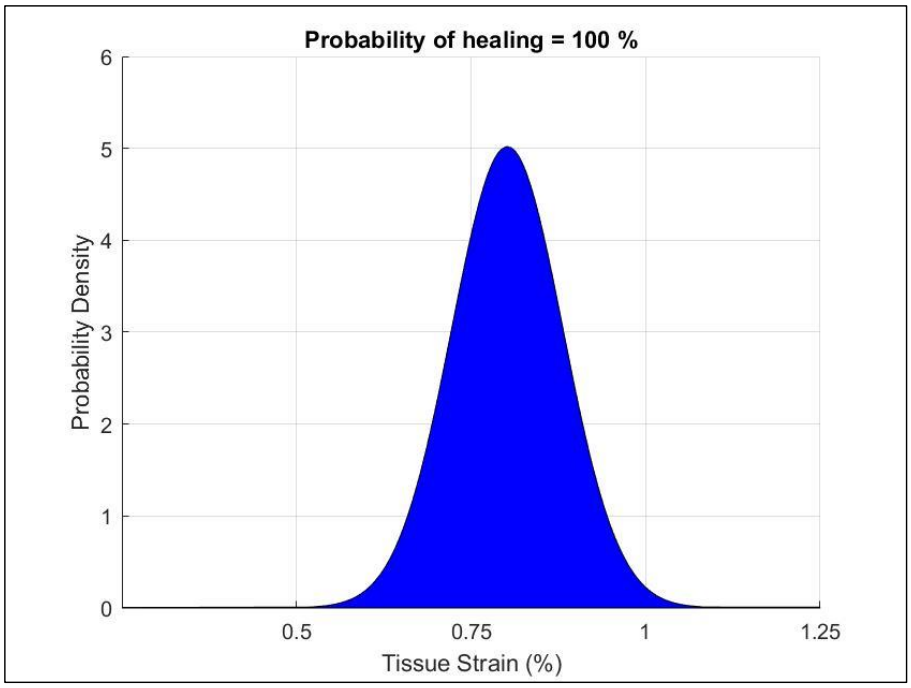

b) COV = 0.5

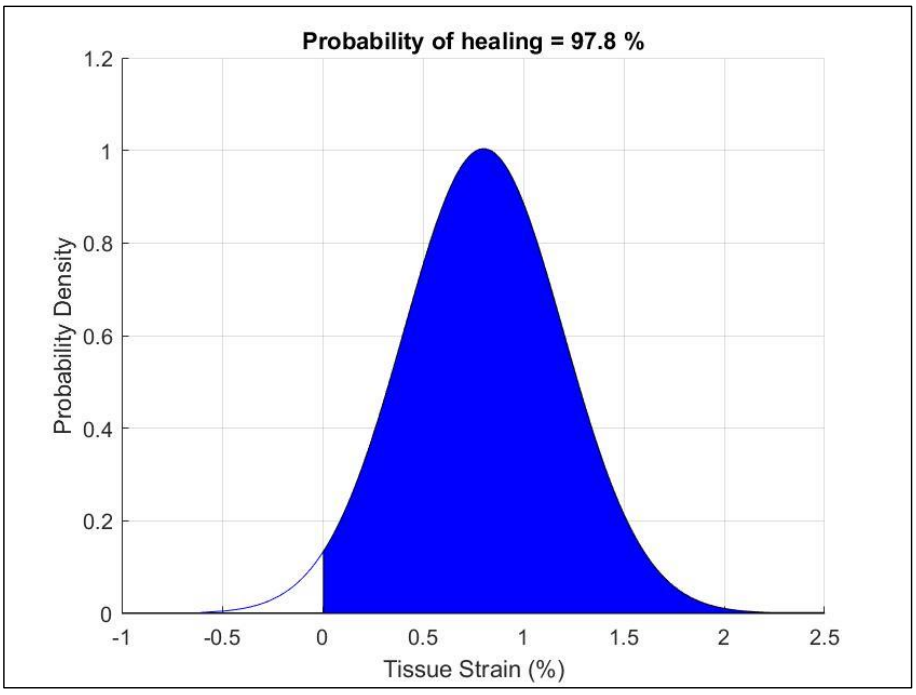

c) COV = 0.9

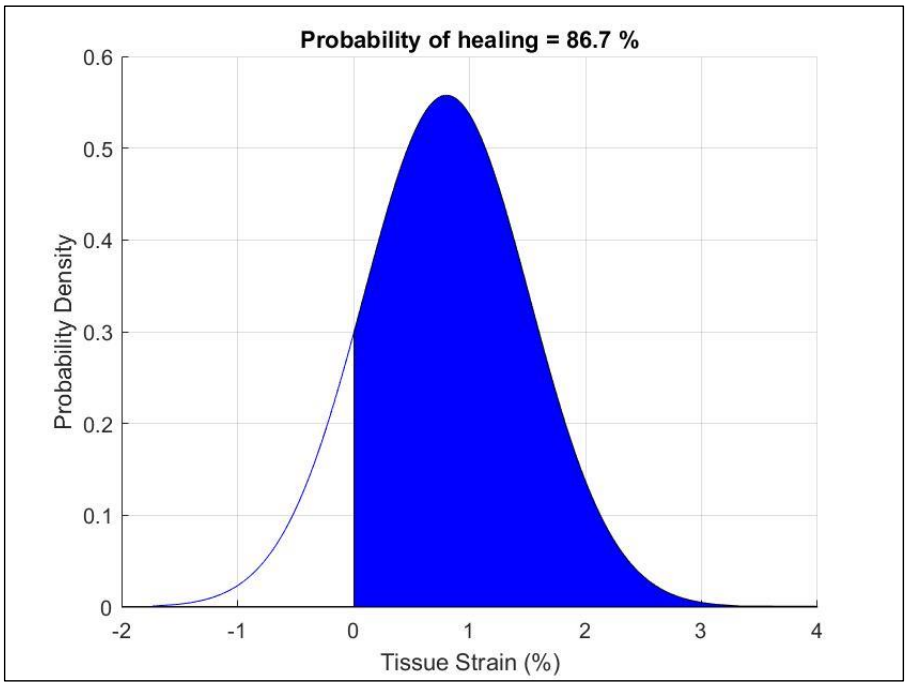

Figure 7.5 Probability of fracture healing (GS = 3 mm, T = 130 kg and WD = 1.8 mm) within the periosteal zone under different levels of uncertainties in weight bearing. (a) COV = 0.1, (b) COV = 0.5 and (c) COV = 0.9.

Taking weight bearing (P) as an example, the process of calculating the probability of fracture healing within the periosteal, cortical and endosteal zones of the callus under different COV values are shown in Figure 7.5, Figure 7.6 and Figure 7.7, respectively. For the mean (μ_P) and each value of COV_P, the corresponding mean (μ_ε) and standard deviation (σ_ε) of ε are calculated using Eq. 7.6 and 7.7, respectively and the probability of healing (PoS) is calculated using Eq. 7.12. It can be seen that PoS within each zone of the callus changes differently as the level of uncertainty in P changes. PoS within each zone were calculated under different COV values for other independent variables (i.e. GS, T and WD) as well. Subsequently the variation of PoS with COV for each variable were plotted as shown in Figure 7.8.

a) COV = 0.1

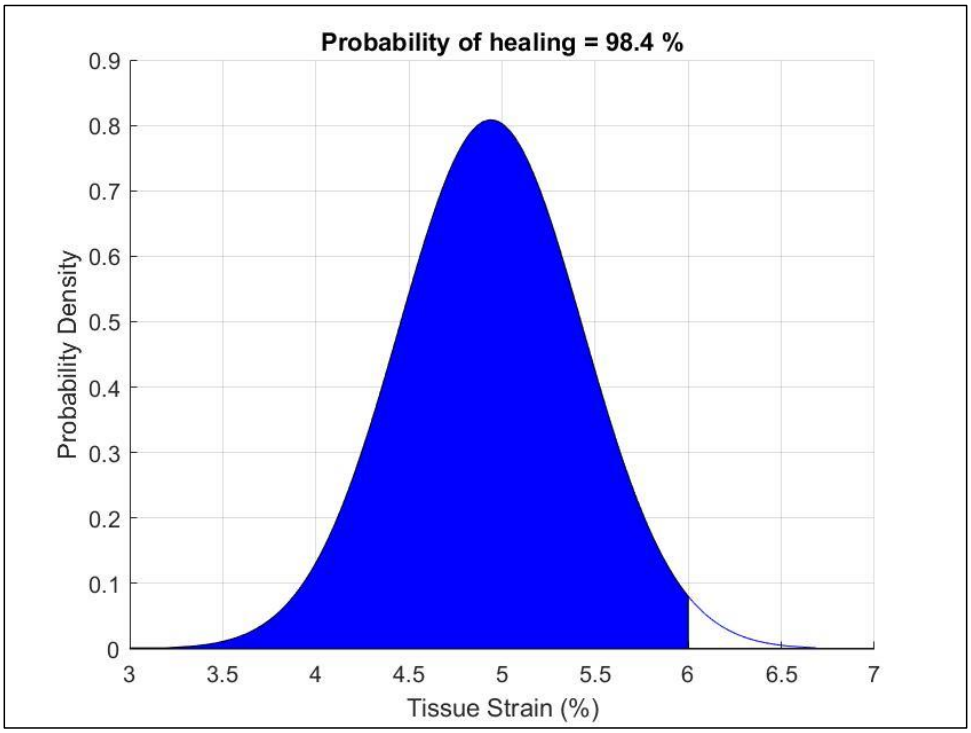

b) COV = 0.5

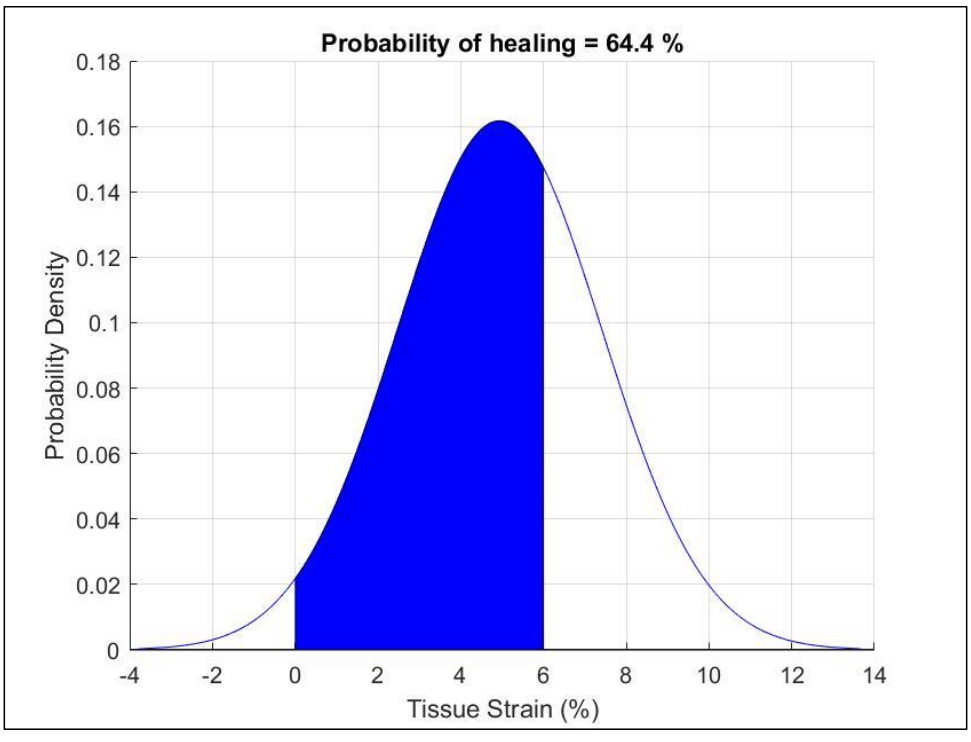

c) COV = 0.9

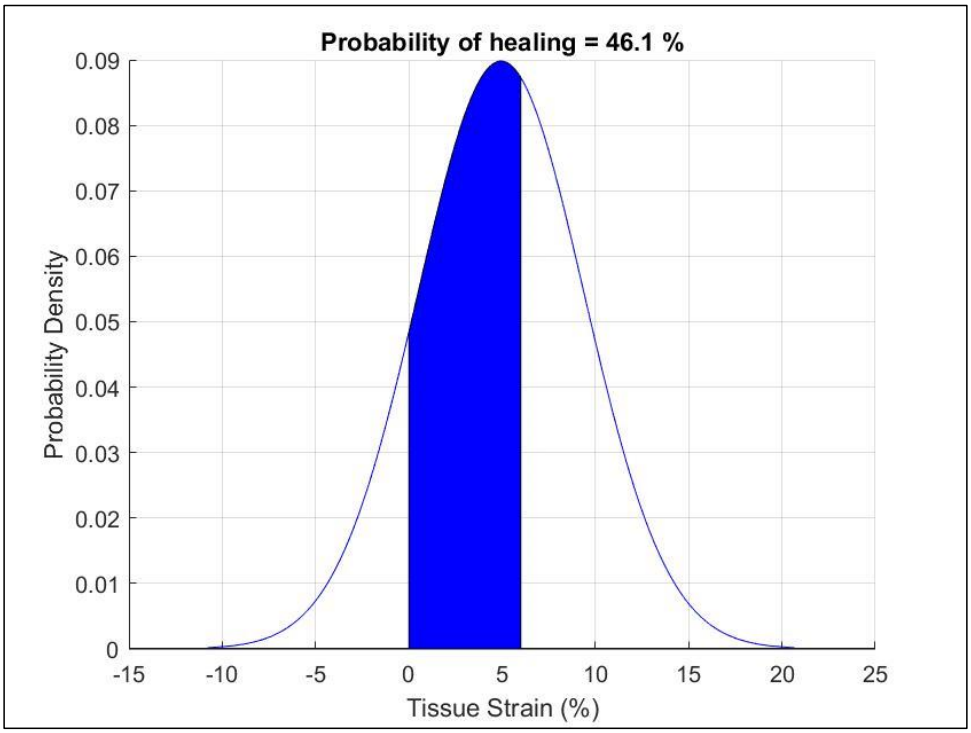

Figure 7.6 Probability of fracture healing (GS = 3 mm, T = 130 kg and WD = 1.8 mm) within the cortical zone under different levels of uncertainties in weight bearing . (a) COV = 0.1, (b) COV = 0.5 and (c) COV = 0.9.

It can be seen from Figure 7.8 that PoS within all callus zones tends to fall with increase in the degree of uncertainty in variables. However, the changes within the periosteal and endosteal zones are not significant except due to uncertainties in weight bearing (P) where the PoS decreased from 100 % to 86 % as COV_P increased from 0 to 0.9. The PoS within periosteal and endosteal zones were insensitive to variabilities in GS, T and WD. The changes in PoS were most significant within the cortical zone of the callus where the PoS decreased from 100 % to 46 %, 70 % and 95 % in response to COV increase from 0 to 0.9 for P, GS and WD, respectively. However, no noticeable changes in PoS was predicted due to uncertainties in wire pretension (T).

a) COV = 0.1

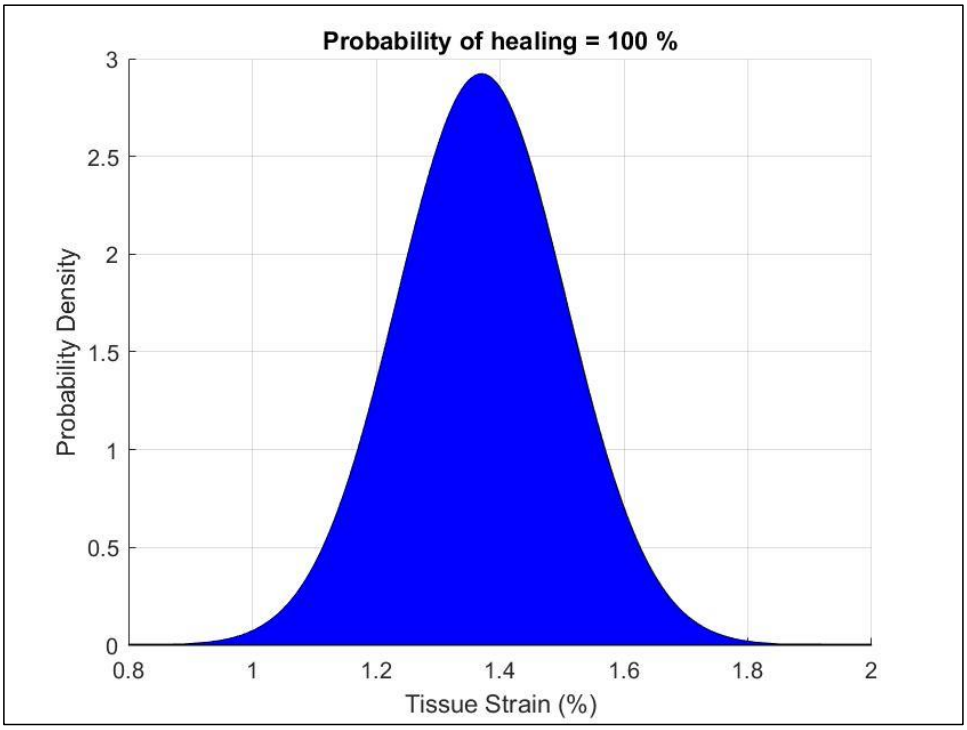

b) COV = 0.5

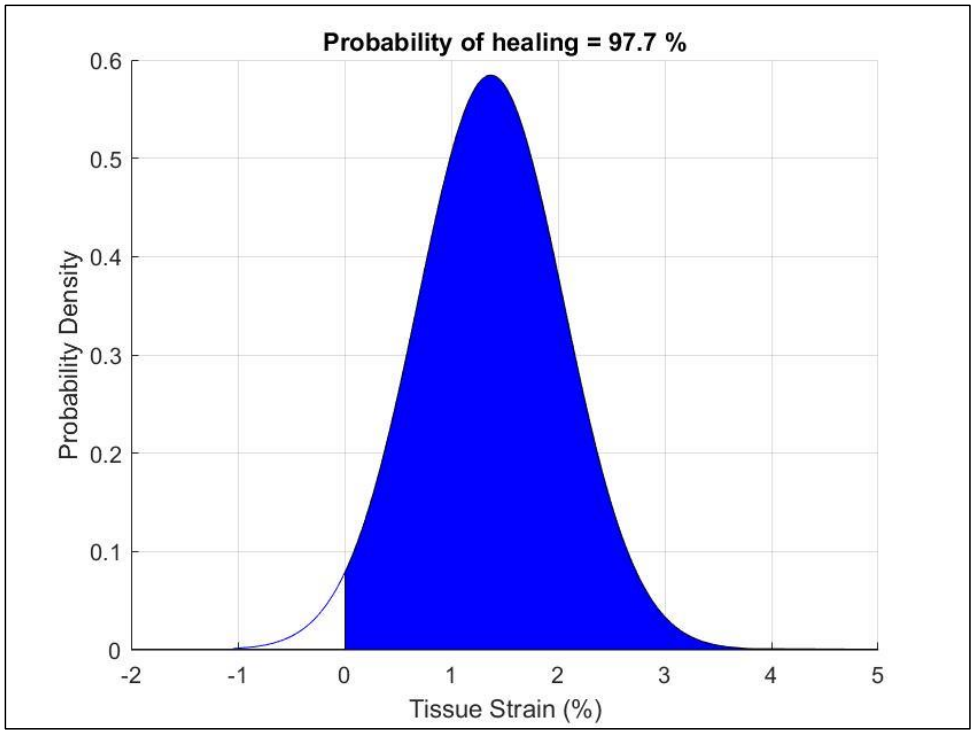

c) COV = 0.9

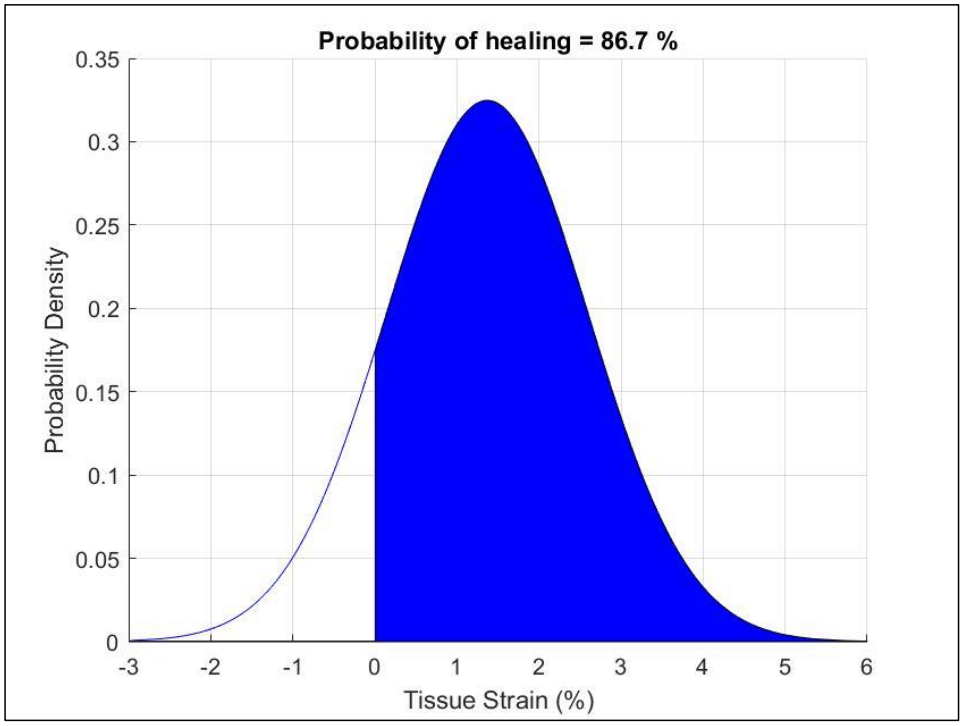

Figure 7.7 Probability of fracture healing (GS = 3 mm, T = 130 kg and WD = 1.8 mm) within the endosteal zone under different levels of uncertainties in weight bearing. (a) COV = 0.1, (b) COV = 0.5 and (c) COV = 0.9.

7.4 Discussion

In this study, computational models were used in conjunction with engineering reliability methods to investigate how the level of uncertainties in mechanical factors affect fracture healing under ICFs. Unlike in most of the existing studies which have taken deterministic approaches, a probabilistic approach was taken in this study to investigate how the uncertainties associated with some of the important mechanical variables affect the probability of fracture healing. It is known that angiogenesis is a prerequisite for successful healing and inhibition to this process could lead to unfavourable healing conditions [226]. Therefore, the fracture site needs to be prevented from excessive movement which can cause rupture of vessels and inhibition of angiogenesis [47].

a)

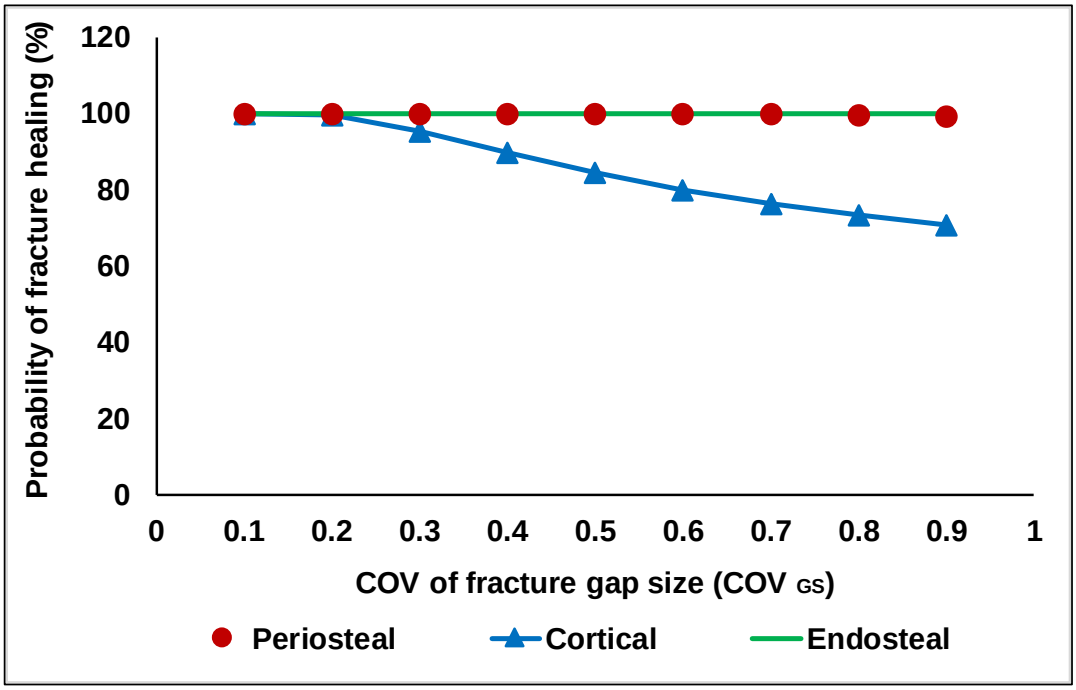
Probability of fracture healing (%)
120
100
80
60
40
20
0
0
0.1
0.2
0.3
0.4
0.5
0.6
0.7
0.8
0.9
1
COV of fracture gap size (COV GS)
Periosteal
Cortical
Endosteal

b)

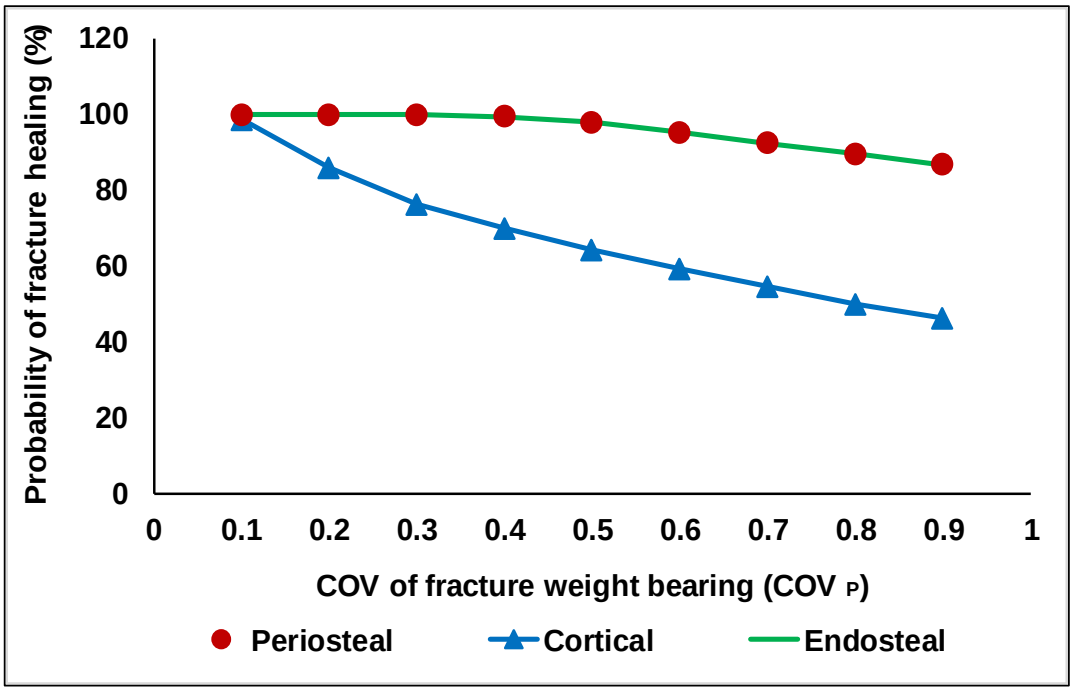
Probability of fracture healing (%)
120
100
80
60
40
20
0
0
0.1
0.2
0.3
0.4
0.5
0.6
0.7
0.8
0.9
1
COV of fracture weight bearing (COV P)
Periosteal
Cortical
Endosteal

c)

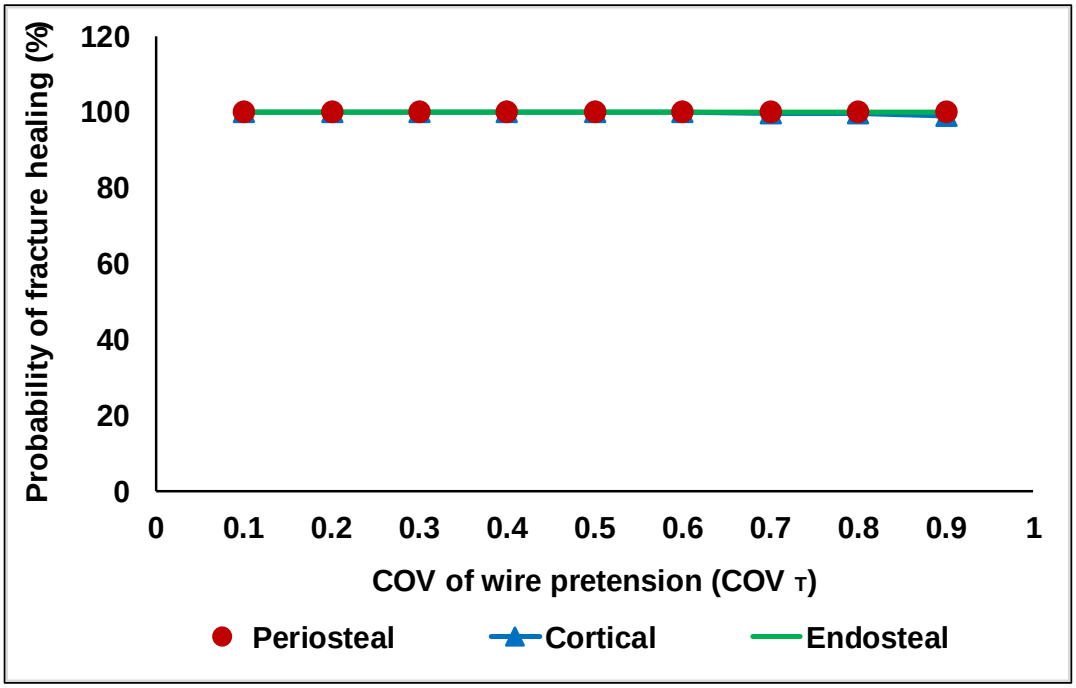

d)

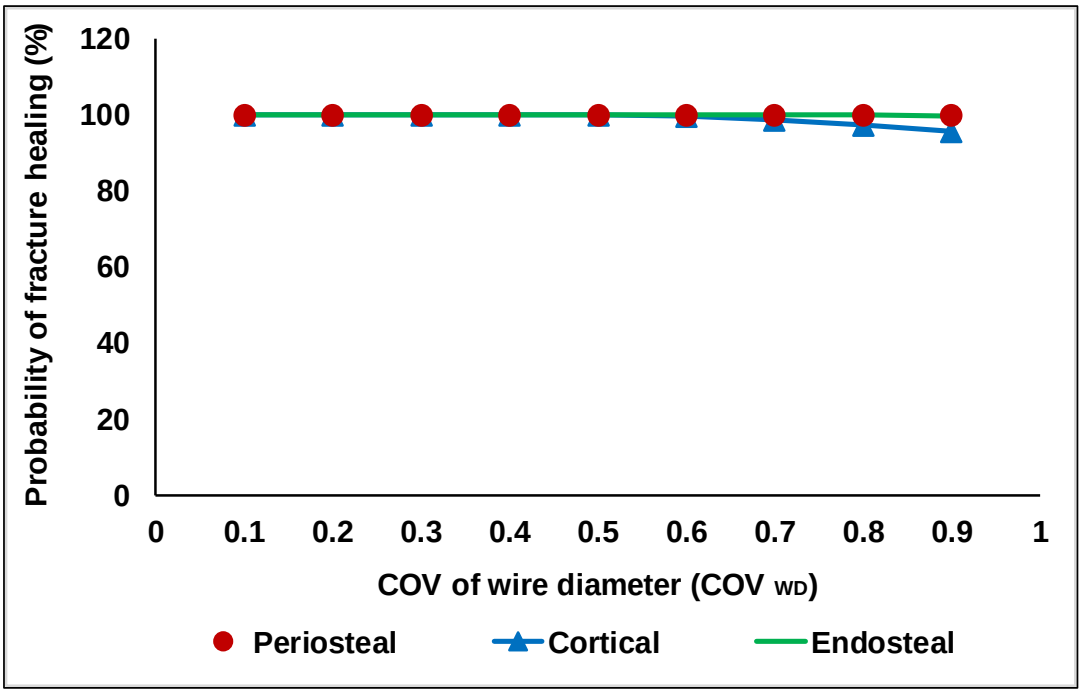

Figure 7.8 The effect of COV on the probability of successful healing (PoS) (a) COV_{GS} ; (b) COV_P ; (c) COV_T ; and (d) COV_{WD}

On the other hand, too little movement at the fracture site can give rise to bone resorption and compromise the quality of bone [81]. Therefore, the success of healing relies on achieving a balance between these two extremities. Based on this, favourable condition for fracture healing was defined in this study as achieving tissue strains between the strain limits for bone resorption and angiogenesis inhibition. This criterion was used to calculate the probabilities of successful healing (PoS) under different levels of uncertainties associated with mechanical variables. Although there is a plethora of uncertain variables that could influence fracture healing under ICF, only some of the most uncertain and influential variables were considered in this study.

As the primary focus of treatment using fixation devices such as ICF is to obtain favourable mechanical conditions within the fracture site to exploit the intrinsic biological healing capacity of bones [7, 9], this study deals with the uncertainties associated with the mechanical variables. The previous chapters of this thesis and studies elsewhere in literature have highlighted the importance of fracture gap size (GS) and weight bearing (P) on fracture healing. These are amongst the most important mechanical variables that influence fracture healing and the fracture site is very sensitive to them [19, 105]. In addition, wire pretension (T) and wire diameter (WD) which are two variables related to the ICF configuration were considered. Although there are various ICF configuration specific variables, T and WD were chosen in this study for two reasons. Firstly, wires are the invasive elements of ICF which connect the bone fragments to ICF and controls IFM. Secondly, a higher degree of uncertainty exists regarding ICF wires. It has been reported that wires could lose pretension due to several reasons such as slippage, yielding etc. [151]. In addition, accuracy of wire tensioners is also a source of uncertainty as errors as high as 37 % are reported with commercially available wire tensioners [263]. Furthermore, there is uncertainty in the effective diameter of the wire due to manufacturing tolerances and stretching (tensioning) of wires. In addition, there is chance of using different diameter wires due to limitations in availability of a specific diameter or even inadvertently as there are many different diameter wires available within the range of 0.7 – 2.0 mm [264, 265], the differences of which are difficult to perceive without high precision measurement.

In this study, the probabilities of successful healing (PoS) were calculated at the beginning of stage III (reparative phase) which refers to the stage when bone formation

within the fracture gap, periosteal bridging and endochondral ossification begins [262]. As the purpose of fracture healing is re-establishment of bone structure within the fracture gap, this point in the healing pathway marks the beginning of the actual repair process. Therefore, this stage is crucial for the success of healing and requires smooth progression of both angiogenesis and osteogenesis. However, there is uncertainty in the time at which this stage is reached as the rate of healing depends on numerous subject specific factors. In this study, this problem was tackled by focusing on a specific point in the healing pathway rather than a specific timepoint during healing. Thus, this analysis inherently assumes that the healing pathway remains the same for all cases and the differences in subject specific variables alter the rate at which the pathway is followed, which is reasonable [262].

The mean values for GS, P, T and WD were obtained from Chapter 6 as these combinations of parameters resulted in optimal healing conditions within the fracture site. Thus, GS = 3 mm, P = 150 N, T = 130 kg and WD = 1.8 mm would result in 100 % probability of fracture healing. By varying the COV of each parameter one by one, the uncertainties in the success of healing was measured by means of calculating PoS.

Out of the four parameters considered (i.e. GS, P, T and WD), tissue strain at the beginning of stage III of secondary healing was most sensitive to weight bearing (P) and then to gap size (GS). Interestingly, the previous chapters focusing on the early post inflammatory stage of healing (Chapters 4 and 5) predicted that the fracture site was more sensitive to GS than P. Therefore, the sensitivity of fracture site to different parameters could vary as healing progresses. Gap size (GS) is regarded as the most critical mechanical parameter in the early stages of healing when the callus is very soft; whereas, weight bearing (P) becomes the most critical parameter as callus stiffens and attracts load.

This phenomenon could possibly be explained by the study of Prat et al. [168], which investigated into load transmission via fracture site stabilized with circular external fixators during different stages of healing. The study [168] involved both theoretical and experimental investigations using rabbit model. Their study demonstrated that, when healing moves from early stages to subsequent stages and callus achieves some nominal mechanical stiffness, drastic change on the load sharing between the fixator and callus would occur (under fixed loading). In the early stages almost all the applied load is

supported by the fixation. This condition reverses to callus taking nearly 85 % of the applied load as callus stiffness increases to just below 1 % of that of intact bone which can occur relatively early during healing. This explains why the fracture site becomes more sensitive to weight bearing (P) as healing moves from early stage to subsequent stages. This has an important clinical implication as post-operative weight bearing exercises need to be carefully designed considering this fact and patients need to strictly adhere to clinical recommendations as PoS is most sensitive to weight bearing during the reparative phase.

An important challenge here is that the degree of uncertainty is relatively high in the level of weight bearing as patients cannot precisely control how much weight is borne by the fractured bone. For example, in sheep, up to 110 % of the body weight may be borne by metatarsal bones during normal walking [92]. However, the recommended weight bearing during the beginning of reparative phase could be around 20 % of the body weight (as per Chapter 6). Therefore, there is a very high degree of uncertainty about the level of weight bearing. The results of this study showed relatively strong positive correlation between P and tissue strains (Figure 7.4b). It was predicted that PoS decrease from 100 % to 46 % within the cortical zone with COV_P increase from 0 to 0.9 (Figure 7.8b). PoS would reduce further if the degree of uncertainty about P increases further, which is suggestive of failure of healing.

Gap size (GS) was predicted to be negatively correlated to tissue strain within the cortical zone (Figure 7.4a). This prediction is consistent with Perren [10] who explained that cells within smaller fracture gaps are subjected to increased mechanical stimuli when compared to those within larger fracture gap sizes. However, this does not suggest that larger gap sizes are preferable over smaller gap sizes as larger gap sizes could lead to relatively high IFMs in the early stages and delay the healing process [19]. It could be noticed from Figure 7.4a that GS is positively correlated to tissue strain within the periosteal zone. Although periosteal callus is not very sensitive to GS at the beginning of stage III, it will be very sensitive to GS in the early stages of healing as reported by Ganadhiepan et al. [21]. Since secondary healing relies on periosteal stabilization of the fracture site, it is essential that conductive mechanical environments to healing is maintained within the periosteal callus during the early stages. Therefore, larger gap sizes

which gives rise to higher tissue strains within the periosteal region in the early stages could lead to delays in healing. Furthermore, the intrinsic healing capacity of bones may not be utilized if the gap size is more than a critical size limit [7]. Nevertheless, clinical studies suggest that very small fracture gaps lead to very high mechanical stimuli and result in unfavourable healing conditions [266]. This emphasises the need for careful preplanning and execution of surgical reduction of fractures considering all the patient specific factors. In this study PoS was predicted to decrease from 100 % to 70 % within the cortical zone as COV_{GS} increased from 0 to 0.9.

The results showed that the uncertainties in ICF configuration parameters (T and WD) have very little effect on the mechanical environment and PoS at the beginning of reparative phase (beginning of stage III) of healing. Figure 7.4 c, d show no significant changes in tissue strains in response to changes in T or WD. In addition, Figure 7.8c, d show insignificant changes in PoS in response to uncertainties in T or WD. This could also be explained by the findings of Prat et al. [168]. As described before, when the fracture moves from the early stages to subsequent stages and begins to harden, a little increase in callus stiffness is enough to attract major fraction of the applied load. As most of the load is transferred via fracture callus, the fixator becomes less effective. Thus, changes made to the fixator will not significantly alter the mechanical environment of the fracture site. This suggests that although there is significant level of uncertainty about ICF configuration, it may not affect the probability of healing significantly during the reparative phase.

This is further supported by the finding of Prat et al. [168], which reported no significant changes in the mechanical behaviour due to differences in fixation rigidities once callus achieves some nominal mechanical properties. Their study compared rigid and dynamized fixation systems and identified noticeable differences in only in the very early stages of healing. Once the elastic modulus of the callus reached around 0.7 % of that of intact bone, no noticeable differences in load transmission were seen between the two fixation types. This is further corroborated by the findings of Terjesen and Svenningsen [267] and Aro et al. [268]. Therefore, the influence of ICF configuration appears to be important only in the early stages of healing to achieve fracture stability. Once callus achieves a nominal stiffness (e.g. around 1 % of intact bone or even less), the fracture site

- ICF interaction (i.e. load transmission) may not show significant differences and thus, not significantly affect the probability of healing.

The results also indicate that the mechanical environment of the periosteal and endosteal zones of the callus are not significantly altered by the mechanical parameters at the beginning of stage III of secondary healing (i.e. beginning of reparative phase) which is in contrast to the predictions made for the early stages of healing (Chapters 4,5). This is due the increase in callus stiffness by stage III which would lead to concentration of stresses closer to the bone ends (i.e. cortical zone) in response to loading.

In summary, the results of the present study emphasise the need for careful surgical reduction of the bone fragment and design of post-operative partial weight bearing exercises. Uncertainties associated with GS and P could not only affect the healing during the early stages (e.g. stage I and II) but also during subsequent stages of healing (e.g. stage III). At the beginning of reparative phase (stage III), P is the most dominant parameter influencing the mechanical environment of the fracture site. Thus, careful controlling of weight bearing is highly recommended during this stage to minimize the uncertainties associated with P. Use of instrumented insoles which allows accurate measurements of weight bearing is a possible way of achieving this [126]. Furthermore, this study suggests that ICF configuration does not significantly affect the probability of healing once callus reaches stage III of secondary healing (reparative phase). Moreover, cortical zone of the callus was predicted to be the most sensitive zone to uncertainties in mechanical parameters.

Limitations

This study has several limitations that needs to be stated. Firstly, simplifications were made to the fracture geometry and loading conditions, most of which are discussed in the previous chapters. In addition, it was assumed that fracture healing pathway remains the same for all the cases considered in this study and the differences in parameters only affect the rate at which the healing path is followed [262]. Moreover, only some of the most important mechanical variables that affect fracture healing under ICF were considered in this study. It should also be noted that the input variables were assumed to be independent and normally distributed which needs to be verified by considering large amount of experimental data. Furthermore, the investigations were carried out only at a

specific stage in the healing pathway. Therefore, future studies need to address these limitations.

Despite these limitations, this study provides useful insights into how uncertainties associated with mechanical variables affect the probability of successful healing. However, large amounts of experimental data are needed to further corroborate the findings of this study.

7.5 Conclusions

This study uses computational models in conjunction with probabilistic methods based on engineering reliability analysis to investigate how fracture healing under ICF is affected by the uncertainties associated with GS, P, T and WD. The probabilities of successful healing (PoS) were calculated under different levels of uncertainties associated with these variables. The main findings of this study are as follows:

- Cortical callus is very sensitive to mechanical variables at the beginning of reparative phase. However, periosteal and endosteal callus appear to be relatively insensitive to the mechanical variables.
- Level of weight bearing (P) is the most critical mechanical variable that affects the probability of successful healing (PoS) at the beginning of reparative phase. As weight bearing is also the most uncertain and easily changeable post-surgery, careful controlling of weight bearing is highly recommended (e.g. via use of instrumented insoles).
- Probability of successful healing (PoS) is sensitive to gap size (GS) during the reparative phase. However, it is not as highly sensitive as it is during the early stages of healing (i.e. post inflammatory and early reparative phases).
- The uncertainties in ICF wire pretension (T) and wire diameter (WD) do not significantly affect the probability of successful healing (PoS) during the reparative phase of healing which suggest that the effectiveness of ICF reduces significantly when the callus gains a nominal stiffness as large proportion of applied load is transmitted directly via callus.

8 Conclusions and Recommendations

8.1 Summary

This thesis significantly contributes to address the gap in the current understanding of the mechanobiology of fracture healing under Ilizarov circular fixators (ICFs). This knowledge gap is a barrier to address many clinical problems associated with ICFs and drives clinical decisions to be made on a trial and error basis without systematic investigations. Consequently, rates of treatment failures and complications are significantly high with ICF treatments. Furthermore, there is also a tendency in surgeons to prefer other fixators over ICF despite its advantages. In this research, computational models were developed, validated using experimental data and used to simulate fracture healing under various conditions to address the research objectives. Wherever possible, model predictions were compared with relevant clinical and experimental studies.

Firstly, a mechanical experiment on surrogate tibial fractures stabilized using ICFs was conducted to capture the interfragmentary movements (IFM) under physiological loadings relevant to early stage partial weight bearing (Chapter 3). Later, this data was used to validate a computational model of tibial fracture stabilized with ICF. After validation, the computational model was used to make predictions for cell differentiations within the fracture site during the early stages of fracture healing under different combinations of fracture geometries, loading and ICF configurations (Chapter 4).

Subsequently, further developments were made to the model to include various cells, growth factors and their transport and interactions within the fracture site (Chapter 5). Then, the model was used to study the spatial and temporal changes in the cell and growth factor concentrations during the early stage healing under physiologically relevant dynamic loading. The influence of different subject specific factors on the concentration changes were also investigated using the model.

Next, the research moved from early stages to the subsequent stages of healing and focused on determining time dependent and patient specific optimal weight bearing range for fracture healing under ICF (Chapter 6). Using sheep model as an example, the optimal weight bearing ranges were established considering the effects of loading on angiogenesis and bone quality. Finally, uncertainties in mechanical variables that influence healing

were incorporated in the analysis to investigate how such uncertainties affect the success of fracture healing under ICF (Chapter 7). This analysis took a probabilistic approach based on engineering reliability analysis techniques.

As ICFs are modular fixators which can be assembled in endless possible configurations, a few different clinically relevant ICF configurations were considered in this thesis. In Chapters 3 and 4, ICF configurations with hexapod system (i.e. TSF) were considered while the conventional ICF configurations (i.e. rings and rods) were considered in Chapters 5 – 7. Since there is only limited amount of data available on the biomechanical properties of TSF, this configuration was chosen for mechanical testing in Chapter 3. Subsequently, the same configuration was used in Chapter 4 as well in the mechanobiological investigations, following validation using the data obtained from Chapter 3. In Chapters 5-7 the conventional ICF configurations with rings and rods were studied. Furthermore, the effect of changing ICF configuration (e.g. changing ring diameter, changing wire diameter, changing wire pretension, use of half pins etc.) was given attention in each chapter. Thus, a reasonable range of clinically relevant ICF configurations have been considered in this thesis.

8.2 Conclusions

The potential of computational models in studying complex biomedical problems is demonstrated in this thesis. By linking our understanding at different observational levels (i.e. cellular, tissue and clinical levels), computational models pave way to make more informed clinical decisions based on systematic investigations rather than trial error. This research provides insights into many aspects of mechanobiology of fracture healing under ICFs and have clinical relevance. The key findings of this thesis are summarised below:

- The investigations on early stage MSC differentiations within the fracture site stabilized with ICF (Chapter 4) suggests that, fracture geometry is the most influential mechanical factor governing the early stage MSC differentiation process. Small gap sizes (e.g. 1 mm) could result in better healing microenvironments throughout the callus; whereas, mid (e.g. 3 mm) and large size (e.g. 5 mm) gaps tend to rely mostly on periosteal stabilization. Furthermore, the roles of loading and ICF configuration on early stage MSC differentiations

are also dictated by fracture gap size. For small gap sizes, MSC differentiations within most parts of the callus would be affected by loading level. But for mid and large gaps, MSC differentiations would be affected significantly by loading only within the periosteal region. This was the case with ICF ring diameter and wire pretension as well. However, these configuration specific parameters would have limited effects of early stage MSC differentiations. These predictions highlight the need for careful fracture reduction with small gap sizes. However, when larger gap sizes (e.g. 3 – 5 mm) are unavoidable, controlling the axial load (i.e. partial weight bearing) would be more effective than adjusting the ICF stiffness by either changing the ring diameter or wire pretension in the early stages of healing.

- Findings of Chapter 5 suggests that, cell and growth factor concentrations within the early fracture callus are significantly enhanced due to physiologically relevant dynamic loading. This could be one of the reasons why fracture healing under ICFs is enhanced due to early weight bearing. The synergistic effects of (i) mechanical stimuli mediated cell differentiation, (ii) advective transport of cells and growth factors and (iii) increased chemical stimuli mediated cell differentiation (due to increased concentrations of growth factors) resulting from dynamic loading are responsible for the enhancement of cell concentrations. An hour of walking with partial weight bearing could result in significantly elevated levels of chondrocyte and growth factors throughout the day. Enhanced chondrocyte content within the fracture callus is beneficial for secondary healing (i.e. via cartilage formation), especially in the early callus development stages. Loading relevant to walking, relatively smaller gap sizes and increased IFM resulting from flexible ICF configurations tend to enhance chondrocyte and growth factor concentrations within the early callus.

- Chapter 6 was focused on determining the optimal levels of weight bearing under ICFs during healing. Although early weight bearing can have beneficial effects on fracture healing, IFMs induced by weight-bearing may inhibit angiogenesis and delay the healing process. The optimal level of weight bearing is time

dependent, subject specific and mainly governed by fracture gap size. The upper and lower limits of optimal weight bearing range could be established by considering the tissue strain limits relevant to angiogenesis inhibition and bone resorption, respectively. In general, weight bearing under conventional ICFs in the early weeks of healing could be detrimental for angiogenesis. For normal body weights (i.e. 75 kg) and mid-sized fracture gaps (e.g. 3mm) , partial weight-bearing could start few weeks post operation (e.g. 4 weeks) and gradually increase to full weight bearing within reasonable timeframes (i.e. 12 weeks). In contrast, for relatively large fracture gap sizes (i.e. 6 mm), even partial weight-bearing is not recommendable within this time frame. Increasing ICF stiffness (e.g. using half pins instead of pretension wires) can increase the level of weight-bearing significantly in the early stages up to a certain time point (e.g. week 8 post-operation). However, no noticeable benefits could be achieved by changing ICF configuration beyond that.

- Chapter 7 emphasised the need for careful surgical reduction of bone fragment and design of post-operative partial weight bearing exercises. The results of Chapter 7 suggested that, uncertainties associated with fracture gap and weight bearing could not only affect fracture healing during the early stages (e.g. post inflammatory stage) but also during subsequent stages of healing (e.g. reparative phase). At the beginning of reparative phase, weight bearing is the most dominant parameter influencing the mechanical environment of the fracture site. Thus, careful controlling of weight bearing (e.g. use of instrumented insoles) is highly recommended during this stage to minimize the uncertainties associated with weight bearing. Furthermore, the results suggested that ICF configuration does not significantly affect the probability of healing once callus reaches stage III of secondary healing (reparative phase). This indicated that the effectiveness of ICF reduces significantly when the callus gains a nominal stiffness as large proportion of applied load is transmitted directly via callus. The results also indicated that, cortical zone is the most sensitive part of the callus to uncertainties in mechanical parameters during the reparative phase of healing.

In summary, by linking ICF mechanics with the biology of fracture healing, this thesis contributes significantly to fill the gap in the current understanding of the mechanobiology of fracture healing under ICFs. The models presented in this thesis could potentially be used to conduct further investigations on many other aspects of fracture healing under ICF and to design patient specific treatment plans.

8.3 Limitations

It should be noted that several assumptions and simplifications were necessary for the development of the computational models presented in this thesis. Therefore, the interpretation of the results and conclusions drawn from this thesis are to be considered in conjunction with the assumptions and simplifications made.

First, only specific aspects of fracture healing were investigated using the models. As there is plethora of factors and processes involved in the fracture healing process, it is practically impossible to incorporate every single factor and process in the models. The model presented in Chapter 4 was focused on early stage MSC differentiations, ignoring other processes such as cell migration and the effects of chemical stimuli (i.e. growth factors).

In Chapter 5, cell migration and the effects of chemical stimuli on fracture healing were considered. However, still the model was focused on cell differentiation pathways during the early stages of healing. The subsequent study (Chapter 6) extended the analysis to cover the entire reparative phase of healing. Nevertheless, to be efficient with computational resources and time, the model had to be simplified. Therefore, angiogenesis was incorporated in the model as the determinant of cell differentiations without explicitly considering the intermediate steps involving growth factors.

In Chapter 7, the investigation on the effects of uncertainties on fracture healing was conducted based on the model developed in Chapter 6. In this investigation, the effects of only some of the most uncertain and influential mechanical variables were considered for analysis. Furthermore, the analysis was focused on a specific point in the healing pathway. The investigation assumed that the variables are independent and normally distributed. In all the chapters, the roles of mechanical factors were given greater

attention. But other factors that influence fracture healing such as age, sex and comorbidities were not considered.

In addition, to minimize the complexity of analysis, only transverse fractures and axial compressive loading were considered throughout the studies. In real bones, more complex fracture geometries and loading conditions can occur and result in significantly different healing environments. Furthermore, following the first model (Chapter 4) which took the complex geometry of bone into account, the bone geometry in the subsequent models were simplified to uniform cylindrical shapes. This simplification enabled to take advantage of axis-symmetry of the fracture site and simulate some of the complex biological processes in 2D domains. This resulted in substantial computational time savings.

It is known that material properties of bone and other tissues and the rates of processes taking place within the fracture site during healing (e.g. rate of cell diffusion, rate of bone formation etc.) are subject specific. The numerical values of such parameters used in the models are typical averages under healthy conditions obtained from existing literature. Therefore, the findings of this study are mostly relevant to typical bone fracture healing under healthy conditions. Moreover, this thesis did not investigate the role of every ICF configuration parameter but only some of most important ones. Finally, and most importantly, more experimental and clinical evidence is required to further corroborate the findings of this thesis.

8.4 Recommendations for future work

Now that the models coupling mechanics of ICF and biology of fracture healing have been developed, many different aspects of fracture healing under ICF that were not studied in this thesis could be studied in the future. Further investigations under various configurations of ICF and various conditions of healing could be carried out. In addition, the models could be extended to capture inflammation and remodelling phases as well. Moreover, the effects of changes to callus geometry during the healing process may also be incorporated.

Another potential application of these models is to investigate the mechano-biology of ‘distraction osteogenesis’: a process by which new bone volumes are grown from existing

fragments by the application of controlled traction. As ICFs are widely used to treat large bone defects with substantial bone losses via distraction osteogenesis, such investigations could be of clinical significance.

In addition, interactive and easy-to-use computational models may be developed to take patient specific factors and healing conditions as inputs; then, construct models as per the user inputs; subsequently, carry out fracture healing simulations and suggests suitable treatment strategies. Such models could have potential for direct clinical uses and serve as tools to assist patient specific treatment planning.

Furthermore, the advancements in imaging techniques (e.g. CT images) in computational model developments have opened new possibilities in developing models directly from clinical images of patients (e.g. CT images). However, there is plenty of room for further research before such techniques can have clinical applications. Finally, further clinical and experimental studies need to be carried out in this research area.

References

[1] T. Meling, K. Harboe, and K. Søreide, "Incidence of traumatic long-bone fractures requiring in-hospital management: a prospective age-and gender-specific analysis of 4890 fractures," *Injury,* vol. 40, no. 11, pp. 1212-1219, 2009.

[2] Z. Li, D. Betts, G. Kuhn, M. Schirmer, R. Müller, and D. Ruffoni, "Mechanical regulation of bone formation and resorption around implants in a mouse model of osteopenic bone," *Journal of the Royal Society Interface,* vol. 16, no. 152, p. 20180667, 2019.

[3] C. Ekegren, E. Edwards, R. de Steiger, and B. Gabbe, "Incidence, costs and predictors of non-union, delayed union and mal-union following long bone fracture," *International journal of environmental research and public health,* vol. 15, no. 12, p. 2845, 2018.

[4] Osteoporosis National Action Plan Working Group, "Osteoporosis National Action Plan 2016," 2016.

[5] D. J. Hak *et al.*, "Delayed union and nonunions: epidemiology, clinical issues, and financial aspects," *Injury,* vol. 45, pp. S3-S7, 2014.

[6] L. Norton and J. Harrison, "Hospital separations due to injury and poisoning, Australia 2006–07," *Injury research and statistics series,* no. 63, 2012.

[7] A. M. Makhdom, L. Nayef, M. Tabrizian, and R. C. Hamdy, "The potential roles of nanobiomaterials in distraction osteogenesis," *Nanomedicine: Nanotechnology, Biology and Medicine,* vol. 11, no. 1, pp. 1-18, 2015.

[8] P. Augat, U. Simon, A. Liedert, and L. Claes, "Mechanics and mechano-biology of fracture healing in normal and osteoporotic bone," *Osteoporosis international,* vol. 16, no. 2, pp. S36-S43, 2005.

[9] P. J. Wraighte and B. E. Scammell, "Principles of fracture healing," *Surgery (Oxford),* vol. 24, no. 6, pp. 198-207, 2006.

[10] S. Perren, "Physical and biological aspects of fracture healing with special reference to internal fixation," *Clinical orthopaedics and related research,* vol. 138, pp. 175-196, 1979.

[11] S. Aitken, T. W. Hamilton, L. Rennie, and B. Caesar, "Nonoperative fracture treatment in the modern era," *Journal of Trauma and Acute Care Surgery,* vol. 69, no. 3, pp. 699-707, 2010.

[12] A. T. Fragomen and S. R. Rozbruch, "The mechanics of external fixation," *HSS Journal,* vol. 3, no. 1, pp. 13-29, 2007.

[13] K. Erler, C. Yildiz, B. Baykal, A. S. Atesalp, M. T. Ozdemir, and M. Basbozkurt, "Reconstruction of defects following bone tumor resections by distraction osteogenesis," *Archives of orthopaedic and trauma surgery,* vol. 125, no. 3, pp. 177-183, 2005.

[14] D. Paley, H. F. Kovelman, and J. E. Herzenberg, "Ilizarov technology," *Advances in Operative Orthopaedics. St. Louis, Mosby-Year Book*, vol. 1, pp. 243-287, 1993.

[15] M. Mullins, A. Davidson, D. Goodier, and M. Barry, "The biomechanics of wire fixation in the Ilizarov system," *Injury*, vol. 34, no. 2, pp. 155-157, 2003.

[16] D. R. Epari, W. R. Taylor, M. O. Heller, and G. N. Duda, "Mechanical conditions in the initial phase of bone healing," *Clinical Biomechanics*, vol. 21, no. 6, pp. 646-655, 2006.

[17] H. Schell, D. Epari, J. Kassi, H. Bragulla, H. Bail, and G. Duda, "The course of bone healing is influenced by the initial shear fixation stability," *Journal of Orthopaedic Research*, vol. 23, no. 5, pp. 1022-1028, 2005.

[18] H. Isaksson, "Recent advances in mechanobiological modeling of bone regeneration," *Mechanics Research Communications*, vol. 42, pp. 22-31, 2012.

[19] L. Claes, P. Augat, G. Suger, and H. J. Wilke, "Influence of size and stability of the osteotomy gap on the success of fracture healing," *Journal of Orthopaedic Research*, vol. 15, no. 4, pp. 577-584, 1997.

[20] L. Claes, K. Eckert-Hübner, and P. Augat, "The fracture gap size influences the local vascularization and tissue differentiation in callus healing," *Langenbeck's archives of surgery*, vol. 388, no. 5, pp. 316-322, 2003.

[21] G. Ganadhiepan, S. Miramini, M. Patel, P. Mendis, and L. Zhang, "Bone fracture healing under Ilizarov fixator: Influence of fixator configuration, fracture geometry, and loading," *International journal for numerical methods in biomedical engineering*, vol. 35, no. 6, p. e3199, 2019.

[22] G. Ganadhiepan *et al.*, "The Effects of Dynamic Loading on Bone Fracture Healing Under Ilizarov Circular Fixators," *Journal of Biomechanical Engineering*, vol. 141, no. 5, pp. 051005-051005-12, 2019.

[23] G. A. Parker and C. A. Picut, *Atlas of histology of the juvenile rat*. Academic Press, 2016.

[24] J. Lowe and P. Anderson, "Chapter 13-Musculoskeletal System," *Stevens & Lowe's Human Histology (Fourth Edition)(Fourth Edition). Philadelphia: Mosby*, 2015.

[25] M. Doblaré and J. Garcıa, "Anisotropic bone remodelling model based on a continuum damage-repair theory," *Journal of biomechanics*, vol. 35, no. 1, pp. 1-17, 2002.

[26] M. Doblaré, J. Garcıa, and M. Gómez, "Modelling bone tissue fracture and healing: a review," *Engineering Fracture Mechanics*, vol. 71, no. 13, pp. 1809-1840, 2004.

[27] J.-Y. Rho, L. Kuhn-Spearing, and P. Zioupos, "Mechanical properties and the hierarchical structure of bone," *Medical engineering & physics*, vol. 20, no. 2, pp. 92-102, 1998.

[28] M. L. Bouxsein and D. Karasik, "Bone geometry and skeletal fragility," *Current osteoporosis reports*, vol. 4, no. 2, pp. 49-56, 2006.

[29] R. S. Taichman, "Blood and bone: two tissues whose fates are intertwined to create the hematopoietic stem-cell niche," *Blood*, vol. 105, no. 7, pp. 2631-2639, 2005.

[30] B. Clarke, "Normal bone anatomy and physiology," *Clinical journal of the American Society of Nephrology*, vol. 3, no. Supplement 3, pp. S131-S139, 2008.

[31] V. Scanlon and T. Sanders, *Essentials of Anatomy and Physiology*. Philadelphia, UNITED STATES: F. A. Davis Company, 2014.

[32] D. B. Burr, "Bone morphology and organization," in *Basic and applied bone biology*: Elsevier, 2019, pp. 3-26.

[33] B. K. Hall, "The embryonic development of bone," *American Scientist*, vol. 76, no. 2, pp. 174-181, 1988.

[34] S. P. Bruder, D. J. Fink, and A. I. Caplan, "Mesenchymal stem cells in bone development, bone repair, and skeletal regenaration therapy," *Journal of cellular biochemistry*, vol. 56, no. 3, pp. 283-294, 1994.

[35] S. A. Hienz, S. Paliwal, and S. Ivanovski, "Mechanisms of bone resorption in periodontitis," *Journal of immunology research*, vol. 2015, 2015.

[36] D. J. Hadjidakis and I. I. Androulakis, "Bone remodeling," *Annals of the New York Academy of Sciences*, vol. 1092, no. 1, pp. 385-396, 2006.

[37] A. L. Firth, W. Yao, and J. X.-J. Yuan, "Identification of Adult Stem and Progenitor Cells in the Pulmonary Vasculature," in *Textbook of Pulmonary Vascular Disease*: Springer, 2011, pp. 621-636.

[38] S. Weiner and H. D. Wagner, "The material bone: structure-mechanical function relations," *Annual review of materials science*, vol. 28, no. 1, pp. 271-298, 1998.

[39] D. R. Carter and W. C. Hayes, "The compressive behavior of bone as a two-phase porous structure," *The Journal of bone and joint surgery. American volume*, vol. 59, no. 7, pp. 954-962, 1977.

[40] J. C. Lotz, T. N. Gerhart, and W. C. Hayes, "Mechanical properties of metaphyseal bone in the proximal femur," *Journal of biomechanics*, vol. 24, no. 5, pp. 317-329, 1991.

[41] J. D. Currey, "The effect of porosity and mineral content on the Young's modulus of elasticity of compact bone," *Journal of biomechanics*, vol. 21, no. 2, pp. 131-139, 1988.

[42] M. B. Schaffler and D. B. Burr, "Stiffness of compact bone: effects of porosity and density," *Journal of biomechanics*, vol. 21, no. 1, pp. 13-16, 1988.

[43] T. S. Keller, "Predicting the compressive mechanical behavior of bone," *Journal of biomechanics*, vol. 27, no. 9, pp. 1159-1168, 1994.

[44] E. A. Zimmermann and R. O. Ritchie, "Bone as a Structural Material," *Advanced Healthcare Materials*, vol. 4, no. 9, pp. 1287-1304, 2015.

[45] T. R. Fleury and R. Stern, "Classification of Long Bone Fractures," *European Surgical Orthopaedics and Traumatology: The EFORT Textbook*, pp. 115-137, 2014.

[46] M. E. Müller, S. Nazarian, P. Koch, and J. Schatzker, *The comprehensive classification of fractures of long bones*. Springer Science & Business Media, 2012.

[47] L. Claes, S. Recknagel, and A. Ignatius, "Fracture healing under healthy and inflammatory conditions," *Nature Reviews Rheumatology*, vol. 8, no. 3, p. 133, 2012.

[48] Z. Ai-Aql, A. S. Alagl, D. T. Graves, L. C. Gerstenfeld, and T. A. Einhorn, "Molecular mechanisms controlling bone formation during fracture healing and distraction osteogenesis," *Journal of dental research*, vol. 87, no. 2, pp. 107-118, 2008.

[49] R. Marsell and T. A. Einhorn, "The biology of fracture healing," *Injury*, vol. 42, no. 6, pp. 551-555, 2011.

[50] R. Dimitriou, E. Tsiridis, and P. V. Giannoudis, "Current concepts of molecular aspects of bone healing," *Injury*, vol. 36, no. 12, pp. 1392-1404, 2005.

[51] C. Ferguson, E. Alpern, T. Miclau, and J. A. Helms, "Does adult fracture repair recapitulate embryonic skeletal formation?," *Mechanisms of development*, vol. 87, no. 1-2, pp. 57-66, 1999.

[52] N. Little, B. Rogers, and M. Flannery, "Bone formation, remodelling and healing," *Surgery (Oxford)*, vol. 29, no. 4, pp. 141-145, 2011.

[53] P. V. Giannoudis, T. A. Einhorn, and D. Marsh, "Fracture healing: the diamond concept," *Injury*, vol. 38, pp. S3-S6, 2007.

[54] P. M. Mountziaris and A. G. Mikos, "Modulation of the inflammatory response for enhanced bone tissue regeneration," *Tissue Engineering Part B: Reviews*, vol. 14, no. 2, pp. 179-186, 2008.

[55] H. Isaksson, C. C. van Donkelaar, R. Huiskes, and K. Ito, "A mechano-regulatory bone-healing model incorporating cell-phenotype specific activity," *Journal of theoretical biology*, vol. 252, no. 2, pp. 230-246, 2008.

[56] R. Dimitriou, E. Jones, D. McGonagle, and P. V. Giannoudis, "Bone regeneration: current concepts and future directions," *BMC medicine*, vol. 9, no. 1, p. 66, 2011.

[57] L. Claes and C. Heigele, "Magnitudes of local stress and strain along bony surfaces predict the course and type of fracture healing," *Journal of biomechanics*, vol. 32, no. 3, pp. 255-266, 1999.

[58] P. Prendergast, R. Huiskes, and K. Søballe, "Biophysical stimuli on cells during tissue differentiation at implant interfaces," *Journal of biomechanics*, vol. 30, no. 6, pp. 539-548, 1997.

[59] L. Geris, A. Gerisch, J. Vander Sloten, R. Weiner, and H. Van Oosterwyck, "Angiogenesis in bone fracture healing: a bioregulatory model," *Journal of theoretical biology,* vol. 251, no. 1, pp. 137-158, 2008.

[60] R. L. Cruess, J. Dumont, and C. Newton, "Healing of bone," *Textbook of small animal orthopaedics,* 1985.

[61] C. E. DeCamp, *Brinker, Piermattei and Flo's handbook of small animal orthopedics and fracture repair*. Elsevier Health Sciences, 2015.

[62] A. P. Matson, K. S. Hamid, and S. B. Adams, "Predictors of time to union after operative fixation of closed ankle fractures," *Foot & ankle specialist,* vol. 10, no. 4, pp. 308-314, 2017.

[63] L. A. Corrales, S. Morshed, M. Bhandari, and T. Miclau III, "Variability in the assessment of fracture-healing in orthopaedic trauma studies," *The Journal of Bone and Joint Surgery. American volume.,* vol. 90, no. 9, p. 1862, 2008.

[64] G. M. Calori *et al.*, "Non-unions," *Clinical Cases in Mineral and Bone Metabolism,* vol. 14, no. 2, p. 186, 2017.

[65] D. M. Nunamaker, F. W. Rhinelander, and R. B. Heppenstall, "Delayed union, nonunion, and malunion," *Textbook of Small Animal Orthopaedics,* vol. 38, 1985.

[66] V. Perumal and C. S. Roberts, "(ii) Factors contributing to non-union of fractures," *Current Orthopaedics,* vol. 21, no. 4, pp. 258-261, 2007.

[67] P. Andrzejowski and P. V. Giannoudis, "The 'diamond concept'for long bone non-union management," *Journal of Orthopaedics and Traumatology,* vol. 20, no. 1, p. 21, 2019.

[68] L. C. Gerstenfeld, D. M. Cullinane, G. L. Barnes, D. T. Graves, and T. A. Einhorn, "Fracture healing as a post-natal developmental process: molecular, spatial, and temporal aspects of its regulation," *Journal of cellular biochemistry,* vol. 88, no. 5, pp. 873-884, 2003.

[69] G. L. Barnes, P. J. Kostenuik, L. C. Gerstenfeld, and T. A. Einhorn, "Growth factor regulation of fracture repair," *Journal of Bone and Mineral Research,* vol. 14, no. 11, pp. 1805-1815, 1999.

[70] F. Rougier, F. Dupuis, and Y. Denizot, "Human bone marrow fibroblasts-an overview of their characterization, proliferation and inflammatory mediator production," *Hematology and Cell Therapy,* vol. 38, no. 3, pp. 241-246, 1996.

[71] J. J. Tomasek, G. Gabbiani, B. Hinz, C. Chaponnier, and R. A. Brown, "Myofibroblasts and mechano-regulation of connective tissue remodelling," *Nature reviews Molecular cell biology,* vol. 3, no. 5, p. 349, 2002.

[72] C. S. Bahney *et al.*, "Cellular biology of fracture healing," *Journal of Orthopaedic Research®,* vol. 37, no. 1, pp. 35-50, 2019.

[73] Z. Bar-Shavit, "The osteoclast: A multinucleated, hematopoietic-origin, bone-resorbing osteoimmune cell," *Journal of cellular biochemistry,* vol. 102, no. 5, pp. 1130-1139, 2007.

[74] V. Peiffer, A. Gerisch, D. Vandepitte, H. Van Oosterwyck, and L. Geris, "A hybrid bioregulatory model of angiogenesis during bone fracture healing," *Biomechanics and modeling in mechanobiology,* vol. 10, no. 3, pp. 383-395, 2011.

[75] C. Sfeir, L. Ho, B. A. Doll, K. Azari, and J. O. Hollinger, "Fracture repair," in *Bone regeneration and repair*: Springer, 2005, pp. 21-44.

[76] B. Beamer, C. Hettrich, and J. Lane, "Vascular endothelial growth factor: an essential component of angiogenesis and fracture healing," *HSS journal,* vol. 6, no. 1, pp. 85-94, 2010.

[77] X. Lu *et al.*, "The ameloblastin extracellular matrix molecule enhances bone fracture resistance and promotes rapid bone fracture healing," *Matrix Biology,* vol. 52, pp. 113-126, 2016.

[78] A. D. Theocharis, S. S. Skandalis, C. Gialeli, and N. K. Karamanos, "Extracellular matrix structure," *Advanced drug delivery reviews,* vol. 97, pp. 4-27, 2016.

[79] A. Goodship, P. Watkins, H. Rigby, and J. Kenwright, "The role of fixator frame stiffness in the control of fracture healing. An experimental study," *Journal of Biomechanics,* vol. 26, no. 9, pp. 1027-1035, 1993.

[80] J. D. Boerckel, Y. M. Kolambkar, H. Y. Stevens, A. S. Lin, K. M. Dupont, and R. E. Guldberg, "Effects of in vivo mechanical loading on large bone defect regeneration," *Journal of Orthopaedic Research,* vol. 30, no. 7, pp. 1067-1075, 2012.

[81] B. Mavčič and V. Antolič, "Optimal mechanical environment of the healing bone fracture/osteotomy," *International orthopaedics,* vol. 36, no. 4, pp. 689-695, 2012.

[82] A. K. Ulstrup, "Biomechanical concepts of fracture healing in weight-bearing long bones," *Acta Orthopaedica Belgica,* vol. 74, no. 3, p. 291, 2008.

[83] P. V. Giannoudis, T. A. Einhorn, G. Schmidmaier, and D. Marsh, "The diamond concept–open questions," *Injury,* vol. 39, pp. S5-S8, 2008.

[84] J. Street *et al.*, "Vascular endothelial growth factor stimulates bone repair by promoting angiogenesis and bone turnover," *Proceedings of the National Academy of Sciences,* vol. 99, no. 15, pp. 9656-9661, 2002.

[85] A. E. Goodship, J. L. Cunningham, and J. Kenwright, "Strain rate and timing of stimulation in mechanical modulation of fracture healing," *Clinical Orthopaedics and Related Research®,* vol. 355, pp. S105-S115, 1998.

[86] J. Kenwright *et al.*, "Axial movement and tibial fractures. A controlled randomised trial of treatment," *Bone & Joint Journal,* vol. 73, no. 4, pp. 654-659, 1991.

[87] N. Amanat, M. McDonald, C. Godfrey, L. Bilston, and D. Little, "Optimal timing of a single dose of zoledronic acid to increase strength in rat fracture repair," *Journal of Bone and Mineral Research,* vol. 22, no. 6, pp. 867-876, 2007.

[88] C. R. Dosier *et al.*, "Effect of cell origin and timing of delivery for stem cell-based bone tissue engineering using biologically functionalized hydrogels," *Tissue Engineering Part A,* vol. 21, no. 1-2, pp. 156-165, 2014.

[89] K. A. Egol, A. Nauth, M. Lee, H.-C. Pape, J. T. Watson, and J. Borrelli Jr, "Bone grafting: sourcing, timing, strategies, and alternatives," *Journal of orthopaedic trauma,* vol. 29, pp. S10-S14, 2015.

[90] V. Glatt, N. Bartnikowski, N. Quirk, M. Schuetz, and C. Evans, "Reverse dynamization: influence of fixator stiffness on the mode and efficiency of large-bone-defect healing at different doses of rhBMP-2," *The Journal of bone and joint surgery. American volume,* vol. 98, no. 8, p. 677, 2016.

[91] S. Larsson, W. Kim, V. L. Caja, E. L. Egger, N. Inoue, and E. Y. Chao, "Effect of early axial dynamization on tibial bone healing: a study in dogs," *Clinical orthopaedics and related research,* vol. 388, pp. 240-251, 2001.

[92] G. N. Duda, K. Eckert-Hübner, R. Sokiranski, A. Kreutner, R. Miller, and L. Claes, "Analysis of inter-fragmentary movement as a function of musculoskeletal loading conditions in sheep," *Journal of biomechanics,* vol. 31, no. 3, pp. 201-210, 1997.

[93] J. A. Auer *et al.*, "Refining animal models in fracture research: seeking consensus in optimising both animal welfare and scientific validity for appropriate biomedical use," *BMC musculoskeletal disorders,* vol. 8, no. 1, p. 72, 2007.

[94] M. S. Ghiasi, J. Chen, A. Vaziri, E. K. Rodriguez, and A. Nazarian, "Bone fracture healing in mechanobiological modeling: A review of principles and methods," *Bone reports,* vol. 6, pp. 87-100, 2017.

[95] D. D. Anderson, T. P. Thomas, A. C. Marin, J. M. Elkins, W. D. Lack, and D. Lacroix, "Computational techniques for the assessment of fracture repair," *Injury,* vol. 45, pp. S23-S31, 2014.

[96] L. Claes and P. Augat, "Models in fracture healing: report from the Reisensburg workshop September 1999," *Journal of orthopaedic trauma,* vol. 14, no. 6, pp. 440-441, 2000.

[97] E. Borgiani, G. N. Duda, and S. Checa, "Multiscale modeling of bone healing: toward a systems biology approach," *Frontiers in physiology,* vol. 8, p. 287, 2017.

[98] M. Wang, N. Yang, and X. Wang, "A review of computational models of bone fracture healing," *Medical & biological engineering & computing,* vol. 55, no. 11, pp. 1895-1914, 2017.

[99] H. Isaksson, C. C. Van Donkelaar, R. Huiskes, and K. Ito, "Corroboration of mechanoregulatory algorithms for tissue differentiation during fracture healing: comparison with in vivo results," *Journal of Orthopaedic Research,* vol. 24, no. 5, pp. 898-907, 2006.

[100] R. Huiskes, W. Van Driel, P. Prendergast, and K. Søballe, "A biomechanical regulatory model for periprosthetic fibrous-tissue differentiation," *Journal of materials science: Materials in medicine,* vol. 8, no. 12, pp. 785-788, 1997.

[101] F. Pauwels, "A new theory on the influence of mechanical stimuli on the differentiation of supporting tissue. The tenth contribution to the functional anatomy and causal morphology of the supporting structure," *Zeitschrift fur Anatomie und Entwicklungsgeschichte,* vol. 121, pp. 478-515, 1960.

[102] D. R. Carter, G. S. Beaupré, N. J. Giori, and J. A. Helms, "Mechanobiology of skeletal regeneration," *Clinical orthopaedics and related research,* vol. 355, pp. S41-S55, 1998.

[103] H. Isaksson, W. Wilson, C. C. van Donkelaar, R. Huiskes, and K. Ito, "Comparison of biophysical stimuli for mechano-regulation of tissue differentiation during fracture healing," *Journal of biomechanics,* vol. 39, no. 8, pp. 1507-1516, 2006.

[104] D. Lacroix, P. Prendergast, G. Li, and D. Marsh, "Biomechanical model to simulate tissue differentiation and bone regeneration: application to fracture healing," *Medical and Biological Engineering and Computing,* vol. 40, no. 1, pp. 14-21, 2002.

[105] D. Lacroix and P. Prendergast, "A mechano-regulation model for tissue differentiation during fracture healing: analysis of gap size and loading," *Journal of biomechanics,* vol. 35, no. 9, pp. 1163-1171, 2002.

[106] M. Steiner, L. Claes, A. Ignatius, F. Niemeyer, U. Simon, and T. Wehner, "Prediction of fracture healing under axial loading, shear loading and bending is possible using distortional and dilatational strains as determining mechanical stimuli," *Journal of the Royal Society Interface,* vol. 10, no. 86, p. 20130389, 2013.

[107] D. P. Burke and D. J. Kelly, "Substrate stiffness and oxygen as regulators of stem cell differentiation during skeletal tissue regeneration: a mechanobiological model," *PLoS One,* vol. 7, no. 7, p. e40737, 2012.

[108] A. OReilly, K. D. Hankenson, and D. J. Kelly, "A computational model to explore the role of angiogenic impairment on endochondral ossification during fracture healing," *Biomechanics and modeling in mechanobiology,* vol. 15, no. 5, pp. 1279-1294, 2016.

[109] S. Checa and P. J. Prendergast, "A mechanobiological model for tissue differentiation that includes angiogenesis: a lattice-based modeling approach," *Annals of biomedical engineering,* vol. 37, no. 1, pp. 129-145, 2009.

[110] A. Bailon-Plaza and M. C. Van Der Meulen, "A mathematical framework to study the effects of growth factor influences on fracture healing," *Journal of Theoretical Biology,* vol. 212, no. 2, pp. 191-209, 2001.

[111] A. Carlier, L. Geris, K. Bentley, G. Carmeliet, P. Carmeliet, and H. Van Oosterwyck, "MOSAIC: a multiscale model of osteogenesis and sprouting angiogenesis with lateral inhibition of endothelial cells," *PLoS computational biology,* vol. 8, no. 10, p. e1002724, 2012.

[112] A. Carlier, L. Geris, N. van Gastel, G. Carmeliet, and H. Van Oosterwyck, "Oxygen as a critical determinant of bone fracture healing—a multiscale model," *Journal of theoretical biology,* vol. 365, pp. 247-264, 2015.

[113] A. Bailón-Plaza and M. C. van der Meulen, "Beneficial effects of moderate, early loading and adverse effects of delayed or excessive loading on bone healing," *Journal of biomechanics,* vol. 36, no. 8, pp. 1069-1077, 2003.

[114] L. Geris, J. V. Sloten, and H. V. Oosterwyck, "Connecting biology and mechanics in fracture healing: an integrated mathematical modeling framework for the study of nonunions," *Biomechanics and modeling in mechanobiology,* vol. 9, no. 6, pp. 713-724, 2010.

[115] S. M. Perren, "Evolution of the internal fixation of long bone fractures," *Bone & Joint Journal,* vol. 84, no. 8, pp. 1093-1110, 2002.

[116] P. Augat, J. Merk, S. Wolf, and L. Claes, "Mechanical stimulation by external application of cyclic tensile strains does not effectively enhance bone healing," *Journal of orthopaedic trauma,* vol. 15, no. 1, pp. 54-60, 2001.

[117] P. Grubor, M. Grubor, and M. Asotic, "Comparison of stability of different types of external fixation," *Medical Archives,* vol. 65, no. 3, p. 157, 2011.

[118] V. Coppa, M. Marinelli, and N. Specchia, "Unilateral uniplanar modular external fixator for percutaneous proximal femoral osteotomy in children: surgical technique," *European Journal of Orthopaedic Surgery & Traumatology,* vol. 29, no. 1, pp. 205-211, 2019.

[119] M. S. Alqahtani, A. Al-Tamimi, H. Almeida, G. Cooper, and P. Bartolo, "A review on the use of additive manufacturing to produce lower limb orthoses," *Progress in Additive Manufacturing,* pp. 1-10, 2019.

[120] M. S. Taljanovic, M. D. Jones, J. T. Ruth, J. B. Benjamin, J. E. Sheppard, and T. B. Hunter, "Fracture fixation," *Radiographics,* vol. 23, no. 6, pp. 1569-1590, 2003.

[121] B. Fleming, D. Paley, T. Kristiansen, and M. Pope, "A biomechanical analysis of the Ilizarov external fixator," *Clinical orthopaedics and related research,* vol. 241, pp. 95-105, 1989.

[122] M. Watson, K. Mathias, N. Maffulli, and D. Hukins, "The effect of clamping a tensioned wire: implications for the Ilizarov external fixation system," *Proceedings of the Institution of Mechanical Engineers, Part H: Journal of Engineering in Medicine,* vol. 217, no. 2, pp. 91-98, 2003.

[123] P. Hillard, A. Harrison, and R. Atkins, "The yielding of tensioned fine wires in the Ilizarov frame," *Proceedings of the Institution of Mechanical Engineers, Part H: Journal of Engineering in Medicine,* vol. 212, no. 1, pp. 37-47, 1998.

[124] F. J. Kummer, "Biomechanics of the Ilizarov external fixator," *Clinical orthopaedics and related research,* vol. 280, pp. 11-14, 1992.

[125] D. Paley, B. Fleming, M. Catagni, T. Kristiansen, and M. Pope, "Mechanical evaluation of external fixators used in limb lengthening," *Clinical orthopaedics and related research,* vol. 250, pp. 50-57, 1990.

[126] S. Miramini, Y. Yang, and L. Zhang, "A probabilistic-based approach for computational simulation of bone fracture healing," *Computer methods and programs in biomedicine,* vol. 180, p. 105011, 2019.

[127] D. J. Henderson, J. L. Rushbrook, P. J. Harwood, and T. D. Stewart, "What Are the Biomechanical Properties of the Taylor Spatial Frame™?," *Clinical Orthopaedics and Related Research®,* vol. 475, no. 5, pp. 1472-1482, 2017.

[128] E. R. Henderson, D. S. Feldman, C. Lusk, H. J. van Bosse, D. Sala, and F. J. Kummer, "Conformational instability of the taylor spatial frame: a case report and biomechanical study," *Journal of Pediatric Orthopaedics,* vol. 28, no. 4, pp. 471-477, 2008.

[129] L. Yang, S. Nayagam, and M. Saleh, "Stiffness characteristics and inter-fragmentary displacements with different hybrid external fixators," *Clinical Biomechanics,* vol. 18, no. 2, pp. 166-172, 2003.

[130] J. Calhoun, F. Li, W. Bauford, T. Lehman, B. Ledbetter, and R. Lowery, "Rigidity of half-pins for the Ilizarov external fixator," *Bulletin (Hospital for Joint Diseases (New York, NY)),* vol. 52, no. 1, pp. 21-26, 1992.

[131] G. N. Duda *et al.*, "Interfragmentary movements in the early phase of healing in distraction and correction osteotomies stabilized with ring fixators," *Langenbeck's Archives of Surgery,* vol. 387, no. 11-12, pp. 433-440, 2003.

[132] G. N. Duda *et al.*, "Interfragmentary motion in tibial osteotomies stabilized with ring fixators," *Clinical orthopaedics and related research,* vol. 396, pp. 163-172, 2002.

[133] Y. Öztürkmen, M. Karamehmetoğlu, H. Karadeniz, İ. Azboy, and M. Caniklioğlu, "Acute treatment of segmental tibial fractures with the Ilizarov method," *Injury,* vol. 40, no. 3, pp. 321-326, 2009.

[134] A. D. Parameswaran, C. S. Roberts, D. Seligson, and M. Voor, "Pin tract infection with contemporary external fixation: how much of a problem?," *Journal of orthopaedic trauma,* vol. 17, no. 7, pp. 503-507, 2003.

[135] A. V. Gubin, D. Y. Borzunov, and T. A. Malkova, "The Ilizarov paradigm: thirty years with the Ilizarov method, current concerns and future research," *International orthopaedics,* vol. 37, no. 8, pp. 1533-1539, 2013.

[136] A. Khurana, C. Byrne, S. Evans, H. Tanaka, and K. Haraharan, "Comparison of transverse wires and half pins in Taylor Spatial Frame: a biomechanical study," *Journal of orthopaedic surgery and research,* vol. 5, no. 1, p. 23, 2010.

[137] E. K. Bliven, M. Greinwald, S. Hackl, and P. Augat, "External fixation of the lower extremities: Biomechanical perspective and recent innovations," *Injury,* vol. 50, pp. S10-S17, 2019.

[138] D. D. Lewis, D. G. Bronson, M. L. Samchukov, R. D. Welch, and J. T. Stallings, "Biomechanics of circular external skeletal fixation," *Veterinary surgery,* vol. 27, no. 5, pp. 454-464, 1998.

[139] D. G. Bronson, M. L. Samchukov, J. G. Birch, R. H. Browne, and R. B. Ashman, "Stability of external circular fixation: a multi-variable biomechanical analysis," *Clinical Biomechanics,* vol. 13, no. 6, pp. 441-448, 1998.

[140] A. R. Cross *et al.*, "Effects of ring diameter and wire tension on the axial biomechanics of four-ring circular external skeletal fixator constructs," *American journal of veterinary research,* vol. 62, no. 7, pp. 1025-1030, 2001.

[141] A. Podolsky and E. Chao, "Mechanical performance of Ilizarov circular external fixators in comparison with other external fixators," *Clinical orthopaedics and related research,* no. 293, pp. 61-70, 1993.

[142] F. Kummer, "evaluation of new Ilizarov rings," *Bulletin of the Hospital for Joint Diseases Orthopaedic Institute,* vol. 50, no. 1, pp. 88-90, 1990.

[143] G. L. Orbay, V. H. Frankel, and F. J. Kummer, "The effect of wire configuration on the stability of the Ilizarov external fixator," *Clinical orthopaedics and related research,* no. 279, pp. 299-302, 1992.

[144] M. Watson, K. Mathias, N. Maffulli, D. Hukins, and D. Shepherd, "Finite element modelling of the Ilizarov external fixation system," *Proceedings of the Institution of Mechanical Engineers, Part H: Journal of Engineering in Medicine,* vol. 221, no. 8, pp. 863-871, 2007.

[145] V. Antoci, M. J. Voor, V. Antoci, and C. S. Roberts, "Effect of wire tension on stiffness of tensioned fine wires in external fixation: a mechanical study," *AMERICAN JOURNAL OF ORTHOPEDICS-BELLE MEAD-,* vol. 36, no. 9, p. 473, 2007.

[146] E. Yilmaz, O. Belhan, L. Karakurt, N. Arslan, and E. Serin, "Mechanical performance of hybrid Ilizarov external fixator in comparison with Ilizarov circular external fixator," *Clinical Biomechanics,* vol. 18, no. 6, pp. 518-522, 2003.

[147] A. Renard, B. Schutte, N. Verdonschot, and A. Van Kampen, "The Ilizarov external fixator: what remains of the wire pretension after dynamic loading?," *Clinical Biomechanics,* vol. 20, no. 10, pp. 1126-1130, 2005.

[148] V. La Russa, B. Skallerud, J. Klaksvik, and O. A. Foss, "Reduction in wire tension caused by dynamic loading. An experimental Ilizarov frame study," *Journal of biomechanics,* vol. 44, no. 8, pp. 1454-1458, 2011.

[149] J. Gessmann, H. Baecker, B. Jettkant, G. Muhr, and D. Seybold, "Direct and indirect loading of the Ilizarov external fixator: the effect on the interfragmentary movements and compressive loads," *Strategies in Trauma and Limb Reconstruction,* vol. 6, no. 1, pp. 27-31, 2011.

[150] J. Gessmann, B. Jettkant, T. A. Schildhauer, and D. Seybold, "Mechanical stress on tensioned wires at direct and indirect loading: a biomechanical study on the Ilizarov external fixator," *Injury,* vol. 42, no. 10, pp. 1107-1111, 2011.

[151] R. Aquarius, A. Van Kampen, and N. Verdonschot, "Rapid pre-tension loss in the Ilizarov external fixator: an in vitro study," *Acta orthopaedica,* vol. 78, no. 5, pp. 654-660, 2007.

[152] L. Claes, K. Eckert-Hübner, and P. Augat, "The effect of mechanical stability on local vascularization and tissue differentiation in callus healing," *Journal of orthopaedic research,* vol. 20, no. 5, pp. 1099-1105, 2002.

[153] T. Ramos, C. Ekholm, B. I. Eriksson, J. Karlsson, and L. Nistor, "The Ilizarov external fixator-a useful alternative for the treatment of proximal tibial fractures A prospective observational study of 30 consecutive patients," *BMC musculoskeletal disorders,* vol. 14, no. 1, p. 11, 2013.

[154] K. Fabry, J. Lammens, P. Delhey, J. Stuyck, and U. Pellenberg, "Ilizarov's method: a solution for infected bone loss," *European Journal of Orthopaedic Surgery & Traumatology,* vol. 16, no. 2, pp. 103-109, 2006.

[155] D. Paley, "Current techniques of limb lengthening," *Journal of Pediatric Orthopaedics,* vol. 8, no. 1, pp. 73-92, 1988.

[156] F. Leung, H. Y. Kwok, T. S. Pun, and S. P. Chow, "Limited open reduction and Ilizarov external fixation in the treatment of distal tibial fractures," *Injury,* vol. 35, no. 3, pp. 278-283, 2004.

[157] G. K. Dendrinos, S. Kontos, D. Katsenis, and A. Dalas, "Treatment of high-energy tibial plateau fractures by the Ilizarov circular fixator," *J Bone Joint Surg Br,* vol. 78, no. 5, pp. 710-717, 1996.

[158] M. Taylor and P. J. Prendergast, "Four decades of finite element analysis of orthopaedic devices: Where are we now and what are the opportunities?," *Journal of biomechanics,* vol. 48, no. 5, pp. 767-778, 2015.

[159] D. Anitha, S. Das De, K. K. Sun, H. K. Doshi, and T. Lee, "Improving stability of locking compression plates through a design modification: a computational investigation," *Computer methods in biomechanics and biomedical engineering,* vol. 18, no. 2, pp. 153-161, 2015.

[160] H. Wee, J. S. Reid, V. M. Chinchilli, and G. S. Lewis, "Finite element-derived surrogate models of locked plate fracture fixation biomechanics," *Annals of biomedical engineering,* vol. 45, no. 3, pp. 668-680, 2017.

[161] C. J. Wilson, M. A. Schütz, and D. R. Epari, "Computational simulation of bone fracture healing under inverse dynamisation," *Biomechanics and modeling in mechanobiology,* pp. 1-10, 2016.

[162] M. Gómez-Benito, J. García-Aznar, J. Kuiper, and M. Doblaré, "A 3D computational simulation of fracture callus formation: influence of the stiffness of the external fixator," *Journal of biomechanical engineering,* vol. 128, no. 3, pp. 290-299, 2006.

[163] D. Lacroix and P. Prendergast, "Three-dimensional simulation of fracture repair in the human tibia," *Computer Methods in Biomechanics & Biomedical Engineering,* vol. 5, no. 5, pp. 369-376, 2002.

[164] D. P. Byrne, D. Lacroix, and P. J. Prendergast, "Simulation of fracture healing in the tibia: mechanoregulation of cell activity using a lattice modeling approach," *Journal of orthopaedic research,* vol. 29, no. 10, pp. 1496-1503, 2011.

[165] S. Miramini *et al.*, "Computational simulation of the early stage of bone healing under different configurations of locking compression plates," *Computer methods in biomechanics and biomedical engineering,* vol. 18, no. 8, pp. 900-913, 2015.

[166] L. Geris, A. A. Reed, J. Vander Sloten, A. H. R. Simpson, and H. Van Oosterwyck, "Occurrence and treatment of bone atrophic non-unions investigated by an integrative approach," *PLoS computational biology,* vol. 6, no. 9, p. e1000915, 2010.

[167] P. Pivonka and C. R. Dunstan, "Role of mathematical modeling in bone fracture healing," *BoneKEy reports,* vol. 1, 2012.

[168] J. Prat *et al.*, "Load transmission through the callus site with external fixation systems: theoretical and experimental analysis," *Journal of biomechanics,* vol. 27, no. 4, pp. 469-478, 1994.

[169] A. Zamani and S. Oyadiji, "Analytical modelling of Kirschner wires in Ilizarov circular external fixator as pretensioned slender beams," *Journal of The Royal Society Interface,* vol. 6, no. 32, pp. 243-256, 2009.

[170] A. Zamani and S. Oyadiji, "Theoretical and finite element modeling of fine Kirschner wires in Ilizarov external fixator," *Journal of Medical Devices,* vol. 4, no. 3, p. 031001, 2010.

[171] G. Zhang, "Geometric and material nonlinearity in tensioned wires of an external fixator," *Clinical Biomechanics,* vol. 19, no. 5, pp. 513-518, 2004.

[172] G. Zhang, "Avoiding the material nonlinearity in an external fixation device," *Clinical Biomechanics,* vol. 19, no. 7, pp. 746-750, 2004.

[173] J. K. Nielsen, C. L. Saltzman, and T. D. Brown, "Determination of ankle external fixation stiffness by expedited interactive finite element analysis," *Journal of orthopaedic research,* vol. 23, no. 6, pp. 1321-1328, 2005.

[174] D. Keshet and M. Eidelman, "Clinical utility of the Taylor spatial frame for limb deformities," *Orthopedic Research and Reviews,* vol. 55, no. unknown, pp. 51-61, 2016.

[175] C. S. Roberts, V. Antoci, and M. J. Voor, "The effect of transfixion wire crossing angle on the stiffness of fine wire external fixation: a biomechanical study," *Injury,* vol. 36, no. 9, pp. 1107-1112, 2005.

[176] B. Tan, R. Shanmugam, R. Gunalan, Y. Chua, G. Hossain, and A. Saw, "A biomechanical comparison between Taylor's Spatial Frame and Ilizarov external fixator," *Malaysian orthopaedic journal,* vol. 8, no. 2, p. 35, 2014.

[177] S. Kold, "CORR Insights®: What Are the Biomechanical Properties of the Taylor Spatial Frame™?," *Clinical Orthopaedics and Related Research®,* vol. 475, no. 5, pp. 1483-1485, 2017.

[178] S. Miramini, L. Zhang, M. Richardson, P. Mendis, and P. R. Ebeling, "Influence of fracture geometry on bone healing under locking plate fixations: A comparison between oblique and transverse tibial fractures," *Medical engineering & physics,* vol. 38, no. 10, pp. 1100-1108, 2016.

[179] L. Zhang *et al.*, "Computational modelling of bone fracture healing under partial weight-bearing exercise," *Medical Engineering & Physics,* vol. 42, pp. 65-72, 2017.

[180] B. Gasser, B. Boman, D. Wyder, and E. Schneider, "Stiffness characteristics of the circular Ilizarov device as opposed to conventional external fixators," 1990.

[181] G. N. Duda, F. Mandruzzato, M. Heller, J.-P. Kassi, C. Khodadadyan, and N. P. Haas, "Mechanical conditions in the internal stabilization of proximal tibial defects," *Clinical Biomechanics,* vol. 17, no. 1, pp. 64-72, 2002.

[182] GOM, "ARAMIS user manual–Software," ed: GOM mbH Braunschweig, Germany, 2013.

[183] L. Zhang, S. Miramini, P. Mendis, M. Richardson, M. Pirpiris, and K. Oloyede, "The effects of flexible fixation on early stage bone fracture healing," *Int J Aerosp Lightweight Struct,* vol. 3, no. 2, pp. 181-189, 2013.

[184] P. Klein *et al.*, "The initial phase of fracture healing is specifically sensitive to mechanical conditions," *Journal of orthopaedic research,* vol. 21, no. 4, pp. 662-669, 2003.

[185] W. McCartney, B. Mac Donald, and M. Hashmi, "Comparative performance of a flexible fixation implant to a rigid implant in static and repetitive incremental loading," *Journal of materials processing technology,* vol. 169, no. 3, pp. 476-484, 2005.

[186] J. R. Davis, *Aluminum and aluminum alloys*. ASM international, 1993.

[187] B. Gardiner, D. Smith, P. Pivonka, A. Grodzinsky, E. Frank, and L. Zhang, "Solute transport in cartilage undergoing cyclic deformation," *Computer methods in biomechanics and biomedical engineering,* vol. 10, no. 4, pp. 265-278, 2007.

[188] G. N. Duda *et al.*, "Mechanical boundary conditions of fracture healing: borderline indications in the treatment of unreamed tibial nailing," *Journal of Biomechanics,* vol. 34, no. 5, pp. 639-650, 2001.

[189] T. A. Einhorn, "The cell and molecular biology of fracture healing," *Clinical orthopaedics and related research,* vol. 355, pp. S7-S21, 1998.

[190] T. A. Einhorn and L. C. Gerstenfeld, "Fracture healing: mechanisms and interventions," *Nature Reviews Rheumatology,* vol. 11, no. 1, p. 45, 2015.

[191] L. Martini, M. Fini, G. Giavaresi, and R. Giardino, "Sheep model in orthopedic research: a literature review," *Comparative medicine,* vol. 51, no. 4, pp. 292-299, 2001.

[192] T. Yamaji, K. Ando, S. Wolf, P. Augat, and L. Claes, "The effect of micromovement on callus formation," *Journal of Orthopaedic Science,* vol. 6, no. 6, pp. 571-575, 2001.

[193] A. Goodship and J. Kenwright, "The influence of induced micromovement upon the healing of experimental tibial fractures," *Bone & Joint Journal,* vol. 67, no. 4, pp. 650-655, 1985.

[194] P. Augat, J. Burger, S. Schorlemmer, T. Henke, M. Peraus, and L. Claes, "Shear movement at the fracture site delays healing in a diaphyseal fracture model," *Journal of orthopaedic research,* vol. 21, no. 6, pp. 1011-1017, 2003.

[195] L. E. Claes *et al.*, "Effects of mechanical factors on the fracture healing process," *Clinical orthopaedics and related research,* vol. 355, pp. S132-S147, 1998.

[196] N. M. Haines, W. D. Lack, R. B. Seymour, and M. J. Bosse, "Defining the lower limit of a “critical bone defect” in open diaphyseal tibial fractures," *Journal of orthopaedic trauma,* vol. 30, no. 5, pp. e158-e163, 2016.

[197] Z. Fan, J. Swadener, J. Rho, M. Roy, and G. Pharr, "Anisotropic properties of human tibial cortical bone as measured by nanoindentation," *Journal of Orthopaedic Research,* vol. 20, no. 4, pp. 806-810, 2002.

[198] J.-Y. Rho, "An ultrasonic method for measuring the elastic properties of human tibial cortical and cancellous bone," *Ultrasonics,* vol. 34, no. 8, pp. 777-783, 1996.

[199] F. Witt, G. N. Duda, C. Bergmann, and A. Petersen, "Cyclic mechanical loading enables solute transport and oxygen supply in bone healing: an in vitro investigation," *Tissue Engineering Part A,* vol. 20, no. 3-4, pp. 486-493, 2014.

[200] B. O'Hara, J. Urban, and A. Maroudas, "Influence of cyclic loading on the nutrition of articular cartilage," *Annals of the rheumatic diseases,* vol. 49, no. 7, pp. 536-539, 1990.

[201] R. L. Mauck, C. T. Hung, and G. A. Ateshian, "Modeling of neutral solute transport in a dynamically loaded porous permeable gel: implications for articular cartilage biosynthesis and tissue engineering," *Journal of biomechanical engineering,* vol. 125, no. 5, pp. 602-614, 2003.

[202] M. J. Gardner, B. F. Ricciardi, T. M. Wright, M. P. Bostrom, and M. C. van der Meulen, "Pause insertions during cyclic in vivo loading affect bone healing," *Clinical orthopaedics and related research,* vol. 466, no. 5, pp. 1232-1238, 2008.

[203] G. N. Duda, B. Bartmeyer, S. Sporrer, W. R. Taylor, M. Raschke, and N. P. Haas, "Does partial weight bearing unload a healing bone in external ring fixation?," *Langenbeck's archives of surgery,* vol. 388, no. 5, pp. 298-304, 2003.

[204] S. Miramini, L. Zhang, M. Richardson, P. Mendis, and P. Ebeling, "Influence of fracture geometry on bone healing under locking plate fixations: A comparison

between oblique and transverse tibial fractures," *Medical Engineering and Physics,* vol. 38, no. 10, pp. 1100-1108, 2016.

[205] J. Aronson, E. Johnson, and J. H. Harp, "Local Bone Transportation for Treatment of Intercalary Defects by the Ilizarov Technique: Biomechanical and Clinical Considerations," *Clinical orthopaedics and related research,* vol. 243, pp. 71-79, 1989.

[206] L. Zhang, S. Miramini, D. W. Smith, B. S. Gardiner, and A. J. Grodzinsky, "Time evolution of deformation in a human cartilage under cyclic loading," *Annals of biomedical engineering,* vol. 43, no. 5, pp. 1166-1177, 2015.

[207] M. Barker and B. Seedhom, "The relationship of the compressive modulus of articular cartilage with its deformation response to cyclic loading: does cartilage optimize its modulus so as to minimize the strains arising in it due to the prevalent loading regime?," *Rheumatology,* vol. 40, no. 3, pp. 274-284, 2001.

[208] L. Zhang, B. S. Gardiner, D. W. Smith, P. Pivonka, and A. J. Grodzinsky, "IGF uptake with competitive binding in articular cartilage," *Journal of Biological Systems,* vol. 16, no. 02, pp. 175-195, 2008.

[209] L. Zhang, S. Miramini, M. Richardson, P. Mendis, and P. Ebeling, "The role of impairment of mesenchymal stem cell function in osteoporotic bone fracture healing," *Australasian physical & engineering sciences in medicine,* vol. 40, no. 3, pp. 603-610, 2017.

[210] A. Andreykiv, F. Van Keulen, and P. Prendergast, "Simulation of fracture healing incorporating mechanoregulation of tissue differentiation and dispersal/proliferation of cells," *Biomechanics and modeling in mechanobiology,* vol. 7, no. 6, pp. 443-461, 2008.

[211] L. Zhang, B. S. Gardiner, D. W. Smith, P. Pivonka, and A. Grodzinsky, "The effect of cyclic deformation and solute binding on solute transport in cartilage," *Archives of biochemistry and biophysics,* vol. 457, no. 1, pp. 47-56, 2007.

[212] R. C. Evans and T. M. Quinn, "Dynamic compression augments interstitial transport of a glucose-like solute in articular cartilage," *Biophysical journal,* vol. 91, no. 4, pp. 1541-1547, 2006.

[213] P. Angele *et al.*, "Cyclic hydrostatic pressure enhances the chondrogenic phenotype of human mesenchymal progenitor cells differentiated in vitro," *Journal of Orthopaedic Research,* vol. 21, no. 3, pp. 451-457, 2003.

[214] S. H. Elder, J. Kimura, L. J. Soslowsky, M. Lavagnino, and S. A. Goldstein, "Effect of compressive loading on chondrocyte differentiation in agarose cultures of chick limb-bud cells," *Journal of Orthopaedic Research,* vol. 18, no. 1, pp. 78-86, 2000.

[215] S. Carroll, C. Buckley, and D. Kelly, "Cyclic hydrostatic pressure promotes a stable cartilage phenotype and enhances the functional development of cartilaginous grafts engineered using multipotent stromal cells isolated from bone marrow and infrapatellar fat pad," *Journal of Biomechanics,* vol. 47, no. 9, pp. 2115-2121, 2014.

[216] T. Vinardell *et al.*, "Hydrostatic pressure acts to stabilise a chondrogenic phenotype in porcine joint tissue derived stem cells," *Eur Cell Mater,* vol. 23, no. 23, pp. 121-132, 2012.

[217] K. Sakao *et al.*, "Induction of chondrogenic phenotype in synovium-derived progenitor cells by intermittent hydrostatic pressure," *Osteoarthritis and cartilage,* vol. 16, no. 7, pp. 805-814, 2008.

[218] C. Y. C. Huang, K. L. Hagar, L. E. Frost, Y. Sun, and H. S. Cheung, "Effects of cyclic compressive loading on chondrogenesis of rabbit bone-marrow derived mesenchymal stem cells," *Stem cells,* vol. 22, no. 3, pp. 313-323, 2004.

[219] L. Claes, H. Wilke, P. Augat, S. Rübenacker, and K. Margevicius, "Effect of dynamization on gap healing of diaphyseal fractures under external fixation," *Clinical Biomechanics,* vol. 10, no. 5, pp. 227-234, 1995.

[220] L. Claes, R. Blakytny, M. Göckelmann, M. Schoen, A. Ignatius, and B. Willie, "Early dynamization by reduced fixation stiffness does not improve fracture healing in a rat femoral osteotomy model," *Journal of Orthopaedic Research,* vol. 27, no. 1, pp. 22-27, 2009.

[221] V. Glatt *et al.*, "Improved healing of large segmental defects in the rat femur by reverse dynamization in the presence of bone morphogenetic protein-2," *The Journal of bone and joint surgery. American volume,* vol. 94, no. 22, p. 2063, 2012.

[222] M. Tägil and P. Aspenberg, "Cartilage induction by controlled mechanical stimulation in vivo," *Journal of Orthopaedic Research,* vol. 17, no. 2, pp. 200-204, 1999.

[223] S. Miramini, L. Zhang, M. Richardson, P. Mendis, A. Oloyede, and P. Ebeling, "The relationship between interfragmentary movement and cell differentiation in early fracture healing under locking plate fixation," *Australasian physical & engineering sciences in medicine,* vol. 39, no. 1, pp. 123-133, 2016.

[224] S. Miramini, L. Zhang, M. Richardson, and P. Mendis, "The Role of Locking Plate Stiffness in Bone Fracture Healing Stabilized by Far Cortical Locking Technique," *International Journal of Computational Methods,* vol. 15, no. 04, p. 1850024, 2018.

[225] L. Zhang, M. Richardson, and P. Mendis, "Role of chemical and mechanical stimuli in mediating bone fracture healing," *Clinical and Experimental Pharmacology and Physiology,* vol. 39, no. 8, pp. 706-710, 2012.

[226] U. Saran, S. G. Piperni, and S. Chatterjee, "Role of angiogenesis in bone repair," *Archives of biochemistry and biophysics,* vol. 561, pp. 109-117, 2014.

[227] L. Claes, N. Meyers, J. Schülke, S. Reitmaier, S. Klose, and A. Ignatius, "The mode of interfragmentary movement affects bone formation and revascularization after callus distraction," *PloS one,* vol. 13, no. 8, p. e0202702, 2018.

[228] G. Shanshan *et al.*, "Robot-assisted weight-bearing exercise for stroke patients with limited mobility," *Journal of Low Frequency Noise, Vibration and Active Control,* vol. 38, no. 2, pp. 879-892, 2019.

[229] N. Bartnikowski *et al.*, "Modulation of fixation stiffness from flexible to stiff in a rat model of bone healing," *Acta orthopaedica,* vol. 88, no. 2, pp. 217-222, 2017.

[230] U. Simon, P. Augat, M. Utz, and L. Claes, "A numerical model of the fracture healing process that describes tissue development and revascularisation," *Computer methods in biomechanics and biomedical engineering,* vol. 14, no. 01, pp. 79-93, 2011.

[231] S. Miramini, L. H. Zhang, M. Richardson, and P. Mendis, "Computational simulation of mechanical microenvironment of early stage of bone healing under locking compression plate with dynamic locking screws," in *Applied Mechanics and Materials*, 2014, vol. 553, pp. 281-286: Trans Tech Publ.

[232] B. Spiegelberg, T. Parratt, S. Dheerendra, W. Khan, R. Jennings, and D. Marsh, "Ilizarov principles of deformity correction," *Annals of The Royal College of Surgeons of England,* vol. 92, no. 2, p. 101, 2010.

[233] S. Ghimire, S. Miramini, M. Richardson, P. Mendis, and L. Zhang, "Role of Dynamic Loading on Early Stage of Bone Fracture Healing," *Annals of biomedical engineering,* pp. 1-17, 2018.

[234] S. Ghimire, S. Miramini, M. Richardson, P. Mendis, and L. Zhang, "Effects of dynamic loading on fracture healing under different locking compression plate configurations: A finite element study," *Journal of the mechanical behavior of biomedical materials,* vol. 94, pp. 74-85, 2019.

[235] G. Chen *et al.*, "Simulation of the nutrient supply in fracture healing," *Journal of biomechanics,* vol. 42, no. 15, pp. 2575-2583, 2009.

[236] G. M. Cooper, R. E. Hausman, and R. E. Hausman, *The cell: a molecular approach*. ASM press Washington, DC, 2000.

[237] I. Pountos and P. V. Giannoudis, "Biology of mesenchymal stem cells," *Injury,* vol. 36, no. 3, pp. S8-S12, 2005.

[238] R. Lanza *et al.*, *Handbook of Stem Cells, Two-Volume Set: Volume 1-Embryonic Stem Cells; Volume 2-Adult & Fetal Stem Cells*. Elsevier, 2004.

[239] X. Zhou, K. von der Mark, S. Henry, W. Norton, H. Adams, and B. de Crombrugghe, "Chondrocytes transdifferentiate into osteoblasts in endochondral bone during development, postnatal growth and fracture healing in mice," *PLoS genetics,* vol. 10, no. 12, p. e1004820, 2014.

[240] M. Ikegame *et al.*, "Tensile stress induces bone morphogenetic protein 4 in preosteoblastic and fibroblastic cells, which later differentiate into osteoblasts leading to osteogenesis in the mouse calvariae in organ culture," *Journal of Bone and Mineral Research,* vol. 16, no. 1, pp. 24-32, 2001.

[241] R. B. Rutherford, M. Moalli, R. T. Franceschi, D. Wang, K. Gu, and P. H. Krebsbach, "Bone morphogenetic protein-transduced human fibroblasts convert

to osteoblasts and form bone in vivo," *Tissue engineering,* vol. 8, no. 3, pp. 441-452, 2002.

[242] C. J. Wilson, M. A. Schuetz, and D. R. Epari, "Effects of strain artefacts arising from a pre-defined callus domain in models of bone healing mechanobiology," *Biomechanics and modeling in mechanobiology,* vol. 14, no. 5, pp. 1129-1141, 2015.

[243] S. Perren and J. Cordey, "The concept of interfragmentary strain," *Current concepts of internal fixation of fractures,* pp. 63-77, 1980.

[244] A. Vetter, F. Witt, O. Sander, G. Duda, and R. Weinkamer, "The spatio-temporal arrangement of different tissues during bone healing as a result of simple mechanobiological rules," *Biomechanics and modeling in mechanobiology,* vol. 11, no. 1, pp. 147-160, 2012.

[245] S. Stegen, N. van Gastel, and G. Carmeliet, "Bringing new life to damaged bone: the importance of angiogenesis in bone repair and regeneration," *Bone,* vol. 70, pp. 19-27, 2015.

[246] M. S. Ghiasi, J. E. Chen, E. K. Rodriguez, A. Vaziri, and A. Nazarian, "Computational Modeling of the Effects of Inflammatory Response and Granulation Tissue Properties on Human Bone Fracture Healing," *arXiv preprint arXiv:1808.04458,* 2018.

[247] Y. Lu and T. Lekszycki, "Modelling of bone fracture healing: influence of gap size and angiogenesis into bioresorbable bone substitute," *Mathematics and Mechanics of Solids,* vol. 22, no. 10, pp. 1997-2010, 2017.

[248] B. Bragdon *et al.*, "Earliest phases of chondrogenesis are dependent upon angiogenesis during ectopic bone formation in mice," *Bone,* vol. 101, pp. 49-61, 2017.

[249] T. Wehner, M. Steiner, A. Ignatius, and L. Claes, "Prediction of the time course of callus stiffness as a function of mechanical parameters in experimental rat fracture healing studies-a numerical study," *PloS one,* vol. 9, no. 12, p. e115695, 2014.

[250] A. I. Leet, C. P. Pichard, and M. C. Ain, "Surgical treatment of femoral fractures in obese children: does excessive body weight increase the rate of complications?," *JBJS,* vol. 87, no. 12, pp. 2609-2613, 2005.

[251] M. Patil and H. Baseer, "Obesity and fracture healing," *Al Ameen Journal of Medical Sciences,* vol. 10, no. 2, pp. 107-111, 2017.

[252] M. A. Karunakar, S. N. Shah, and S. Jerabek, "Body mass index as a predictor of complications after operative treatment of acetabular fractures," *JBJS,* vol. 87, no. 7, pp. 1498-1502, 2005.

[253] U. C. Okoroafor, L. K. Cannada, and J. L. McGinty, "Obesity and failure of nonsurgical management of pediatric both-bone forearm fractures," *The Journal of hand surgery,* vol. 42, no. 9, pp. 711-716, 2017.

[254] T. H. Meadows, J. T. Bronk, Y. Chao, and P. J. Kelly, "Effect of weight-bearing on healing of cortical defects in the canine tibia," *The Journal of bone and joint surgery. American volume,* vol. 72, no. 7, pp. 1074-1080, 1990.

[255] G. A. Ilizarov, "The apparatus: components and biomechanical principles of application," in *Transosseous osteosynthesis*: Springer, 1992, pp. 63-136.

[256] J. R. Ebert, T. R. Ackland, D. G. Lloyd, and D. J. Wood, "Accuracy of partial weight bearing after autologous chondrocyte implantation," *Archives of physical medicine and rehabilitation,* vol. 89, no. 8, pp. 1528-1534, 2008.

[257] F. E. Donaldson, P. Pankaj, and A. H. R. Simpson, "Investigation of factors affecting loosening of ilizarov ring-wire external fixator systems at the bone-wire interface," *Journal of Orthopaedic Research,* vol. 30, no. 5, pp. 726-732, 2012.

[258] L. Mehrez and M. Browne, "A numerically validated probabilistic model of a simplified total hip replacement construct," *Computer methods in biomechanics and biomedical engineering,* vol. 15, no. 8, pp. 845-858, 2012.

[259] C. Dopico-González, A. M. New, and M. Browne, "A computational tool for the probabilistic finite element analysis of an uncemented total hip replacement considering variability in bone–implant version angle," *Computer methods in biomechanics and biomedical engineering,* vol. 13, no. 1, pp. 1-9, 2010.

[260] C. K. Fitzpatrick, C. W. Clary, and P. J. Rullkoetter, "The role of patient, surgical, and implant design variation in total knee replacement performance," *Journal of biomechanics,* vol. 45, no. 12, pp. 2092-2102, 2012.

[261] O. Kayabasi and B. Ekici, "Probabilistic design of a newly designed cemented hip prosthesis using finite element method," *Materials & Design,* vol. 29, no. 5, pp. 963-971, 2008.

[262] A. Vetter *et al.*, "Temporal tissue patterns in bone healing of sheep," *Journal of Orthopaedic Research,* vol. 28, no. 11, pp. 1440-1447, 2010.

[263] C. S. Roberts, V. Antoci, V. Antoci Jr, and M. J. Voor, "The accuracy of fine wire tensioners: a comparison of five tensioners used in hybrid and ring external fixation," *Journal of orthopaedic trauma,* vol. 18, no. 3, pp. 158-162, 2004.

[264] R. Kajiwara, O. Ishida, K. Kawasaki, N. Adachi, Y. Yasunaga, and M. Ochi, "Effective repair of a fresh osteochondral defect in the rabbit knee joint by articulated joint distraction following subchondral drilling," *Journal of orthopaedic research,* vol. 23, no. 4, pp. 909-915, 2005.

[265] B. Franssen, A. H. Schuurman, A. M. Van Der Molen, and M. Kon, "One century of Kirschner wires and Kirschner wire insertion techniques: a historical review," *Acta Orthop Belg,* vol. 76, no. 1, pp. 1-6, 2010.

[266] S. M. Perren, "Evolution of the internal fixation of long bone fractures: the scientific basis of biological internal fixation: choosing a new balance between stability and biology," *The Journal of bone and joint surgery. British volume,* vol. 84, no. 8, pp. 1093-1110, 2002.

[267] T. Terjesen and S. Svenningsen, "The effects of function and fixation stiffness on experimental bone heating," *Acta Orthopaedica Scandinavica*, vol. 59, no. 6, pp. 712-715, 1988.

[268] H. T. Aro, P. J. Kelly, D. G. Lewallen, and E. Chao, "The effects of physiologic dynamic compression on bone healing under external fixation," *Clinical orthopaedics and related research*, no. 256, pp. 260-273, 1990.

Appendix: Additional outcomes of this research

Additional outcomes (publications) of this research that are not included in the chapters are presented in this section. This section includes the following two publications:

1. **The effects of direct and indirect loading on bone fracture healing under Ilizarov circular fixator** published in the **proceedings of the 6th International Conference on Computational and Mathematical Biomedical Engineering** (published on 10/06/2019)
2. **The role of physiological loading on bone fracture healing under Ilizarov circular fixator : the effects of load duration and loading frequency** which is published by **Lecture Notes in Computational Vision and Biomechanics** book series (published on 01/04/2020)

6th International Conference on Computational and Mathematical Biomedical Engineering – CMBE2019
10-12 June 2019, Japan
P. Nithiarasu, M. Ohta, M. Oshima (Eds.)

THE EFFECTS OF DIRECT AND INDIRECT LOADING ON BONE FRACTURE HEALING UNDER ILIZAROV CIRCULAR FIXATOR

Ganesharajah Ganadhiepan[1], Saeed Miramini[1], Priyan Mendis[1], and Lihai Zhang[1]
[1] Department of Infrastructure Engineering, The University of Melbourne, Australia.
{ganadhiepang,s.miramini, pamendis, lihzhang}@unimelb.edu.au

SUMMARY

In this study, a validated 3D computational model of a fractured tibia stabilized with Ilizarov circular fixator (ICF) has been used to investigate the influence of two different weight transmission modes of ICF (namely, (i) direct loading and (ii) indirect loading) on the early stage cell differentiations within the fracture callus. Furthermore, how the effects of direct and indirect loading vary with patient specific parameters such as fracture gap size and loading level are also investigated in this study. The results provide insights into the interrelationships between load transmission modes and the spatially dependent cellular differentiation within the callus.

Key words: *Ilizarov circular fixator, mechano-regulation, direct loading, indirect loading*

1 INTRODUCTION

Ilizarov circular fixator (ICF) is an external bone fixator device used to treat number of bone defects including fractures, non-unions and deformities [1]. Its advantages include: (i) being minimally invasive with only very small pretensioned wires (e.g. 1.8 mm diameter) passing through the bones (ii) being tailorable throughout the course of healing depending on the healing progression and (iii) allowing early weight bearing. Although the mechanical performance of ICF under different configurations has been investigated so far, the influence of its mechanical behaviour on the fracture microenvironment has not been investigated clearly yet. One such behaviour that lacks mechanobiological investigation is the effect of the mode of load transmission through ICF on the fracture microenvironment.

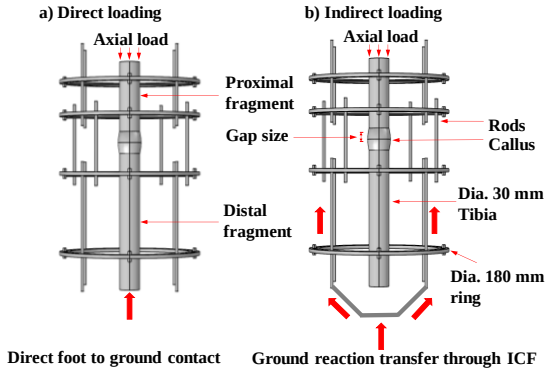

Fig. 1 Direct and indirect loading in ICF

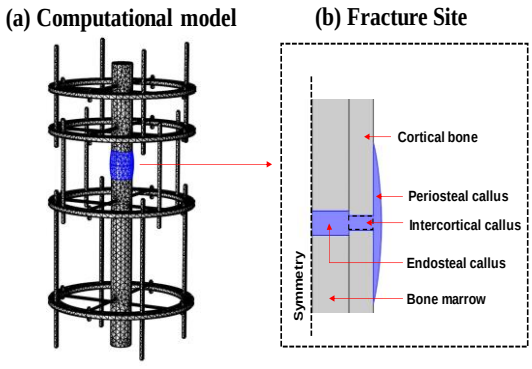

Fig. 2 Computational model and fracture site

In general, ICF could allow weight bearing in two modes: (i) Direct loading (Fig. 1a) – where the foot contacts the ground directly to transmit the load and (ii) Indirect loading (Fig. 1b) – where the distal end of the frame is extended and connected to a weight bearing platform which permits no direct contact

of the foot to the ground during weight bearing [2, 3]. These two loading modes could result in two significantly different mechanical microenvironments within a given fracture site (i.e. callus). However, how these different load transmission modes affect the cell differentiations within the fracture site has not been investigated yet. The purpose of this study is to investigate this. Furthermore, how the effect of direct and indirect loading varies with patient specific parameters such as fracture gap size and loading level are also investigated in this study. We specifically focused on the early stage of healing as this is when the cells commit to differential pathway which is decisive of the healing outcome [4, 5].

2 METHODOLOGY

In this study, a validated fully coupled 3D computational model of a fractured tibia stabilized with a four ring Ilizarov fixator (Fig. 2a) was used to predict the mesenchymal stem cell differentiations within the early callus (consisting mainly of granulation tissue) under direct and indirect loading conditions. To simplify the bone geometry, the tibia was assumed to be cylindrical with a 30 mm diameter outer cortex and an 18 mm diameter inner bone marrow. The Ilizarov fixator had two mutually perpendicular 1.8 mm diameter pretension wires (with 883 N wire pretension) per ring and four 180 mm diameter (internal) rings (two per fragment) connected together using twelve 4.69 mm diameter rods. The bone tissues (i.e. cortical bone, bone marrow and soft fracture callus) were treated as bi-phasic poroelastic materials and the fixator components (i.e. pretension wires, rings and rods) were modelled with linear elastic stainless-steel material (all material properties were adopted from our previous study [6]). Assuming quasi static condition for the tissues and neglecting the body forces, the governing equations for poro-elastic formulation could be written as follows [6]:

$$\boldsymbol{\sigma} = -p\mathbf{I} + \boldsymbol{\sigma}^{\mathbf{e}} \tag{1}$$

$$\nabla.\boldsymbol{\sigma} = -\nabla p + \nabla.\boldsymbol{\sigma}^{\mathbf{e}} = \mathbf{0} \tag{2}$$

$$\nabla.(\mathbf{v}^{\mathbf{s}} - \mathbf{k}\nabla p) = \mathbf{0} \tag{3}$$

where, $\boldsymbol{\sigma}$ – stress tensor of the callus; p - incremental interstitial fluid pressure; $\mathbf{I}$ - identity matrix; $\boldsymbol{\sigma}^{\mathbf{e}}$ - elastic stress of solid matrix; $\mathbf{v}^{\mathbf{s}}$ - solid phase velocity and $\mathbf{k}$ - tissue permeability tensor. To simulate the cell differentiations with the fracture callus, the mechano-regulatory theory of Prendergast et al. [7, 8] for poro-elastic formulations were used. According to this theory, MSC differentiation within the early callus is governed by the stimulation index S defined as

$$S = \gamma/a + v/b \tag{4}$$

where, γ - octahedral shear strain of solid phase; v - interstitial fluid velocity, a = 0.0375 and b = 3 μm s^{-1}. The mechano-regulatory theory suggests that, larger values of S (i.e. S > 3) are conductive to fibroblast differentiation; intermediate values of S (i.e. 1<S<3) are conductive to chondrocyte differentiation and smaller values of S (S<1) are conductive to osteoblast differentiation.

2.1 Numerical solution and parametric study

The fracture callus was assumed to be fluid saturated and initially filled with MSC. The external boundaries of all bone materials were assumed to be impermeable to fluid flow and the wire pretension was applied as initial axial stress to the wires. In the direct loading condition, the bottom end of the distal fragment was assigned a fixed boundary condition. However, for the indirect loading condition, the bottom end of the distal fragment was left free and the bottom ends of the four bottom rods were assigned fixed boundary condition to represent load transmission through the weight bearing platform.

The axial load was applied as a ramp load over 0.5 s to the top surface of cortical bone (proximal fragment) to represent physiological loading and the model was meshed and solved using the time dependent solver of COMSOL MULTIPHYSICS (COMSOL AB, Stockholm, Sweden). To account for the stress stiffening effect of the wires, geometric non-linearity of the wires was taken into consideration

in the analysis. Since the mechanical microenvironment of the fracture site is very sensitive to the gap size and loading levels, the influence of these parameters was also investigated in this study to better understand the effect of direct and indirect loading on the microenvironment of the fracture site. Relatively small and large gap sizes (i.e. 3 mm and 5 mm) and physiologically relevant low and high axial loads (i.e. 150 N and 300 N) were considered for both direct and indirect loading scenarios.

3 RESULTS AND CONCLUSIONS

As different zones within the fracture callus are within different microenvironments, the cell differentiations were calculated within three distinct zones of the callus, namely, (i) periosteal callus (ii) intercortical callus and (iii) endosteal callus (Fig.2b). Figure 3 shows the percentage of each cell within these zones of the callus. It could be seen that the intercortical callus is generally affected very much by the interfragmentary movement (IFM) and mostly consists of fibroblasts (always > 90 %) irrespective of the gap size, axial load or load transmission mode (i.e. direct or indirect).

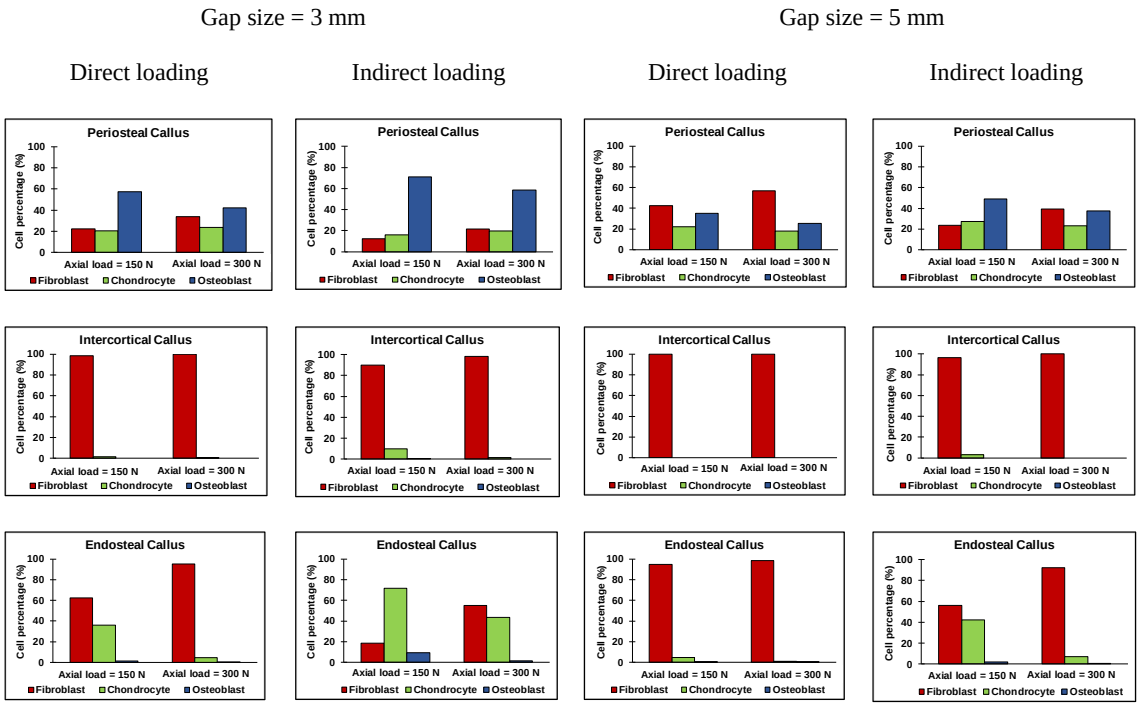

Fig. 3 Cell percentages within different regions of the callus under different gap sizes, axial loads and loading modes.

Under direct loading, noticeable osteoblasts were predicted only in the periosteal zone and the percentage of osteoblasts dropped with increase of gap size or axial load. Chondrocytes were also noticeable only in the periosteal zone except for small gap (3 mm) and small axial load (150 N) case, where the endosteal zone consisted of 36 % of chondrocytes. Fibroblasts were the most dominant in the endosteal zone (always > 62 %) in general and under large gap size (5 mm), its dominance was noticed even in the periosteal callus (i.e. greater than 42 % and 56 % for respectively for 150 N and 300 N axial loads). This suggests that the mechanical microenvironment within the fracture gap is relatively unstable and mostly conductive to fibroblast differentiation. Reduction of IFM due to reduction of gap size or lowering of axial load tends to promote better environments mostly within the periosteal region which is the most important region for fracture stabilization in the early stages. However, under relatively small gaps (i.e. 3 mm), lowering the load tends to promote bridging within the endosteal region as well. These predictions are in good agreement with in vivo sheep experimental studies on transverse osteotomies stabilized with ring fixators [9-11].

Indirect loading was predicted to enhance the microenvironment further within the callus. It could be seen that the osteoblast differentiation within the periosteal zone significantly increased in all indirect loading cases compared to the corresponding cases of direct loading. In addition, noticeable chondrocyte differentiation was predicted within the endosteal zone for all indirect load cases. Under small gap size (i.e. 3 mm) and low axial load (i.e. 150 N) noticeable chondrocytes (around 10 %) were predicted even within the intercortical zone. Furthermore, the percentage of fibroblast was observed to drop within the periosteal and endosteal zones with the change of load transmission mode from direct to indirect. These results suggest that indirect loading using weight bearing platforms could significantly improve the mechanical microenvironment within the fracture callus in the early stages of fracture healing. This could be particularly beneficial when larger fracture gaps are unavoidable, which could normally lead to unstable fracture microenvironments. In addition, indirect loading significantly enhances early weight bearing capacity. This could also be beneficial for early mobility of patients without having adverse effects on the fracture site. Therefore, indirect loading using weight bearing platforms appears to widen the allowable range of gap size and weight bearing, providing more flexibility to surgeons. However, further animal experiments and clinical studies are required to support the outcomes of this study.

4 ACKNOWLEDGEMENTS AND DISCLOSURES

The authors would like to thank Prof. Minoo Patel of Epworth Hospital (Richmond) for this support. Also, the authors have no conflicts of interest to disclose.

REFERENCES

[1] K. Erler, C. Yildiz, B. Baykal, A. S. Atesalp, M. T. Ozdemir, and M. Basbozkurt, Reconstruction of defects following bone tumor resections by distraction osteogenesis, Archives of orthopaedic and trauma surgery, vol. 125, no. 3, pp. 177-183, 2005.

[2] J. Gessmann, H. Baecker, B. Jettkant, G. Muhr, and D. Seybold, Direct and indirect loading of the Ilizarov external fixator: the effect on the interfragmentary movements and compressive loads, Strategies in Trauma and Limb Reconstruction, vol. 6, no. 1, pp. 27-31, 2011.

[3] J. Gessmann, B. Jettkant, T. A. Schildhauer, and D. Seybold, Mechanical stress on tensioned wires at direct and indirect loading: a biomechanical study on the Ilizarov external fixator, Injury, vol. 42, no. 10, pp. 1107-1111, 2011.

[4] D. R. Epari, W. R. Taylor, M. O. Heller, and G. N. Duda, Mechanical conditions in the initial phase of bone healing, Clinical Biomechanics, vol. 21, no. 6, pp. 646-655, 2006.

[5] P. Klein et al., The initial phase of fracture healing is specifically sensitive to mechanical conditions, Journal of orthopaedic research, vol. 21, no. 4, pp. 662-669, 2003.

[6] S. Miramini et al., Computational simulation of the early stage of bone healing under different configurations of locking compression plates, Computer methods in biomechanics and biomedical engineering, vol. 18, no. 8, pp. 900-913, 2015.

[7] R. Huiskes, W. Van Driel, P. Prendergast, and K. Søballe, A biomechanical regulatory model for periprosthetic fibrous-tissue differentiation, Journal of materials science: Materials in medicine, vol. 8, no. 12, pp. 785-788, 1997.

[8] P. Prendergast, R. Huiskes, and K. Søballe, Biophysical stimuli on cells during tissue differentiation at implant interfaces, Journal of biomechanics, vol. 30, no. 6, pp. 539-548, 1997.

[9] L. Claes, P. Augat, G. Suger, and H. J. Wilke, Influence of size and stability of the osteotomy gap on the success of fracture healing, Journal of orthopaedic research, vol. 15, no. 4, pp. 577-584, 1997.

[10] L. E. Claes et al., Effects of mechanical factors on the fracture healing process, Clinical orthopaedics and related research, vol. 355, pp. S132-S147, 1998.

[11] T. Yamaji, K. Ando, S. Wolf, P. Augat, and L. Claes, The effect of micromovement on callus formation, Journal of Orthopaedic Science, vol. 6, no. 6, pp. 571-575, 2001.